POLITECHNIKA ŚLĄSKA

Wydział Górnictwa, Inżynierii Bezpieczeństwa i Automatyki Przemysłowej

Katedra Geoinżynierii i Eksploatacji Surowców

mgr inż. Dawid Franke

ROZPRAWA DOKTORSKA

Eko-efektywna technologia odzysku metali z płyt obwodów drukowanych

Promotor: **dr hab. inż. Tomasz Suponik, prof. PŚ**

Promotor pomocniczy: **dr inż. Paweł Nuckowski**

Gliwice 2023

Podziękowania

Na powstanie i ostateczny kształt mojej pracy doktorskiej miało wpływ wiele osób, którym chciałbym w tym miejscu podziękować.

Jako pierwszemu serdecznie dziękuję mojemu promotorowi dr hab. inż., prof. PŚ Tomaszowi Suponikowi, za zaangażowanie i niewiarygodną cierpliwość w trakcie mojej drogi naukowej. Jego wiedza, doświadczenie i nieoceniona pomoc pozwoliły mi na osiągnięcie tego etapu.

Chciałbym również podziękować mojemu promotorowi pomocniczemu dr inż. Pawłowi Nuckowskiemu, za wspaniałą współpracę i przekazaną wiedzą oraz cenne wskazówki. Dzięki nim mogłem znacząco rozwinąć swoją pracę.

Osobne, równie ważne, podziękowania składam na ręce moich rodziców. Nie mógłbym tego osiągnąć bez ogromnego wsparcia i zrozumienia z ich strony. Dziękuję również moim przyjaciołom, którzy przez całą tę drogę towarzyszyli mi swoją przyjaźnią i cierpliwością.

Streszczenie

Zużyty sprzęt elektryczny i elektroniczny (ZSEE) jest obecnie jednym z najszybciej rosnących strumieni odpadów. Niewłaściwe magazynowanie lub przetwarzanie ZEEE może być przyczyną problemów środowiskowych i degradacji środowiska przyrodniczego. Dynamicznie rosnąca ilość tych odpadów staje się wyzwaniem dla firm odzyskujących wartościowe substancje, a znaczący wzrost popytu na urządzenia elektroniczne spowodowany m.in. COVID-19 może dodatkowo zwiększyć produkcję ZSEE w najbliższych latach. Elementem występującym niemal we wszystkich ZSEE są płyty obwodów drukowanych (ang. *Printed Cicruit Boards*, PCB). Najczęściej stosowanymi są PCB typu FR-4, które zbudowane są z podłoża wykonanego z włókna szklanego i żywicy epoksydowej. W kompozycie zużytych płyt obwodów drukowanych (ang. *Waste Printed Cicruit Boards,* WPCB) FR-4 zatopione są metaliczne ścieżki zawierające duże ilości metali takich jak Cu, Fe, Al, Sn, pierwiastki ziem rzadkich, Ta, Ga i innych z grupy lantanowców oraz metale szlachetne: Au, Ag i Pd. WPCB FR-4 zawierają również metale niebezpieczne dla zdrowia i życia ludzi oraz środowiska przyrodniczego, takie jak Cr, Pb, Be, Hg, Cd, Zn, Ni. Dlatego w celu ochrony złóż i środowiska WPCB powinny być przetwarzane zgodnie z zasadami gospodarki o obiegu zamkniętym oraz zrównoważonej produkcji.

Najczęściej stosowanymi metodami recyklingu WPCB są metody chemiczne polegające na ich roztwarzaniu w kwasach lub spalaniu. Poza wysokim stopniem skomplikowania tych metod oraz wysokimi emisjami do środowiska przyrodniczego, następuje utrata części niemetalicznych, które mogłyby być wykorzystane do innych procesów produkcyjnych lub wytwórczych. Alternatywnymi sposobami przetwarzania WPCB są metody fizyczne i fizykochemiczne z zakresu inżynierii mineralnej. Wykazują one znacznie mniejszy wpływ na środowisko przyrodnicze, jednak z uwagi na trudność uwolnienia metali z kompozytu WPCB polegające na konieczności stosowania szeregu procesów technologicznych, są one rzadziej stosowane.

Wobec powyższego, głównym celem pracy było opracowanie eko-efektywnej technologii recyklingu WPCB z wykorzystaniem metod fizycznych i fizykochemicznych z zakresu inżynierii mineralnej. W pierwszym etapie badań dokonano oceny procesów jednostkowych, a następnie dobrano komponenty technologii odzysku metali z WPCB. Ocenę zrealizowano na trzech poziomach: sprawność rozdziału, koszty procesowe i inwestycyjne oraz oddziaływanie na środowisko przyrodnicze. W szczególności w pracy przedstawiono wyniki badań rozdrabniania, separacji elektrostatycznej, flotacji, separacji grawitacyjnej przy użyciu separatora cyklofluidalnego i stołu koncentracyjnego oraz zabezpieczenia produktów do transportu. Oceniono następnie czystość produktów recyklingu oraz oddziaływanie procesów separacji na środowisko przyrodnicze i człowieka. Ponadto oszacowano parametry ekonomiczne technologii recyklingu wpływające na koszty procesowe i inwestycyjne.

Spis treści

Lista głównych publikacji 9

Lista zgłoszeń patentowych 11

Lista pozostałych publikacji 12

1 Wprowadzenie 15

2 Przegląd metod recyklingu zużytych płyt odwodów drukowanych 21

3 Cel i zakres pracy 25

4 Metodyka badawcza 27

4.1 Przygotowanie zużytych płyt obwodów drukowanych do procesów rozdziału 27

4.2 Zastosowane metod separacji 28

4.3 Metody analityczne 31

5 Wyniki i dyskusja 33

5.1 Rozdrabnianie 33

5.2 Metody rozdziału 34

5.3 Ocena procesów jednostkowych 48

6 Podsumowanie 55

Bibliografia 57

Wykaz publikacji 63

Lista głównych publikacji

M1. ***Impact of grinding of printed circuit boards on the efficiency of metal recovery by means of electrostatic separation.***

Suponik T., **Franke D.**, Nuckowski P., Matusiak P., Kowol D., Tora B.,
Minerals, vol. 11, nr 3, 2021, 281, s. 1-21, DOI:10.3390/min11030281,
(MEiN=100, IF=2,818)

D.F. był odpowiedzialny za przeprowadzenie badań rozdrabniania w młynie nożowym i separacji elektrostatycznej zużytych płyt obwodów drukowanych. D.F. wykonał analizę granulometryczną, gęstości właściwej i mikroskopową otrzymanych produktów. Ponadto D.F. przygotował *rysunki 1 – 4* i *9* oraz sporządził *tabele 1 – 3* i *6*.

M2. ***Recovery of metals from printed circuit boards by means of electrostatic separation.***

Franke D., Suponik T., Nuckowski P., Gołombek K., Hyra K.,
Management Systems in Production Engineering, P.A. NOVA S.A., vol. 28, nr 4, 2020, s. 213-219, DOI:10.2478/mspe-2020-0031,
(MEiN=70, IF=1,003)

D.F. był odpowiedzialny za sporządzenie przeglądu literaturowego i przygotowanie zużytych płyt obwodów drukowanych do procesów rozdrabniania. D.F. zbadał możliwość zastosowania separacji elektrostatyczne do rozdziału metali od tworzyw sztucznych z rozdrobnionych zużytych płyt obwodów drukowanych. Ponadto D.F. przygotował r*ysunek 1* i *tabele 1 – 3*.

M3. ***Evaluation of the efficiency of metal recovery from printed circuit boards using gravity processes.***

Franke D., Suponik T., Nuckowski P., Dubaj J.,
Physicochemical Problems of Mineral Processing, vol. 57, nr 4, 2021, s. 63-77, DOI:10.37190/ppmp/138471,
(MEiN=70, IF=1,047)

D.F. był odpowiedzialny za zaplanowanie i przeprowadzenie badań zastosowania grawitacyjnych metod separacji do rozdziału metali od tworzyw sztucznych z rozdrobnionych zużytych płyt obwodów drukowanych. D.F. zbadał możliwość wykorzystania stołu koncentracyjnego i laboratoryjnego separatora cyklofluidalnego oraz wykonał analizę mikroskopową i gęstości właściwej otrzymanych produktów separacji. Ponadto D.F. był odpowiedzialny za projekt i wykonanie podajnika, umożliwiającego podawanie nadawy w sposób jednorodny. Autor przygotował *rysunki 1 – 3, 7* oraz *tabele 1 – 4*.

M4. ***Evaluation of the use of flotation for the separation of ground printed circuit boards.***

Franke D., Kar U., Suponik T., Siudyga T.,

Gospodarka Surowcami Mineralnymi – Mineral Resources Management, Polska Akademia Nauk, vol. 38, nr 1, 2022, s. 171-188, DOI:10.24425/gsm.2022.140605,

(MEiN=100 punktów, IF=0,938)

D.F. był odpowiedzialny za zaplanowanie i przeprowadzenie badań flotacji rozdrobnionych zużytych płyt obwodów drukowanych. D.F. wykonał analizę mikroskopową oraz gęstości właściwej otrzymanych produktów separacji. Ponadto autor przygotował *rysunki 1 – 3* oraz *tabele 1 – 3* i *7*.

M5. ***Recycling of waste printed circuit boards – application potential and selection of eco-efficient methods.***

Franke D., Suponik T.,

Journal of Cleaner Production, Elsevier (manuskrypt w trakcie recenzji)

(MEiN=140, IF=11,1)

D.F. był odpowiedzialny za przygotowanie przeglądu literaturowego, porównanie pod względem aspektów środowiskowych i technologicznych metod chemicznych oraz fizycznych stosowanych podczas recyklingu zużytych płyt obwodów drukowanych. Autor dokonał oceny procesów jednostkowych technologii ze szczególnym uwzględnieniem ich oddziaływania na człowieka i środowisko przyrodnicze, parametrów technicznych oraz kosztów inwestycyjnych i eksploatacyjnych. Ponadto D.F. opracował *tabele 1 – 2* i *rysunki 1 – 5*.

M6. ***Morphology, phase and chemical analysis of leachate after bioleaching metals from printed circuit boards***

Hyra K., Nuckowski P., Willner J., Suponik T., **Franke D.**, Pawlyta M., Matus K., Kwaśny W.,

Materials, MDPI, vol. 15, nr 13, 2022, 4373, s. 1-17, DOI:10.3390/ma15134373,

(MEiN=140, IF=3,4)

D.F. był odpowiedzialny za przygotowanie i przeprowadzenie eksperymentu bioługowania półproduktu pochodzącego z separacji elektrostatycznej rozdrobnionych zużytych płyt obwodów drukowanych. Autor przeprowadził i koordynował badania bioługowania przy użyciu dwóch szczepów bakterii *Acidithiobacillus ferrooxidans* i *Acidithiobacillus thiooxidans* w kontrolowanych warunkach laboratoryjnych, osobno dla każdego szczepu bakterii. Wyniki badań przedstawiono również w raporcie PBL i publikacji pt. *Odzysk metali z odpadów elektronicznych,* PM NEWS PM News, nr 23, 2020, s. 25.

Lista zgłoszeń patentowych

P1. ***Sposób rozdziału metali od tworzyw sztucznych z płyt obwodów drukowanych***
Franke D., Suponik T.,
zgłoszenie patentowe nr. P.438999, Urząd Patentowy Rzeczypospolitej Polskiej, 21.09.2021
D.F. był odpowiedzialny za integrację komponentów wynalazku w skali laboratoryjnej oraz współautorstwo opisu zgłoszenia patentowego.

Lista pozostałych publikacji

Publikacje z zakresu tematyki rozprawy doktorskiej:

O1. ***Physical processing in waste printed circuit boards recycling: current state of research***

Franke D., Suponik T., Nuckowski P.,

w *Global challenges for a sustainable society. EURECA-PRO. The European university for responsible consumption and production*, Springer Proceedings in Earth and Environmental Sciences, Springer. J. Benítez-Andrades, P. García-Llamas, Á. Taboada, L. Estévez-Mauriz, R. Baelo, Red. 2023, s. 51-57.

(MEiN=20)

D.F. był odpowiedzialny za przygotowanie publikacji, w której przedstawiono podsumowanie wyników prac badawczych dot. separacji metali z rozdrobnionych płyt obwodów drukowanych za pomocą metod fizycznych, tj. separacji elektrostatycznej, separacji grawitacyjnej i flotacji.

O2. ***Przegląd piśmiennictwa z zakresu gospodarowania elektroodpadami oraz metod odzysku metali z płyt obwodu drukowanego (PCB)***

Hyra K., Nuckowski P., Kwaśny W., Suponik T., **Franke D.**,

w *Interdyscyplinarne badania młodych naukowców*, Wydawnictwo Politechniki Śląskiej, B. Balon, Red. 2023, s. 136–164.

(MEiN=20)

D.F. był odpowiedzialny za opis badań separacji elektrostatycznej oraz opracowanie *rysunku 9*. Publikacja przedstawia stosowane procesy recyklingu zużytych płyt obwodów drukowanych oraz podkreśla potrzebę holistycznego projektowania technologii recyklingu, zwracając uwagę na aspekty gospodarcze, ekonomiczne i środowiskowe.

O3. ***Metals recovery from e-scrap using gravity, electrostatic and magnetic separations.***

Franke D., Suponik T.,

Innovative Mining Technologies: IMTech 2019 Scientific and Technical Conference, 25-27 Marca 2019, Szczyrk, Polska, IOP Conference Series: Materials Science and Engineering, nr 545, 2019, IOP Publishing, art. no. 012016 1-9, DOI:10.1088/1757-899X/545/1/012016,

(MEiN=20)

D.F. był odpowiedzialny za przeprowadzenie badań separacji elektrostatycznej, magnetycznej i grawitacyjnej w cieczy ciężkiej rozdrobnionych płyt obwodów drukowanych. W publikacji przedstawiono ocenę możliwości zastosowania powyższych metod, w celu wyboru komponentów eko-efektywnej technologii recyklingu zużytych płyt obwodów drukowanych.

O4. ***Electrostatic and magnetic separations for the recovery of metals from electronic waste.***

Suponik T., **Franke D.**, Nuckowski P.,

Mineral Engineering Conference: MEC 2019, 16-19 Września 2019, Kocierz, Beskid Mały, Poland, IOP Conference Series: Materials Science and Engineering, nr 641, 012017, 2019, IOP Publishing, s. 1-8, DOI:10.1088/1757-899X/641/1/012017,

(MEiN=20)

D.F. przeprowadził analizę granulometryczną i separację elektrostatyczną rozdrobnionych płyt obrodów drukowanych. Autor był odpowiedzialny za opracowanie publikacji, w której przedstawiono wyniki separacji elektrostatycznej w wyselekcjonowanych klasach ziarnowych oraz wyniki analizy składu fazowego otrzymanych produktów.

O5. ***Gospodarka obiegu zamkniętego: Odzysk metali z płyt obwodów drukowanych.***

Willner J., Fornalczyk A., Saternus M., **Franke D.**, Suponik T., Turek M., Dydo P., Jakóbik-Kolon A., Kluczka J., Mitko K.,

w *Ochrona klimatu i środowiska, nowoczesna energetyka*: Praca zbiorowa pod red. Werle S., Ferdyn-Grygierek J., Szczygieł M., Monografia, Politechnika Śląska, vol. 909, 2021, Politechnika Śląska, ISBN 978-83-7880-790-2, s. 71-102,

(MEiN=20)

D.F. był odpowiedzialny za opracowanie rozdziału *3.3. Odzysk metali z płyt obwodów drukowanych*, w którym przedstawiono problem oraz potencjał ekonomiczny recyklingu tego typu odpadów.

O6. ***Odzysk metali z odpadów elektronicznych.***

Suponik T., Nuckowski P., Willner J., ***Franke D.***, Hyra K., Polak J., Lewandowski D., Gaweł M.,

w *PM News: Czasopismo Koła Zarządzania Projektami SOLVER*, nr 23, 2020, s. 25

D.F. opracował rozdział pt. *Odzysk metali z odpadów elektronicznych.* Publikacja przedstawia podsumowanie badań separacji elektrostatycznej rozdrobnionych płyt obrodów drukowanych, przeprowadzonych w ramach realizacji projektu nr. POWR-03.05.00-00-Z098/17-00.

Publikacje spoza zakresu tematyki rozprawy doktorskiej:

O7. ***Influence of citrus fruit waste filler on the physical properties of silicone-based composites.***
Mrówka M., **Franke D.**, Ošlejšek M., Jureczko M.
Materials, MDPI, vol. 16, nr 19, 2023; 6569, s. 1-15, DOI:10.3390/ma16196569,
(MEiN=140, IF=3,4)

O8. ***Prediction and Potential Treatment of Underground Contaminated Water Based on Monitoring of pH and Salinity in a Coal Mine Waste Heap, Southern Poland.***
Suponik T., **Franke D.**, Neculita C., Mzyk T., Frączek R.,
Minerals, MDPI, vol. 12, nr 4, 2022, 391, s. 1-17, DOI:10.3390/min12040391,
(MEiN=100, IF=2,818)

O9. ***A study on the hard coal grindability dependence on selected parameters.***
Kogut K., Cablik V., Matusiak P., Kowol D., Suponik T., **Franke D.**, Tora B., Pomykała R.,
Energies, vol. 14, nr 23, 2021, 8158, s. 1-9, DOI:10.3390/en14238158,
(MEiN=140, IF=3,252)

O10. ***Selective crushing of run-of-mine as an important part of the hard coal beneficiation process.***
Matusiak P., Kowol D., Suponik T., **Franke D.**, Nuckowski P., Tora B., Pomykała R.,
Energies, vol. 14, nr 11, 2021, 3167, s. 1-15, DOI:10.3390/en14113167,
(MEiN=140, IF=3,252)

O11. ***The impact of precipitation on the groundwater of coal waste dump.***
Suponik T., **Franke D.**, Frączek R., Nowińska K., Pierzyna P., Różański Z., Wrona P.,
Journal of Sustainable Mining, vol. 20, nr 1, 2021, 5, s. 11-19, DOI:10.46873/2300-3960.1031,
(MEiN=70)

O12. ***The testing of waste from the installation of salt debris leaching.***
Suponik T., Pierzyna P., **Franke D.**, Adamczyk Z.,
Mineral Engineering Conference: MEC 2018, 26-29 Wrzesień 2018, Zawiercie, Poland: Lutyński M., Suponik T. (red.), IOP Conference Series: Materials Science and Engineering, nr 427, 2018, IOP Publishing, art. nr 012040, s. 1-9, DOI:10.1088/1757-899X/427/1/012040,
(MEiN=20)

O13. ***Zrównoważone certyfikowane budynki.***
Franke D., Kuczera A.,
Polskie Stowarzyszenie Budownictwa Ekologicznego PLGBC, 2023

O14. ***Certyfikacja zrównoważonych budynków w Polsce.***
Franke D.
Real Estate Magazine 3/2023, 2023

1 Wprowadzenie

Szybki rozwój światowych gospodarek przyczynił się do nadmiernego zużycia zasobów naturalnych, a wraz z rozwojem nowych technologii wzrasta zapotrzebowanie na niektóre surowce krytyczne, których złoża są ograniczone i mogą w bliskiej przyszłości ulec wyczerpaniu. Powodem tego był ówcześnie funkcjonujący model gospodarczy, który polegał na wydobyciu materiałów, produkcji dóbr, ich użytkowaniu, a następnie po utracie wartości użytkowej pozbyciu się ich, nie uwzględniając dalszego przetwarzania w celu pozyskania surowców wtórnych. Takie postępowanie spowodowało, że surowce, nawet te wartościowe, stawały się odpadami [1]. Głównymi czynnikami przyczyniającymi się do tego zjawiska były przede wszystkim aspekty ekonomiczne, ale także brak zaawansowanych technologii i systemów zarządzania odpadami [2] oraz brak regulacji prawnych nakazujących lub zachęcających do odpowiedniego gospodarowania odpadami. Zmiana starego liniowego modelu ekonomicznego rozpoczęła się w erze rosnących cen energii i dostrzeżenia problemu wyczerpujących się złóż. Zaczęto wdrażać do różnych gałęzi gospodarek nowy model biznesowy, którego celem jest wydłużenie cyklu życia surowców przy jednoczesnym zachowaniu ich wartości rezydualnej [1,3]. Model ten został określony mianem gospodarki o obiegu zamkniętym, której wdrożenie jest niezbędne dla zapewnienia bezpieczeństwa surowców. Ponadto ta nowa koncepcja daje szanse na obniżenie śladu środowiskowego produktów i tym samym uznaje się ją za zgodną z zasadami zrównoważonej produkcji [4].

Współcześnie rozwijającym się sektorem gospodarki, charakteryzującym się znacznym wzrostem i nieustannym zapotrzebowaniem na metale ziem rzadkich oraz inne wartościowe pierwiastki, jest przemysł elektryczny i elektroniczny. Od końca XX wieku sektor ten dynamicznie poszerza swoje możliwości i stanowi kluczowy filar współczesnej gospodarki, odgrywając istotną rolę w wielu dziedzinach życia społecznego i technologicznego postępu. Wraz z ilością wyprodukowanych urządzeń wzrasta liczba zużytych sprzętów elektrycznych i elektronicznych (ZSEE). Szacuje się, że jest to jeden z najszybciej rosnących strumieni odpadów. Według *United Nation Institute for Training and Research* w roku 2019 wygenerowanych zostało 53,6 Tg ZSEE, których wartość wynosiła 57 mld USD. Szacuje się, że strumień tych odpadów w 2030 r. wzrośnie do 74,7 Tg, a w 2050 r. aż do 110 Tg [5]. Niewłaściwe magazynowanie lub przetwarzanie ZSEE stanowi zagrożenie dla zdrowia ludzi i może być przyczyną degradacji środowiska przyrodniczego. Szybko rosnąca ilość ZSEE staje się więc obecnym wyzwaniem, szczególnie dla firm odzyskujących z nich wartościowe substancje.

Istotnym aspektem wpływającym na zwiększającą się ilość ZSEE była pandemia COVID-19 [6]. Masowe przejścia na zdalną pracę i naukę spowodowały gwałtowny wzrost popytu na produkty elektroniczne. Zmieniła się również aktywność rekreacyjna, przybierając częściej formę cyfrową, która niejednokrotnie wymaga zakupu nowych urządzeń takich jak telewizory, komputery osobiste,

konsole do gier lub innego sprzętu służącego do rekreacji. [7]. Świadczą o tym m.in. wzrosty sprzedaży komputerów o ponad 11,2% [8] oraz konsol do gier o 155% w roku 2020 [9]. Pandemia COVID-19 była również przyczyną ograniczonej dostępności produktów elektronicznych, co może stanowić doskonały przykład odpowiedzi gospodarki na brak wystarczającej ilości zasobów [1]. Zwiększony popyt na urządzenia elektroniczne spowodował konieczność zwiększenia produkcji, a wprowadzone obostrzenia wprowadziły zakłócenia w niemal wszystkich początkowych etapach cyklu życia urządzeń elektronicznych. Deficyty materiałów rozpoczęły się już na poziomie wydobycia surowców, bowiem niektóre z działalności górniczych zaopatrujących gospodarkę w metale zmniejszyły swoje wydobycie. Niedobór surowców i zmniejszona dostępność siły roboczej były z kolei główną przyczyną przestojów w produkcji urządzeń elektronicznych. Nie należy również zapominać o problemach logistycznych związanych z wprowadzaniem na rynek już gotowych wyrobów, tj. zakłócenia w transporcie lub punktach sprzedaży [7]. Tym samym powszechnie dostępny produkt stał się wyrobem wyłącznie na zamówienie z długim okresem oczekiwania. Wobec powyższego braki dostępności zasobów mogą spowodować znaczące przeszkody w prawidłowym funkcjonowaniu gospodarek. Dlatego niezwykle istotne jest zamykanie obiegów surowców w gospodarkach, szczególnie tych ubogich w zasoby metali stanowiących podstawę rozwoju nowych technologii [10].

Szacuje się, że w krajach Unii Europejskiej (UE) strumień ZSEE wzrasta średnio o około 2% w skali roku. W Polsce ilość zebranych odpadów jest ściśle powiązana z ilością sprzętu wprowadzonego do obiegu w poprzedzającym roku (Rys. 1.1). Na polski rynek w roku 2018 wprowadzono 660 437 Mg sprzętu elektronicznego oraz zebrano 255 625 Mg ZSEE, co stanowi ok. 39% masy wprowadzonych do obiegu urządzeń [11]. Wobec tego szacuje się, że w roku 2030 ilość ZSEE zwiększy się do około 320 000 Mg, co będzie stanowić wyzwanie dla firm zajmujących się przetwarzaniem tego typu odpadów.

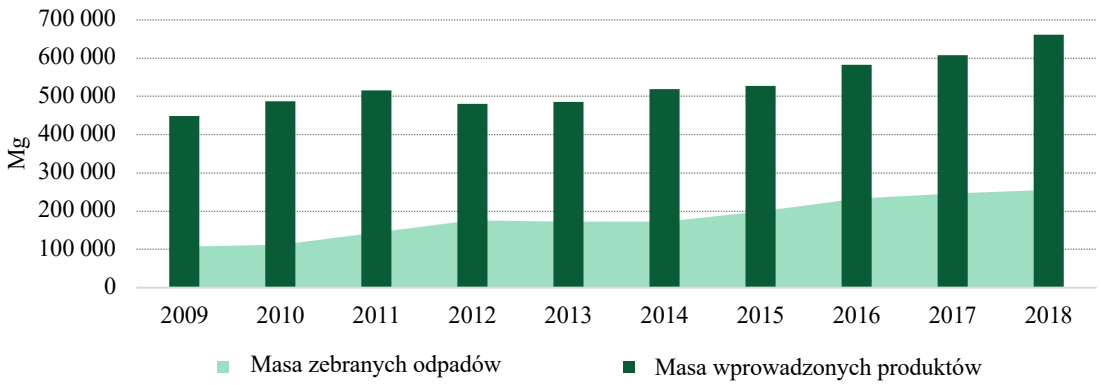

Rysunek 1.1. Ilość wprowadzonego na rynek sprzętu elektronicznego oraz zebranego ZSEE w Polsce w latach 2009 - 2018 [11].

Fundamentalnym elementem niemal wszystkich urządzeń elektronicznych są płyty obwodów drukowanych (ang. *Printed Cicruit Boards*, PCB). Stanowią one nieodzowną podstawę elektroniki, pełniąc istotną funkcję w prawidłowym funkcjonowaniu i integracji komponentów elektronicznych. PCB zawierają duże ilości metali takich jak: Cu, Fe, Al, Sn, pierwiastki ziem rzadkich, Ta, Ga i innych z grupy lantanowców oraz metale szlachetne Au, Ag i Pd [12]. W składzie PCB można znaleźć również metale uznane za niebezpieczne dla zdrowia i życia ludzi oraz środowiska przyrodniczego, takie jak Cr, Pb, Be, Hg, Cd, Zn, Ni [13,14]. Wartym podkreślenia jest również fakt, że stężenia metali zawartych w PCB są dziesiątki, a nawet setki razy wyższe niż w wydobywanych rudach [15].

Płyty obwodów drukowanych zbudowane są z dielektrycznych materiałów kompozytowych (laminatów), które zostały pokryte metalicznymi ścieżkami, zazwyczaj z miedzi, i zawierają punkty lutownicze bądź elementy kontaktowe wykonane z metali lub ich stopów, tj. In, Ga, Fe, Cu, Ag, Au, Pt, Be, Al, An, Pb, Cd, Sn – Pb, Ag – Pb – Sn, Sn – Sb, Be – Sn i In – Sn [16]. W zależności od roku produkcji, przeznaczenia i producenta, laminat PCB może być wykonany z różnych materiałów i posiadać określoną sztywność. Laminat zbudowany jest z minimum dwóch warstw: miedzi i materiału dielektrycznego. Najczęściej jednak jest wielowarstwowy, w którym liczba warstw miedzi jest zwykle parzysta. Zakres i skład materiałów wykorzystywanych do produkcji PCB określa *National Electrical Manufacturers Association*, która wprowadziła również klasyfikację opartą o następujące parametry: niepalność, pochłanianie wilgoci oraz stabilność w wysokiej temperaturze. Klasyfikacja ta standaryzuje laminaty najczęściej według klas łatwopalności od 1 do 5 (ang. *flame resistance*, FR), przy czym 1 oznacza najmniejszą odporność, a 5 największą [10].

Z uwagi na doskonałe parametry, zarówno mechaniczne, jak i elektryczne, najczęściej spotykaną klasą PCB jest FR-4, której laminat wykonany jest z włókna szklanego i żywicy epoksydowej. Szacuje się, że około 35% masy FR-4 stanowią metale, głownie takie jak Cu, Sn, Zn, Fe, Al, Ni i śladowe ilości Au, Ag, Pd oraz Pd (Rys. 1.2). Wśród nich najwartościowszymi metalami są złoto, pallad, srebro i miedź. Odzysk tych metali może przynieść znaczące korzyści ekonomiczne podmiotom zajmującym się ich odzyskiem [17]. Recykling zużytych płyt obwodów drukowanych (ang. *Waste Printed Circuit Boards*, WPCB) jest zatem konieczny z uwagi na ochronę zasobów naturalnych i bezpieczeństwo surowców. Potwierdza to opracowany przez *Royal Society of Chemistry* wskaźnik ryzyka dostaw surowców, który ocenia problemy z dostępnością surowców w przyszłości. Przy określaniu indeksu przeanalizowano takie czynniki jak: zasobność skorupy ziemskiej, rozmieszczenie i ilość rezerw, koncentrację produkcji, zastępowalność, stopień recyklingu i stabilność polityczną. Większość metali, z których składają się PCB, posiada indeks powyżej sześciu w 10-punktowej skali, gdzie 1 oznacza bardzo niskie ryzyko dostaw, a 10 bardzo wysokie (Rys. 1.2).

Metal	Zawartość w WPCB, %	Szacunkowa wartość metali w 1 Mg WPCB, USD	Wskaźnik ryzyka dostaw ⓘ
Cu	6 – 27	507 – 2 280	4,3
Al	2,0 – 7,2	48 – 171	4,8
Pb	1 – 4,2	23 – 93	6,2
Zn	0,2 – 2,2	6 – 66	4,8
Ni	0,3 – 5,4	91 – 1 643	6,2
Sn	1 – 5,6	247 – 1 385	6,7
Ag	0,011 – 0,45	84 – 3 446	6,2
Au	0,025 – 0,205	14 516 – 119 034	5,7
Pd	0,005 – 0,4	2 868 – 229 428	7,6
Pt	0,0005 –0,003	164 - 984	7,6
Σ	10,54 – 52,66	18 553 – 358 531	-

ⓘ Relatywne ryzyko dostaw: 1 (bardzo małe ryzyko) - 10 (bardzo duże ryzyko).

Rysunek 1.2. Szacunkowa zawartość metali w obwodach drukowanych i ich wartość monetarna oraz współczynnik ryzyka dostaw [13,18,19] **(M5)**.

Jak podaje Główny Inspektor Środowiska w raporcie o funkcjonowaniu systemu gospodarki zużytym sprzętem elektrycznym i elektronicznym, w roku 2017 zebrano 33 493 Mg zużytego sprzętu informatycznego i telekomunikacyjnego [21]. Szacuje się, że masa WPCB w tej grupie odpadu stanowi około 3% [5]. Wobec tego można przypuszczać, że w roku 2017 w Polsce zebrano około 1 005 Mg WPCB. Biorąc pod uwagę średnie zawartości metali w WPCB i ich cenę, wartość zebranych WPCB wynosiła ok. 95 254 609 USD, dlatego rynek WPCB w Polsce stanowi znaczną perspektywę rozwoju dla firm **(M5)**.

Należy mieć na uwadze, że wpływ na środowisko nieodpowiedniego recyklingu WPCB może być większy niż w przypadku wydobycia metali ze złóż [20]. Dlatego w celu ochrony środowiska przyrodniczego, WPCB powinny być przetwarzane zgodnie z zasadami gospodarki o obiegu zamkniętym i zrównoważonej produkcji. Zasady te powinny zostać wdrożone już na etapie projektowania technologii recyklingu, która powinna być efektywna i charakteryzować się niskim oddziaływaniem na środowisko oraz nie przyczyniać się do zubożania zasobów naturalnych. Technologię, która uwzględnia powyższe kryteria, można określić jako eko-efektywną. Za najważniejszą i jedną z pierwszych definicji pojęcia eko-efektywności w kontekście technologii

uznaje się za tę opracowaną w 1993 r. przez World Business Council for Sustainable Development., która brzmi:

„*Wytwarzanie dóbr i usług konkurencyjnych cenowo, spełniających potrzeby ludzkie i podnoszących jakość życia z równoczesną redukcją oddziaływania na środowisko i zachowaniem zużycia surowców naturalnych na poziomie dostosowanym do możliwości Ziemi*" [21].

Wdrożenie zasad eko-efektywności w projektowaniu technologii recyklingu WPCB może przyczynić się m.in. do obniżenia zużycia materiałów, zmniejszenia ilości odpadów i ograniczenia emisji, a w efekcie zwiększenia konkurencyjności i wizerunku firm poprzez zastosowanie zrównoważonych rozwiązań oraz postępu w zakresie ochrony środowiska [22]. W związku z powyższym opracowanie eko-efektywnej technologii recyklingu WPCB stanowi ogromny potencjał dla podmiotów zajmujących się przetwarzaniem odpadów elektronicznych, jak również szansę redukcji wpływu na środowisko wynikającej z zastosowania niskoemisyjnych technologii recyklingu oraz z pozyskania metali ze źródeł wtórnych i ograniczenia ich wydobywania z zasobów naturalnych.

2 Przegląd metod recyklingu zużytych płyt odwodów drukowanych

Z uwagi na skomplikowaną budowę WPCB, ich recykling jest procesem złożonym i wymaga podjęcia działań przygotowawczych. Najważniejszym z nich jest demontaż, który polega na usunięciu z powierzchni WPCB komponentów możliwych do ponownego użycia lub zawierających toksyczne substancje. W zależności do przyjętej metody recyklingu z WPCB usuwane są również elementy, których występowanie mogłoby zakłócić dalsze procesy. Przygotowane w ten sposób WPCB mogą być skierowane do procesów odzysku surowców, które mogą być prowadzone za pomocą metod chemicznych, metod fizycznych opartych wyłącznie na oddziaływaniach mechanicznych lub metod mieszanych. Do metod chemicznych zaliczyć można hydrometalurgię i bio-hydrometalurgię, pirometalurgię i plazmę, natomiast wśród metod fizycznych wyróżnia się m.in. separację elektrostatyczną, magnetyczną, grawitacyjną i niezbędne w tym przypadku metody dezintegracji i rozdrabniania [23]. Powyższe metody charakteryzują się indywidualnymi cechami, które determinują sposób oddziaływania na środowisko (Rys. 2.1.)**(M5)**.

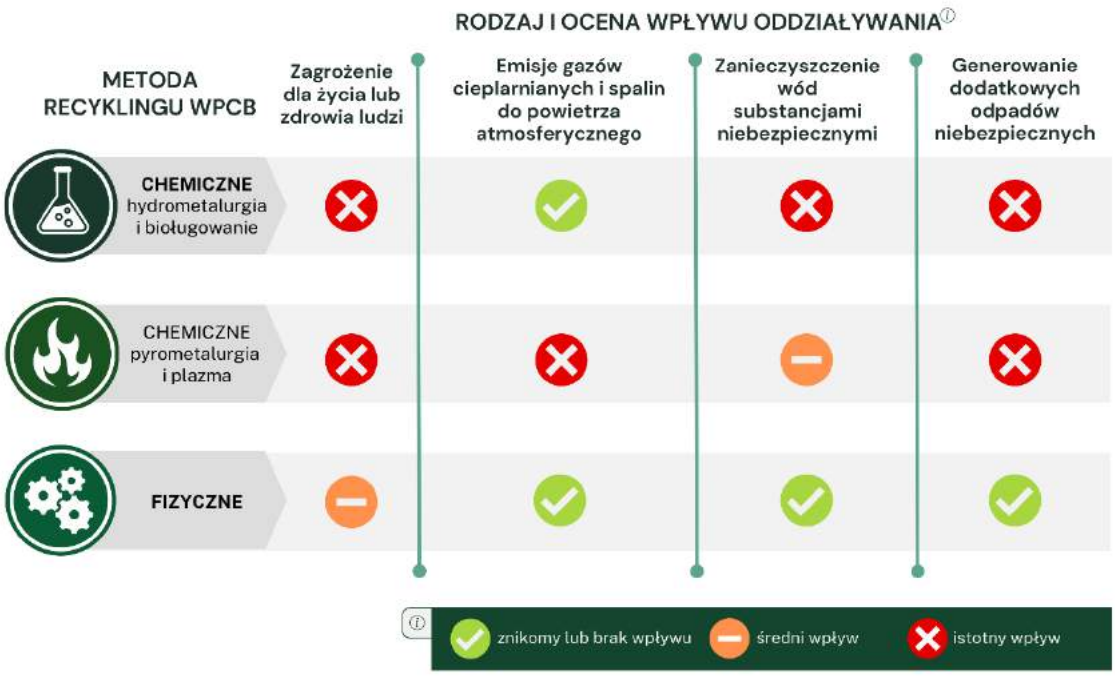

Rysunek 2.1. Rodzaj i ocena wpływu oddziaływania na środowisko przyrodnicze głównych metod recyklingu WPCB **(M5)**

Za najczęściej stosowaną metodą chemiczną stosowaną w recyklingu WPCB uznaje się hydrometalurgię [24], w której wykorzystuje się toksyczne związki chemiczne takie jak cyjanki, halogenki, tiomocznik, tiosiarczany i in. negatywnie wpływające na środowisko przyrodnicze. Mimo że metoda ta należy do jednej z nielicznych pozwalających na niemal pełny rozdział i odzysk metali, jest jednocześnie jedną z najbardziej obciążających środowisko [25]. Wariantem tej metody jest biohydrometalurgia, w której wykorzystuje się mikroorganizmy jako katalizatory procesu. Do odzysku metali najczęściej stosuje się szczep bakterii *Acidithiobacillus ferrooxidans*, za pomocą którego, w kontrolowanych warunkach, możliwe jest roztworzenie metali zawartych w WPCB **(M6)**. Jednakże z uwagi na mechanikę procesu i jego stosunkowo niewielką wydajność, biohydrometalurgia jest zwykle stosowana jako metoda pomocnicza [26–28]. Kolejną powszechnie stosowaną metodą chemiczną jest pirometalurgia [29], która pomimo relatywnej dużej szybkości procesu, jest pod względem inwestycyjnym i procesowym metodą drogą. Ponadto, pirometalurgia znacząco oddziałuje na środowisko przyrodnicze, głównie poprzez emisję pyłów i gazów do atmosfery oraz generowanie odpadów przemysłowych [30]. W tym przypadku konieczne jest wykorzystanie instalacji oczyszczania spalin, co zmniejsza opłacalność recyklingu WPCB [31]. Wśród metod polegających na rozkładzie termicznym wyróżnić można również technologie plazmowe, które charakteryzują się mniejszym wpływem na środowisko, jednakże większą energochłonnością procesu recyklingu [32]. Istotnym aspektem stosowania metod chemicznych jest utrata części niemetalicznych WPCB. Występujące w laminacie tworzywa sztuczne i włókno szklane ulegają przemianom w reakcjach chemicznych lub zanieczyszczeniu innymi substancjami, w wyniku czego stanowią odpad lub są źródłem emisji do środowiska **(M5)**.

W przeciwieństwie do powyższych, metody oparte o oddziaływania mechaniczne charakteryzują się mniejszym wpływem na środowisko przyrodnicze [33,34]. Recykling prowadzony w ten sposób umożliwia odzyskanie wartościowych substancji (metali) i wykorzystanie pozostałych (włókna szklanego i tworzyw sztucznych) do wytwarzania nowych produktów. Tym samym metody fizyczne stanowią szanse na niemal bezodpadowy recykling WPCB. Niemetaliczna część rozdrobnionego laminatu WPCB nie ulega zmianom chemicznym, co stwarza szerokie możliwości zastosowania, np. do produkcji materiałów kompozytowych. Należy jednak zaznaczyć, że zastosowanie metod fizycznych nie umożliwia pełnego odzysku, czyli pozyskania metali w postaci indywiduum (Rys. 2.2). Otrzymuje się mieszaninę metali uwolnioną od części niemetalicznych, z której na drodze przemian chemicznych można produkować poszczególne metale na zerowym stopniu utlenienia. Z uwagi na dobrze rozwinięty przemysł metalurgiczny w Polsce, możliwe jest przekazanie mieszaniny metali pochodzącej z odzysku PCB do istniejących już instalacji produkcji lub odzyskiwania metali.

Jednym z najważniejszych procesów poprzedzających metody separacji jest rozdrabnianie, którego celem jest uwolnienie metali od pozostałych części WPCB. Niewłaściwe rozdrobnienie WPCB

powoduje pewną losowość we właściwościach fizycznych ziaren, co jest główną przyczyną niepoprawnej separacji i tym samym przenikania ziaren do niewłaściwych produktów. Dlatego odpowiednie uwolnienie metali od pozostałych elementów niemetalicznych jest kluczowe do uzyskania wysokiej sprawności separacji. Rozdrabnianie WPCB najczęściej obejmuje dwa etapy. Pierwszy z nich polega na zmniejszeniu rozmiaru WPCB za pomocą dezintegratora do wymiarów nieprzekraczających ok. 5 cm [35,36]. Kolejnym krokiem jest zmielenie wstępnie rozdrobnionych WPCB przy użyciu młynów młotkowych [37–39] lub nożowych [36]. Uzyskany w ten sposób proszek WPCB stanowi nadawę na procesy separacji.

W procesach recyklingu WPCB opartych na metodach fizycznych zazwyczaj stosuje się metody kombinowane składające się z kilku procesów separacji. Wynika to w głównej mierze z zakresu oddziaływań poszczególnych metod, ograniczających się zazwyczaj do jednej właściwości materiału poddawanego separacji, np. właściwości magnetycznych, gęstości właściwej, hydrofobowości lub zdolności gromadzenia ładunków powierzchniowych. Metody te łączy się ze sobą etapowo lub warunkowo w zależności od klasy ziarnowej albo innej właściwości fizycznej materiału.

Najczęściej stosowaną metodą fizyczną w recyklingu WPCB jest separacja elektrostatyczna [13,40–42], w której rozdział jest możliwy dzięki występowaniu różnic w przewodności elektrycznej materiałów budujących WPCB [43]. Separacja elektrostatyczna prowadzona jest na sucho, a najczęściej stosowanym urządzenia jest elektrodynamiczny separator bębnowy [44]. Z uwagi na występowanie dużego gradientu gęstości metali i tworzyw sztucznych do recyklingu WPCB stosuje się również metody grawitacyjne. Obejmują one rodzaje separacji prowadzone na sucho (np. cyklony, separatory pneumatyczne [45] i powietrzne stoły koncentracyjne [46]) oraz na mokro (np. stoły koncentracyjne [47,48], hydrocyklony [49] oraz metody polegające na fluidyzacji [50]). Zastosowanie poszczególnych rodzajów separacji grawitacyjnych jest ściśle uzależnione od wielkości ziaren nadawy. W recyklingu WPBC znalazła również zastosowanie flotacja, która możliwa jest dzięki występowaniu różnic we właściwościach hydrofobowych materiałów. W celu zapewnienia wysokiej wydajności flotacji konieczne jest użycie odczynników flotacyjnych często o toksycznych właściwościach [51]. Uzupełnieniem powyższych metod jest separacja magnetyczna, która pozwala oddzielić żelazo od pozostałych metali [47,52]. Jednakże z uwagi na właściwości magnetyczne tworzyw sztucznych i metali takich jak złoto, srebro i miedź, separacja magnetyczna nie jest stosowana jako samodzielna metoda [17].

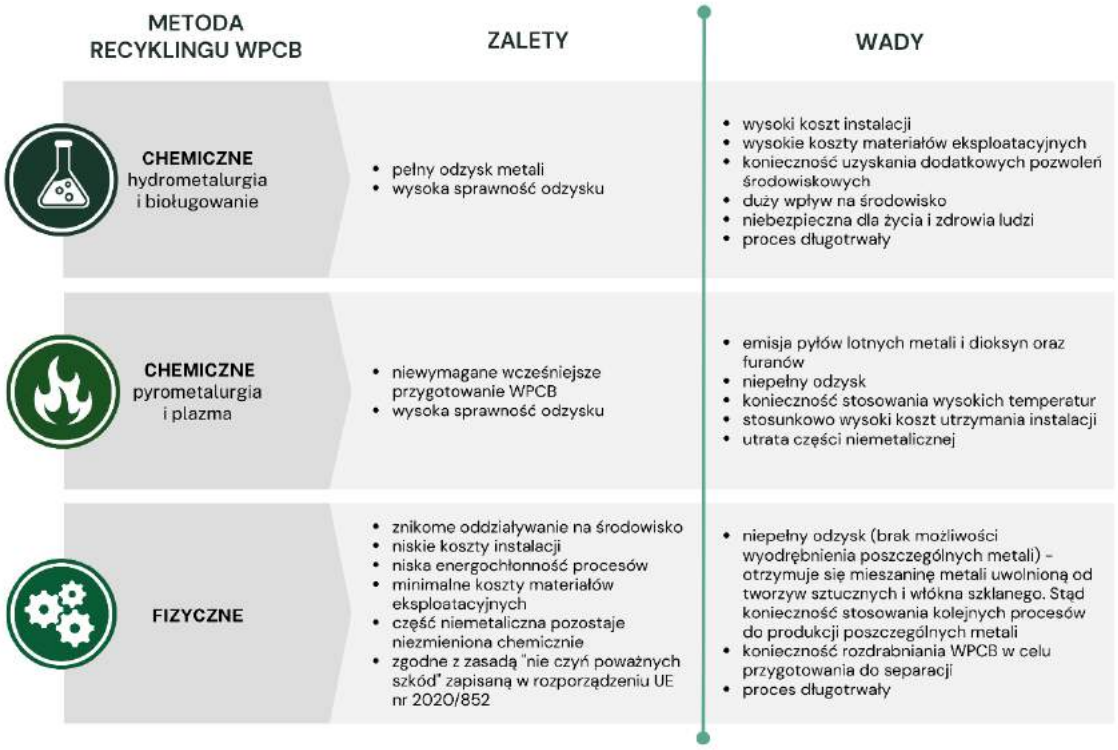

Rysunek 2.2. Podstawowe wady i zalety głównych metod recyklingu WPCB [24,25,31] **(M5)**

Wobec powyższego metody fizyczne stanowią szansę na opracowanie eko-efektywnej technologii recyklingu WPCB, która może być zgodna z zasadami zrównoważonego produkcji i gospodarki o obiegu zamkniętym. Metody fizyczne stanowią zatem duży potencjał do ograniczenia wpływu recyklingu WPCB na środowiskowo i efektywnego odzysku surowców.

3 Teza, cel i zakres rozprawy doktorskiej

3.1 Teza

Na podstawie przeglądu piśmiennictwa oraz dostępnych danych dotyczących polskiego rynku zajmującego się przetwarzaniem zużytego sprzętu elektrycznego i elektronicznego określono lukę badawczą w zakresie istniejących technologii recyklingu zużytych płyt odwodów drukowanych zgodnych z zasadami zrównoważonej produkcji i gospodarki o obiegu zamkniętym. Wobec powyższego sformułowano następującą tezę rozprawy: **istnieje możliwość opracowania i zastosowania eko-efektywnej technologii do recyklingu zużytych płyt obwodów drukowanych, która wykorzystuje procesy fizyczne z zakresu inżynierii mineralnej i jest zgodna z zasadami zrównoważonej produkcji i gospodarki o obiegu zamkniętym.**

3.2 Cel

Głównym celem rozprawy było eksperymentalne zweryfikowanie możliwości zastosowania znanych metod z zakresu inżynierii mineralnej, których zintegrowanie pozwoli opracować efektywną i ekonomicznie uzasadnioną technologię recyklingu zużytych płyt obwodów drukowanych zgodną z zasadami zrównoważonej produkcji i gospodarki o obiegu zamkniętym.

3.3 Zakres

W rozprawie doktorskiej zidentyfikowano i dobrano odpowiednie metody recyklingu zużytych płyt obwodów drukowanych prowadzące do uwolnienia metali od kompozytu WPCB. Następnie przeprowadzono badania eksperymentalne mielenia w młynie nożowym **(M1)** i zastosowano metody separacji fizycznej i fizykochemicznej z obszaru inżynierii mineralnej mające największy potencjał technologiczny. Należały do nich separacja elektrostatyczna za pomocą laboratoryjnego, bębnowego separatora elektrostatycznego **(M1, M2)**, separacja grawitacyjna przy użyciu laboratoryjnego stołu koncentracyjnego i separatora cyklofluidalnego **(M3)** oraz flotacja w laboratoryjnej maszynce flotacyjnej **(M4)**. Dla każdej z metod przeprowadzono analizę otrzymanych produktów rozdziału, oceniono efektywność procesu oraz jego wpływ na środowisko przyrodnicze i człowieka. Oszacowano również ewentualne koszty inwestycyjne i eksploatacyjne dla poszczególnych metod recyklingu **(M5)**. Ocenę wykonano ponadto dla procesu dezintegracji i pakowania produktów **(M5)**. W pracy zbadano również możliwość zastosowania bioługowania, przy użyciu bakterii *Acidithiobacillus ferrooxidans*, w celu odzysku metali z półproduktu otrzymanego w wyniku separacji elektrostatycznej **(M6)**. Na podstawie przeprowadzonych analiz opracowano eko-efektywną technologię recyklingu WPCB.

4 Metodyka badawcza

4.1 Przygotowanie zużytych płyt obwodów drukowanych do procesów rozdziału

W badaniach zastosowano płyty główne wyprodukowane przez Gigabyte, Intel, Nvidia, MSI, Asus w latach 2007-2009. Pierwszym etapem badań było oddzielenie z powierzchni WPCB komponentów, które mogłyby powodować trudności podczas dalszych procesów lub które zawierały toksyczne substancje. Komponenty te zostały zdemontowane z powierzchni płytek przy użyciu ręcznych narzędzi warsztatowych, takich jak śrubokręty, kombinerki i małe łomy do podważania. Oddzielone elementy obejmowały rezystory (zawierające: Ni, Cr, Cd, Al, Pb i Ta), tranzystory (Pb i Cu), baterie, chipy (Pb, Ni, Sn, Ga, Al i Ag), kondensatory (Sn, Cu i Zn), filtry zakłóceń elektromagnetycznych (Fe, Cu i Zn), złącza (Pb, Ni, Fe i Sn), śruby i gniazda wykonane z tworzyw sztucznych [53]. Następnie, ze względu na ograniczenia materiału wsadowego do młyna, oczyszczone WPCB zostały rozdrobnione w dezintegratorze na kawałki o wymiarach nieprzekraczających 1 × 1 cm.

Kolejnym krokiem badań był wybór efektywnego sposobu uwolnienia metali od pozostałych części WPCB za pomocą młyna nożowego LMN-100 (Testchem, Radlin, Polska) **(M1)**. Młyn ten posiada stalowe ostrza zamontowane na korpusie komory mielenia i rotatorze oraz wyposażony jest w sito, które umożliwia określenie wielkości zmielonego materiału. Mielenie zostało przeprowadzone przy prędkości 2815 obrotów na minutę i szczelinie pomiędzy nożami równej 0,5 mm. W celu określenia efektywnego poziomu rozdrobnienia i sposobu mielenia, w procesie tym zastosowano następujące różne warunki (warianty) procesu:

- wariant 1 – perforacja w sicie 1 mm, obciążenie młyna (wydajność podawania materiału na młyn) 5 g/min,
- wariant 2 – perforacja w sicie 1 mm, schładzanie nadawy ciekłym azotem, obciążenie młyna 20 g/min,
- wariant 3 – perforacja w sicie 2 mm, obciążenie młyna 10 g/min,
- wariant 4 – perforacja w sicie 3 mm, obciążenie młyna 10 g/min.

Podczas rozdrabniania WPCB nie dopuszczano do przeciążenia młyna, które mogłoby przyczynić się do powstania w komorze roboczej rozdrabniania temperatur powodujących tworzenie się konglomeratów – ziaren o stałych połączeniach metal-tworzywo sztuczne. W celu obserwacji tego zjawiska w wariantach zastosowano różne obciążenia młyna. W wariancie 2, kawałki WPCB zostały uprzednio umieszczone w zbiorniku YDS-5-200 (Cryogen, Drogomyśl, Polska) wypełnionego ciekłym azotem i schłodzone do temperatur kriogenicznych, a następnie zmielone w młynie nożowym, w sposób podobny jak w przypadku pozostałych wariantów. Kawałki WPCB

schładzano do momentu zakończenia wrzenia ciekłego azotu. Nadawę na procesy separacji stanowił produkt otrzymany z najefektywniejszego wariantu rozdrabniania.

4.2 Zastosowane metod separacji

W ramach przeprowadzonych badań postanowiono zastosować i ocenić wybrane metody zakresu inżynierii mineralnej charakteryzujące się odmiennymi sposobami oddziaływań fizycznych, aby wybrać i stworzyć z jej wykorzystaniem eko-efektywną technologię recyklingu**(M5)**. Rozdział metali od kompozytu WPCB przeprowadzono za pomocą czterech urządzeń laboratoryjnych o różnym sposobie oddziaływania, tj. bębnowego separatora elektrostatycznego **(M1 i M2)**, stołu koncentracyjnego, separatora cyklofluidalnego **(M3)** i maszynki flotacyjnej **(M4)**. Nadawę na urządzenia stanowił ten sam materiał, z którego wydzielono cztery próbki reprezentatywne. Dla wszystkich zastosowanych metod rozdziału została przeprowadzona optymalizacja parametrów separacji. Badania rozdrabniania oraz separacji zostały wykonane w Pracowni Recyklingu i Gospodarki o Obiegu Zamkniętym Wydziału Górnictwa, Inżynierii Bezpieczeństwa i Automatyki Przemysłowej Politechniki Śląskiej

Pierwszym zbadanym procesem rozdziału była separacja elektrostatyczna, która zachodzi dzięki różnicy w zdolnościach gromadzenia ładunku powierzchniowego i przewodności ziaren. Do separacji elektrostatycznej użyto laboratoryjnego bębnowego separatora elektrostatycznego (Boxmag-rapid, Aston, Birmingham, Wielka Brytania), którego konstrukcja umożliwia odbiór trzech produktów, tj. ziaren metali, konglomeratów i ziaren tworzyw sztucznych (Rys. 4.1.). Separację wykonano przy następujących parametrach: prędkość obrotowa wału 100 obr/min, napięcie 17 kV, odległość między elektrodą a bębnem 0,03 m **(M1, M2, P1)**.

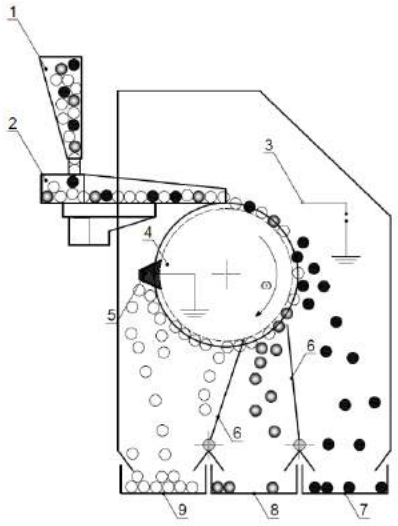

Rysunek 4.1. Schemat separatora elektrostatycznego: 1 – zasobnik nadawy, 2 – podajnik wibracyjny, 3 – elektroda, 4 – bęben obrotowy, 5 – szczotka, 6 – przegrody, 7 – pojemnik produktu przewodzącego, 8 – pojemnik półproduktu, 9 – pojemnik materiału nieprzewodzącego.

Kolejną zastosowaną metodą była separacja grawitacyjna **(M3)**, w której rozdział ziaren jest możliwy w przypadku występowania różnicy w gęstości ziaren. Z uwagi na szeroki zakres urządzeń i różnych konstrukcji w obrębie tego rodzaju separacji postanowiono zastosować dwa rodzaje separatorów oddziaływających na ziarna w odrębny sposób. W obu przypadkach separacja zachodziła w ośrodku wodnym. Pierwszym zastosowanym urządzeniem w ramach separacji grawitacyjnej był laboratoryjny stół koncentracyjny. W tym przypadku rozdział ziaren odbywa się na podłużnej, rowkowanej płycie roboczej, która jest nachylona o maksymalnie 10^{o} w kierunku poprzecznym do osi (Rys. 4.2.). Płyta wykonuje ruchy posuwisto-zwrotne, dzięki czemu podawane na powierzchnie płyty ziarna w postaci zawiesiny rozdzielane są względem ich gęstości wzdłuż płyty. Najlżejsze ziarna (tworzywa sztuczne) zostają najszybciej strącone z powierzchni płyty, natomiast najcięższe ziarna (metale) pokonują napór hydrostatyczny cieczy i zostaną przeniesione wzdłuż płyty w wyniku jej ruchów. W górnej części płyty umieszone są dysze natryskowe, które powodują zwiększenie efektywności procesu rozdziału. Parametry separacji były następujące: obciążenie stołu: 9 dm^3/min (zawiesina wody z materiałem), natężenie przepływu wody pierwszej dyszy 5,7 dm^3/min, natężenie przepływu wody drugiej dyszy 5,4 dm^3/min; skok stołu 1,5 mm, częstotliwość ruchu stołu 260 skoków/min, kąt nachylenia wzdłużnego 1^{o}, kąt nachylenia poprzecznego: 6^{o} **(M3)**.

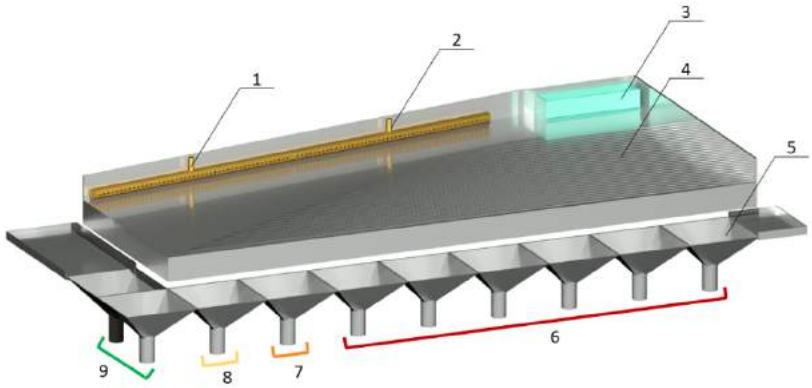

Rysunek 4.2. Schemat stołu koncentracyjnego: 1 – dysza I, 2 – dysza II, 3 – miejsce podawania nadawy, 4 – rowki płyty stołu, 5 – odbiorniki produktów, 6 – najlżejsze ziarna (tworzywa sztuczne), 7– półprodukt I, 8 – półprodukt II, 9 – koncentrat.

Drugim urządzeniem z zakresu metod grawitacyjnych był laboratoryjny separator cyklofluidalny (Rys. 4.3.), w którym rozdział zachodzi dzięki fluidyzacji ziaren w kierunku pionowym. Zasada działania laboratoryjnego separatora cyklofluidalnego odpowiada półprzemysłowemu separatorowi cyklofluidalnemu w kształcie litery „U" o ruchu ciągłym (zgłoszenie patentowe nr P.424161, Polska)[54]. W wyniku pionowych ruchów cieczy następuje rozdział ziaren według ich gęstości: najcięższe ziarna (metale) opadają na dno separatora, a najlżejsze są unoszone na jego powierzchnię. Separator ten wyposażony jest w zbiornik wypełniony wodą, w którym umieszczony jest cylinder. Cylinder, w którym znajduje się zawiesina z proszkiem WPCB, od dołu

zamknięty jest sitem o wielkości perforacji oczek wynoszącej 0,5 mm i wykonuje pionowy ruch posuwisto-zwrotny. Dzięki temu powstaje cykliczny napór cieczy w cylindrze i możliwy jest gęstościowy rozdział ziaren. Podczas tego procesu zastosowano następujące parametry: objętość wody 13 dm^3, skok cylindra 4 cm, częstotliwość ruchu cylindra 53 ruchy/min **(M3)**.

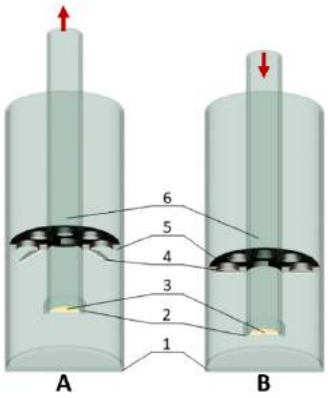

Rysunek 4.3. Schemat laboratoryjnego separatora cyklofluidalnego: A – położenie górne, B – położenie dolne, 1 – zbiornik cylindryczny ($Ø_{wew.}$ 19,5 cm), 2 – obejma sita, 3 – sito (wymiary oczek 0,5 x 0,5 mm), 4 – zawory, 5 – opaska, 6 – komora rozdziału (robocza): $Ø_{wew.}$ 5 cm **(M3)**.

Ostatnim zbadanym procesem separacji z zakresu inżynierii mineralnej była flotacja, która polega na rozdziale ziaren w wyniku różnic we właściwościach hydrofobowych. Proces flotacji zachodzi w wodzie, która poddana jest aeracji. Dzięki temu ziarna hydrofilne (metale), z uwagi na ich zdolność, „przylegają" do cząsteczek powietrza i unoszone są na powierzchnię zbiornika. Podczas flotacji możliwe jest stosowanie różnych odczynników flotacyjnych, które mogą powodować zmiany we właściwościach powierzchniowych ziaren lub tworzenie się stabilnej piany, w której będą utrzymywać się uniesione ziarna. Z uwagi na stosunkowo niską gęstość tworzyw sztucznych, która wynosi od 0,9 g/cm^3 do 3,5 g/cm^3, w badaniach zastosowano proces odwróconej flotacji **(M3)**.

Badania flotacji przeprowadzono przy użyciu laboratoryjnej maszyny flotacyjnej typu Mechanobr (Zakład Budowy Aparatury Instytutu Metali Nieżelaznych, Gliwice, Polska) przy użyciu litrowego zbiornika flotacyjnego. Pierwszym etapem był wybór odpowiedniego odczynnika chemicznego przy takiej samej zawartości materiału i wydatku powietrza, wynoszących odpowiednio 25 g/dm^3 i 200 dm^3/godz. Zbadano możliwości zastosowania odczynników flotacyjnych takich jak: kwas taninowy (w stężeniu 60mg/dm^3), glikol dipropylenowy (450 mg/dm^3), 2-oktanol (450 mg/dm^3) i ich kombinacji. Następnie po wyborze najefektywniejszego wariantu zbadano kolejno wpływ stężenia odczynnika flotacyjnego, wydatku poddawanego powietrza i ilości materiału. We wszystkich testach prędkość obrotowa rotatora w zbiorniku flotacyjnym oraz czas flotacji pozostawały stałe i wynosiły odpowiednio 400 obr./min i 5 minut.

Dla otrzymanych półproduktów zawierających ziarna konglomeratów, które charakteryzują się silnymi wiązaniami pomiędzy metalami i tworzywami sztucznymi, postanowiono zastosować alternatywną metodę. Z uwagi na trudność ponownego rozdrobnienia ziaren konglomeratu,

oceniono możliwość zastosowania metody chemicznej o niskim wpływie na środowisko, jaką jest bio-hydrometalurgia. W tym celu wykorzystano acydofilnych bakterii z gatunku *Acidithiobacillus ferrooxidans*. Eksperyment został przeprowadzony w warunkach laboratoryjnych przez okres 64 dni. Bioługowanie przeprowadzono w kolbach Erlenmeyera o pojemności 0,3 dm^3, zawierających 3 g półproduktu otrzymanego w wyniku separacji elektrostatycznej. W doświadczeniu wykonano również sterylne próbki kontrolne w identycznych warunkach eksperymentu (wymywanie chemiczne), które zostały odseparowane od prób bakteryjnych, w celu uniknięcia niepożądanego zaszczepienia bakteriami prób kontrolnych. Temperatura otoczenia wynosiła od 21,3°C do 23,9°C. Do każdej z prób przygotowano minimum dwa osobne roztwory ługujące. W próbach z udziałem bakterii *Acidithiobacillus ferrooxidans* oraz w próbie kontrolnej z udziałem pożywki Silvermana i Lundgrena 9K badano pH roztworu i potencjał oksydacyjno-redukcyjny Eh. W celu zapewnienia optymalnych warunków pH roztworu, konieczne było zakwaszanie roztworów ługujących za pomocą pięciomolowego roztworu kwasu siarkowego (VI), utrzymując odczyn na poziomie pH=2. Po zakończeniu bioługowania roztwory przefiltrowano, oddzielając pozostałą ciecz za pomocą bibuły filtracyjnej (Macherey-Nagel, Allentown, PA, USA, MN 640 d, 18,5 cm ∅) **(M6)**.

4.3 Metody analityczne

Po rozdrobnieniu WPCB w młynie nożowym przeprowadzono analizę granulometryczną otrzymanego materiału za pomocą:

- zestawu sit (Fritsch, Niemcy) o rozmiarach oczek: 3,15 mm, 2,00 mm, 1,40 mm, 1,00 mm, 0,71 mm, 0,5 mm, 0,355 mm, 0,25 mm, 0,18 mm, 0,125 mm, 0,09 mm,
- laserowego analizatora wielkości cząstek ANALYSETTE 22 MicroTec Plus (Fritsch, Niemcy) – ze względu na ograniczenia w pomiarze wielkości ziaren pomiar nie był prowadzony dla materiału otrzymanego z rozdrabniania w młynie z sitem o perforacji 2 i 3 mm. Najdrobniejsze cząstki trudno zwilżalne, które występowały w niewielkiej ilości, zostały usunięte przed przeprowadzeniem analizy.

Produkty rozdrabniania oraz produkty otrzymane za pomocą separatora elektrostatycznego, stołu koncentracyjnego i separatora cyklofluidalnego poddano następującym analizom:

- optycznej spektrometrii emisyjnej z plazmą sprzężoną indukcyjnie (ICP-OES) za pomocą spektrometru Jy2000 (Yobin-Yvon, Hessen, Niemcy). Źródłem indukcji był palnik plazmowy sprzężony z generatorem częstotliwości 40.68 MHz,
- gęstości właściwej za pomocą piknometrów piknometrów Gay-Lussaca na podstawie PN- EN 1097-7:2001 z wykorzystaniem alkoholu etylowego o gęstości 0,7893 g/cm^3,
- analizy mikroskopowej korzystając z mikroskopu stereoskopowego Zeiss SteREO Discovery (Carl Zeiss AG, Niemcy).

W przypadku produktów otrzymanych za pomocą maszynki flotacyjnej dokonano następujących analiz:

- energodyspersyjnej fluorescencji rentgenowskiej (ang. *Energy Dispersive X-ray Fluorescence*, ED/XRF) za pomocą spektrofotometru ED-XRF Epsilon 4 Spectofotometer (Malvern Panalytical, Malvern, United Kingdom), wyposażonego w lampę rentgenowską o mocy 10 W z anodą Ag, detektor typu Silicon Drift i system płukania helem,
- gęstości właściwej za pomocą piknometrów piknometrów Gay-Lussaca na podstawie PN- EN 1097-7:2001 z wykorzystaniem alkoholu etylowego o gęstości 0,7893 g/cm^3,
- analizy mikroskopowej korzystając z mikroskopu stereoskopowego Zeiss SteREO Discovery (Carl Zeiss AG, Niemcy).

Koncentrat oraz półprodukt otrzymany z separacji elektrostatycznej najefektywniejszego wariantu rozdrabniania WPCB dodatkowo oceniono za pomocą:

- skaningowego mikroskopu elektronowego wysokiej rozdzielczości Zeiss SUPRA 35 (Carl Zeiss AG, Germany), wyposażonego w system analizy składu chemicznego EDAX – spektroskopii rentgenowskiej z dyspersją energii (ang. *Energy Dispersive X-ray Spectroscopy*, EDS) (EDAX, Stany Zjednoczone),
- rentgenowskiej jakościowej analizy fazowej przy użyciu dyfraktometru Panalytical X'Pert Pro MPD (Panalytical, Holandia), wykorzystując filtrowane promieniowanie lampy z anodą kobaltową ($\lambda K\alpha$ = 0,179 nm). Linie dyfrakcyjne rejestrowano w geometrii Bragga-Brentano, metodą skanowania krokowego za pomocą detektora PIXcell 3D, w zakresie kątów od 20–100° [2θ] (krok 0.05°, czas kroku 200 s). Uzyskane dyfraktogramy analizowano przy użyciu oprogramowania Panalytical High Score Plus (v. 3.0e) posiadającego bazę danych PAN-ICSD.

Ze względu na występowanie dużej ilości tworzyw sztucznych w nadawie i produktach niemetalicznych z separacji elektrostatycznej i możliwość uszkodzenia urządzeń, nie przeprowadzono analiz SEM-EDS oraz XRD dla tych produktów.

W przypadku eksperymentu bioługowania pomiary zostały wykonane za pomocą pH-metru KnickPortamesstype 913 (Knick, Berlin, Niemcy) z elektrodą WTW pH-ElectrodeSenTix 41 z automatyczną kompensacją temperatury oraz miernika Eh CP-551 (Elmetron, Zabrze, Polska) z elektrodą Radelkis OP-7171-1A. Próbki roztworów i pozostałości (osadów) otrzymanych w wyniku zastosowania *Acidithiobacillus ferrooxidans* poddano analizie ICP-OES za pomocą spektrometru Jy2000 (Yobin-Yvon, Hessen, Niemcy) **(M6)**. Badania analityczne zostały wykonane w Laboratorium Badania Materiałów Wydziału Mechanicznego Technologicznego Politechniki Śląskiej oraz Pracowni Recyklingu i Gospodarki o Obiegu Zamkniętym Wydziału Górnictwa, Inżynierii Bezpieczeństwa i Automatyki Przemysłowej Politechniki Śląskiej

5 Wyniki i dyskusja

5.1 Rozdrabnianie

Wyniki analizy granulometrycznej rozdrobnionych w młynie nożowym WPCB dla różnych wariantów procesu przedstawiono w tabeli 5.1. Ze względu na włóknisty (iglasty) kształt rozdrobnionych ziaren żywicy epoksydowej i włókna szklanego, różnorodne kształty rozdrobnionych cząstek metali oraz znaczne różnice w zwilżalności, jednoznaczne określenie i ocena wielkości ziaren była trudna do przeprowadzenia.

Jak można było przewidzieć wraz ze wzrostem perforacji sita w młynie nożowym (wariant 3 i 4) otrzymany produkt cechował się większymi rozmiarami. W wariantach 3 i 4 największy udział stanowiły odpowiednio klasy ziarnowe 1,4 – 0,355 mm oraz 2,0 – 0,5 mm (Tab. 5.1.). Natomiast dla wariantów 1 i 2 rozdrobniony materiał występował głównie w klasach od 1,0 – 0,25 mm i poniżej 0,09 mm, przy czym dla wariantu 2 ziarna charakteryzowały się nieznacznie mniejszą wielkością. Różnice w wynikach między zastosowanymi metodami analizy wynikają z różnych kształtów, jaki przyjmowały ziarna. I tak dla metali, ziarna przybierały głównie kształt globularny, płatkowy i iglasty, a dla tworzyw sztucznych włóknisty i płatkowy **(M1)**.

Tabela 5.1. Wychody klas ziarnowych produktów rozdrabniania **(M1)**

Klasa ziarnowa, mm	**Wychód, %**					
	Wariant 1[a]	**Wariant 1[b]**	**Wariant 2[a]**	**Wariant 2[b]**	**Wariant 3[a]**	**Wariant 4[a]**
>3,15	0,0	0,0	0,0	0,0	0,0	0,0
3,15 – 2,0	0,0	0,0	0,0	0,0	0,0	0,2
2,0 – 1,4	0,0	0,0	0,0	0,0	0,4	13,7
1,4 – 1,0	0,3	0,0	0,4	0,0	11,1	24,6
1,0 – 0,71	5,7	5,2	3,6	1,6	25,6	16,8
0,71 – 0,5	14,1	14,8	13,0	10,4	15,6	10,7
0,5 – 0,355	19,3	22,0	19,5	22,1	11,6	8,4
0,355 – 0,25	17,0	10,4	17,0	14,2	8,6	6,3
0,25 – 0,18	9,6	5,6	10,6	6,5	5,0	4,1
0,18 – 0,125	8,5	4,9	10,8	5,3	4,5	4,5
0,125 – 0,09	9,1	3,8	8,5	4,3	3,6	4,2
<0,09	16,3	33,3	16,6	35,6	13,9	6,5

[a] analiza wykonana za pomocą sit Fritsch, [b] analiza wykonana za pomocą analizatora wielkości cząstek

W produktach rozdrabniania dla wariantów 3 i 4 zauważono, że ziarna metali posiadają liczne połączenia metal-tworzywo sztuczne, co nie jest widoczne dla wariantu 1, a szczególnie 2. Materiał otrzymany z wariantu 2 charakteryzował się znacznie mniejszym udziałem ziaren konglomeratów. Co więcej, proces rozdrabniania z wykorzystaniem ciekłego azotu charakteryzował się znacznie wyższą wydajnością. W tym przypadku wzrost temperatury komory młyna był znacznie mniejszy, co może ograniczyć zjawisko powstawania konglomeratów i ograniczyć zużycie noży oraz innych elementów. Wobec tego, najbardziej efektywne rozdrabnianie WPCB uzyskano dla wariantu z wykorzystaniem ciekłego azotu i otrzymany w ten sposób produkt stanowił nadawę na procesy separacji. Zauważono, że pełne uwolnienie metali od tworzyw sztucznych wystąpiło dla ziaren poniżej 0,3 mm, a w mniejszym stopniu dla ziaren mniejszych od 0,8 mm **(M1)**. Według pracy Li i in. 2007 [55] pełne uwolnienie metali zachodzi dla ziaren poniżej 0,6 mm, zaś Kaya 2016 [12] podaje, że dopiero dla ziaren poniżej 0,15 mm. W obu wymienionych pracach w badaniach zastosowano wielostopniowe rozdrabnianie w młynach młotkowych oraz użyto innych WPCB, co mogło mieć wpływ na rezultaty prac.

5.2 Metody rozdziału

Pierwszą zastosowaną metodą rozdziału była separacja elektrostatyczna, którą przeprowadzono dla wszystkich produktów otrzymanych z procesu rozdrabniania. Biorąc pod uwagę gęstości tworzyw sztucznych i metali, można określić, że produkty separacji dla wariantu 4 są silnie zanieczyszczone **(M1)**. Związane jest to z niskim stopniem rozdrobnienia, który nie pozwolił na wystarczające uwolnienie substancji użytecznych (metali w stanie wolnym) z kompozytu WPCB. Świadczą o tym relatywnie wysokie wychody koncentratu na poziomie 43% i jego niska gęstość wynosząca 5,5 g/cm^3. W przypadku wariantu 1, 2 i 3 koncentrat stanowił odpowiednio 25,8%, 26,2% i 27,2% wszystkich produktów, a jego gęstość wynosiła odpowiednio 8,8 g/cm^3, 8,9 g/cm^3 (Tab. 5.2.) i 7,3 g/cm^3 **(M1)**.

Powyższe wartości mogą sugerować o bardzo zbliżonych jakościowo produktach, jednakże w wyniku analizy składu chemicznego potwierdzono, że najlepsze pod względem czystości produkty otrzymano w wyniku separacji materiału pochodzącego z wariantu 2. I tak, w koncentracie dla tego wariantu zidentyfikowano ponad 93% wartościowych metali (tj. Cu, Al, Pb, Zn, Ni, Fe, Sn, Cr, Ti, Ag, Au) (Tab. 5.3.), natomiast w przypadku pozostałych było to odpowiednio 87%, 76% i 54%. Stosunkowo wysoką czystość koncentratu oraz odpadu otrzymano również dla wariantu 1. Jednak w niskich temperaturach (wariant 2) dzięki zastosowaniu ciekłego azotu do schłodzenia nadawy, dodatkowo nie następował znaczący wzrost temperatury w komorze roboczej młyna i uplastycznienie rozdrabnianego materiału, i nie tworzyły się, lub tworzyły się w mniejszym stopniu, konglomeraty stałych połączeń metal-tworzywo sztuczne.

Na Rysunku 5.1. przedstawiono zdjęcia mikroskopowe produktów separacji elektrostatycznej z wariantu 2. Potwierdzają one wysoką czystość uzyskanego koncentratu i produktu zawierającego tworzywa sztuczne. W półprodukcie można zauważyć występowanie głównie ziaren konglomeratów, których rozdział za pomocą separacji mechanicznej jest niemożliwy. Aby to zrobić, ziarna te należałoby ponownie rozdrobnić lub wykorzystać inne metody spoza zakresu inżynierii mineralnej. W produkcie zawierającym tworzywa sztuczne zidentyfikowano śladowe ilości drobnych ziaren metali (poniżej 200 μm), które uwięzły we włóknistej strukturze ziaren włókna szklanego.

Można byłoby przyjąć, że ze względu na wielowarstwową budowę PCB korzystne jest uzyskanie jak najmniejszych ziaren. Wu i in. 2008 jednak podają [56], że bardzo drobne ziarna, tj. poniżej 0,125 mm, mogą przyczynić się do nieefektywnej separacji elektrostatycznej spowodowanej efektem agregacji ziaren na powierzchni bębna oraz elektrody. W pracy Wu i in. 2009 [57] przedstawiono, że efekt ten może mieć istotny wpływ na stabilność procesu separacji. Osiadanie pyłu zbudowanego z tworzyw sztucznych na powierzchni elektrody było obserwowane w prezentowanych w niniejszej pracy badaniach. Natomiast zauważono, że efekt agregacji był mocno ograniczony w przypadku separacji materiału pochodzącego z wariantu 2 rozdrabniania.

Można więc podsumować, że schładzanie materiału do temperatur kriogenicznych ma pozytywny wpływ na wielkość i kształt ziaren, a co za tym idzie, zgodnie z konkluzjami Lu et al. 2008. [58], na sprawność odzysku metali z WPCB. Należy podkreślić, że schłodzony materiał znacznie szybciej ulegał rozdrabnianiu, a stopień uwolnienia metali był wyższy.

Tabela 5.2. Wychody oraz gęstość produktów otrzymanych z separacji elektrostatycznej (wariant 2) **(M1)**

Produkty	**Koncentrat**	**Półprodukt**	**Tworzywa sztuczne**
Wychód, %	26,2	2,8	71,0
Gęstość właściwa, g/cm^3	8,87	5,33	2,29

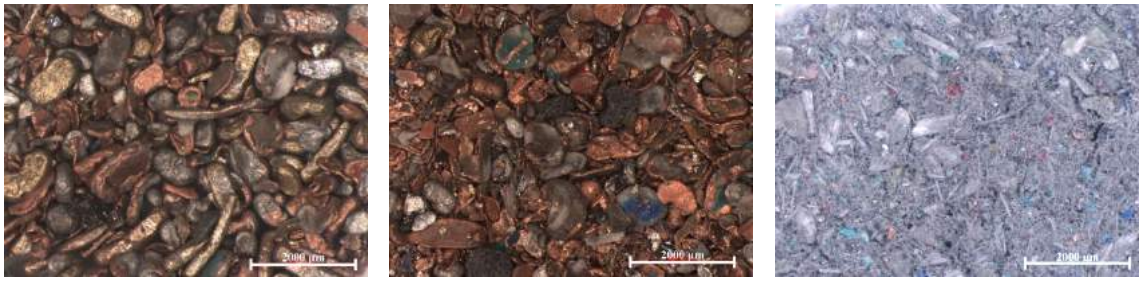

(a) (b) ©

Rysunek. 5.1. Zdjęcia mikroskopowe produktów separacji elektrostatycznej (wariant 2): (a) – koncentrat, (b) – półprodukt, (c) – tworzywa sztuczne **(M1).**

Tabela 5.3. Skład chemiczny nadawy i produktów separacji elektrostatycznej (wariant 2) **(M1)**.

Pierwiastek		**Zawartość pierwiastka w produkcie, %**			
		Nadawa	**Koncentrat**	**Półprodukt**	**Tworzywa sztuczne**
Wartościowe pierwiastki	Cu	17,70	68,50	6,68	0,17
	Al	1,95	6,82	1,34	0,07
	Pb	0,39	1,5	0,74	0,001
	Zn	0,69	2,5	0,94	-*
	Ni	0,19	0,75	0,31	-*
	Fe	0,38	0,95	1,50	0,09
	Sn	2,92	11,5	1,18	0,02
	Cr	0,06	0,15	0,04	0,001
	Ti	0,26	0,51	0,39	0,18
	Ag	0,0301	0,1074	-*	-*
	Au	0,0029	0,0092	-*	-*
	Suma	**24,57**	**93,30**	**13,12**	**0,54**
Pierwiastki o niskiej wartości	Sb	0,22	0,61	0,18	0,01
	Ca	6,56	0,92	2,41	7,51
	Br	1,64	0,03	1,12	1,28
	Ba	0,31	-*	0,41	0,77
	Mg	0,57	0,05	1,51	2,50
	Si	12,00	0,40	3,19	13,92
	Mn	0,01	0,03	-*	-*
	Suma	**21,26**	**2,01**	**8,82**	**26,00**

*poniżej progu detekcji

W celu zbadania morfologii ziaren koncentratu i półproduktu otrzymanych z wariantu 2 oraz określenia składu chemicznego w mikroobszarach ziaren wykonano zdjęcia wykorzystując metodę detekcji elektronów z rozproszeniem wstecznym (Rys. 5.2.) oraz przeprowadzono pomiary z wykorzystaniem EDS (Tab. 5.4.). Różnice kontrastu ziaren wskazują na ich niejednorodny skład chemiczny. Jaśniejsze obszary świadczą o występowaniu pierwiastków o wyższej liczbie atomowej, natomiast ciemne o niższej. Jednak należy mieć na uwadze możliwość gromadzenia ładunków powierzchniowych przez tworzywa sztuczne, które w przypadku naelektryzowania mogą również przejawiać się jako jasne obszary. W koncentracie (Rys. 5.2.a) występowały w większości ziarna jednorodne, znajdowały się w nim również nieliczne ziarna tworzące połączenia metal-metal lub metal-tworzywo sztuczne, zaś w półprodukcie (Rys. 5.2.b) występowały głównie ziarna niejednorodne.

Ziarna występujące w koncentracie (Rys. 5.2.a) o wielkości poniżej 0,3 mm były głównie jednorodne. Ziarna płatkowe i powstałe z nich ziarna o kształcie nieregularnym zbudowane były głownie z miedzi (Tab. 5.4.). W przypadku ziaren płatkowych o wielkości powyżej 0,6 mm obserwuje się niewystarczający stopień uwolnienia metali od pierwiastków. Ziarna podłużne wykazują najwyższą czystość niezależnie od ich wielkości. Można więc przypuszczać, że ziarna te pochodziły głównie z elementów WPCB, które nie miały połączeń z kompozytem.

Na podstawie przedstawionej analizy i obserwacji wszystkich ziaren koncentratu można podsumować, że metale zawarte w ziarnach o wielkości powyżej 800 μm są niewystarczająco uwolnione od tworzyw sztucznych.

W porównaniu do koncentratu, ziarna występujące w półprodukcie były większe, tj. w zakresie od około 0,5 mm do 1,0 mm (Rys. 5.2.b). Niemalże na każdym ziarnie można zauważyć charakterystyczną dla tworzyw sztucznych budowę włóknistą. Kształt ziaren, ich obustronne połączenia z tworzywami sztucznymi oraz duża zawartość miedzi (Tab. 5.4.) mogą wskazywać, że ziarna te pochodzą głównie z wewnętrznych warstw PCB. Ze względu na wielkość ziaren półprodukt można skierować do ponownego rozdrabniania lub poddać go roztwarzaniu roztworami ługującymi.

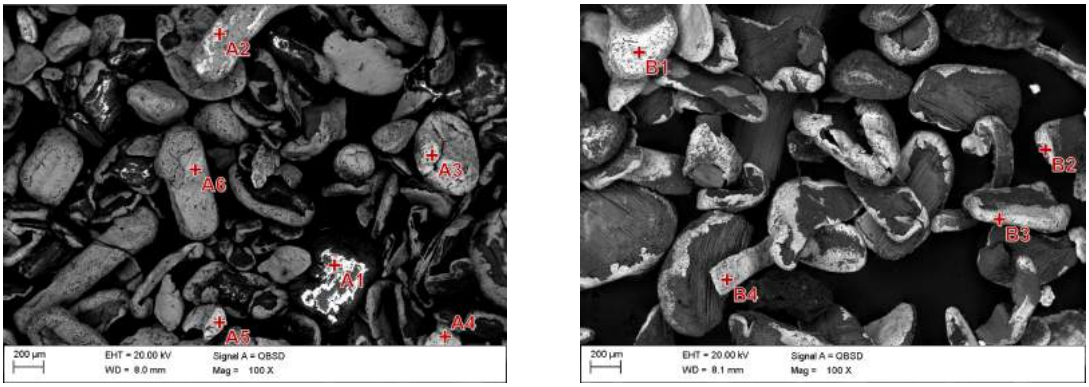

(a) (b)

Rysunek. 5.2. Zdjęcia SEM koncentratu (a) i półproduktu (b) otrzymanego w wyniku separacji elektrostatycznej (wariant 2) **(M1)**.

Tabela 5.4. Stężenia pierwiastków [% at.] zmierzone za pomocą EDS w mikroobszarach zaznaczonych na rysunku 5.4. **(M1)**.

Pierwiastek	**Punk analizy**									
	A1	**A2**	**A3**	**A4**	**A5**	**A6**	**B1**	**B2**	**B3**	**B4**
Mg	6,2	-	-	-	-	-	-	-	1,8	-
Al	93,8	22,4	4,1	5,5	34,9	4,0	6,8	2,4	8,5	9,9
Si	-	-	-	-	3,6	1,7	-	1,2	-	1,2
Sc	-	-	-	0,2	-	0,2	0,3	-	-	-
Fe	-	3,2	-	-	-	-	-	-	-	-
Ni	-	26,4	-	-	-	37,0	-	-	-	-
Cu	-	12	-	3,1	50,9	45,8	5,9	96,4	89,7	87,3
Sn	-	-	95,9	89,7	10,7	10,6	83,6	-	-	-
Sb	-	-	-	1,6	-	0,7	0,8	-	-	-
Ag	-	-	-	-	-	-	2,5	-	-	-
Au	-	36	-	-	-	-	-	-	-	-
Ca	-	-	4,7	1,3	-	-	-	-	-	-
Mn	-	-	0,2	-	-	-	-	-	-	-
S	-	-	0,5	-	-	-	-	-	-	-
Cl	-	-	-	0,3	-	-	-	-	-	1,6
Cr	-	-	6,7	-	-	-	-	-	-	-
Ba	-	-	0,2	-	-	-	-	-	-	-

Analiza składu fazowego dla koncentratu (Rys. 5.3.a) nie wykazała faz mogących świadczyć o występowaniu zanieczyszczeń, w przeciwieństwie do półproduktu (Rys. 5.3.b), w którym zidentyfikowano linie dyfrakcyjne pochodzące od krzemu. W koncentracie (Rys. 5.3.a) zidentyfikowano fazy takie jak miedź, cyna oraz brąz, zaś w półprodukcie (Rys. 5.3.b) poza krzemem również miedź i aluminium. Ze względu na ograniczoną czułość metody nie można wykluczyć występowania w małych ilościach innych faz metalicznych/niemetalicznych.

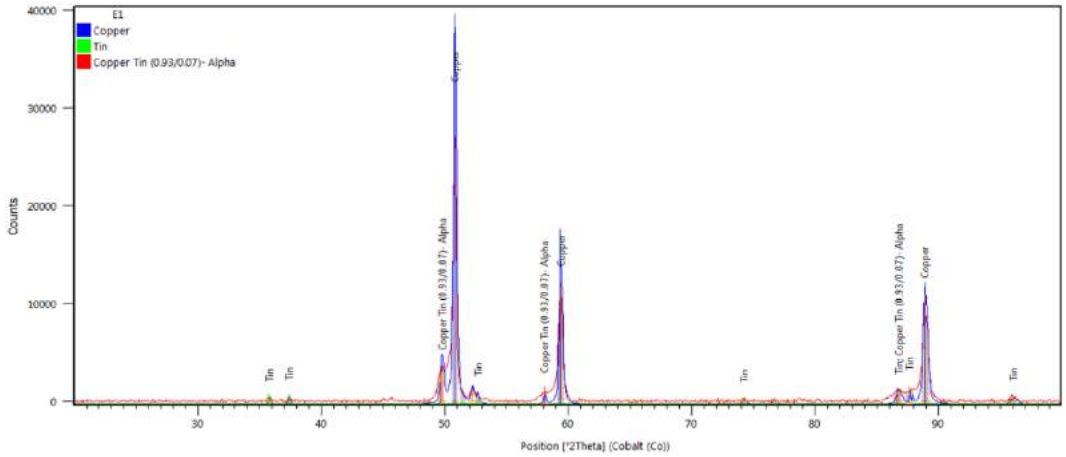

(a)

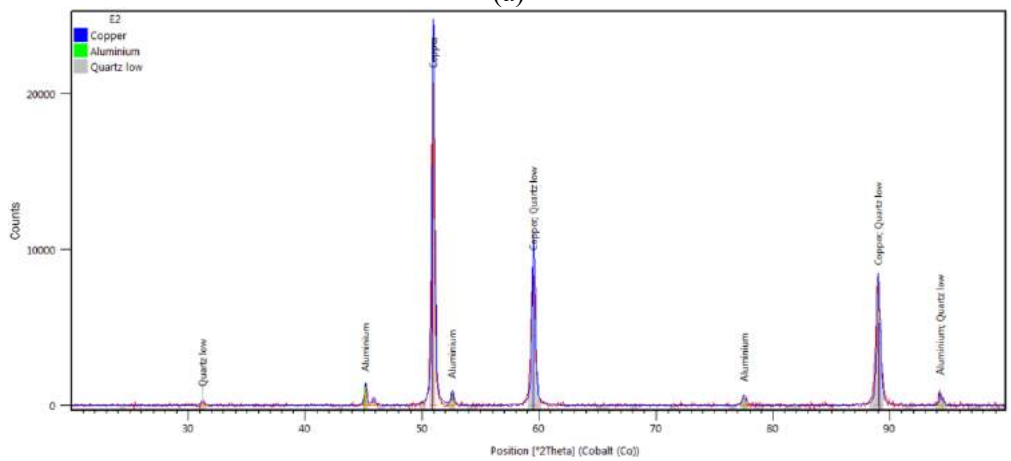

(b)

Rysunek 5.3. Dyfraktogram rentgenowski koncentratu (a) i półproduktu (b) separacji elektrostatycznej (wariant 2) **(M1)**.

Następną zastosowaną metodą rozdziału WPCB była separacja grawitacyjna przy użyciu stołu koncentracyjnego i separatora cyklofluidalnego **(M3)**. Nadawę na oba urządzenia stanowił materiał pochodzący z wariantu 2. W wyniku separacji na stole koncentracyjnym otrzymano cztery produkty, tj. T1 – T4, natomiast w przypadku separatora cyklofluidalnego uzyskano siedem produktów, tj, C1 – C7. W obu przypadkach usunięto przed separacją unoszący się na wodzie materiał (T0 i C0), który stanowił około 3% nadawy.

Wychód koncentratu T1 (Tab. 5.5.) był porównywalny do koncentratu otrzymanego w wyniku separacji elektrostatycznej, natomiast cechował się niższą gęstością. W przypadku separatora cyklofluidalnego otrzymano dwa produkty, tj. C1 i C2, które z uwagi na gęstość można zaklasyfikować jako koncentrat (Tab. 5.6.) Produkt C1 był również podobny pod względem jakościowym do koncentratu separacji elektrostatycznej, jednak jego wychód był znacznie mniejszy i wynosił 6,4%. W produkcie T1 przedstawionym na Rysunku 5.4.a można zauważyć zarówno ziarna metali, jak i ziarna konglomeratów, co świadczy o niskiej sprawności separacji. Potwierdzeniem tego była analiza składu chemicznego, za pomocą której w T1 zidentyfikowano 74% wartościowych pierwiastków (Tab. 5.7.). W porównaniu do T1, produkty C1 i C2 charakteryzowały się wyższą czystością. W C1 nie zidentyfikowano ziaren konglomeratów i ziaren tworzy sztucznych (Rys. 5.5.), natomiast w C2 można odnaleźć sporadyczne ziarna konglomeratów. Oba te produkty zawierały podobnie wysoką zawartość wartościowych pierwiastków wynoszącą około 88% **(M3)**.

Półprodukty separacji fizycznej stanowią największy udział wśród wszystkich otrzymanych produktów. Z uwagi na gęstość zaklasyfikowano T2 oraz C3 – C5 jako półprodukty. Wychód T2 wynosił blisko 29% (Tab. 5.5), co w porównaniu do separacji elektrostatycznej stanowi około 10 razy więcej. Na zdjęciach mikroskopowych można zauważyć znaczną ilość ziaren większych od 1 mm, wśród których znajdują się metale, konglomeraty, jak i tworzywa sztuczne (Rys. 5.4.b). W składzie chemicznym T2 zidentyfikowano ponad 17% wartościowych pierwiastków, co świadczy o występowaniu znacznej liczby ziaren metali (Tab. 5.7.). Wychód półproduktów otrzymanych w wyniku separacji za pomocą separatora cyklofluidalnego wynosił blisko 26% (Tab. 5.6). Podobnie jak w T2, dominowały tutaj ziarna powyżej 1 mm (Rys. 5.5.), natomiast w składzie chemicznym produkty C3-C5 zawierały około 13,5% metali (Tab. 5.8.). Należy zaznaczyć, że uzyskanie dużych wychodów półproduktów było zjawiskiem niepożądanym, bowiem nie stanowią one produktów końcowych i konieczne jest ich dalsze przetwarzanie.

W wyniku separacji grawitacyjnej otrzymano również produkty zbudowane z tworzyw sztucznych, tj. T3 i T4 oraz C6 i C7. Produkty te charakteryzowały się relatywnie niską gęstością i niską zawartością metali nieprzekraczająca 6% (Tab. 5.7. i Tab. 5.8.). Należy zaznaczyć, że w przypadku procesów grawitacyjnych wystąpiła klasyfikacja ziaren tworzyw sztucznych z uwagi na ich wielkość, co może ułatwić ich potencjalne zastosowanie do innych procesów, np. produkcji materiałów kompozytowych. W przypadku produktów T3 i C6 występują głównie ziarna większe od 0,5 mm, natomiast w produktach T4 i C7 ziarna mniejsze od 0,2 mm (Rys. 5.4 i Rys. 5.5.).

Ze względów ekonomicznych i ochrony środowiska należy zwrócić uwagę na konieczność użycia wody procesowej w zastosowanych procesach separacji grawitacyjnej. W przypadku rozdziału prowadzonego z wykorzystaniem stołu koncentracyjnego nieprzerwanie dostarczano wodę. Istnieje

możliwość zamknięcia obiegu wody, jednak w tym przypadku należy wyposażyć stanowisko w instalacje filtrującą, w celu oczyszczania jej z drobnych cząstek. Podczas separacji za pomocą separatora cyklofluidalnego zużycie wody nastąpiło wskutek napełnienia zbiorników oraz podczas odbioru produktów, które pozostały na sicie. Podczas badań z wykorzystaniem stołu koncentracyjnego zużyto około 77 l wody, natomiast w przypadku separatora cyklofluidalnego 13 l. W obu przypadkach otrzymane produkty poddano procesowi długotrwałego suszenia, co związane było również z wykorzystaniem energii.

Tabela 5.5. Wychody oraz gęstość produktów otrzymanych ze stołu koncentracyjnego **(M3).**

Produkty	**T0**	**T1**	**T2**	**T3**	**T4**
Wychód, %	2,8	25,7	28,9	8,9	33,7
Gęstość właściwa, g/cm^3	1,9	8,0	4,5	2,9	2,4

Tabela 5.6. Wychody oraz gęstość produktów otrzymanych z laboratoryjnego separatora cyklofluidalnego **(M3)**.

Produkty	**C0**	**C1**	**C2**	**C3**	**C4**	**C5**	**C6**	**C7**
Wychód, %	3,1	6,4	12,5	12,1	7,1	6,3	8,5	44,0
Gęstość właściwa, g/cm^3	2,0	8,9	8,1	7,0	5,3	4,1	3,1	2,3

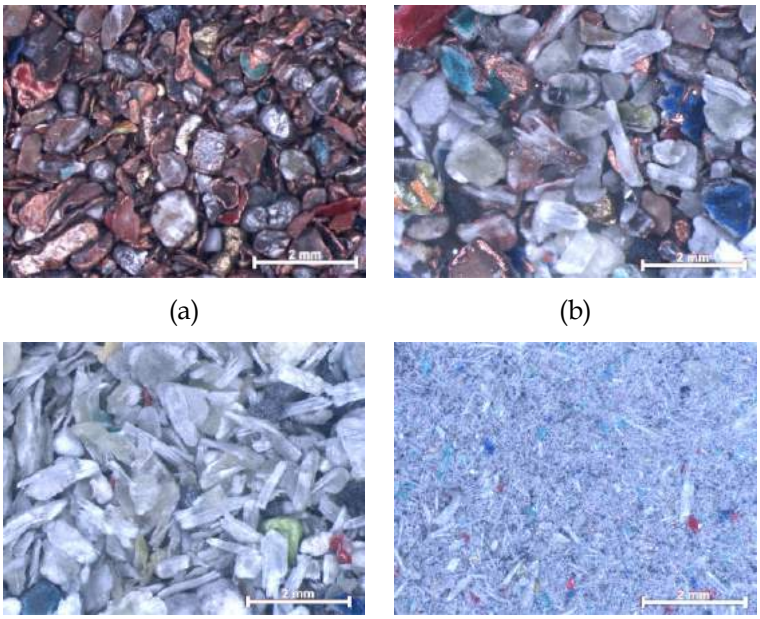

(a) (b)

(c) (d)

Rysunek. 5.4. Zdjęcia mikroskopowe produktów otrzymanych ze stołu koncentracyjnego: (a) – koncentrat (T1), (b) – półprodukt (T2), (c) – tworzywa sztuczne (T3), (d) – tworzywa sztuczne (T4) **(M3)**.

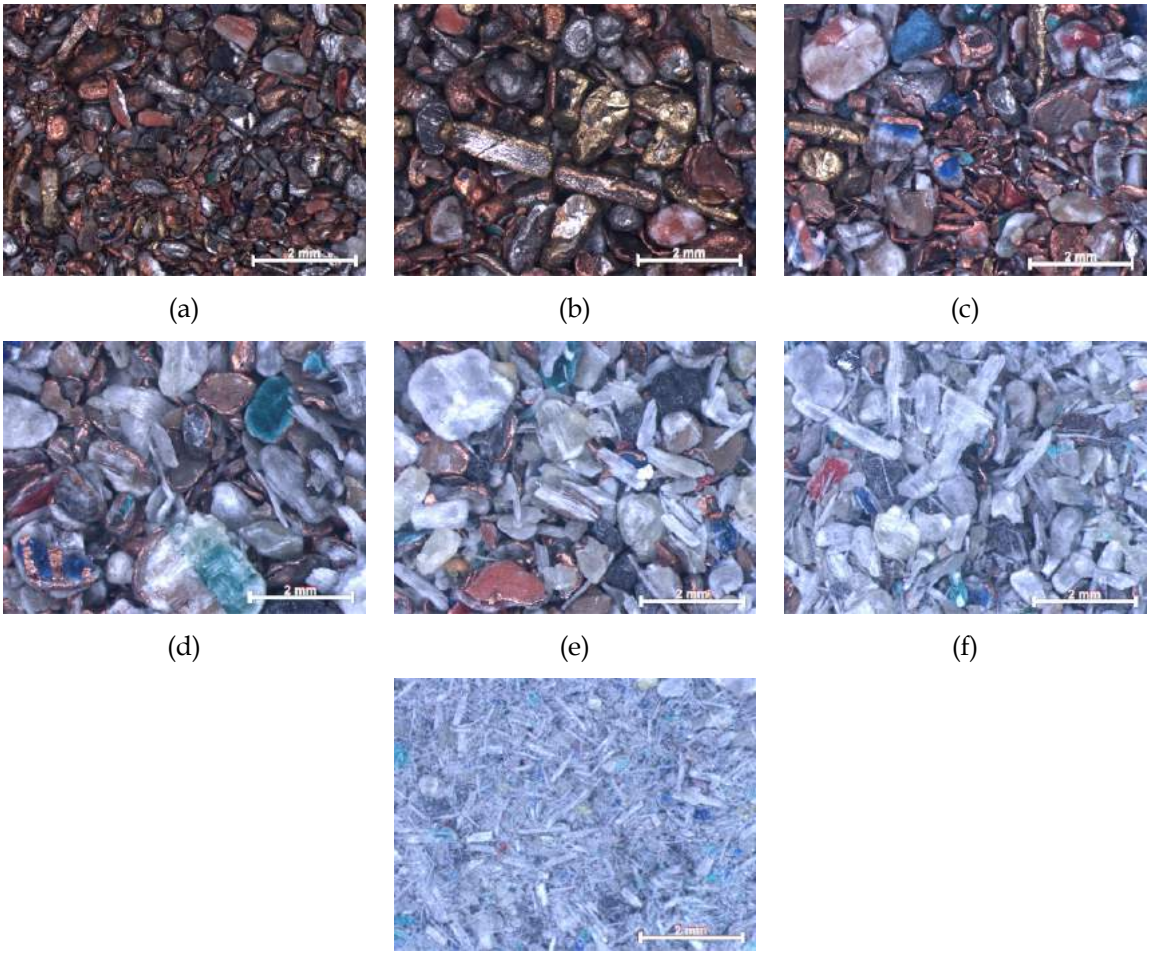

Rysunek. 5.5. Zdjęcia mikroskopowe produktów otrzymanych z laboratoryjnego separatora cyklofluidalnego: (a) – koncentrat (C1), (b) – koncentrat (C2), (c) – półprodukt (C3), (d) – półprodukt (C4), (e) – półprodukt (C5), (f) – tworzywa sztuczne (C6), (g) – od tworzywa sztuczne pad (C7) **(M3)**.

Tabela 5.7. Skład chemiczny nadawy i produktów otrzymanych ze stołu koncentracyjnego **(M3)**.

Pierwiastek		**Zawartość pierwiastka w produkcie, %**				
		Nadawa	**T1**	**T2**	**T3**	**T4**
Wartościowe pierwiastki	Cu	17,70	59,20	9,50	2,44	1,55
	Al	1,95	0,89	1,61	3,30	3,02
	Pb	0,39	1,10	0,64	0,02	0,02
	Zn	0,69	1,90	0,60	0,11	0,06
	Ni	0,19	0,59	0,19	0,08	0,06
	Fe	0,38	0,94	0,25	0,38	0,28
	Sn	2,92	6,30	2,67	0,27	0,36
	Cr	0,06	0,14	0,07	0,08	0,06
	Ti	0,26	0,91	0,15	0,13	0,09
	Ag	0,0301	0,0216	-*	-*	-*
	Au	0,0029	0,0072	-*	-*	-*
	Suma	**24,57**	**72,00**	**15,68**	**6,81**	**5,50**
Pierwiastki o niskiej wartości	Sb	0,22	0,10	0,34	0,18	0,11
	Ca	6,56	0,90	5,10	6,99	8,10
	Br	1,64	0,53	0,78	0,92	1,89
	Ba	0,31	0,71	0,15	0,19	0,12
	Si	12,00	3,10	9,30	15,10	13,10
	Mn	0,01	0,0065	0,0022	-*	-*
	Suma	**21,26**	5,35	15,67	23,38	23,32

*poniżej progu detekcji

Tabela 5.8. Skład chemiczny nadawy i produktów otrzymanych z separatora cyklofluidalnego **(M3)**.

Pierwiastek		**Zawartość pierwiastka w produkcie, %**							
		Nadawa	**C1**	**C2**	**C3**	**C4**	**C5**	**C6**	**C7**
Wartościowe pierwiastki	Cu	17,70	72,10	68,10	11,30	10,20	2,88	2,55	1,88
	Al	1,95	1,09	0,85	1,57	2,17	2,88	2,86	2,49
	Pb	0,39	1,50	1,40	0,88	0,91	0,05	0,02	0,01
	Zn	0,69	2,30	2,40	0,65	0,54	0,18	0,11	0,05
	Ni	0,19	1,09	1,07	0,32	0,36	0,08	0,06	0,01
	Fe	0,38	1,35	1,44	0,36	0,27	0,41	0,38	0,18
	Sn	2,92	8,10	11,40	1,10	0,90	0,10	0,11	0,07
	Cr	0,06	0,21	0,14	0,07	0,08	0,09	0,13	0,08
	Ti	0,26	0,99	0,89	0,24	0,21	0,15	0,21	0,13
	Ag	0,0301	0,0582	0,0078	0,0012	-*	-*	-*	-*
	Au	0,0029	0,0096	0,0078	-*	-*	-*	-*	-*
	Suma	**24,57**	**88,79**	**87,78**	**15,48**	**16,65**	**6,81**	**6,44**	**4,89**
Pierwiastki o niskiej wartości	Sb	0,22	0,50	0,30	0,09	0,08	0,15	0,17	0,12
	Ca	6,56	0,98	1,20	6,10	5,40	7,10	7,40	6,90
	Br	1,64	0,32	0,45	0,52	0,96	1,50	2,11	2,30
	Ba	0,31	0,92	0,84	0,09	0,07	0,21	0,25	0,22
	Si	12,00	0,92	5,50	6,30	9,20	13,80	15,20	9,80
	Mn	0,01	0,0078	0,0067	0,0054	0,0056	0,0077	0,0062	0,0012
	Suma	**21,26**	**3,65**	**8,30**	**13,11**	**15,72**	**22,77**	**25,14**	**19,34**

*poniżej progu detekcji

Ostatnią zastosowaną metodą rozdziału metali od tworzyw sztucznych była flotacja **(M4)**. W pierwszym etapie badań dobrano odczynnik flotacyjny w celu uzyskania największej efektywności procesu. Na podstawie gęstości produktu dolnego (metali) i górnego (tworzyw sztucznych) określono, że spośród zbadanych odczynników najlepsze efekty osiągnięto przy zastosowaniu glikolu dipropylenowego. Następie przeprowadzono testy użycia różnych stężeń odczynnika, wydatku powietrza i ilości materiału. Optymalne warunki flotacji uzyskano przy stężeniu 157 mg/dm^3, strumieniu powietrza 200 dm^3/h i 25g/dm^3 materiału.

W wyniku flotacji rozdrobnionych WPCB (wariant 2) oraz przy zastosowaniu powyższych parametrów procesu uzyskano niemal 57% produktu dolnego, oraz 43% produktu górnego (Tab.5.9.). Z uwagi na konstrukcję urządzenia oraz dynamikę procesu wydzielenie półproduktu było niemożliwe. Produkt dolny był silnie zanieczyszczony ziarnami tworzyw sztucznych (głównie o kształcie płatkowym) i ziarnami konglomeratu (Rys. 5.6.a). Natomiast produkt górny charakteryzował się wysoką czystością, podobnie jak w przypadku separacji elektrostatycznej zaobserwowano śladowe ilości ziaren o średnicy poniżej 0,2 mm (Rys. 5.6.b). Jak wynika również z analizy składu chemicznego, produkt dolny, którego około połowę stanowiły metale, był silnie zanieczyszczony tworzywami sztucznymi (Tab. 5.10.). Przenikanie ziaren zbudowanych z kompozytów WPCB do produktu dolnego było niepożądane ze względu na pogorszenie czystości koncentratu. Było to prawdopodobnie spowodowane dużym rozmiarem tych ziaren i wskazuje to na potrzebę przeprowadzenia flotacji w określonych klasach ziarnowych.

Tabela 5.9. Wychody oraz gęstość produktów otrzymanych z flotacji **(M4)**.

Produkty	**Produkt dolny (koncentrat)**	**Produkt górny (tworzywa sztuczne)**
Wychód, %	56,6	43,4
Gęstość właściwa, g/cm^3	7,4	2,7

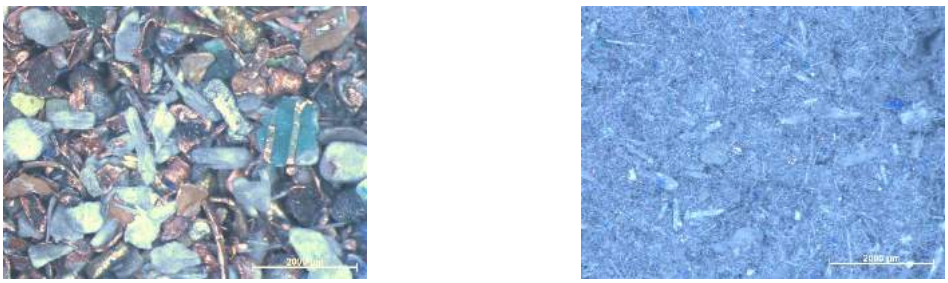

(a) (b)

Rysunek. 5.6. Zdjęcia mikroskopowe produktów otrzymanych z flotacji: (a) – produkt dolny (koncentrat), (b) – produkt górny (tworzywa sztuczne) **(M4)**.

Tabela 5.10. Skład chemiczny nadawy i produktów otrzymanych z flotacji **(M4)**.

Pierwiastek		Zawartość pierwiastka w produkcie, %		
		Nadawa	**Produkt dolny (koncentrat)**	**Produkt górny (tworzywa sztuczne)**
Wartościowe pierwiastki	Cu	17,70	39,94	2,33
	Al	1,95	1,10	1,71
	Zn	0,69	0,92	0,69
	Ni	0,19	0,64	0,34
	Fe	0,38	0,97	0,49
	Sn	2,92	7,80	1,12
	Cr	0,06	0,05	0,31
	Ti	0,26	0,49	0,52
	Ag	0,0301	0,5797	0,0918
	Au	0,0029	0,0140	0,0048
	Suma	**24,57**	**53,13**	**8,01**
Pierwiastki o niskiej wartości	Sb	0,22	0,09	10,40
	Ca	6,56	3,24	2,89
	Br	1,64	2,16	0,69
	Ba	0,31	0,73	0,0065
	Si	12,00	5,02	15,84
	Mn	0,01	0,0083	0,0014
	Suma	**21,26**	**11,29**	**29,82**

Z uwagi na występowanie niewielkich ilości półproduktu otrzymanego w wyniku separacji elektrostatycznej możliwe było przeprowadzenie eksperymentu bioługowania przy użyciu szczepu bakterii *Acidithiobacillus ferrooxidans*. Na rysunku 5.7. przedstawiono zmiany w czasie potencjału Eh oraz pH podczas trwania eksperymentu. Dla prób bakteryjnych, w ciągu pierwszych 25 dni zaobserwowano gwałtowny wzrost Eh - od wartości początkowej 255 mV do około 620 mV, a następnie zaobserwowano stabilny wzrost do wartości 700 mV uzyskanej w 52 dniu eksperymentu (Rys. 5.7.). O biologicznym przebiegu reakcji oraz wzroście mikroorganizmów świadczyło niskie pH, przy jednoczesnym utrzymywaniu się wartości Eh w roztworze kontrolnym w zakresie 300-400 mV. Ze względu na zasadowy charakter WPCB [28] oraz w celu zapewnienia

korzystnych warunków dla mikroorganizmów, próbki bakteryjne zakwaszano przy użyciu pięciomolowego roztworu kwasu siarkowego (VI). Efekt samo zakwaszenia przy utrzymującej się wartości pH = 2 zaobserwowano w 9 dniu prowadzonego procesu. W przypadku roztworu kontrolnego korekta pH była przeprowadzana regularnie, zapewniając w ten sposób kwaśne środowisko podczas 64 dni chemicznego ługowania **(M6)**.

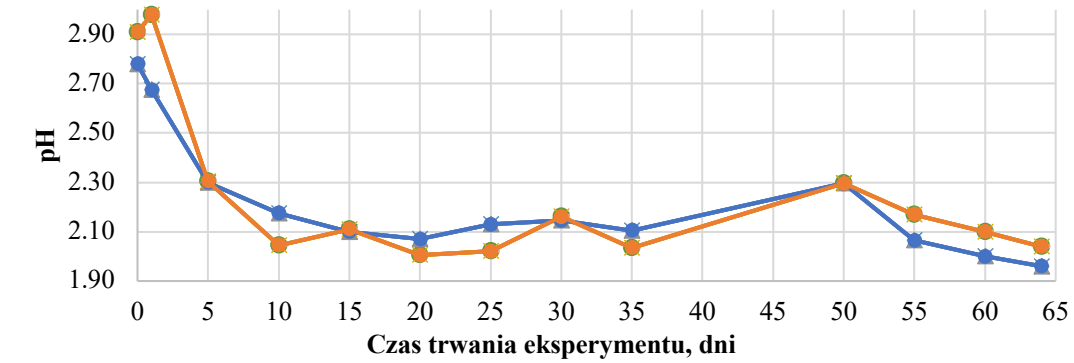

(a)

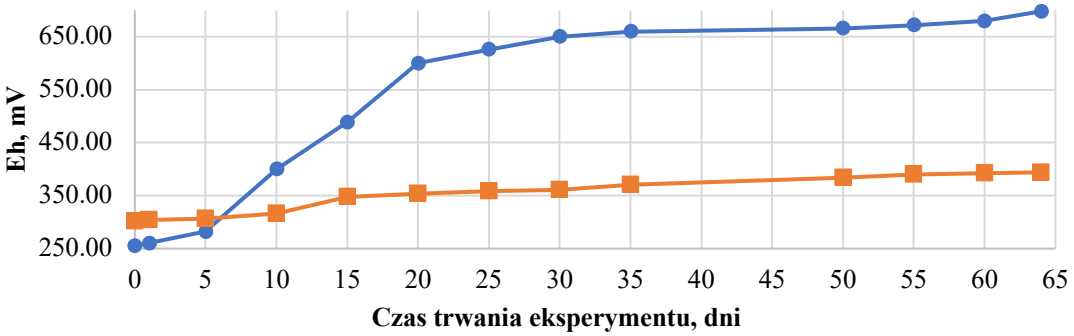

(b)

Rysunek 5.7. Wykresy zmian w czasie trwania eksperymentu bioługowania: (a) – potencjału redoks (Eh), (b) – pH, podczas wymywania bakteryjnego (niebieska linia) i chemicznego (pomarańczowa linia) **(M6)**.

Na podstawie analizy składu chemicznego odcieku i osadu (pozostałości) (Tab. 5.11.) można zaobserwować, że bioługowanie za pomocą bakterii *A. ferrooxidans*, nie jest efektywne dla wszystkich metali. W przypadku miedzi, aluminium, cynku i niklu większa ilość każdej substancji zostaje wyługowana. Natomiast nie można tego było zaobserwować dla ołowiu i cyny, gdzie w osadzie zidentyfikowano większą ilość pierwiastków. Wobec powyższego bioługowanie półproduktu pochodzącego z separacji elektrostatycznej przy użyciu *A. ferrooxidans* było możliwe, a proces był najbardziej wydajny dla miedzi, a następnie dla cynku, niklu i aluminium.

Tabela 5.11. Skład chemiczny eluatu i osadu (pozostałości) otrzymanych z eksperymentu bioługowania **(M6)**.

Pierwiastek	Zawartość pierwiastka, ppm		
	Materiał wsadowy	**Eluat**	**Osad (pozostałość)**
Cu	1000	700	250
Al	200	150	60
Pb	110	20	70
Zn	140	75	60
Ni	50	34	20
Sn	180	10	200

5.3 Ocena procesów jednostkowych

Jednym z ważniejszych aspektów wpływających na wybór metod recyklingu WPCB jest ekonomiczne uzasadnienie przedsięwzięcia. W tym przypadku czynnikiem decydującym były wychody i wartość monetarna produktów separacji, który określono za pomocą parametrów jakościowych i ilościowych (Rys. 5.8.). Zestawiając ze sobą wychody produktów i zawartość w nich wartościowych pierwiastków, jak również zawartości pierwiastków należących do kompozytu, oceniono jakość produktów i efektywność separacji **(M5)**. Biorąc pod uwagę powyższe, najlepsze produkty uzyskano w wyniku separacji elektrostatycznej. Produkt metaliczny stanowił około 26% i składał się w ponad 93% z tzw. metali wartościowych. Natomiast w produkcie zawierającym tworzywa sztuczne zidentyfikowano blisko 0,5% wartościowych metali, co świadczy o bardzo wysokim poziomie recyklingu i sprawności urządzenia. W wyniku separacji elektrostatycznej otrzymano również niemal 3% półproduktu, który zbudowany był z ziaren konglomeratów, składających się w około 13% z wartościowych metali. Wobec powyższego sprawność recyklingu wartościowych metali za pomocą separatora elektrostatycznego można określić na poziomie powyżej 95%. Efektywność separacji elektrostatycznej została również potwierdzona w pracach autorów Mir i Dhawan 2022 [17], De Olivieira i in. 2022 [59], Hamerski i in. 2019 [60] oraz Dascalescu i in. 1992 [61].

W przypadku innych procesów separacji otrzymane produkty cechowały się niższą czystością. Na przykład produkt metali otrzymany za pomocą stołu koncentracyjnego, charakteryzował się zawartością metali na poziomie 71% i zanieczyszczeniem ok. 7,5%, natomiast produkt zawierający tworzywa sztuczne zawierał ponad 5% wartościowych metali. W pracy De Oliveira i in. 2022 [59] do badań również wykorzystano stół koncentracyjny uzyskując wyższe

sprawności, jednakże proces separacji odbywał się w wyselekcjonowanych klasach ziarnowych. Dla nadawy o wielkości ziaren 0,3 mm – 0,6 mm i 0,6 mm – 1,18 mm, w produkcie metalicznym autorzy zidentyfikowali zawartość metali na poziomie odpowiednio 89% i 76%. W przypadku badań przeprowadzonych przez Burat i Ozer 2018 [48] konieczna była integracja stołu koncentracyjnego z separatorem elektrostatycznym i magnetycznym, bowiem zastosowanie wyłącznie procesów grawitacyjnych było niewystarczające. Co więcej, separacja odbywała się również z podziałem na trzy klasy ziarnowe. W wyniku zastosowanych procesów uzyskano sprawność odzysku metali na poziomie 95,4%, czyli podobnej jak w przypadku separacji elektrostatycznej przeprowadzonej w niniejszych badaniach. Należy zaznaczyć, że wielkość ziaren znacząco determinuje sprawność separacji metodami fizycznymi. Dzięki zawężonym klasom możliwa jest dokładniejsza optymalizacja procesu, jednak zwiększa to poziom skomplikowania technologii.

Najgorsze parametry jakościowe produktów otrzymano w wyniku flotacji. Produkt metali zawierał ok 53% wartościowych pierwiastków. W przypadku pracy Yao i in. 2020 [62] również zastosowano proces flotacji odwróconej i uzyskano poziom odzysku metali wynoszący 92,7%, jednak nadawa składała się z ziaren o wielkości od 0,25 mm do 0,5 mm, a do badań użyto odczynnika w postaci alkoholu bezwodnego. W pracy innego autora Jeon in. 2018 [63] zwiększono poziom odzysku Au z 32% do 51% przy użyciu MIBC jako spieniacza i nafty jako kolektora. W przypadku pracy Han i in. 2018 [64] uzyskano poziom odzysku miedzi wynoszący niemal 91% stosując kwas taninowy przy stężeniu 60 mg/cm^3. Wartym podkreślenia jest konieczność stosowania podczas flotacji odczynników chemicznych, których użycie jest wątpliwe podczas projektowania eko- efektywnych technologii. Nie wszystkie odczynniki wykazują działania toksyczne lub kancerogenne, jednakże stwarza to problemy z zagospodarowaniem lub oczyszczaniem wody procesowej, a w niektórych przypadkach stężenie substancji może negatywnie wpływać na zdrowie ludzi.

Rysunek 5.8. Zestawienie parametrów jakościowych i ilościowych otrzymanych produktów separacji **(M5)**.

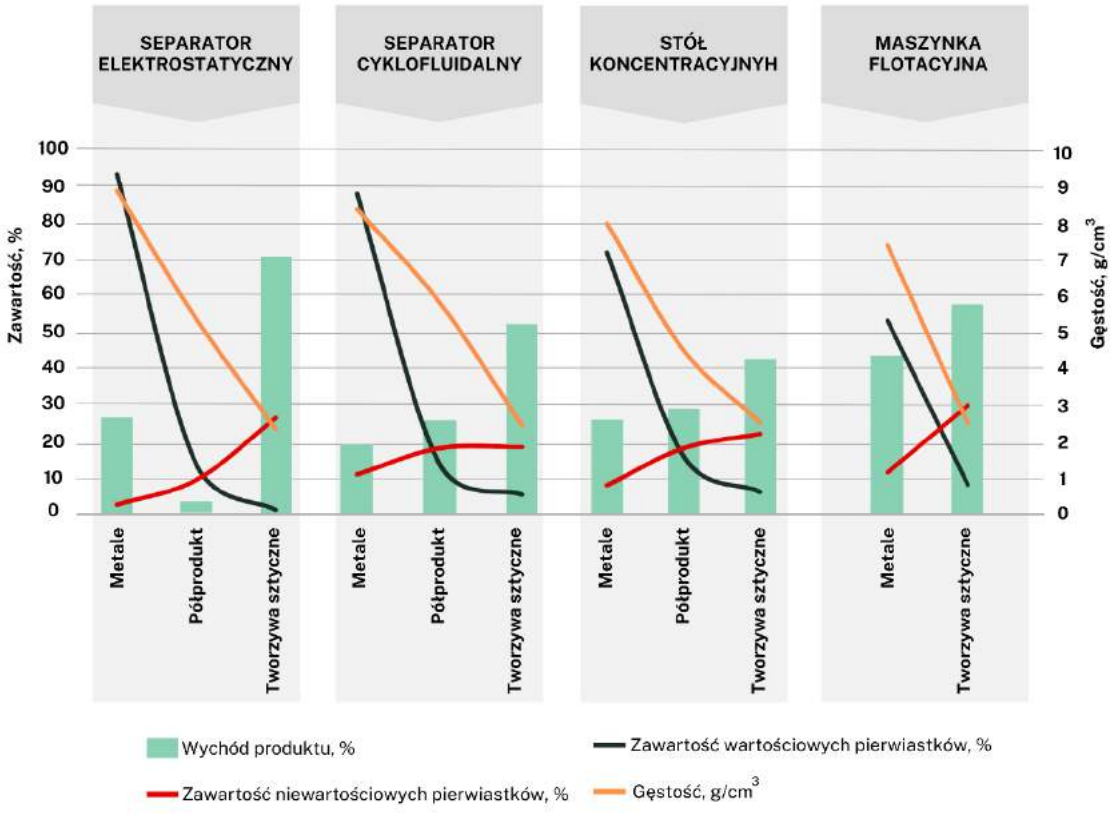

Eko-efektywna technologia, poza wysoką wydajnością, powinna również cechować się niskim oddziaływaniem na człowieka i środowisko przyrodnicze oraz być możliwie niskokosztowa. W celu oceny powyższych parametrów opracowano i zweryfikowano w skali laboratoryjnej poszczególne procesy (etapy) prowadzących do efektywnego rozdziału metali z WPCB za pomocą wymienionych wcześniej metod. Na podstawie przeprowadzonych prac badawczych określono następujące etapy technologii recyklingu WPCB:

- etap I – demontaż,
- etap II – rozdrabnianie,
- etap III – mielenie,
- etap IV – separacja,

W ramach każdego z powyższych etapów przeprowadzono na poziomie laboratoryjnym wstępne analizy środowiskowe oraz ekonomiczne każdego z procesów recyklingu. W pierwszej kolejności przeprowadzono zidentyfikowano oraz oceniono czynniki szkodliwe i niebezpieczne na stanowisku pracy oraz potencjalne oddziaływania na środowisko przyrodnicze (Tab. 5.12), a następie wyznaczono parametry techniczne i ekonomiczne (Tab. 5.13) **(M5)**.

Zidentyfikowanymi czynnikami szkodliwymi występującymi na stanowisku pracy było zapylenie i hałas wynikających z pracy urządzeń. Najwyższa wartość zapylenia w przeliczeniu na ośmiogodzinny dzień pracy rozpoznano podczas separacji elektrostatycznej, a następnie podczas procesu mielenia i pakowania. Z kolei najwyższy poziom hałasu zidentyfikowano podczas separacji grawitacyjnej na stole koncentracyjnym, a następnie podczas mielenia i rozdrabniania oraz procesu flotacji, których wartości nie przekraczały odpowiednio 133 dB, 132 dB, 117 i 116 dB. Identyfikację czynników niebezpiecznych przeprowadzono w oparciu o wiedzę starszego inspektora ds. BHP. Zagrożenia te wynikały głównie z ruchomych i ostrych elementów maszyn. Jednakże w przypadku separacji elektrostatycznej występowało również ryzyko porażenia wysokim napięciem o wartości ponad 15kV, a podczas mielenia możliwy był bezpośredni kontakt z bardzo niskimi temperaturami wynikającymi z zastosowania ciekłego azotu.

Analizę środowiskową przeprowadzono uwzględniając wyłącznie bezpośrednie emisje zanieczyszczeń do środowiska wynikające z pracy urządzeń. Podobnie jak w przypadku zapylenia, najwyższą potencjalną ilość emisji pyłów zidentyfikowano podczas separacji elektrostatycznej i mielenia. W przypadku separacji elektrostatycznej poziom zapylenia wynikał głównie z nieszczelności obudowy. Podczas procesów grawitacyjnych i flotacji zapylenie występowało wyłącznie podczas początkowego etapu mieszania rozdrobionych WPCB z woda, a więc jego wartości były marginalne. Jednakże w przypadku tych procesów powstały emisje wody procesowej. Największy strumień wody koniecznej do zagospodarowania zidentyfikowano podczas separacji na stole koncentracyjnym i wynosi ponad 1 000 l/h. Podczas flotacji stosowany był glikol dipropylenowy, który nie jest uznany za toksyczny i nieulegający bioakumulacji. Jednakże konieczne było odpowiednie zagospodarowanie zanieczyszczonej nim wody procesowej.

Jednym z najważniejszych ocenionych parametrów ekonomicznych technologii była wydajność poszczególnych procesów (Tab. 5.13.). Najwyższą wydajność uzyskano podczas rozdrabniania w wykorzystaniem dezintegratora (20 kg_{WPCB}/h), która wynika z półtechnicznej skali urządzenia. Natomiast najwyższą wydajność wśród zastosowanych procesów rozdziału uzyskano dla separatora cyklofluidalnego (7,5 kg_{WPCB}/h), a następnie stołu koncentracyjnego (6 kg_{WPCB}/h) i separacji elektrostatycznej (2 kg_{WPCB}/h). W przypadku flotacji otrzymano najniższą sprawność wynoszącą 0,15 kg_{WPCB}/h. Należy zaznaczyć, że podczas procesów separacji grawitacyjnej i flotacji konieczne było suszenie produktów o szacunkowej wydajności 2,5 kg_{WPCB}/h **(M5)**.

Kolejnym istotnym zbadanym parametrem była energochłonność urządzeń zastosowanych w procesach recyklingu. Największe zapotrzebowanie na energie (7,5 kW/h) rozpoznano podczas rozdrabniania WPCB za pomocą dezintegratora. Następnym wysoko energochłonnym procesem było suszenie produktów separacji (3 kW/h). Podobne zapotrzebowanie na energię (3 kW/h) określono dla procesu flotacji, co wynikało z konieczności zastosowania kompresora

wytwarzającego sprężone powietrze. Innym aspektem, który bezpośrednio wynikał z energochłonności były koszty eksploatacji urządzeń, które uwzględniały również zużycie wody procesowej, koszty pracownika i innych materiałów eksploatacyjnych wymaganych do prawidłowego funkcjonowania urządzeń. Średni sumaryczny koszt eksploatacyjny, poniesiony na przygotowanie WPCB do procesów separacji wynosił 44,80 zł/kg_{WPCB}, natomiast największy udział kosztów (blisko 80%) wynikał z mielenia WPCB. Najbardziej kosztowną metodą rozdziału była flotacja, w wyniku której poniesiono najwyższy koszt energii elektrycznej w przeliczeniu na jeden kilogram WPCB (ponad 10 zł/kg_{WPCB}). Podczas flotacji wymagana była również filtracja i zakup odczynnika flotacyjnego. Z uwagi na najniższą wydajność procesu, podczas flotacji występuje również najwyższy koszt obliczeniowy poniesiony na pracownika (117,13 zł/kg_{WPCB}). Wobec tego sumaryczne koszty eksploatacyjne zastosowania flotacji wyniosły ponad 176 zł/kg_{WPCB}, co może przekraczać wartość metali zawartych w WPCB. Natomiast najniższe sumaryczne koszty eksploatacyjne (3,8 zł/kg_{WPCB}) poniesiono w wyniku separacji cyklofluidalnej.

Biorąc pod uwagę czystość otrzymanych produktów, wydajność procesów separacji, ich oddziaływanie na środowisko przyrodnicze i człowieka oraz parametry ekonomiczne, najefektywniejszą wśród zbadanych metod rozdziału jest separacja elektrostatyczna. Zatem metoda ta może być uznana za najlepiej wpisują w koncepcję eko-efektywnej technologii. Dodatkowo jej zastosowanie w procesach recyklingu WPCB, w połączeniu z rozdrabnianiem w młynie nożowym w temperaturach kriogenicznych ogranicza poziom skomplikowania technologii i może zwiększyć korzyści ekonomiczne recyklingu WPCB.

Tabela 5.12. Ocena procesów jednostkowych technologii pod względem oddziaływania na pracownika i środowisko przyrodnicze **(M5)**.

KATEGORIE / ETAPY			I Demontaż	II Rozdrabnianie	III Mielenie		IV Separacja						
					IIIA Schładzanie	IIIB Mielenie	Separator elektrostatyczny	Stół koncentracyjny		Separator cyklofluidalny		Maszynka flotacyjna	
								IVA rozdział	IVB suszenie	IVA rozdział	IVB suszenie	IVA rozdział	IVB suszenie
Identyfikacja czynników szkodliwych i niebezpiecznych na stanowisku pracy	Czynniki szkodliwe	Zapylenie[1], g/m^2×8h	brak	brak	brak	0,048	0,064	brak	brak	brak	brak	brak	brak
		Hałas[2], dB	brak	<89, szczytowy <117	brak	<94, szczytowy <132	<71	<133	<50	<102	<50	<116	<50
	Czynniki niebezpieczne	Rodzaj czynnika niebezpiecznego	ostre części narzędzi	części ruchome dezintegratora	temperatury - 198^{o}c (ciekły azot)	ostre elementy ruchome	elementy ruchome separatora, wysokie napięcie ok. 15kV	ruchome części separatora	brak	ruchome części separatora	brak	ruchome części separatora	brak
Oddziaływanie na środowisko przyrodnicze		Emisja pyłów do powietrza[1], g/m^2×h	brak	brak	brak	0,006	0,008	brak	brak	brak	brak	brak	brak
		Emisja wody procesowej, l/h	brak	brak	brak	brak	brak	1 020	Brak	375	Brak	3	brak

[1] Pomiar poglądowy na własny użytek. Pomiar polegał na określeniu masy opadu pyłu, zgromadzonego w czasie jednej godziny na powierzchni szklanej płytki, która została umieszczona w odległości 1 m od źródła zapylenia.
[2] Pomiar poglądowy na własny użytek. Wykonany przy użyciu sonometru Bentech GM1356.

Tabela 5.13. Ocena procesów jednostkowych technologii pod względem parametrów techniczno-eksploatacyjnych i ekonomicznych **(M5)**.

KATEGORIE / ETAPY			I Demontaż	II Rozdrabnianie	III Mielenie		IV Separacja						
					IIIA Schładzanie	IIIB Mielenie	Separator elektro -statyczny	Stół koncentracyjny		Separator cyklofluidalny		Maszynka flotacyjna	
								IVA rozdział	IVB suszenie	IVA rozdział	IVB suszenie	IVA rozdział	IVB suszenie
Parametry techniczne		Szacunkowa wydajność procesu[3], kg_{WPCB}/h	12	20	2,5		2	6	2,5	7,5	2,5	0,15	2,5
		Liczba pracowników	1										
		Zapotrzebowanie na energię, kWh	brak	7,5	brak	2,2	1,5	2,0	3	0,7	3	3	3
		Zużycie wody procesowej, l/kg_{WPCB}	0	0	0	0	0	170	0	50	0	20	0
Parametry ekonomiczne	**Koszty inwestycyjne**	Zakup urządzeń[4], zł	3 000	66 000	4 500	25 000	31 000	26 000	4 500	20 000	4 500	18 000	4 500
	Aspekty eksploatacyjno -ruchowe	Koszt energii[5], zł/kg_{WPCB}	0	0,20	0	0,47	0,40	0,18	0,63	0,05	0,63	10,57	0,63
		Kosz wody procesowej, zł/kg_{WPCB}	0	0	0	0	0	2,19	0	0,64	0	0,26	0
		Koszt pracownika[6], zł/kg_{WPCB}	2,49	1,50	11,97		8,79	2,93		2,34		117,13	
		Materiały eksploatacyjne i ich zapotrzebowanie[3]	brak	elementy wału tnącego (36 szt./2 Mg_{WPCB})	ciekły azot (1 l/kg_{WPCB})	noże młyna (7szt./50 kg_{WPCB})	elektroda (1szt/4 Mg_{WPCB})	brak	worek do filtracji cieczy 5um, 1 szt./250l	brak	Worek do filtracji cieczy 5um, 1 szt./250l	Odczynnik flotacyjny 157 ml /dm^3	Worek do filtracji 5um, 1 szt./250l
		Koszty materiałów eksploatacyjnych[7], zł/kg_{WPCB}	0	4,62	4,20	19,56	<0,01	0	3,24	0	0,76	32,45	15,27

[3] Wartości wyznaczone na podstawie badań laboratoryjnych.
[4] Ceny netto urządzeń eksploatacyjnych zostały wyznaczone na podstawie rozeznania rynkowego.
[5] Koszt energii został obliczony na podstawie energochłonności urządzeń i rynkowej ceny energii elektrycznej [65].
[6] Koszt pracownika wyznaczono uwzględniając obciążenie pracownika wynikające z szacunkowej wydajności procesu oraz średniego miesięcznego kosztu ponoszonego przez pracodawcę w 2023 r.
[7] Ceny netto materiałów eksploatacyjnych zostały wyznaczone na podstawie rozeznania rynkowego.

6 Podsumowanie

W pracy zidentyfikowano i oceniono pod względem sprawności, kosztów i oddziaływania na środowisko przyrodnicze oraz człowieka poszczególne etapy recyklingu prowadzące do odzysku metali z WPCB. Najlepsze wyniki w tym zakresie dla zbadanych metod fizycznych i fizykochemicznych uzyskano dla separacji elektrostatycznej. Dla tego procesu otrzymano blisko 26% wysokiej czystości koncentrat, o zawartości metali powyżej 93%. Najważniejszym z podjętych działań było mielenie z wykorzystaniem ciekłego azotu, w wyniku którego uzyskano odpowiedni poziom uwolnienia metali, co z kolei umożliwiło wysoką sprawność separacji. Na podstawie przeprowadzonych badań opracowano cztery najważniejsze etapy eko- efektywnej technologii recyklingu WPCB typu FR-4:

- Etap I – demontaż: polega na usunięciu z powierzchni płytki podzespołów zawierających toksyczne substancje lub mogących zakłócić prawidłowy przebieg dalszych procesów. Należą do nich m.in. rezystory, tranzystory, baterie, chipy, kondensatory, złącza, śruby i gniazda wykonane z tworzyw sztucznych. Podzespoły te można poddać innym procesom recyklingu lub ponownie wykorzystać.
- Etap II – rozdrabnianie: zadaniem tego procesu jest zmniejszenie rozmiarów WPCB za pomocą dezintegratora do wymiarów nie większych niż 1 x 1 cm.
- Etap III – mielenie: w pierwszym kroku kawałki WPCB umieszcza się w zbiorniku z ciekłym azotem, a następnie mieli w młynie nożowym wyposażonym w sito o perforacji oczek 1 mm.
- Etap IV – separacja: za pomocą bębnowego separatora elektrostatycznego (prędkość obrotowa wału 100 obr/min, napięcie 17 kV, odległość między elektrodą a bębnem 0,03 m) rozdziela się proszek WPCB na koncentrat, półprodukt i tworzywa sztuczne.

Otrzymany w ten sposób koncentrat (26,2%), z uwagi na wysoką czystość i zawartość cennych pierwiastków, może być przekazany dalszym podmiotom zajmującym się produkcją lub przetwarzaniem metali i stanowić znaczącą korzyść finansową dla podmiotu zajmującego się recyklingiem WPCB. W przypadku półproduktu (2,8%), zawierającego ok. 13% metali, możliwe jest jego przetwarzanie za pomocą bioługowania z wykorzystaniem bakterii *Acidithiobacillus ferrooxidans*. Natomiast produkt zawierający tworzywa sztuczne (71,0%) może być wykorzystany jako wypełniacz stosowany w materiałach kompozytowych, których osnowę stanowi żywica epoksydowa lub poliestrowa.

Nie należy zapominać o tym, że w wyniku metod fizycznych uzyskuje się wyłącznie mieszaninę metali, którą należy poddać obróbce chemicznej w celu ich wyodrębnienia. Pomimo tego zastosowanie eko-efektywnej technologii recyklingu przyczynia się do ograniczenia negatywnego wpływu na środowisko, ponieważ tworzywa sztuczne są wcześniej wydzielone i mogą być zastosowane do wytwarzania innych dóbr konsumpcyjnych. Co więcej, z uwagi na relatywnie niski stopień jej skomplikowania i niskokosztowość, stanowi szansę na zwiększenie liczby instalacji recyklingu WPCB

w krajach Unii Europejskiej, tym samym zachowując cenne pierwiastki w gospodarce UE, jak również tworząc nowe miejsca pracy.

Ostatnim etapem eko-efektywnej technologii recyklingu WPCB jest zabezpieczenie produktów (mieszaniny metali i kompozytu) za pomocą opakowań jednostkowych, które zostaną przekazane odpowiednim podmiotom w celu wyodrębnienia metali w postaci indywiduum i produkcji materiałów kompozytowych.

Wobec powyższego potwierdzono przedstawioną w rozprawie doktorskiej tezę i opracowano technologię recyklingu WPCB (Rys. 6.1.), którą można uznać za eko-efektywną i zgodną z zasadami zrównoważonej produkcji oraz gospodarki o obiegu zamkniętym.

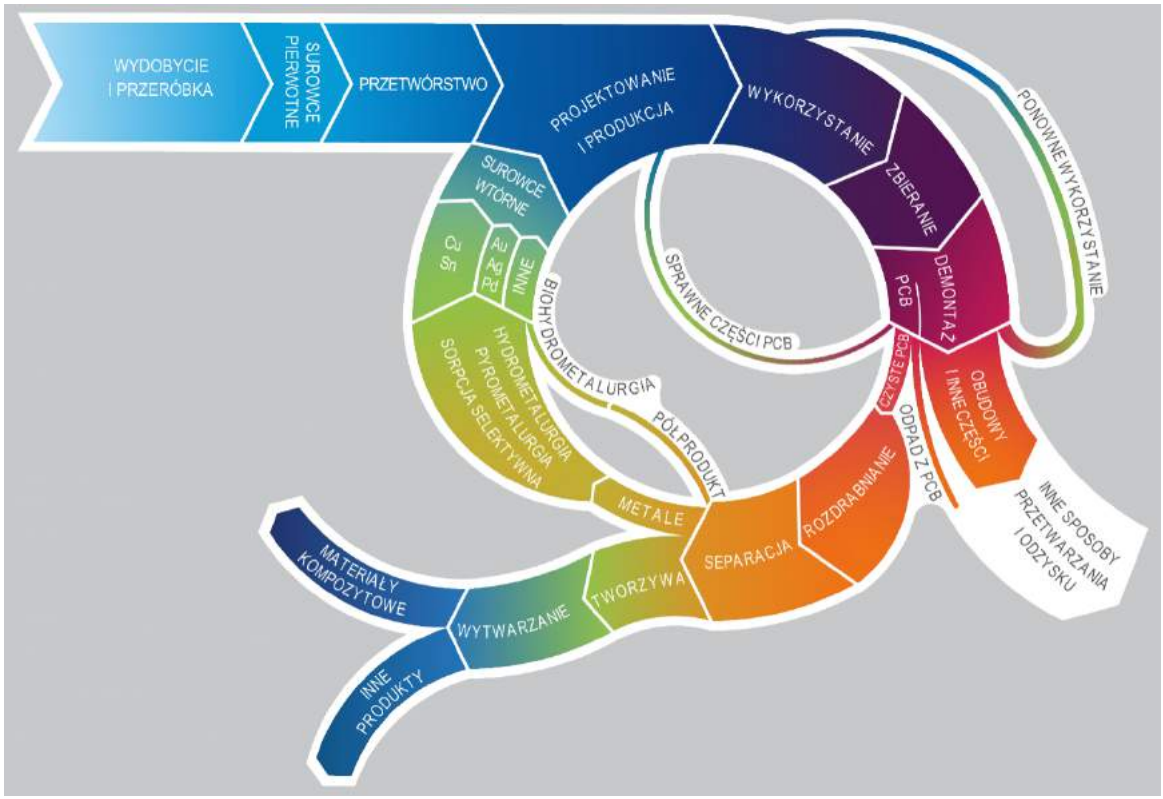

Rys. 6.1. Schemat ideowy eko-efektywnej technologii recyklingu zużytych płyt odwodów drukowanych typu FR-4.

Podsumowując, głównym osiągnięciem pracy było opracowanie, na podstawie badań technologicznych, analizy środowiskowej i finansowej, zintegrowanej technologii recyklingu WPCB stanowiącej alternatywę dla obecnie stosowanych chemicznych metod recyklingu. Uzyskano wysoki poziom uwolnienia metali od kompozytu WPCB stosując kriogeniczne temperatury podczas mielenia płyt w młynie nożowym, jak również wysoką sprawność rozdziału metali od kompozytu przy zastosowaniu separacji elektrostatycznej. Ponadto, na podstawie analiz ekonomicznych i ocen oddziaływania na środowisko przyrodnicze oraz człowieka, wykazano, że zaproponowana technologia jest niskokosztowa i wysokosprawna, jak również może być uznana za zgodną z zasadami zrównoważonej produkcji i gospodarki o obiegu zamkniętym.

Bibliografia

1. Xavier, L.H.; Giese, E.C.; Ribeiro-Duthie, A.C.; Lins, F.A.F. Sustainability and the Circular Economy: A Theoretical Approach Focused on e-Waste Urban Mining. *Resources Policy* **2021**, *74*, 101467, doi:10.1016/j.resourpol.2019.101467.
2. Araujo Galvão, G.D.; de Nadae, J.; Clemente, D.H.; Chinen, G.; de Carvalho, M.M. Circular Economy: Overview of Barriers. *Procedia CIRP* **2018**, *73*, 79–85, doi:10.1016/j.procir.2018.04.011.
3. Morseletto, P. Targets for a Circular Economy. *Resources, Conservation and Recycling* **2020**, *153*, 104553, doi:10.1016/j.resconrec.2019.104553.
4. Dantas, T.E.T.; de-Souza, E.D.; Destro, I.R.; Hammes, G.; Rodriguez, C.M.T.; Soares, S.R. How the Combination of Circular Economy and Industry 4.0 Can Contribute towards Achieving the Sustainable Development Goals. *Sustainable Production and Consumption* **2021**, *26*, 213–227, doi:10.1016/j.spc.2020.10.005.
5. Forti, V.; Baldé, C.P.; Kuehr, R.; Bel, G. The Global E-Waste Monitor 2020: Quantities, Flows and the Circular Economy Potential. *United Nations University (UNU)/United Nations Institute for Training and Research (UNITAR) – co-hosted SCYCLE Programme, International Telecommunication Union (ITU) & International Solid Waste Association (ISWA),* **2020**, 1-120.
6. Dutta, D.; Arya, S.; Kumar, S.; Lichtfouse, E. Electronic Waste Pollution and the COVID-19 Pandemic. *Environ Chem Lett* **2022**, *20*, 971–974, doi:10.1007/s10311-021-01286-9.
7. Yu, D.E.C.; Yu, K.D.S.; Tan, R.R. Implications of the Pandemic-Induced Electronic Equipment Demand Surge on Essential Technology Metals. *Cleaner and Responsible Consumption* **2020**, *1*, 100005, doi:10.1016/j.clrc.2020.100005.
8. International Data Corporation Traditional PC Shipments Continue to Grow Amid Global Economic Slowdown, According to IDC Dostępny online: https://www.businesswire.com/news/home/20200709005963/en/Traditional-PC-Shipments-Continue-to-Grow-Amid-Global-Economic-Slowdown-According-to-IDC (dostęp 28 grudnia 2022).
9. GamesIndustry.biz; Dring, C. What Is Happening with Video Game Sales during Coronavirus Dostępny online: https://www.gamesindustry.biz/what-is-happening-with-video-game-sales-during-coronavirus (dostęp 28 grudnia 2022).
10. Hyra, K.; Nuckowski, P.M.; Kwaśny, W.; Suponik, T.; Franke, D.M. *Przegląd Piśmiennictwa z Zakresu Gospodarowania Elektroodpadami Oraz Metod Odzysku Metali z Płyt Obwodu Drukowanego (PCB)*, w Interdyscyplinarne badania młodych naukowców, Wydawnictwo Politechniki Śląskiej, B. Balon, Red. **2023**, s. 136–164.

11. Eurostat Waste Electrical and Electronic Equipment (WEEE) by Waste Management Operations Dostępny online: https://ec.europa.eu/eurostat/databrowser/view/ENV_WASELEE__custom_4207254/default/table (dostęp 28 grudnia 2022).
12. Kaya, M. Recovery of Metals and Nonmetals from Electronic Waste by Physical and Chemical Recycling Processes. *Waste Management* **2016**, *57*, 64–90, doi:10.1016/j.wasman.2016.08.004.
13. Kaya, M. Recovery of Metals and Nonmetals from Waste Printed Circuit Boards (PCBs) by Physical Recycling Techniques. In *Energy Technology 2017*; Zhang, L., Drelich, J.W., Neelameggham, N.R., Guillen, D.P., Haque, N., Zhu, J., Sun, Z., Wang, T., Howarter, J.A., Tesfaye, F., Ikhmayies, S., Olivetti, E., Kennedy, M.W., Eds.; Springer International Publishing: Cham, 2017; pp. 433–451 ISBN 978-3-319-52191-6.
14. Zhang, Y.; Liu, S.; Xie, H.; Zeng, X.; Li, J. Current Status on Leaching Precious Metals from Waste Printed Circuit Boards. *Procedia Environmental Sciences* **2012**, *16*, 560–568, doi:10.1016/j.proenv.2012.10.077.
15. Muwanguzi, A.J.B.; Karasev, A.V.; Byaruhanga, J.K.; Jönsson, P.G. Characterization of Chemical Composition and Microstructure of Natural Iron Ore from Muko Deposits. *ISRN Materials Science* **2012**, *2012*, 1–9, doi:10.5402/2012/174803.
16. Menad, N.; Van Houwelingen, J. Identification and Recovery of Rare Metals in Electric and Electronic Scrap: A Review. *Tirtheenth International Waste Man-agement and Landfill Symposium* **2011**.
17. Mir, S.; Dhawan, N. A Comprehensive Review on the Recycling of Discarded Printed Circuit Boards for Resource Recovery. *Resources, Conservation and Recycling* **2022**, *178*, 106027, doi:10.1016/j.resconrec.2021.106027.
18. The London Metal Exchange, Dostępny online: https://www.lme.com/en/ (dostęp 29 grudnia 2022).
19. Royal Society of Chemistry Periotic Table, Dostępny online: https://www.rsc.org/periodic-table/ (dostęp 29 grudnia 2022).
20. Pokhrel, P.; Lin, S.-L.; Tsai, C.-T. Environmental and Economic Performance Analysis of Recycling Waste Printed Circuit Boards Using Life Cycle Assessment. *Journal of Environmental Management* **2020**, *276*, 111276, doi:10.1016/j.jenvman.2020.111276.
21. Madden, K.; Young, R.; Brady, K.; Hall, J. *Eco-Efficiency Learning Module*; World Business Council for Sustainable Development (WBCSD), 2006; ISBN 2-940240-84-1.
22. Kleiber, M.; Czaplicka-Kolarz, K. *Ekoefektywnosc technologii: praca zbiorowa*; Wydawnictwo Naukowe Instytutu Technologii Eksploatacji - Panstwowego Instytutu Badawczego: Radom, 2011; ISBN 978-83-7789-050-9.

23. Ghosh, B.; Ghosh, M.K.; Parhi, P.; Mukherjee, P.S.; Mishra, B.K. Waste Printed Circuit Boards Recycling: An Extensive Assessment of Current Status. *Journal of Cleaner Production* **2015**, *94*, 5–19, doi:10.1016/j.jclepro.2015.02.024.
24. Maurice, A.A.; Dinh, K.N.; Charpentier, N.M.; Brambilla, A.; Gabriel, J.-C.P. Dismantling of Printed Circuit Boards Enabling Electronic Components Sorting and Their Subsequent Treatment Open Improved Elemental Sustainability Opportunities. *Sustainability* **2021**, *13*, 10357, doi:10.3390/su131810357.
25. Yaashikaa, P.R.; Priyanka, B.; Senthil Kumar, P.; Karishma, S.; Jeevanantham, S.; Indraganti, S. A Review on Recent Advancements in Recovery of Valuable and Toxic Metals from E-Waste Using Bioleaching Approach. *Chemosphere* **2022**, *287*, 132230, doi:10.1016/j.chemosphere.2021.132230.
26. Argumedo-Delira, R.; Gómez-Martínez, M.J.; Soto, B.J. Gold Bioleaching from Printed Circuit Boards of Mobile Phones by Aspergillus Niger in a Culture without Agitation and with Glucose as a Carbon Source. *Metals* **2019**, *9*, 521, doi:10.3390/met9050521.
27. Hołda, A.; Krawczykowska, A. Extraction of Selected Metals from Waste Printed Circuit Boards by Bioleaching Acidophilic Bacteria. *IM* **2021**, *1*, doi:10.29227/IM-2021-01-06.
28. Hyra, K.; Nuckowski, P.M.; Willner, J.; Suponik, T.; Franke, D.; Pawlyta, M.; Matus, K.; Kwaśny, W. Morphology, Phase and Chemical Analysis of Leachate after Bioleaching Metals from Printed Circuit Boards. *Materials* **2022**, *15*, 4373, doi:10.3390/ma15134373.
29. Niu, B.; Chen, Z.; Xu, Z. Recovery of Valuable Materials from Waste Tantalum Capacitors by Vacuum Pyrolysis Combined with Mechanical–Physical Separation. *ACS Sustainable Chem. Eng.* **2017**, *5*, 2639–2647, doi:10.1021/acssuschemeng.6b02988.
30. Ahirwar, R.; Tripathi, A.K. E-Waste Management: A Review of Recycling Process, Environmental and Occupational Health Hazards, and Potential Solutions. *Environmental Nanotechnology, Monitoring & Management* **2021**, *15*, 100409, doi:10.1016/j.enmm.2020.100409.
31. Ma, E. Recovery of Waste Printed Circuit Boards Through Pyrometallurgy. In *Electronic Waste Management and Treatment Technology*; Elsevier, 2019; pp. 247–267 ISBN 978-0-12-816190-6.
32. Changming, D.; Chao, S.; Gong, X.; Ting, W.; Xiange, W. Plasma Methods for Metals Recovery from Metal–Containing Waste. *Waste Management* **2018**, *77*, 373–387, doi:10.1016/j.wasman.2018.04.026.
33. Suponik, T.; Franke, D.; Nuckowski, P.; Matusiak, P.; Kowol, D.; Tora, B. Impact of Grinding of Printed Circuit Boards on the Efficiency of Metal Recovery by Means of Electrostatic Separation. *Minerals* **2021**, *11*, 281, doi:10.3390/min11030281.
34. Franke, D.M.; Kar, U.; Suponik, T.; Siudyga, T. Evaluation of the Use of Flotation for the Separation of Ground Printed Circuit Boards. **2022**, doi:10.24425/GSM.2022.140605.

35. Kaya, M. *Electronic Waste and Printed Circuit Board Recycling Technologies*; The Minerals, Metals & Materials Series; Springer International Publishing: Cham, 2019; ISBN 978-3-030-26592-2.
36. Kozłowski, J.; Mikłasz, W.; Lewandowski, D.; Czyżyk, H. Research on hazardous waste - management part I. **2013**, *15*, 8.
37. Otsuki, A.; Pereira Gonçalves, P.; Leroy, E. Selective Milling and Elemental Assay of Printed Circuit Board Particles for Their Recycling Purpose. *Metals* **2019**, *9*, 899, doi:10.3390/met9080899.
38. Verma, H.R.; Singh, K.K.; Basha, S.M. Effect of Milling Parameters on the Concentration of Copper Content of Hammer-Milled Waste PCBs: A Case Study. *J. Sustain. Metall.* **2018**, *4*, 187–193, doi:10.1007/s40831-018-0179-z.
39. Khaliq, A.; Rhamdhani, M.; Brooks, G.; Masood, S. Metal Extraction Processes for Electronic Waste and Existing Industrial Routes: A Review and Australian Perspective. *Resources* **2014**, *3*, 152–179, doi:10.3390/resources3010152.
40. Wu, J.; Li, J.; Xu, Z. Electrostatic Separation for Multi-Size Granule of Crushed Printed Circuit Board Waste Using Two-Roll Separator. *Journal of Hazardous Materials* **2008**, *159*, 230–234, doi:10.1016/j.jhazmat.2008.02.013.
41. Li, J.; Xu, Z.; Zhou, Y. Application of Corona Discharge and Electrostatic Force to Separate Metals and Nonmetals from Crushed Particles of Waste Printed Circuit Boards. *Journal of Electrostatics* **2007**, *65*, 233–238, doi:10.1016/j.elstat.2006.08.004.
42. Aksa, W.; Medles, K.; Rezoug, M.; Boukhoulda, M.F.; Bilici, M.; Dascalescu, L. Two Stage Electrostatic Separator for the Recycling of Plastics from Waste Electrical and Electronic Equipment. *Journal of Electrostatics* **2013**, *71*, 681–688, doi:10.1016/j.elstat.2013.03.009.
43. Skowron, M.; Syrek, P.; Surowiak, A. The Application of the Electrodynamic Separator in Minerals Beneficiation. *IOP Conf. Ser.: Mater. Sci. Eng.* **2017**, *200*, 012017, doi:10.1088/1757-899X/200/1/012017.
44. Cieśla, A.; Kraszewski, W.; Skowron, M.; Surowiak, A.; Syrek, P. Wykorzystanie bębnowego separatora elektrodynamicznego do separacji odpadów elektronicznych. *Gospodarka Surowcami Mineralnymi* **2016**, *32*, 155–174, doi:10.1515/gospo-2016-0007.
45. Kumar, V.; Lee, J.; Jeong, J.; Jha, M.K.; Kim, B.; Singh, R. Recycling of Printed Circuit Boards (PCBs) to Generate Enriched Rare Metal Concentrate. *Journal of Industrial and Engineering Chemistry* **2015**, *21*, 805–813, doi:10.1016/j.jiec.2014.04.016.
46. Vermeșan, H.; Tiuc, A.-E.; Purcar, M. Advanced Recovery Techniques for Waste Materials from IT and Telecommunication Equipment Printed Circuit Boards. *Sustainability* **2019**, *12*, 74, doi:10.3390/su12010074.

47. Zhu, X.; Nie, C.; Wang, S.; Xie, Y.; Zhang, H.; Lyu, X.; Qiu, J.; Li, L. Cleaner Approach to the Recycling of Metals in Waste Printed Circuit Boards by Magnetic and Gravity Separation. *Journal of Cleaner Production* **2020**, *248*, 119235, doi:10.1016/j.jclepro.2019.119235.
48. Burat, F.; Özer, M. Physical Separation Route for Printed Circuit Boards. *Physicochemical Problems of Mineral Processing; ISSN 2084-4735* **2018**, doi:10.5277/PPMP1858.
49. Bilesan, M.R.; Makarova, I.; Wickman, B.; Repo, E. Efficient Separation of Precious Metals from Computer Waste Printed Circuit Boards by Hydrocyclone and Dilution-Gravity Methods. *Journal of Cleaner Production* **2021**, *286*, 125505, doi:10.1016/j.jclepro.2020.125505.
50. Barnwal, A.; Dhawan, N. Recovery of Copper Values from Discarded Random Access Memory Cards via Fluidization and Thermal Exposure. *Journal of Cleaner Production* **2020**, *256*, 120516, doi:10.1016/j.jclepro.2020.120516.
51. Ximei, L.; Yunfan, W.; Mingze, M.; Shuixiang, S.; Ying, Z.; Jiushuai, D.; Jian, L. Role of Dissolved Mineral Species in Quartz Flotation and Siderite Solubility Simulation. *Physicochemical Problems of Mineral Processing; ISSN 2084-4735* **2017**, doi:10.5277/PPMP170243.
52. Veit, H.M.; Diehl, T.R.; Salami, A.P.; Rodrigues, J.S.; Bernardes, A.M.; Tenório, J.A.S. Utilization of Magnetic and Electrostatic Separation in the Recycling of Printed Circuit Boards Scrap. *Waste Management* **2005**, *25*, 67–74, doi:10.1016/j.wasman.2004.09.009.
53. Lee, J.; Kim, Y.; Lee, J. Disassembly and Physical Separation of Electric/Electronic Components Layered in Printed Circuit Boards (PCB). *Journal of Hazardous Materials* **2012**, *241–242*, 387–394, doi:10.1016/j.jhazmat.2012.09.053.
54. Błaszczyński, S.; Plewa, F.; Szpyrka, J.; Suponik, T.; Lutyński, M.; Kujawska, M.; Dittrich, N.; Hadrian, H. Urządzenie Do Rozdziału Mieszanin Drobno-Uziarnionych Składników w Ośrodku Wodnym - Różniących Się Gęstością, Zgłoszenie Patentowe Nr P.424161, 2018.
55. Li, J.; Lu, H.; Guo, J.; Xu, Z.; Zhou, Y. Recycle Technology for Recovering Resources and Products from Waste Printed Circuit Boards. *Environ. Sci. Technol.* **2007**, *41*, 1995–2000, doi:10.1021/es0618245.
56. Wu, J.; Li, J.; Xu, Z. Electrostatic Separation for Recovering Metals and Nonmetals from Waste Printed Circuit Board: Problems and Improvements. *Environ. Sci. Technol.* **2008**, *42*, 5272–5276, doi:10.1021/es800868m.
57. Wu, J.; Qin, Y.; Zhou, Q.; Xu, Z. Impact of Nonconductive Powder on Electrostatic Separation for Recycling Crushed Waste Printed Circuit Board. *Journal of Hazardous Materials* **2009**, *164*, 1352–1358, doi:10.1016/j.jhazmat.2008.09.061.
58. Lu, H.; Li, J.; Guo, J.; Xu, Z. Movement Behavior in Electrostatic Separation: Recycling of Metal Materials from Waste Printed Circuit Board. *Journal of Materials Processing Technology* **2008**, *197*, 101–108, doi:10.1016/j.jmatprotec.2007.06.004.

59. De Oliveira, C.M.; Bellopede, R.; Tori, A.; Zanetti, G.; Marini, P. Gravity and Electrostatic Separation for Recovering Metals from Obsolete Printed Circuit Board. *Materials* **2022**, *15*, 1874, doi:10.3390/ma15051874.
60. Hamerski, F.; Krummenauer, A.; Bernardes, A.M.; Veit, H.M. Improved Settings of a Corona-Electrostatic Separator for Copper Concentration from Waste Printed Circuit Boards. *Journal of Environmental Chemical Engineering* **2019**, *7*, 102896, doi:10.1016/j.jece.2019.102896.
61. Dascalescu, L.; Iuga, A.; Morar, R. Corona–Electrostatic Separation: An Efficient Technique for the Recovery of Metals and Plastics From Industrial Wastes. *Magnetic and Electrical Separation* **1992**, *4*, 241–255, doi:10.1155/1993/59037.
62. Yao, Y.; Bai, Q.; He, J.; Zhu, L.; Zhou, K.; Zhao, Y. Reverse Flotation Efficiency and Mechanism of Various Collectors for Recycling Waste Printed Circuit Boards. *Waste Management* **2020**, *103*, 218–227, doi:10.1016/j.wasman.2019.12.030.
63. Jeon, S.; Ito, M.; Tabelin, C.B.; Pongsumrankul, R.; Kitajima, N.; Park, I.; Hiroyoshi, N. Gold Recovery from Shredder Light Fraction of E-Waste Recycling Plant by Flotation-Ammonium Thiosulfate Leaching. *Waste Management* **2018**, *77*, 195–202, doi:10.1016/j.wasman.2018.04.039.
64. Han, J.; Duan, C.; Li, G.; Huang, L.; Chai, X.; Wang, D. The Influence of Waste Printed Circuit Boards Characteristics and Nonmetal Surface Energy Regulation on Flotation. *Waste Management* **2018**, *80*, 81–88, doi:10.1016/j.wasman.2018.09.002.
65. Polskie Sieci Elektroenergetyczne Rynkowa Cena Energii Elektrycznej z Dnia 25.04.2023 Dostępny online: https://www.pse.pl/dane-systemowe/funkcjonowanie-rb/raporty-dobowe-z-funkcjonowania-rb/podstawowe-wskazniki-cenowe-i-kosztowe/rynkowa-cena-energii-elektrycznej-rce (dostęp 25 kwietnia 2023).

Wykaz publikacji

Lp.	Publikacja	Punkty MEiN	Impact Factor
	GŁÓWNE PUBLIKACJE		
1.	*Recovery of metals from printed circuit boards by means of electrostatic separation,* Franke D., Suponik T., Nuckowski P., Gołombek K., Hyra K., Management Systems in Production Engineering, P.A. NOVA S.A., vol. 28, nr 4, 2020, s. 213-219, DOI:10.2478/mspe-2020-0031	70	1,003
2.	*Impact of grinding of printed circuit boards on the efficiency of metal recovery by means of electrostatic separation,* Suponik T., Franke D., Nuckowski P., Matusiak P., Kowol D., Tora B., Minerals, vol. 11, nr 3, 2021, 281, s. 1-21, DOI:10.3390/min11030281	100	2,818
3.	*Evaluation of the efficiency of metal recovery from printed circuit boards using gravity processes.,* Franke D., Suponik T., Nuckowski P., Dubaj J., Physicochemical Problems of Mineral Processing, vol. 57, nr 4, 2021, s. 63-77, DOI:10.37190/ppmp/138471	70	1,047
4.	*Evaluation of the use of flotation for the separation of ground printed circuit boards,* Franke D., Kar U., Suponik T., Siudyga T., Gospodarka Surowcami Mineralnymi – Mineral Resources Management, Polska Akademia Nauk, vol. 38, nr 1, 2022, s. 171-188, DOI:10.24425/gsm.2022.140605	100	0,938
5.	*Morphology, phase and chemical analysis of leachate after bioleaching metals from printed circuit boards,* Hyra K., Nuckowski P., Willner J., Suponik T., Franke D., Pawlyta M., Matus K., Kwaśny W., Materials, MDPI, vol. 15, nr 13, 2022, 4373, s. 1-17, DOI:10.3390/ma15134373	140	3,4
6.	*Recycling of waste printed circuit boards – application potential and selection of eco-efficient methods,* Franke D., Suponik T., Journal of Cleaner Production, Elsevier (manuskrypt w trakcie recenzji)	-	-
	Suma wskaźników bibliometrycznych głównych publikacji:	**480**	**9,206**
	POZOSTAŁE PUBLIKACJE Z ZAKRESU ROZPRAWY DOKTORSKIEJ		
7.	*Metals recovery from e-scrap using gravity, electrostatic and magnetic separations,* Franke D., Suponik T., Innovative Mining Technologies: IMTech 2019 Scientific and Technical Conference, 25-27 Marca 2019, Szczyrk, Polska, IOP Conference Series: Materials Science and Engineering, nr 545, 2019, IOP Publishing, art. no. 012016 1-9, DOI:10.1088/1757-899X/545/1/012016	20	0
8.	*Electrostatic and magnetic separations for the recovery of metals from electronic waste.* Suponik T., Franke D., Nuckowski P., Mineral Engineering Conference: MEC 2019, 16-19 Września 2019, Kocierz, Beskid Mały, Poland, IOP Conference Series: Materials Science and Engineering, nr 641, 012017, 2019, IOP Publishing, s. 1-8, DOI:10.1088/1757-899X/641/1/012017	20	0
9.	*Odzysk metali z odpadów elektronicznych,* Suponik T., Nuckowski P., Willner J., *Franke D.*, Hyra K., Polak J., Lewandowski D., Gaweł M., w *PM News: Czasopismo Koła Zarządzania Projektami SOLVER*, nr 23, 2020, s. 25	0	0
10.	*Physical processing in waste printed circuit boards recycling: current state of research,* Franke D., Suponik T., Nuckowski P., w *Global challenges for a sustainable society. EURECA-PRO. The*	20	0

	European university for responsible consumption and production, Springer Proceedings in Earth and Environmental Sciences, Springer. J. Benítez-Andrades, P. García-Llamas, Á. Taboada, L. Estévez-Mauriz, R. Baelo, Red. 2023, s. 51-57		
11.	*Przegląd piśmiennictwa z zakresu gospodarowania elektroodpadami oraz metod odzysku metali z płyt obwodu drukowanego (PCB),* Hyra K., Nuckowski P., Kwaśny W., Suponik T., Franke D., w *Interdyscyplinarne badania młodych naukowców*, Wydawnictwo Politechniki Śląskiej, B. Balon, Red. 2023, s. 136–164	20	0
12.	*Gospodarka obiegu zamkniętego: Odzysk metali z płyt obwodów drukowanych,* Willner J., Fornalczyk A., Saternus M., Franke D., Suponik T., Turek M., Dydo P., Jakóbik-Kolon A., Kluczka J., Mitko K., w Ochrona klimatu i środowiska, nowoczesna energetyka: Praca zbiorowa pod red. Werle S., Ferdyn-Grygierek J., Szczygieł M., Monografia, Politechnika Śląska, vol. 909, 2021, Politechnika Śląska, ISBN 978-83-7880-790-2, s. 71-102	20	0
Suma wskaźników bibliometrycznych pozostałych publikacji z zakresu rozprawy doktorskiej:		**100**	**0**
POZOSTAŁE PUBLIKACJE ZPOZA ZAKRESU ROZPRAWY DOKTORSKIEJ			
13.	*The testing of waste from the installation of salt debris leaching,* Suponik T., Pierzyna P., Franke D., Adamczyk Z., Mineral Engineering Conference: MEC 2018, 26-29 Wrzesień 2018, Zawiercie, Poland: Lutyński M., Suponik T. (red.), IOP Conference Series: Materials Science and Engineering, nr 427, 2018, IOP Publishing, art. nr 012040, s. 1-9, DOI:10.1088/1757-899X/427/1/012040	20	0
14.	*The impact of precipitation on the groundwater of coal waste dump,* Suponik T., Franke D., Frączek R., Nowińska K., Pierzyna P., Różański Z., Wrona P.,Journal of Sustainable Mining, vol. 20, nr 1, 2021, 5, s. 11-19, DOI:10.46873/2300-3960.1031	70	0
15.	*Prediction and Potential Treatment of Underground Contaminated Water Based on Monitoring of pH and Salinity in a Coal Mine Waste Heap, Southern Poland,* Suponik T., Franke D., Neculita C., Mzyk T., Frączek R., Minerals, MDPI, vol. 12, nr 4, 2022, 391, s. 1-17, DOI:10.3390/min12040391	100	2,818
16.	*Selective crushing of run-of-mine as an important part of the hard coal beneficiation process,* Matusiak P., Kowol D., Suponik T., Franke D., Nuckowski P., Tora B., Pomykała R., Energies, vol. 14, nr 11, 2021, 3167, s. 1-15, DOI:10.3390/en14113167	140	3,252
17.	*A study on the hard coal grindability dependence on selected parameters,* Kogut K., Cablik V., Matusiak P., Kowol D., Suponik T., Franke D., Tora B., Pomykała R., Energies, vol. 14, nr 23, 2021, 8158, s. 1-9, DOI:10.3390/en14238158	140	3,252
18.	*Zrównoważone certyfikowane budynki,* Franke D., Kuczera A., Polskie Stowarzyszenie Budownictwa Ekologicznego PLGBC, 2023	0	0
19.	*Certyfikacja zrównoważonych budynków w Polsce,* Franke D, Real Estate Magazine 3/2023, 2023	0	0
20.	*Influence of citrus fruit waste filler on the physical properties of silicone-based composites,* Mrówka M., Franke D., Ošlejšek M., Jureczko M., Materials, MDPI, vol. 16, nr 19, 2023; 6569, s. 1-15, DOI:10.3390/ma16196569	140	3,4
Suma wskaźników bibliometrycznych pozostałych publikacji spoza zakresu rozprawy doktorskiej:		**610**	**11,722**
SUMA WSKAŹNIKÓW BIBLIOMETRYCZNYCH:		**1 190**	**20,928**

Główne publikacje

minerals

MDPI

Article

Impact of Grinding of Printed Circuit Boards on the Efficiency of Metal Recovery by Means of Electrostatic Separation

Tomasz Suponik [1,*], Dawid M. Franke [1], Paweł M. Nuckowski [2], Piotr Matusiak [3], Daniel Kowol [3] and Barbara Tora [4]

[1] Institute of Mining, Faculty of Mining, Safety Engineering and Industrial Automation, Silesian University of Technology, 2 Akademicka Street, 44-100 Gliwice, Poland; dawid.franke@polsl.pl
[2] Materials Research Laboratory, Faculty of Mechanical Engineering, Silesian University of Technology, 18A Konarskiego Street, 44-100 Gliwice, Poland; pawel.nuckowski@polsl.pl
[3] KOMAG Institute of Mining Technology, 37 Pszczynska, 44-101 Gliwice, Poland; pmatusiak@komag.eu (P.M.); dkowol@komag.eu (D.K.)
[4] Faculty of Mining and Geoengineering, AGH University of Science and Technology, 30 Mickiewicza, 30-059 Kraków, Poland; tora@agh.edu.pl
* Correspondence: tomasz.suponik@polsl.pl

Abstract: This paper analyses the impact of the method of grinding printed circuit boards (PCBs) in a knife mill on the efficiency and purity of products obtained during electrostatic separation. The separated metals and plastics and ceramics can be used as secondary raw materials. This is in line with the principle of circular economy. Three different screen perforations were used in the mill to obtain different sizes of ground grains. Moreover, the effect of cooling the feed to cryogenic temperature on the final products of separation was investigated. The level of contamination of the concentrate, intermediate, and waste obtained as a result of the application of fixed, determined electrostatic separation parameters was assessed using ICP-AES, SEM–EDS, XRD, and microscopic analysis as well as specific density. The yields of grain classes obtained from grinding in a knife mill were tested through sieve analysis and by using a particle size analyser. The test results indicate that using a knife mill with a 1 mm screen perforation along with cooling the feed to cryogenic temperature significantly improves the efficiency of the process. The grinding products were characterised by the highest release level of the useful substance—metals in the free state. The purity of the concentrate and waste obtained from electrostatic separation was satisfactory, and the content of the intermediate, in which conglomerates of solid metal–plastic connections were present, was very low. The yield of concentrate and waste amounted to 26.2% and 71.0%, respectively. Their purity, reflected in the content of the identified metals (valuable metals), was at the level of 93.3% and 0.5%, respectively. In order to achieve effective recovery of metals from PCBs by means of electrostatic separation, one should strive to obtain a feed composed of grains <1000 μm and, optimally, <800 μm.

Keywords: metals recovery; printed circuit board; cryogenic grinding; electrostatic separation; atomic emission spectroscopy; scanning electron microscopy (SEM); X-ray diffraction (XRD)

Citation: Suponik, T.; Franke, D.M.; Nuckowski, P.M.; Matusiak, P.; Kowol, D.; Tora, B. Impact of Grinding of Printed Circuit Boards on the Efficiency of Metal Recovery by Means of Electrostatic Separation. *Minerals* **2021**, *11*, x. https://doi.org/10.3390/xxxxx

Academic Editor: Zenixole Tshentu, Durga Parajuli

Received: 20 January 2021
Accepted: 2 March 2021
Published: date

1. Introduction

In line with the circular economy principle, and for economic and environmental reasons, the recovery of metals from printed circuit boards (PCBs) is not only required—it is obligatory. The production process created for this purpose should be characterised by high efficiency, low costs, and a low impact on the natural environment. The method for preparing PCBs for separation processes is crucial in terms of purity and efficiency of the products obtained. The correct method for PCB grinding can facilitate the full release

of useful components (i.e., metals in the free state) to produce pure concentrate in the separation processes and minimise the effect of penetration of metals into waste.

According to Vermesan et al. [1], PCB recycling directions should include disassembly (i.e., removal of hazardous products, such as batteries and capacitors), treatment (i.e., reduction of PCB dimensions), and finally, processing of the obtained products. This approach can provide economic and environmental benefits in the recovery of metals, but also of plastics and ceramics from PCBs.

The rapid advancement of computer technologies has contributed to a change in consumption patterns, which has resulted in a mass replacement of devices with new ones with much higher efficiencies [2]. In 2019, 53.6 million tonnes of electronic waste was generated. It is 9.2 million tonnes more compared with that in 2014 [3]. As a result, even greater amounts of waste electrical and electronic equipment (WEEE) are generated. They contain toxic heavy metals and halogenated flame retardants [4], which may penetrate into the aquatic environment. One of the basic building blocks of WEEE are PCBs [2]. Their content of metals is significantly higher than in natural metal ores [5–8]. PCBs are composed of about 30% metals in the free state and about 70% components, such as glass fibre, epoxy resin, and polyester. For the sake of simplicity, these components of PCBs are hereinafter referred to as plastic and ceramic materials [9,10]. Depending on the material used to build the laminate (dielectric materials), there are many types of PCBs, such as FR-2 to 6, G-10, G-11, and CEM-1 to 8 [10,11]. The most common type is FR-4, whose laminate mainly consists of epoxy resin reinforced with glass fibres and SiO_2 (approximately 40%), CaO (approximately 20%), and smaller amounts of Al_2O_3, MgO, and BaO [12]. This type of boards allows for the use of high operating temperatures (130 °C and above). To improve this property of PCBs, flame retardants are used, which include bromine and antimony compounds [11,13]. PCBs, depending on the manufacturer, production date, and destination, exhibit different metal contents. The estimated contents of noble (Au, Ag, and Pd) and seminoble (Cu) metals in PCBs are 0.05%, 0.03%, 0.01%, and 16%, respectively. Moreover, other metals occur in small concentrations in PCBs: 3% Fe, 3% Sn, 2% Pb, 1% Zn, and trace amounts of Al, Ni, Cr, Na, Cd, Mo, Ti, and Co [10,14,15]. Due to their properties, noble metals have found their application in the production of PCBs, mainly as contact metals [16]. Gold is used in bonding wires, contacts, and integrated circuits. Silver is used as contacts, switches, and solders, while palladium and platinum are used for multilayer capacitors and connectors as well as hard disks, thermocouples, and fuel cells, respectively [17]. As a seminoble (but the most abundant) metal, copper is used in the production of cables, wires, connectors, and other components [17]. The amount of precious metals, such as gold, silver, and palladium, contained in e-waste is increasing rapidly, with used mobile phones having the largest share [18]. According to the work of Hagelüken [19], about 350 g/t Au, 1380 g/t Ag, and 210 g/t Pd are present in PCBs and other components of mobile phones.

E-waste raw materials were estimated to be worth USD 57 billion in 2019. This concerns about 17% of e-waste documented in that year. The value of the processed waste can be estimated to be about USD 10 billion. However, the processing of about 83% of e-waste generated in 2019 was not documented, which contributed to environmental interference and the impact on employees' health [3,20]. Therefore, proper recycling of WEEE is necessary, not only for the protection of the environment and natural resources, but also for economic reasons, creation of new jobs, and reduction of the impact of landfills on the landscape [21,22].

The methods for recovering metals from PCBs can be divided into physical and chemical methods [23], including the use of microorganisms (bioleaching) [24]. Some of the chemical ones, especially pyro- and hydro-metallurgical methods, have a significant impact on the natural environment, including water and air pollution and waste generation [25–27]. Compared with other chemical methods, bioleaching has a negligible impact on the environment; however, these are long-term methods [28]. Therefore, the possibility

of using known, cheap, and environmentally friendly solutions is being analysed. These certainly include the methods of grinding and electrostatic separation.

The efficiency of metal recovery using these methods depends on the degree of metal release. Therefore, in order to ensure high efficiency of electrostatic separation, PCBs should be ground to release the useful components (i.e., metals) from plastic and ceramic materials. This process is characterised by high energy consumption [9,29]. PCBs are characterised by a complicated structure, as they are composed of many conductive layers (mainly copper) placed on nonconductive substrates [24,30]. Each component may consist of various elements mechanically connected with each other [31,32]. Additionally, the materials used in PCBs are characterised by varied mechanical properties. Most boards have a glass fibre substrate that breaks easily when shear forces are applied. Selective grounding of PCBs can be performed in knife or hammer mills [22,33]. In order to adjust the process, multistage grinding or grinding with liquid nitrogen can be used [22,33–35].

The recovery of metals from PCBs with the use of electrostatic separation has already found application in some places of the globe [8,36–38]. It consists of grain separation due to the differences in the ability to accumulate surface charges and electric current conductivity properties [29,39,40]. The literature contains two main solutions for the construction of electrostatic separators: drum and free-fall electrostatic separators [41,42]. In the case of drum separators, the separation efficiency depends on the voltage, the rotational speed of the drum, the electrode position, and the feed efficiency (separator load) [43,44]. The selection of separation parameters depends mainly on the design of the device and grain size. With the inappropriate selection of parameters, electrostatic separation will not be effective and may even damage the electrode through spark discharge [40]. Large grains are often combinations of metals with plastic and ceramic materials, and thus the efficiency of metal recovery from PCBs may be low [36,45]. Depending on the conditions of the separation process, the type of feed fed to the separator, the following product ranges can be obtained: 9%–27% conductive grains (metals), 2%–6% mixed grains, and 67%–85% nonconductive grains [38,43].

The aim of the study was to assess the impact of the PCB grinding method in a knife mill on the purity of products obtained during electrostatic separation. The level of contamination of the concentrate, intermediate, and waste obtained as a result of the application of fixed, determined electrostatic separation parameters was assessed using inductively coupled plasma atomic emission spectroscopy (ICP-AES), specific density analysis using a pycnometer and ethyl alcohol (PN-EN 1097-7 No. 2001), scanning electron microscope (SEM) with energy dispersive X-ray spectroscopy (EDS), microscopic analysis using stereo microscope, and X-ray powder diffraction (XRD).

2. Materials and Methods

2.1. Grinding Materials and Methods

Motherboards manufactured by Gigabyte, Intel, Nvidia, MSI, and Asus in 2007–2009 were used in the tests. These are the most common FR-4 boards, the laminate of which is made of fibre glass with epoxy resin [31,46]. Before commencing the grinding, the boards were manually disassembled with the use of workshop tools (screwdrivers and pliers) [47], and components of a different physical and chemical nature, which could have disturbed the process of grinding and electrostatic separation, were easily removed. These components included resistors (Ni, Cr, Cd, Al, Pb, and Ta), transistors (Pb and Cu), batteries, chips (Pb, Ni, Sn, Ga, Al, and Ag), capacitors (Sn, Cu, and Zn), electromagnetic interference filters (Fe, Cu, and Zn), connectors (Pb, Ni, and Sn), screws, and switches [48].

A LMN-100 knife mill from Testchem (Radlin, Poland) [49] was used in the grinding processes. In mills of this type, the grinding takes place by cutting the material by knives mounted on the device body and a rotator. These mills are equipped with a screen to determine the size of the ground material. The feed to the mill were PCBs cut into 3 × 3 cm pieces. The following different process conditions (options) were used to produce the grinding product in different grain classes:

- option 1—1 mm screen perforation, mill load (capacity of feeding the material to the mill): 5 g/min;
- option 2—1 mm screen perforation, cooling the feed with liquid nitrogen, mill load: 20 g/min;
- option 3—2 mm screen perforation, mill load: 10 g/min;
- option 4—3 mm screen perforation, mill load: 10 g/min.

The other process parameters remained unchanged and were as follows:

- rotator speed: 2815 min^{-1};
- gap between the knives in the mill: 0.5 mm.

During the PCB grinding, the mill was not allowed to overload, which could contribute to high temperatures in the grinding working chamber, causing the formation of conglomerates—solid metal–plastic–ceramic compounds. Therefore, different mill loads were used in different options. Despite this, it was noticed that the temperature in the working chamber of the mill was increasing. In option 2, liquid nitrogen was used to reduce the temperature of the ground PCBs to the level of cryogenic temperatures (below −150 °C). The cooling process consisted in placing the feed into a container filled with liquid nitrogen. The feed was cooled until liquid nitrogen ceased to boil.

2.2. Electrostatic Separation

In order to recover metals from ground PCBs, electrostatic separation was used consisting in grain separation due to differences in the ability to accumulate surface charges and the properties of electric current conductivity [29,39,40]. The tests were carried out in a drum electrostatic separator from Boxmag-rapid Ltc. (Aston, Birmingham, UK), which allows for a three-product separation into waste, intermediate, and concentrate. The design of the device allows for the optimisation of the separation conditions by means of changing the rotational speed of the shaft (i.e., the material feeding efficiency, the voltage flowing through the electrode, and its distance from the shaft). The diagram and structure of the device is shown in Figure 1.

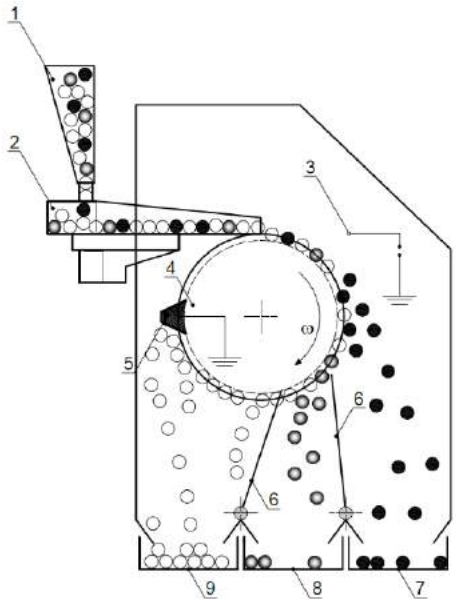

Figure 1. Diagram of the electrostatic separator: 1—feed container, 2—vibrating feeder, 3—electrode, 4—drum, 5—brush, 6—partition, 7—conductor container (concentrate), 8—container for complex grains folded with metals and nonmetals, and 9—nonconductor container (waste).

In the case of perfect separation, grains with good electrically conductive properties (e.g., metals in the free state) will be the first to detach from the drum to form a concentrate, while nonconductive grains (plastics and ceramics) will detach last or will be pulled

off with a brush, creating waste. Grains that show moderate conductive properties or poor capacity to accumulate surface charges (e.g., solid metal–plastic–ceramic compounds) will detach between the concentrate and the waste and form the intermediate. On the basis of preliminary tests and previous studies by Suponik and Franke [50,51], it was decided that electrostatic separation, aimed at selecting the optimal option of PCB grinding, would be performed for the following technical parameters: shaft rotation speed of 100 rpm, voltage of 17 kV, distance between electrode and drum of 0.03 m.

2.3. Product Analysis

After PCB grinding, particle size analysis of the obtained material was carried out using the following:

- Fritsch screens with mesh sizes of 2 mm, 1.4 mm, 1 mm, 710 μm, 500 μm, 355 μm, 250 μm, 180 μm, 125 μm, and 90 μm.
- ANALYSETTE 22 MicroTec Plus Laser Particle Sizer (Fritsch, Germany)—the measurement was not carried out on material obtained from grinding in a mill with a screen with 2 and 3 mm perforation due to limitations in the measurement of grain size.

Two methods of analysis were used in the study, as the grains had different sizes, shapes, and wettability. In the particle size analyser, the tiniest hardly wettable particles, occurring in low amounts, were removed prior to the analysis.

The electrostatic separation products obtained for the analysed options of PCB grinding were analysed via the following:

- ICP-AES—using the JY2000 Optical Emission Spectrometer (by Jobin Yvon) in order to assess the content of elements in products. The source of the induction was a plasma torch coupled with a 40.68 MHz frequency generator; the products were previously dissolved.
- Specific density analysis—using Gay-Lussac pycnometers on the basis of PN-EN 1097-7:2001 with the use of ethyl alcohol with a density of 0.7893 g/cm^3.
- Microscope analysis with Zeiss SteREO Discovery Modular Stereo Microscope (Carl Zeiss AG, Jena, Germany).

For the best selected option of PCB grinding, the obtained concentrate and intermediate were subsequently analysed using the following:

- High-resolution Zeiss SUPRA 35 scanning electron microscope (Carl Zeiss AG, Germany), equipped with EDAX energy dispersive X-ray spectroscopy (EDS) chemical analysis system (EDAX, Mahwah, NJ, USA).
- Qualitative phase analysis was performed with the use of a Panalytical X'Pert Pro MPD diffractometer (Panalytical, Almelo, The Netherlands), utilising filtered radiation of a cobalt anode lamp ($\lambda_{K\alpha}$ = 0.179 nm). The diffraction lines were recorded in the Bragg–Brentano geometry, using the step-scanning method by means of a PIXcell 3D detector on the diffracted beam axis, in the angle range of 20°–100° [2θ] (step, 0.05°; count time per step, 200 s). The obtained diffractograms were analysed with the use of Panalytical HighScore Plus (v. 3.0e) software with the PAN-ICSD database.

Due to the presence of large amounts of plastics in the feed and waste from electrostatic separation and the possibility of damaging the equipment, SEM-EDS and XRD analyses were not performed for these products.

3. Results

3.1. Grinding

The results of the grain analysis of the PCBs ground in a knife mill for various process options are presented in Table 1. Due to the fibrous/needle shape of the ground grains of epoxy resin and glass fibre (Figure 2) and various shapes of the fragmented metal particles (Figures 3 and 4), it was difficult to unambiguously determine and assess the grain size.

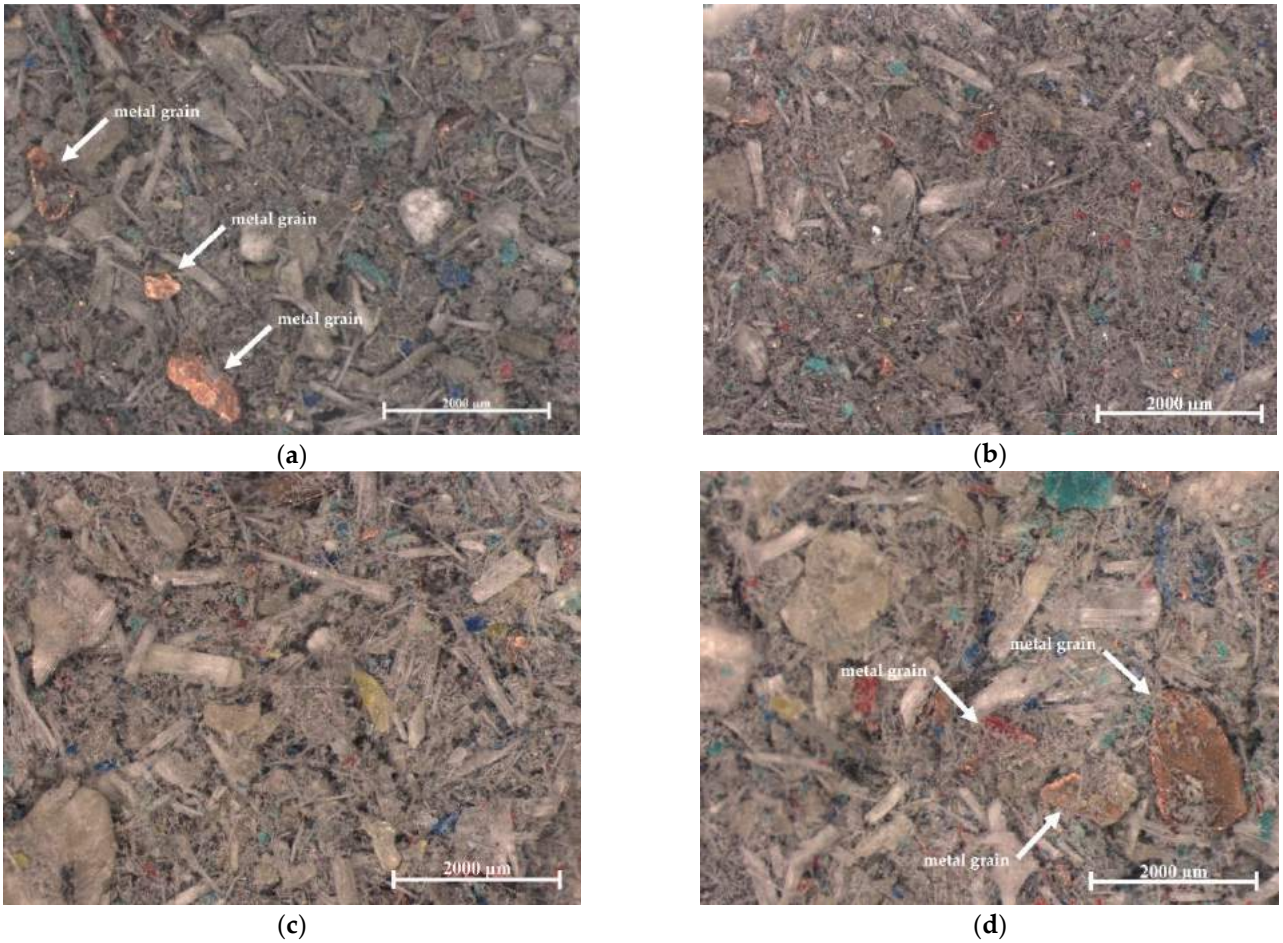

Figure 2. Waste from electrostatic separation (stereo microscope): (**a**) option 1, (**b**) option 2, (**c**) option 3, (**d**) and option 4.

Table 1. Yield of grinding product grain classes.

Grain Class, mm	Yield of Product, %					
	Option 1 [a]	Option 1 [b]	Option 2 [a]	Option 2 [b]	Option 3 [a]	Option 4 [a]
>2.0	0.0	0.0	0.0	0.0	0.0	0.2
2.0–1.4	0.0	0.0	0.0	0.0	0.4	13.7
1.4–1.0	0.3	0.0	0.4	0.0	11.1	24.6
1.0–0.71	5.7	5.2	3.6	1.6	25.6	16.8
0.71–0.50	14.1	14.8	13.0	10.4	15.6	10.7
0.50–0.36	19.3	22.0	19.5	22.1	11.6	8.4
0.36–0.25	17.0	10.4	17.0	14.2	8.6	6.3
0.25–0.18	9.6	5.6	10.6	6.5	5.0	4.1
0.18–0.13	8.5	4.9	10.8	5.3	4.5	4.5
0.13–0.09	9.1	3.8	8.5	4.3	3.6	4.2
<0.09	16.3	33.3	16.6	35.6	13.9	6.5

[a] analysis carried out with Fritsch screens, [b] analysis carried out with the particle size analyser.

As could be expected, however, with the increase of the screen perforation in the knife mill (options 3 and 4), the material obtained after grinding was characterised by larger grain sizes. The largest content in options 3 and 4 was represented by 1.4–0.355 mm and 2.0–0.5 mm grain classes, respectively (Table 1). For options 1 and 2 (i.e., with the use of a screen with a 1 mm perforation), respectively, without and with cooling the feed to cryogenic temperatures, the shredded material was obtained mainly in classes from 1.0 to

0.25 mm and <0.09 mm, while for option 2, the grains were generally slightly smaller (Table 1). For example, material with a size <0.5 mm was represented at 88% for this option and at 80% for option 1. The differences in the results between the sieve analysis and the particle size analyser are due to the different shapes of the grains. For metals, the grains were mainly globular, patch, and needle shaped, and for plastic and ceramic materials, fibrous and patch shaped.

3.2. Analysis of the Electrostatic Separation Efficiency

Based on the density of the products obtained from electrostatic separation (Table 2), it can be concluded that its efficiency, manifested by the purity of the concentrate (the presence of metals with a minimum amount of plastic and ceramic materials) and waste (the presence of plastic and ceramic materials with a minimum amount of metals), increases with the degree of PCB grinding. The higher the density of the separation product, the higher the metal content and the lower the plastic and ceramic content. The highest and lowest densities of the concentrate and the lowest and highest densities of waste were obtained for options 2 and 4, respectively. This is correlated with the grain size, which in turn is related to the release of useful components (i.e., metals). A high purity of the concentrate and waste was also achieved for option 1. However, at low temperatures (option 2 of the grinding process), due to the use of liquid nitrogen to cool the feed, there was no significant increase in temperature in the mill's working chamber, and no plasticisation of the shredded material, and no (or less) solid metal–plastic–ceramic compounds.

However, the yield of concentrates and intermediates in options 1 and 2 is the lowest. In both cases, as previously noted, the presence of plastic and ceramic materials was minimised. The most concentrate and the least waste were obtained for option 4. However, taking into account the densities of plastics, ceramics, and metals, it is concluded that the separation products for option 4 are highly contaminated. This is due to the low degree of grinding, which did not allow the sufficient release of useful substances (metals in the free state) from the PCB composite.

Table 2. Yield and density of electrostatic separation products.

Grinding Option	Yield of Product, %			Density, g/cc		
	Waste	Intermediate	Concentrate	Waste	Intermediate	Concentrate
Option 1	71.5	2.8	25.8	2.61	5.98	8.78
Option 2	71.0	2.8	26.2	2.29	5.33	8.87
Option 3	66.7	6.1	27.2	2.92	3.76	7.32
Option 4	50.4	6.3	43.2	3.35	3.5	5.51

Figures 2–4 present pictures of the waste, intermediate, and concentrate (made with a stereo microscope), respectively, from the electrostatic separation process obtained for different grinding options. They confirm that the sizes of all grains decreased along with the reduction of perforation in the knife mill screens. Using additional cooling of the feed in option 2, the smallest grain sizes were obtained, which is particularly noticeable for the intermediate (Figure 3b).

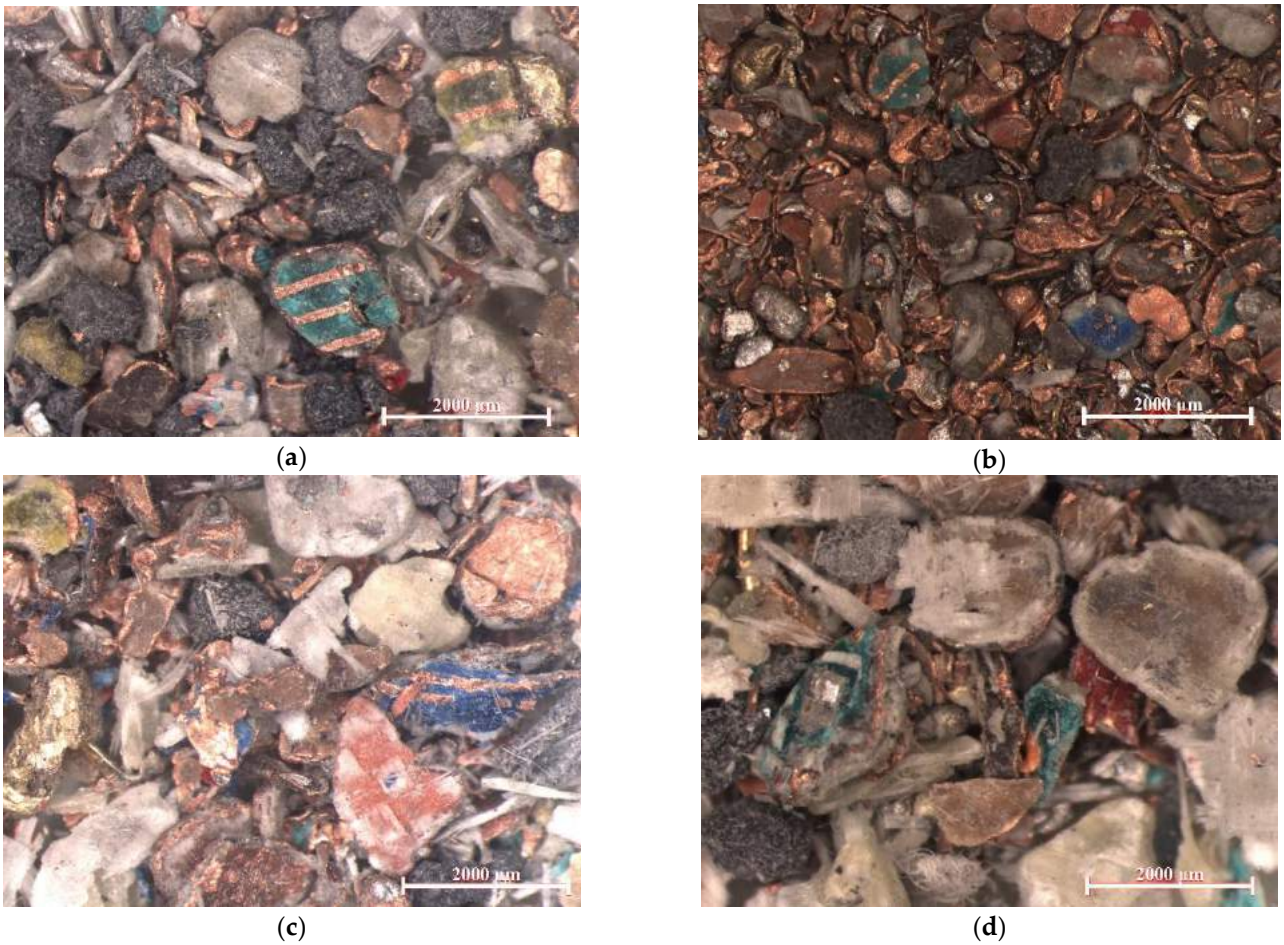

(**a**) (**b**)

(**c**) (**d**)

Figure 3. Intermediate from electrostatic separation (stereo microscope): (**a**) option 1, (**b**) option 2, (**c**) option 3, (**d**) and option 4.

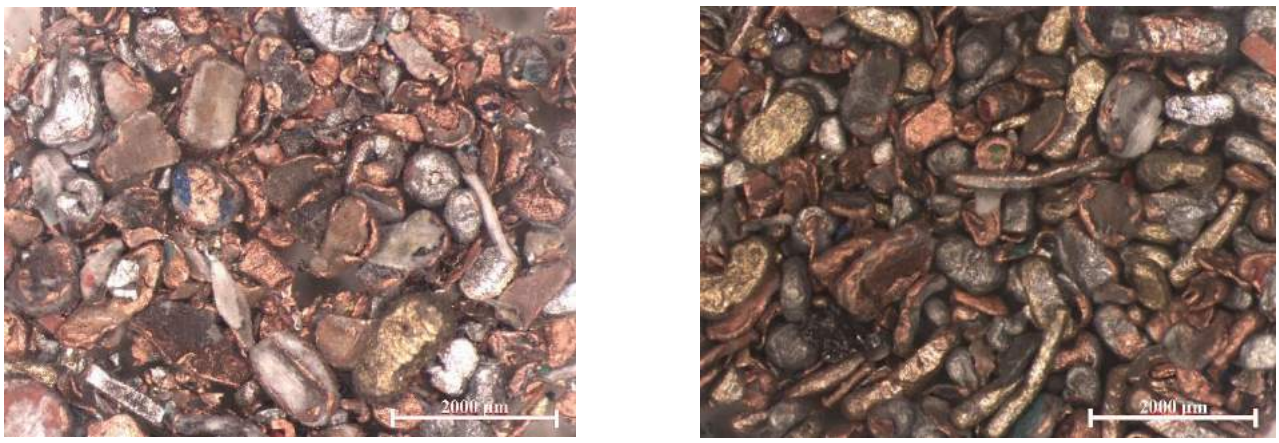

(**a**) (**b**)

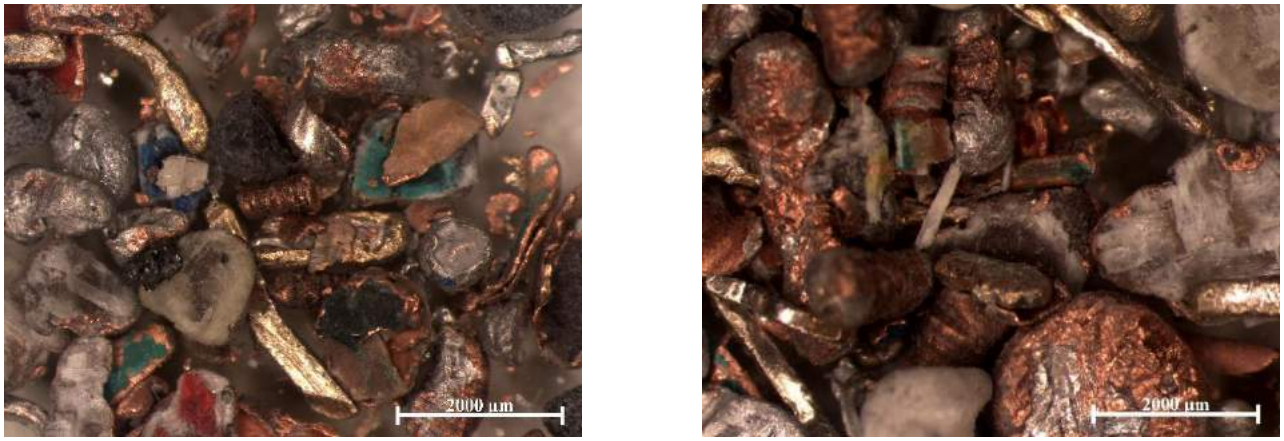

(**c**) (**d**)

Figure 4. Concentrate from electrostatic separation (stereo microscope): (**a**) option 1, (**b**) option 2, (**c**) option 3, (**d**) and option 4.

In the waste for all grinding options (Figure 2), there were small amounts of metal grains or metal–plastic–ceramic conglomerates, while in the intermediates (Figure 3), there were many grains that clearly indicated these compounds. The waste (Figure 2) consisted mainly of fibrous and needle-shaped grains. Compared with other separation products, the greatest diversity of grains was observed in terms of their size, from less than 50 µm (fibre/needle thickness) to over 2000 µm. However, in the waste for options 1 and 2, grains larger than 1000 µm were relatively the scarcest. The penetration of grains larger than the screen used in the mill resulted from the elongated shape of the grains. The intermediates (Figure 3) consisted mainly of patch grains and globular grains. The grains presented in Figure 3c,d have a layer structure characteristic of PCBs. This shows that the level of grinding is insufficient. For option 2, the grain size was the least diversified (Figure 2b). There were mainly thin patch grains with a diameter of 150 to 1000 µm. The yield of intermediates for options 1 and 2 was, however, very small, amounting to 2.8%. This shows that only a small fraction of the metals was not released sufficiently in the grinding process. In the intermediate of option 2, the least compounds of this type are observed, which may indicate the highest degree of release of the useful substance from the composite among the options. This part can be recycled for further grinding or processed using other metal recovery methods, such as bioleaching [28,52].

For the concentrates obtained in the third and fourth grinding options (Figure 4c,d), numerous metal–plastic–ceramic compounds are visible, which is not the case for option 1 (Figure 4a), and especially option 2 (Figure 4b). In the group of all concentrates (Figure 4), the greatest differentiation in terms of grain shape can be observed. There were polyhedral, globular, patch, and irregular grains here. The concentrate for option 2 (Figure 4b), as compared with the others, was characterised by the smallest differentiation in terms of grain size and shape (the grains were more rounded). This shows that the strength properties of PCBs have changed at cryogenic temperatures due to the application of liquid nitrogen. Option 2 was dominated by grains of globular shape (most abundant in the range of 250–500 µm) and patch shape (patch thickness, >30 µm; width, ~500 µm). In the case of polyhedral grains, the transverse dimensions ranged from 200 to 350 µm. Irregular grains were probably created as a result of crushing the patch grains.

In order to improve the efficiency of electrostatic separation, the process can be optimised by adjusting the voltage applied to the electrode, the distance between the electrode and the device's shaft, and the shaft rotation speed. Failure to adjust the last of the mentioned parameters could cause very fine metal particles to penetrate into the intermediate and waste. These particles were affected by a very small centrifugal force due to the movement of the separator shaft.

The grains of metals, probably copper, with dimensions of 450, 800, and 1200 μm, visible in Figure 2a,d, characterised by a patch shape, could have penetrated into the waste and the intermediate due to the presence of plastic and ceramic materials in the grain or as a result of being covered by grains made of plastic and ceramic materials (aggregation effect) [36]. The results of the tests of the chemical compositions of the feed and electrostatic separation products for all analysed grinding options are presented in Table 3 (the measurements were made using ICP-AES). In the feed, the main identified elements were Cu (17.70%), Si (12.02%), Ca (6.56%), Sn (2.92%), Al (1.95%), Br (1.64%), and less than 1% of Zn, Mg, Pb, Fe, Ba, Ti, Sb, Ni, Cr, Mn, and Ag (0.0301%), and Au (0.0029%). The remaining unidentified part of the feed probably consists of the components of epoxy resins, which mainly include polyphenols, less often polyglycols, and epichlorohydrin or oligomers [53–55].

Concentrates obtained from electrostatic separation, first, second, third, and fourth grinding options, contained 86.6%, 93.3%, 76.0%, and 54.4% of valuable metals, respectively, among which for the most effective option 2, 68.5% Cu, 0.1074% Ag, 0.0142% Au, and 2.7%, 2.0%, 9.6%, and 9.8% residues constituting nonvaluable elements were identified. The second group of elements includes Sb, Ca, Br, Ba, Mg, Mn—components of epoxy resins used to improve the properties of PCBs, especially as flame retardants [12]—and Si, a component of glass fabrics [10].

In the concentrate for option 2, the share of precious metals was clearly visible, which was 0.1074% for silver and 0.0092% for gold. The most abundant metal in the concentrate was copper (68.5%), followed by tin (11.5%) and aluminium (6.8%). Higher amounts of metals as compared with the other options also applied to metals such as zinc, magnesium, lead, barium, calcium, iron, nickel, titanium, and chromium.

As can be seen above, the concentrate obtained from option 2 contained much larger amounts of valuable metals than those from options 3 and 4 and slightly larger amounts than that from option 1. This demonstrates that the efficiency of the electrostatic separation process is influenced by the method of preparing the feed for the separator—first, the perforation in the knife mill screen, and then the cooling of the feed to the knife mill to cryogenic temperatures.

The yield of intermediates from the electrostatic separation process ranged, for the tested options of PCB grinding, from 2.8% for options 1 and 2 to 6.3% for option 4 (Table 2). This is a small amount, especially for the first two grinding options. The ICP tests identified 22% (option 2) to 27% (option 3) of elements. The remaining part are probably, as for the remaining separation products, organic substances in the form of the previously mentioned polyphenols or polyglycols. Of the identified elements, 45%–60% were valuable elements. For the most effective grinding option, they were Cu (6.68%), Fe (1.50%), Al (1.34%), and Sn (1.18%). Among the nonvaluable elements, Si (3.19%), Ca (2.41%), Mg (1.51%), and Br (1.12%) should be mentioned.

There were small amounts of metals in the waste from electrostatic separation, especially in options 1 (1.99%) and 2 (0.54%). In this end product, apart from unidentified organic substances, Si (approximately 14%) and Ca (approximately 8%) as well as Mg and Br (approximately 2%) were identified. The waste yield in option 2 was as high as 71%. Taking into account the fact that there were almost no metals in the free state, it can be used for the production of various components/prefabricates [12].

Table 3. Elemental content in the feed and electrostatic separation products for all grinding options.

	Element	Content of the Element, %, in											
		Feed	Concentrate				Intermediate				Waste			
			Option 1	Option 2	Option 3	Option 4	Option 1	Option 2	Option 3	Option 4	Option 1	Option 2	Option 3	Option 4
Valuable elements	Cu	17.70 ± 1.77	64.17 ± 6.42	68.50 ± 6.85	54.29 ± 5.43	38.45 ± 3.85	5.14 ± 0.51	6.68 ± 0.67	6.42 ± 0.64	7.47 ± 0.75	1.24 ± 0.12	0.17 ± 0.02	3.20 ± 0.32	3.89 ± 0.39
	Al	1.95 ± 0.20	5.28 ± 0.53	6.82 ± 0.68	4.58 ± 0.46	4.08 ± 0.41	1.18 ± 0.12	1.34 ± 0.13	0.84 ± 0.08	0.54 ± 0.05	0.2 ± 0.02	0.07 ± 0.01	0.48 ± 0.05	0.29 ± 0.03
	Pb	0.39 ± 0.04	2.04 ± 0.20	1.5 ± 0.15	2.54 ± 0.25	1.74 ± 0.17	1.28 ± 0.13	0.74 ± 0.07	0.47 ± 0.04	0.08 ± 0.01	BDL *	0.001 ± 0.0001	BDL *	0.02 ± 0.002
	Zn	0.69 ± 0.07	1.22 ± 0.12	2.5 ± 0.25	1.87 ± 0.19	0.87 ± 0.09	0.74 ± 0.07	0.94 ± 0.09	0.40 ± 0.04	0.94 ± 0.09	0.14 ± 0.01	BDL *	0.08 ± 0.01	BDL *
	Ni	0.19 ± 0.02	1.28 ± 0.13	0.75 ± 0.08	0.49 ± 0.05	0.34 ± 0.03	0.75 ± 0.07	0.31 ± 0.03	0.41 ± 0.04	0.21 ± 0.02	BDL *	BDL *	0.18 ± 0.02	BDL *
	Fe	0.38 ± 0.04	2.42 ± 0.24	0.95 ± 0.10	1.87 ± 0.19	1.11 ± 0.11	0.61 ± 0.06	1.50 ± 0.15	1.64 ± 0.16	0.84 ± 0.08	0.04 ± 0.004	0.09 ± 0.01	0.15 ± 0.02	0.40 ± 0.04
	Sn	2.92 ± 0.29	9.54 ± 0.95	11.5 ± 1.15	9.78 ± 0.98	7.21 ± 0.72	2.57 ± 0.26	1.18 ± 0.12	1.88 ± 0.19	0.58 ± 0.06	0.15 ± 0.02	0.02 ± 0.002	1.14 ± 0.11	1.19 ± 0.12
	Cr	0.06 ± 0.06	0.18 ± 0.02	0.15 ± 0.02	0.09 ± 0.01	0.04 ± 0.004	0.02 ± 0.002	0.04 ± 0.004	0.47 ± 0.05	0.27 ± 0.03	0.001 ± 0.0001	0.001 ± 0.0001	BDL *	0.04 ± 0.004
	Ti	0.26 ± 0.03	0.39 ± 0.04	0.51 ± 0.05	0.51 ± 0.05	0.51 ± 0.05	BDL *	0.39 ± 0.04	0.40 ± 0.04	0.22 ± 0.02	0.21 ± 0.02	0.18 ± 0.02	0.28 ± 0.03	BDL *
	Ag	0.030 ± 0.003	0.0647 ± 0.0067	0.1074 ± 0.0011	0.0221 ± 0.0022	0.0054 ± 0.0005	BDL *	BDL *	0.0007 ± 0.0001	BDL *	BDL *	BDL *	BDL *	0.0002 ± 0.00002
	Au	0.0029 ± 0.0003	0.0010 ± 0.0001	0.0092 ± 0.0009	0.0005 ± 0.0001	0.0007 ± 0.0001	BDL *	BDL *	BDL *	BDL *	BDL *	BDL *	BDL *	BDL *
	Sum	**24.57**	**86.58**	**93.30**	**76.04**	**54.36**	**12.29**	**13.12**	**12.93**	**11.15**	**1.99**	**0.54**	**5.51**	**5.83**
Nonvaluable elements	Sb	0.22 ± 0.02	0.27 ± 0.03	0.61 ± 0.06	0.19 ± 0.02	0.08 ± 0.01	BDL *	0.18 ± 0.02	0.18 ± 0.02	0.12 ± 0.01	0.21 ± 0.02	0.01 ± 0.001	0.27 ± 0.03	0.33 ± 0.03
	Ca	6.56 ± 0.66	0.98 ± 0.10	0.92 ± 0.09	1.12 ± 0.11	2.24 ± 0.22	2.81 ± 0.28	2.41 ± 0.24	4.78 ± 0.48	3.91 ± 0.39	8.43 ± 0.84	7.51 ± 0.75	6.93 ± 0.70	9.05 ± 0.91
	Br	1.64 ± 0.08	0.08 ± 0.01	0.03 ± 0.003	0.35 ± 0.04	0.78 ± 0.08	0.78 ± 0.08	1.12 ± 0.12	1.49 ± 0.15	1.21 ± 0.12	2.11 ± 0.21	1.28 ± 0.13	1.69 ± 0.17	1.41 ± 0.14
	Ba	0.31 ± 0.03	0.10 ± 0.01	BDL *	0.2 ± 0.02	0.15 ± 0.02	BDL *	0.41 ± 0.04	0.12 ± 0.01	0.32 ± 0.03	0.64 ± 0.06	0.77 ± 0.08	0.59 ± 0.06	0.59 ± 0.06
	Mg	0.57 ± 0.06	0.05 ± 0.01	0.05 ± 0.01	0.28 ± 0.03	0.43 ± 0.04	0.95 ± 0.09	1.51 ± 0.15	0.64 ± 0.06	0.44 ± 0.04	2.01 ± 0.20	2.50 ± 0.25	2.10 ± 0.21	1.48 ± 0.15
	Si	12.00 ± 1.20	1.21 ± 0.12	0.40 ± 0.04	7.45 ± 0.75	6.15 ± 0.62	5.68 ± 0.57	3.19 ± 0.32	6.78 ± 0.68	7.28 ± 0.73	14.48 ± 1.45	13.92 ± 1.39	11.21 ± 1.12	12.1 ± 1.21
	Mn	0.01 ± 0.001	0.03 ± 0.003	0.03 ± 0.003	0.03 ± 0.003	0.03 ± 0.003	BDL *	BDL *	BDL *	BDL *	BDL *	BDL *	BDL *	BDL *
	Sum	**21.26**	**2.69**	**2.01**	**9.59**	**9.83**	**10.22**	**8.82**	**13.99**	**13.28**	**27.88**	**26.00**	**22.79**	**24.93**

* BDL—below detection limit.

In order to investigate the morphology of the concentrate and intermediate grains obtained from the most effective option for preparing the feed for an electrostatic separator (option 2), and to determine the chemical composition in grain micro-areas, as well as to demonstrate the number and type of metal–plastic–ceramic or metal–metal compounds, photographs were taken using quadrant backscatter diffraction (QBSD) (Figures 5 and 6), and measurements were performed using EDS (Tables 4 and 5). The differences in grain contrast in these figures indicate their heterogeneous chemical composition. The lighter areas indicate the presence of elements with a higher atomic number, while the dark ones indicate the elements with a lower atomic number. However, one should take into account the possibility of accumulation of surface charges by plastics, which, in the case of electrification, can also appear as bright areas. The concentrate (Figure 5) contained mostly homogeneous grains, without contrast. There were also a few grains forming metal–metal or metal–plastic–ceramic compounds. One the other hand, in the intermediate (Figure 6), the opposite was true; mainly nonhomogeneous grains appeared—all grains are in two shades.

The concentrations of the elements measured for the selected micro-areas of the concentrate grains (Figure 5) and the intermediate grains (Figure 6) are presented in Tables 4 and 5, respectively. The grains in the concentrate (Figure 5) below 300 μm in size were mainly homogeneous—they did not display any contrast. The patch grains and the irregular grains obtained were mainly made up of copper (e.g., points A1 and A2 in Figure 5). In the case of patch grains >600 μm in size (e.g., point A3 in Figure 5 marked on a grain with a diameter of 900 μm), an insufficient degree of metal release from nonvaluable elements is observed, from Si and Al in this case. The investigated micro-area of this grain consisted of 66% of these elements. In the remaining micro-areas of Si concentrate grains examined by means of EDS, it was absent or there was only a small amount (less than 5%). At point A5 (Figure 5, Table 4), the presence of gold was indicated for the elongated grain. It can be assumed that the grain came from gold-plated contacts. Elongated grains exhibit the highest purity, regardless of their size. It can therefore be assumed that these grains came mainly from contacts that had no connections with the PCB composite. Each tested area in the concentrate contained different amounts of aluminium.

On the basis of the presented analysis and observation of all concentrate grains, it can be summarised and generalised that metals contained in grains with size >800 μm are insufficiently released from plastic and ceramic materials. They should be ground again under the conditions in line with option 2.

Compared with the concentrate, the grains present in the intermediate were larger and ranged from about 500 μm to 1000 μm (Figure 6). The fibrous structure characteristic of ceramics can be seen in almost every grain. The grains' shape, their two-sided connections with plastic and ceramic materials, and their high copper content (Table 5) may indicate that these grains mainly come from the internal PCB layers. Due to the size of the grains, the intermediate can be reground or subjected to digestion with leaching solutions.

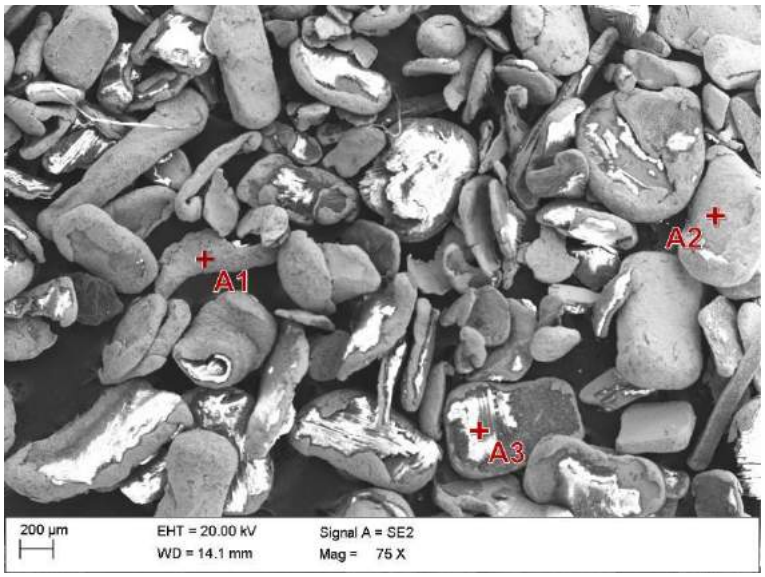

(**a**)

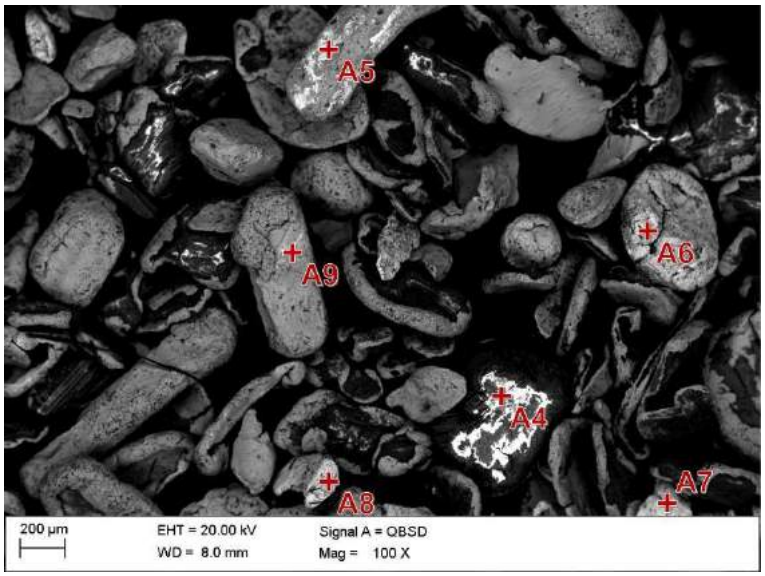

(**b**)

Figure 5. Concentrate from the electrostatic separation (SEM, QBSD mode (Table 4)) with marked EDS analysis points: (**a**) A1 – A3 and (**b**) A5 – A9.

Table 4. Elemental concentrations (% at.) measured with EDS in the micro-areas marked in Figure 5.

Element	Point of Analysis								
	A1	**A2**	**A3**	**A4**	**A5**	**A6**	**A7**	**A8**	**A9**
Mg	-	-	-	6.2	-	-	-	-	-
Al	1.4	2.3	19.0	93.8	22.4	4.1	5.5	34.9	4.0
Si	-	1.0	46.8	-	-	-	-	3.6	1.7
Sc	-	-	-	-	-	-	0.2	-	0.2
Fe	-	-	-	-	3.2	-	-	-	-
Ni	-	-	-	-	26.4	-	-	-	37.0
Cu	98.6	96.8	5.0	-	12	-	3.1	50.9	45.8
Sn	-	-	-	-	-	95.9	89.7	10.7	10.6
Sb	-	-	-	-	-	-	1.6	-	0.7
Au	-	-	-	-	36	-	-	-	-

Na	-	-	1.0	-	-	-	-	-	-

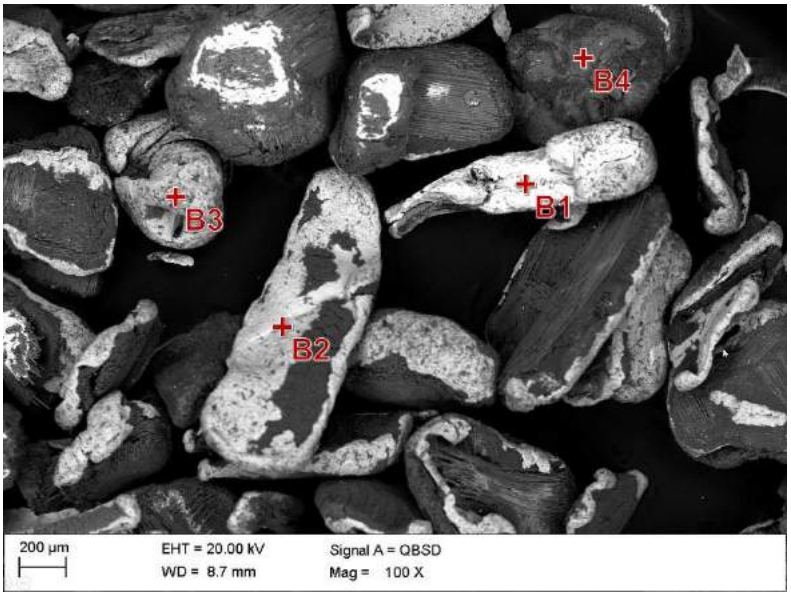

(**a**)

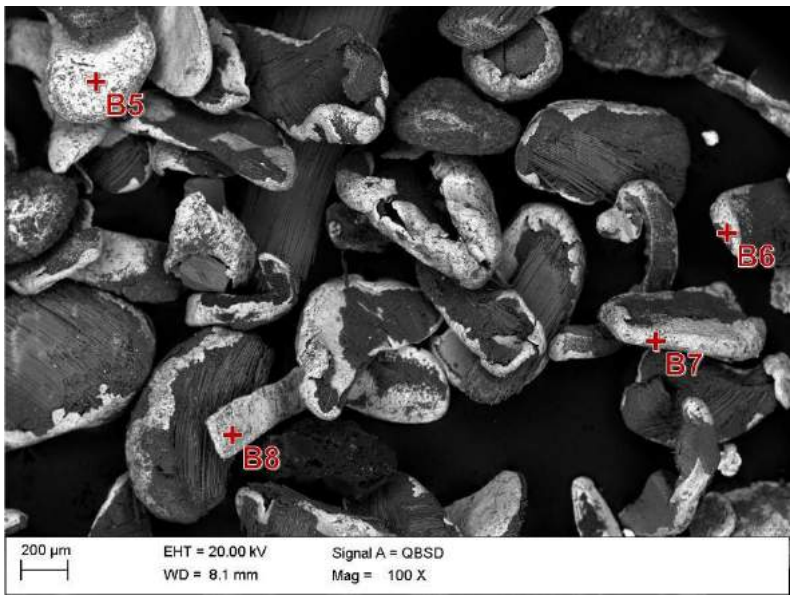

(**b**)

Figure 6. Intermediate from the electrostatic separation (SEM, QBSD mode (Table 5)) with marked EDS analysis points: (**a**) B1 – B4 and (**b**) B5 – B8.

Table 5. Elemental concentrations [% at.] measured with EDS in the micro-areas marked in Figure 6.

Element	Point of Analysis							
	B1	**B2**	**B3**	**B4**	**B5**	**B6**	**B7**	**B8**
Mg	-	-	1.5	-	-	-	1.8	-
Al	3.4	4.6	13.7	74.8	6.8	2.4	8.5	9.9
Si	-	-	20.4	4.6	-	1.2	-	1.2
Sc	-	-	-	-	0.3	-	-	-
Fe	-	-	23.1	1.7	-	-	-	-
Ni	4.3	-	2.0	-	-	-	-	-

Cu	17.2	95.4	26.9	10.6	5.9	96.4	89.7	87.3
Ag	1.2	-	-	-	2.5	-	-	-
Sn	73.9	-	-	6.6	83.6	-	-	-
Sb	-	-	-	-	0.8	-	-	-
Ca	-	-	4.7	1.3	-	-	-	-
Mn	-	-	0.2	-	-	-	-	-
S	-	-	0.5	-	-	-	-	-
Cl	-	-	-	0.3	-	-	-	1.6
Cr	-	-	6.7	-	-	-	-	-
Ba	-	-	0.2	-	-	-	-	-

X-ray qualitative phase analysis was carried out for the concentrate and the intermediate also obtained from the most effective option for preparing the feed for an electrostatic separator (i.e., option 2). The analysis of the phase composition of the concentrate (Figure 7) did not indicate phases that could suggest the presence of impurities, nonvaluable elements, unlike that of the intermediate (Figure 8), where the diffraction lines from silicon were identified. Phases such as copper, tin, and CuSn (bronze) were identified in the concentrate (Figure 7), while in the intermediate, apart from silicon, copper and aluminium were also present. Due to the limited sensitivity of the method, the presence of other metallic/nonmetallic phases in small amounts cannot be excluded.

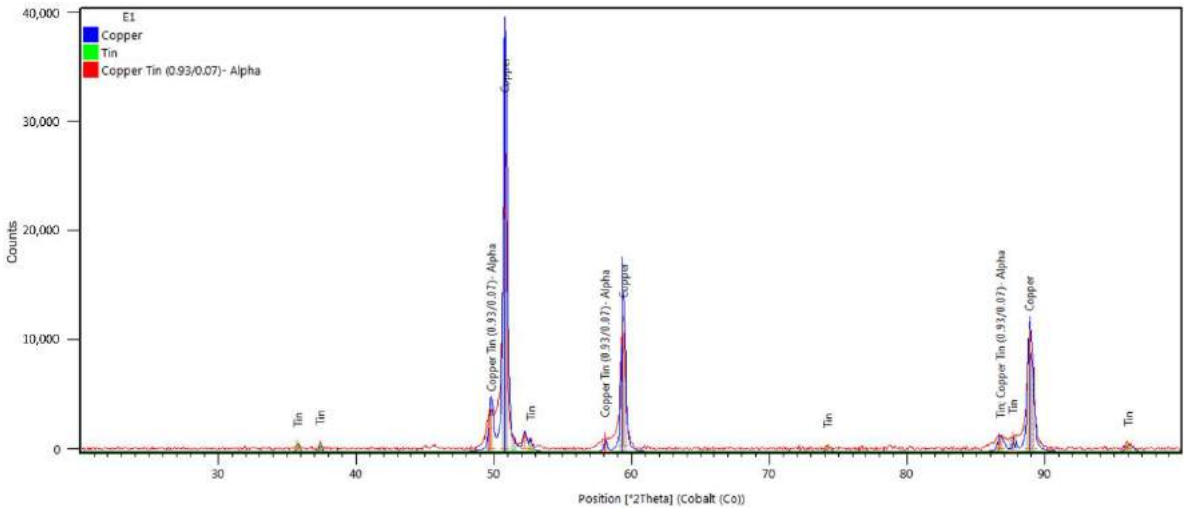

Figure 7. X-ray diffraction patterns of the concentrate.

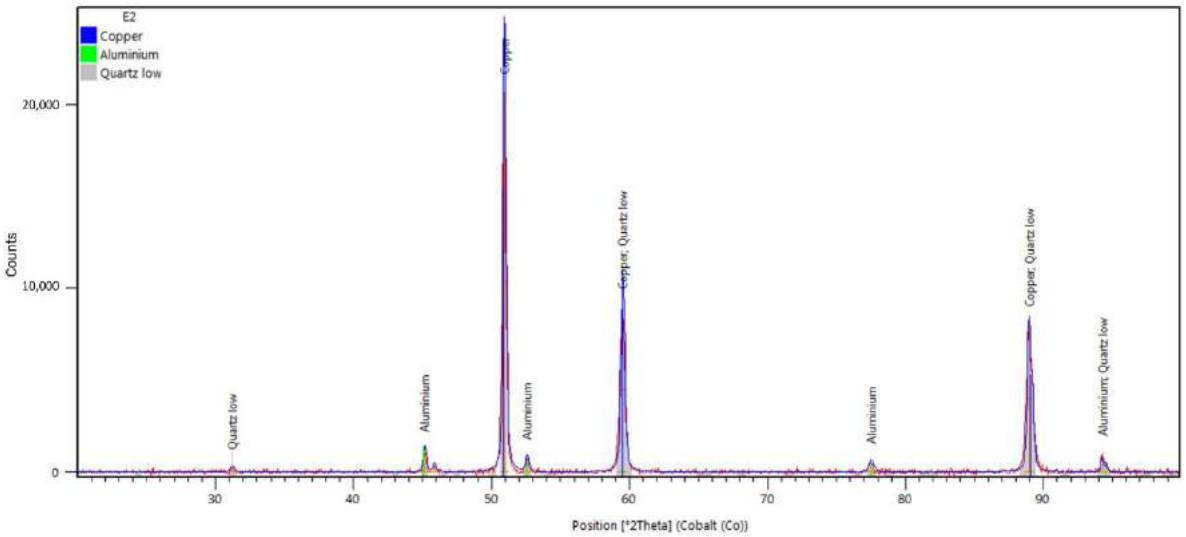

Figure 8. X-ray diffraction patterns of the intermediate.

4. Discussion

The obtained results of metal recovery efficiency tests using electrostatic separation for various options of PCB grinding confirm that the method and degree of grinding significantly affect the purity of the concentrate and waste, and thus the efficiency of the process. Significant indicators of the grinding degree were the limit dimensions of the ground grains, as well as the resulting level of metal release from plastic and ceramic materials.

According to the work of Li et al. [7], full metal release occurs for grains <0.6 mm, while Kaya [24] reports that it occurs only for grains <0.15 mm. In both of the above-mentioned papers, the research involved multistage grinding in hammer mills and the use of various PCBs, which could have had an impact on the results. Based on the results of the research presented in this article, it can be seen that the complete release of metals from plastic and ceramic materials occurred for grains <0.3 mm and, to a lesser extent, for grains smaller than 0.8 mm. Grinding was carried out with a knife mill, and the feed was cooled to cryogenic temperature. So far, little research was done to assess the efficiency of PCB grinding using knife mills and cryogenic temperatures in detail. Grinding, cooling the feed to cryogenic temperature, and the preprocessing steps are energy-consuming processes. The validity of using these methods should be confirmed by economic analysis and compared with other methods for recovering useful substances from PCBs.

It can be assumed that the degree of grinding for which the metals are fully released depends, to some extent, on the type of PCB. At this point, it should be added after authors Li et al. [7] and Wu et al. [40] that electrostatic separation may be effective for grains <1.2 mm. In addition, the separation efficiency is influenced by the optimisation of the process (i.e., for the drum electrostatic separator, the adjustment of the voltage, the shaft rotational speed, and the load of the separator). These parameters were not analysed in this paper.

In this work, the separation efficiency was analysed in terms of product yield, the penetration of inappropriate grains into individual products, and the presence of mixed grains in them (i.e., conglomerates—solid metal–plastic–ceramic compounds). The concentrate from electrostatic separation for the option of grinding using a 3 mm screen perforation in the knife mill was the one most contaminated with plastic and ceramic materials. In this case, a fairly large amount of metals also penetrated into the waste. This is explained by the fact that as much as 38.5% of the grains after grinding were larger than 1 mm. In the grinding option using a 2 mm screen perforation, the content of grains >1 mm was 11.5%. This resulted in an increase in the content of metals in the concentrate, but not a sufficient one. The low separation efficiency for these grinding options could also be caused by an insufficient electrostatic force. According to Wu et al. [40], a 20 kV voltage is suitable for efficient electrostatic separation of fine grains. For larger ones, it may be insufficient, and increasing the voltage may negatively affect the overall efficiency of the process.

A much better efficiency of recovering metals from PCBs was obtained for the options of grinding using a screen with a 1 mm perforation, without and with cooling the feed to cryogenic temperatures, respectively. In these cases, grains >1 mm were not present in the grinding products. The share of grains <0.5 mm was substantial. The yields of separation products for these options were very similar, but for the option with a reduced feed temperature per grain mill, they were generally slightly smaller. For this case, the purity of the concentrate and waste was the highest. Only small amounts of fine metal grains (below 200 μm) that were trapped in the fibrous structure of the glass fibre grains were identified in the waste. It can therefore be concluded that cooling the material to cryogenic temperatures has a positive effect on the size and shape of the grains, and thus, in line with the conclusions of Lu et al. [44], on the recovery of metals from PCBs. It should be added that the cooled material was ground much faster, and the degree of metal release was higher.

It could be assumed that due to the multilayer structure of PCBs, it is advantageous to obtain the smallest possible grain [31,46]. Wu et al., however, report [40] that very fine grains below 0.091–0.125 mm may contribute to ineffective electrostatic separation caused by the grain aggregation effect on the drum and electrode surface. According to Wu et al. [56], this effect may have a significant impact on the stability of the separation process. Considering the above, in order to obtain the appropriate electrostatic separation efficiency, a very narrow grain class should be used with the separator. The settling of dust made of plastic and ceramic materials on the electrode surface was observed in the research papers presented in this paper. On the other hand, aggregation on the drum surface was very limited when using cryogenic temperatures for the preparation of the feed.

For the concentrate obtained from electrostatic separation, for the option of PCB grinding using cryogenic temperatures and 1 mm screen perforation, the value of valuable metals that can be obtained was estimated on the basis of the London Metal Exchange. The metal content in the concentrate for this grinding option is shown (based on Table 3) in Figure 9. The estimated value refers to pure metals and does not include the costs required for PCB processing. As can be seen from Table 6, gold and copper have the decisive share in the final value, accounting for 39% and 37% of the total, respectively, followed by tin at 15.5% and silver at 6%. Due to the low gold content of PCBs, the recovery process should be adapted to minimise the loss of this metal. In this case, the PCB grinding process may be a critical stage. In order to improve the efficiency of copper recovery, which creates numerous connections with plastic and ceramic materials due to the PCB structure, the grinding process should be carried out in such a way as to obtain the highest possible release of this metal.

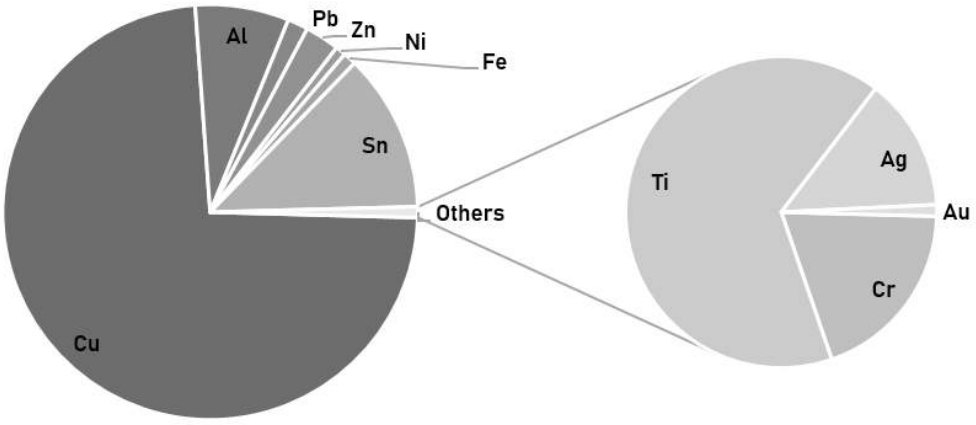

Figure 9. Metal content in the concentrate obtained from electrostatic separation for the option of PCB grinding using cryogenic temperatures and 1 mm screen perforation.

At high temperatures occurring in the mill's working chamber, when cryogenic temperatures are not used to prepare the feed, gold becomes plastic, which may lead to coating of the mill elements and other grains of harder metals. When liquid nitrogen was used to cool the feed, this unfavourable effect was minimised.

Table 6. The value of metals recoverable from the concentrate obtained from electrostatic separation for the option of PCB grinding using cryogenic temperatures and 1 mm screen perforation.

Metal	Price*, ($/Mg)	Metal Content in the Concentrate (Data from Table 3), %	Metal Recovery Level Related to the Initial PCB Mass (after Dismantling), %	Prices of Metals Obtained from 100 g of PCB, $
Cu	7635	68.5	17.95	1.4
Al	1986	6.82	1.79	0.035
Pb	2063	1.5	0.39	0.008
Zn	2762	2,5	0.66	0.018
Ni	16,390	0.75	0.20	0.032
Fe	553	0.95	0.25	0.001
Sn	19,128	11.5	3.01	0.576
Ag	7.91×10^5	0.1074	0.0281	0.223
Au	6.01×10^7	0.0092	0.0024	1.4
			Suma, $	3.7

* According to the London Metal Exchange (December 2020).

5. Conclusions

The use of a knife mill with the use of a 1 mm screen perforation along with cooling the feed to cryogenic temperature significantly improves the full release of useful components from PCBs. After grinding, the mixture of fine grains can be transferred to the electrostatic separation process in order to separate metals in the free state from plastics and ceramic materials, while before grinding, hazardous products, such as batteries, capacitors, and radiators, must be disassembled from the PCBs. Similar directions of activities in the field of PCB recycling were presented by Vermesan et al. [1]. This is in line with the circular economy policy. In this way, metals can be recovered (economic benefits), but also the negative impact of human activity on the environment can be reduced by limiting the extraction and processing of metal ores and the amount of waste.

The recovered mixture of metals, the concentrate from the electrostatic separation process, can be transferred to metallurgical processing, where metals are produced along with the concentrate from the processing of nonferrous metal ores, while plastic and ceramic materials, the waste from the electrostatic separation, can be used as secondary raw materials for the production of various components/prefabricates. The purity of the concentrate and the waste obtained from electrostatic separation was satisfactory, and the proportion of the intermediate, in which the conglomerates of solid metal–plastic–ceramic compounds were present, was very low. The yield of the concentrate and the waste amounted to 26.2% and 71.0%, respectively, and their purity, reflected in the content of the identified valuable metals, was at the level of 93.3% and 0.5%, respectively.

Author Contributions: Research concept, T.S. and D.M.F.; conduct of the process of grinding and electrostatic separation, D.M.F.; XRD analysis, P.M.N.; analysis of grinding, T.S. and B.T.; analysis of the yield of separation products and their density, D.M.F., P.M., and D.K.; microscopic and ICP analysis, D.M.F. and T.S.; investigation, T.S. and D.M.F.; writing—original draft preparation, D.M.F. and T.S.; writing—review and editing, D.M.F., T.S., P.M.N., B.T., D.K., and P.M. All authors have read and agreed to the published version of the manuscript.

Funding: The project was funded under the statutory financial grant BK-06/050/BK_20/0101 for the year 2020 of the Faculty of Mining, Safety Engineering and Industrial Automation, Silesian University of Technology.

Institutional Review Board Statement: Not applicable.

Informed Consent Statement: Not applicable.

Data Availability Statement: Data sharing not applicable.

Acknowledgments: The authors thank Krzysztof Matus for SEM characterization.

Conflicts of Interest: The authors declare no conflicts of interest. The funders had no role in the design of the study; in the collection, analyses, or interpretation of data; in the writing of the manuscript; or in the decision to publish the results.

References

1. Vermeșan, H.; Tiuc, A.-E.; Purcar, M. Advanced Recovery Techniques for Waste Materials from IT and Telecommunication Equipment Printed Circuit Boards. *Sustainability* **2019**, *12*, 74, doi:10.3390/su12010074.
2. Kumar, V.; Lee, J.; Jeong, J.; Jha, M.K.; Kim, B.; Singh, R. Recycling of Printed Circuit Boards (PCBs) to Generate Enriched Rare Metal Concentrate. *J. Ind. Eng. Chem.* **2015**, *21*, 805–813, doi:10.1016/j.jiec.2014.04.016.
3. Sohaili, J.; Muniyandi, S.K.; Mohamad, S.S. A Review on Printed Circuit Board Recycling Technology. *J. Emerg. Trends Eng. Appl. Sci.* **2012**, *3*, 12–18.
4. Tsydenova, O.; Bengtsson, M. Chemical Hazards Associated with Treatment of Waste Electrical and Electronic Equipment. *Waste Manag.* **2011**, *31*, 45–58, doi:10.1016/j.wasman.2010.08.014.
5. Johnson, J.; Harper, E.M.; Lifset, R.; Graedel, T.E. Supporting Information for "Dining at the Periodic Table: Metals"Concentrations as They Relate to Recycling. *Environ. Sci. Technol.* **2007**, *41*, 1759–1765, doi:10.1021/es060736h.
6. Tuncuk, A.; Stazi, V.; Akcil, A.; Yazici, E.Y.; Deveci, H. Aqueous Metal Recovery Techniques from E-Scrap: Hydrometallurgy in Recycling. *Miner. Eng.* **2012**, *25*, 28–37, doi:10.1016/j.mineng.2011.09.019.
7. Li, J.; Lu, H.; Guo, J.; Xu, Z.; Zhou, Y. Recycle Technology for Recovering Resources and Products from Waste Printed Circuit Boards. *Environ. Sci. Technol.* **2007**, *41*, 1995–2000, doi:10.1021/es0618245.
8. Dascalescu, L.; Iuga, A.; Morar, R. Corona–Electrostatic Separation: An Efficient Technique for the Recovery of Metals and Plastics From Industrial Wastes. *Magn. Electr. Sep.* **1900**, *4*, 059037, doi:10.1155/1993/59037.
9. Huang, K.; Guo, J.; Xu, Z. Recycling of Waste Printed Circuit Boards: A Review of Current Technologies and Treatment Status in China. *J. Hazard. Mater.* **2009**, *164*, 399–408, doi:10.1016/j.jhazmat.2008.08.051.
10. Kumar, A.; Holuszko, M.E.; Janke, T. Characterization of the Non-Metal Fraction of the Processed Waste Printed Circuit Boards. *Waste Manag.* **2018**, *75*, 94–102, doi:10.1016/j.wasman.2018.02.010.
11. Weil, E.D.; Levchik, S. A Review of Current Flame Retardant Systems for Epoxy Resins. *J. Fire Sci.* **2004**, *22*, 25–40, doi:10.1177/0734904104038107.
12. Muniyandi, S.K.; Sohaili, J.; Hassan, A. Encapsulation of Nonmetallic Fractions Recovered from Printed Circuit Boards Waste with Thermoplastic. *J. Air Waste Manag. Assoc.* **2014**, *64*, 1085–1092, doi:10.1080/10962247.2014.911221.
13. Duan, H.; Hu, J.; Yuan, W.; Wang, Y.; Yu, D.; Song, Q.; Li, J. Characterizing the Environmental Implications of the Recycling of Non-Metallic Fractions from Waste Printed Circuit Boards. *J. Clean. Prod.* **2016**, *137*, 546–554, doi:10.1016/j.jclepro.2016.07.131.
14. Bizzo, W.; Figueiredo, R.; de Andrade, V. Characterization of Printed Circuit Boards for Metal and Energy Recovery after Milling and Mechanical Separation. *Materials* **2014**, *7*, 4555–4566, doi:10.3390/ma7064555.
15. Charles, R.G.; Douglas, P.; Hallin, I.L.; Matthews, I.; Liversage, G. An Investigation of Trends in Precious Metal and Copper Content of RAM Modules in WEEE: Implications for Long Term Recycling Potential. *Waste Manag.* **2017**, *60*, 505–520, doi:10.1016/j.wasman.2016.11.018.
16. Cayumil, R.; Khanna, R.; Rajarao, R.; Mukherjee, P.S.; Sahajwalla, V. Concentration of Precious Metals during Their Recovery from Electronic Waste. *Waste Manag.* **2016**, *57*, 121–130, doi:10.1016/j.wasman.2015.12.004.
17. Schluep, M.; Hagelueken, C.; Kuehr, R.; Magalini, F.; Maurer, C. Recycling—from e-Waste to Resources. In *Sustainable Innovation and Technology Transfer Industrial Sector Studies*; Nairobi and Bonn, UNEP and STeP, **2006**.
18. Mao, S.; Kang, Y.; Zhang, Y.; Xiao, X.; Zhu, H. Fractional Grey Model Based on Non-Singular Exponential Kernel and Its Application in the Prediction of Electronic Waste Precious Metal Content. *ISA Trans.* **2020**, *107*, 12–26, doi:10.1016/j.isatra.2020.07.023.
19. Hagelüken, C. Recycling of Electronic Scrap at Umicore's Integrated Metals Smelter and Refinery. *World of Metallurgy* **2006**, 11
20. Song, Q.; Zeng, X.; Li, J.; Duan, H.; Yuan, W. Environmental Risk Assessment of CRT and PCB Workshops in a Mobile E-Waste Recycling Plant. *Environ. Sci. Pollut. Res.* **2015**, *22*, 12366–12373, doi:10.1007/s11356-015-4350-9.
21. Dervišević, I.; Minić, D.; Kamberović, Ž.; Ćosović, V.; Ristić, M. Characterization of PCBs from Computers and Mobile Phones, and the Proposal of Newly Developed Materials for Substitution of Gold, Lead and Arsenic. *Environ. Sci. Pollut. Res.* **2013**, *20*, 4278–4292, doi:10.1007/s11356-012-1448-1.
22. Niu, Q.; Xiang, D.; Liu, X.; Duan, G.; Shi, C. The Recycle Model of Printed Circuit Board and Its Economy Evaluation. In *Proceedings of the 2007 IEEE International Symposium on Electronics and the Environment*; IEEE: Orlando, FL, USA, 2007; pp. 106–111.
23. Guo, C.; Wang, H.; Liang, W.; Fu, J.; Yi, X. Liberation Characteristic and Physical Separation of Printed Circuit Board (PCB). *Waste Manag.* **2011**, *31*, 2161–2166, doi:10.1016/j.wasman.2011.05.011.
24. Kaya, M. Recovery of Metals and Nonmetals from Electronic Waste by Physical and Chemical Recycling Processes. *Waste Manag.* **2016**, *57*, 64–90, doi:10.1016/j.wasman.2016.08.004.
25. Leung, A.O.W.; Luksemburg, W.J.; Wong, A.S.; Wong, M.H. Spatial Distribution of Polybrominated Diphenyl Ethers and Polychlorinated Dibenzo-p-Dioxins and Dibenzofurans in Soil and Combusted Residue at Guiyu, an Electronic Waste Recycling Site in Southeast China. *Environ. Sci. Technol.* **2007**, *41*, 2730–2737.

26. Qiu, R.; Lin, M.; Ruan, J.; Fu, Y.; Hu, J.; Deng, M.; Tang, Y.; Qiu, R. Recovering Full Metallic Resources from Waste Printed Circuit Boards: A Refined Review. *J. Clean. Prod.* **2020**, *244*, 118690, doi:10.1016/j.jclepro.2019.118690.
27. Xiang, D.; Mou, P.; Wang, J.; Duan, G.; Zhang, H.C. Printed Circuit Board Recycling Process and Its Environmental Impact Assessment. *Int. J. Adv. Manuf. Technol.* **2007**, *34*, 1030–1036, doi:10.1007/s00170-006-0656-6.
28. Argumedo-Delira, R.; Gómez-Martínez, M.J.; Soto, B.J. Gold Bioleaching from Printed Circuit Boards of Mobile Phones by Aspergillus Niger in a Culture without Agitation and with Glucose as a Carbon Source. *Metals* **2019**, *9*, 521, doi:10.3390/met9050521.
29. Drzymała, J.; Swatek, A. *Mineral Processing: Foundations of Theory and Practice of Minerallurgy*; University of Technology: Wroclaw, Poland, **2007**; ISBN 978-83-7493-362-9.
30. Tatariants, M.; Yousef, S.; Sidaraviciute, R.; Denafas, G.; Bendikiene, R. Characterization of Waste Printed Circuit Boards Recycled Using a Dissolution Approach and Ultrasonic Treatment at Low Temperatures. *RSC Adv.* **2017**, *7*, 37729–37738, doi:10.1039/C7RA07034A.
31. Forti, V.; Baldé, C.P.; Kuehr, R.; Bel, G. The Global E-waste Monitor 2020: Quantities, flows and the circular economy potential; *United Nations University (UNU)/United Nations Institute for Training and Research (UNITAR) – co-hosted SCYCLE Programme, International Telecommunication Union (ITU) & International Solid Waste Association (ISWA),* Bonn/Geneva/Rotterdam, **2020**; p. 120.
32. Bidini, G.; Fantozzi, F.; Bartocci, P.; D'Alessandro, B.; D'Amico, M.; Laranci, P.; Scozza, E.; Zagaroli, M. Recovery of Precious Metals from Scrap Printed Circuit Boards through Pyrolysis. *J. Anal. Appl. Pyrolysis* **2015**, *111*, 140–147, doi:10.1016/j.jaap.2014.11.020.
33. LaDou, J. Printed Circuit Board Industry. *Int. J. Hyg. Environ. Health* **2006**, *209*, 211–219, doi:10.1016/j.ijheh.2006.02.001.
34. Ernst, T.; Popp, R.; Wolf, M.; van Eldik, R. Analysis of Eco-Relevant Elements and Noble Metals in Printed Wiring Boards Using AAS, ICP–AES and EDXRF. *Anal. Bioanal. Chem.* **2003**, *375*, 805–814, doi:10.1007/s00216-003-1802-8.
35. Koyanaka, S.; Endoh, S.; Ohya, H. Effect of Impact Velocity Control on Selective Grinding of Waste Printed Circuit Boards. *Adv. Powder Technol.* **2006**, *17*, 113–126, doi:10.1163/156855206775123467.
36. Li, J.; Xu, Z.; Zhou, Y. Application of Corona Discharge and Electrostatic Force to Separate Metals and Nonmetals from Crushed Particles of Waste Printed Circuit Boards. *J. Electrost.* **2007**, *65*, 233–238, doi:10.1016/j.elstat.2006.08.004.
37. Khaliq, A.; Rhamdhani, M.; Brooks, G.; Masood, S. Metal Extraction Processes for Electronic Waste and Existing Industrial Routes: A Review and Australian Perspective. *Resources* **2014**, *3*, 152–179, doi:10.3390/resources3010152.
38. Dascalescu, L.; Tilmatine, A.; Aman, F.; Mihailescu, M. Optimization of Electrostatic Separation Processes Using Response Surface Modeling. *IEEE Trans. Ind. Applicat.* **2004**, *40*, 53–59, doi:10.1109/TIA.2003.821812.
39. Zenkiewicz, M.; Zuk, T. Physical basis of tribocharging and electrostatic separation of plastics. *Polimery* **2014**, *59*, 314–323, doi:10.14314/polimery.2014.314.
40. Wu, J.; Li, J.; Xu, Z. Electrostatic Separation for Recovering Metals and Nonmetals from Waste Printed Circuit Board: Problems and Improvements. *Environ. Sci. Technol.* **2008**, *42*, 5272–5276, doi:10.1021/es800868m.
41. Wei, J.; Realff, M.J. Design and Optimization of Free-Fall Electrostatic Separators for Plastics Recycling. *AIChE J.* **2003**, *49*, 3138–3149, doi:10.1002/aic.690491214.
42. Tilmatine, A.; Medles, K.; Bendimerad, S.-E.; Boukholda, F.; Dascalescu, L. Electrostatic Separators of Particles: Application to Plastic/Metal, Metal/Metal and Plastic/Plastic Mixtures. *Waste Manag.* **2009**, *29*, 228–232, doi:10.1016/j.wasman.2008.06.008.
43. Hou, S.; Wu, J.; Qin, Y.; Xu, Z. Electrostatic Separation for Recycling Waste Printed Circuit Board: A Study on External Factor and a Robust Design for Optimization. *Environ. Sci. Technol.* **2010**, *44*, 5177–5181, doi:10.1021/es903936m.
44. Lu, H.; Li, J.; Guo, J.; Xu, Z. Movement Behavior in Electrostatic Separation: Recycling of Metal Materials from Waste Printed Circuit Board. *J. Mater. Process. Technol.* **2008**, *197*, 101–108, doi:10.1016/j.jmatprotec.2007.06.004.
45. Li, J.; Zhou, Q.; Xu, Z. Real-Time Monitoring System for Improving Corona Electrostatic Separation in the Process of Recovering Waste Printed Circuit Boards. *Waste Manag. Res.* **2014**, *32*, 1227–1234, doi:10.1177/0734242X14554647.
46. Sanapala, R. Characterization of FR-4 Printed Circuit Board Laminates Before and After Exposure to Lead-Free Soldering Conditions. Ph.D. Thesis, University of Maryland: College Park, USA, **2008**.
47. Franke, D.; Suponik, T. Metals Recovery from E-Scrap Using Gravity, Electrostatic and Magnetic Separations. *IOP Conf. Ser. Mater. Sci. Eng.* **2019**, *545*, 012016, doi:10.1088/1757-899X/545/1/012016
48. Lee, J.; Kim, Y.; Lee, J. Disassembly and Physical Separation of Electric/Electronic Components Layered in Printed Circuit Boards (PCB). *J. Hazard. Mater.* **2012**, *241–242*, 387–394, doi:10.1016/j.jhazmat.2012.09.053.
49. Available online: www.testchem.pl/en/testchem-products/sample-preparing/grinders-and-crushers/knife-lab-grinders/ (accessed on 4 December **2020**).
50. Franke, D.; Suponik, T.; Nuckowski, P.M.; Gołombek, K.; Hyra, K. Recovery of Metals from Printed Circuit Boards By Means of Electrostatic Separation. *Manag. Syst. Prod. Eng.* **2020**, *28*, 213–219, doi:10.2478/mspe-2020-0031.
51. Suponik, T.; Franke, D.; Nuckowski, P. Electrostatic and Magnetic Separations for the Recovery of Metals from Electronic Waste. *IOP Conf. Ser. Mater. Sci. Eng.* **2019**, *641*, 012017, doi:10.1088/1757-899X/641/1/012017.
52. Wu, W.; Liu, X.; Zhang, X.; Zhu, M.; Tan, W. Bioleaching of Copper from Waste Printed Circuit Boards by Bacteria-Free Cultural Supernatant of Iron–Sulfur-Oxidizing Bacteria. *Bioresour. Bioprocess.* **2018**, *5*, 10, doi:10.1186/s40643-018-0196-6.
53. Pham, H.Q.; Marks, M.J. Epoxy Resins. In *Ullmann's Encyclopedia of Industrial Chemistry*; Wiley-VCH Verlag GmbH & Co. KGaA, Ed.; Wiley-VCH Verlag GmbH & Co. KGaA: Weinheim, Germany, 2005; p. 155-244, ISBN 978-3-527-30673-2.

54. Sood, B.; Sanapala, R.; Das, D.; Pecht, M.; Huang, C.Y.; Tsai, M.Y. Comparison of Printed Circuit Board Property Variations in Response to Simulated Lead-Free Soldering. *IEEE Trans. Electron. Packag. Manufact.* **2010**, *33*, 98–111, doi:10.1109/TEPM.2010.2042453.
55. Sood, B.; Pecht, M. The Effect of Epoxy/Glass Interfaces on CAF Failures in Printed Circuit Boards. *Microelectron. Reliab.* **2018**, *82*, 235–243, doi:10.1016/j.microrel.2017.10.027.
56. Wu, J.; Qin, Y.; Zhou, Q.; Xu, Z. Impact of Nonconductive Powder on Electrostatic Separation for Recycling Crushed Waste Printed Circuit Board. *J. Hazard. Mater.* **2009**, *164*, 1352–1358, doi:10.1016/j.jhazmat.2008.09.061.

sciendo

Management Systems in Production Engineering

2020, Volume 28, Issue 4, pp. 213-219

Date of submission of the article to the Editor: 03/2020
Date of acceptance of the article by the Editor: 07/2020

DOI 10.2478/mspe-2020-0031

RECOVERY OF METALS FROM PRINTED CIRCUIT BOARDS BY MEANS OF ELECTROSTATIC SEPARATION

Dawid FRANKE, Tomasz SUPONIK, Paweł M. NUCKOWSKI, Klaudiusz GOŁOMBEK, Kamila HYRA
Silesian University of Technology

Abstract:
Without the use of appropriate recycling technologies, the growing amount of electronic waste in the world can be a threat to the development of new technologies, and in the case of improper waste management, may have a negative impact on the environment. This is due to the fact that this waste contains large amounts of valuable metals and toxic polymers. Therefore, it should be recycled in accordance with the assumptions of the circular economy. The methods of mechanical recovery of metals from electronic waste, including printed circuits, may be widely used in the future by waste management companies as well as metal production and processing companies. That is why, a well-known and easily applicable electrostatic separation (ES) method was used to recover metals from printed circuit boards. The grain class of 0.32 - 0.10 mm, obtained after grinding the boards, was fed to a separator. Feed and separation products were analyzed by means of ICP-AES, SEM/EDS and XRD. The concentrate yield obtained after electrostatic separation amounted to 32.3% of the feed. Its density was 11.1 g/cc. Out of the 91.44% elements identified in the concentrate, over 90% were metals. XRD, SEM observations and EDS analysis confirmed the presence of non-metallic materials in the concentrate. This relatively high content of impurities indicates the need to grind printed circuit board into grain classes smaller than 0.32-0.10 mm.

Key words: *electrostatic separation, metals recovery, PCB, SEM, XRD*

INTRODUCTION

The production of Waste Electrical and Electronic Equipment (WEEE) is growing at an alarming rate. In 2016, 44.7 million metric tonnes of WEEE were generated, but is expected to increase to 55 million metric tonnes by 2021 [5, 25]. People can process them, degrading the environment to a greater or lesser extent [24]. Effective management of WEEE has become a global problem, because in the event of improper management and recycling, they can have a significantly impact on the environment.

Considering environmental protection, depleting of metal deposits and economic benefit, environmentally friendly and high-efficiency methods of recovering metals from printed circuit boards (PCB) should be sought. Basically, the methods of recovering metals from PCB are divided into physical and chemical [15]. Since chemical methods usually have a negative impact on the environment, the authors of the study focused on one of the physical methods, i.e. electrostatic separation (ES) [15, 23, 30].

The aim of the article was to assess the efficiency of metal recovery from PCB using ES. The article contains the results of the tests on the recovery of metals from grinded PCB with a grain size of 0.1-0.32 mm, using an ES.

In order to obtain accurate test results and eliminate potential measurement errors, the following analysis methods were used: X-ray Powder Diffraction (XRD), Scanning Electron Microscopy (SEM) with the Energy Dispersive Spectroscopy (EDS) system and Inductively Coupled Plasma atomic emission spectroscopy (ICP-AES). As a result of the tests, non-metallic and metallic parts were separated from PCB.

LITERATURE REVIEW

The basic element of the construction of most WEEE are PCB which contain about 70% of non-metallic parts, such as fiberglass, epoxy resin, polyester, woven glass, as well as 30% of metallic parts [2]. It is difficult to determine the type and amount of metals in PCB. It can be estimated that a PCB contains about 16% Cu, 3% Fe, 3% Sn, 2% Pb, 1% Zn 0.05% Au, 0.03% Ag, 0.01% Pd and others metals such as Cr, Na, Cd, Mo, Ti, Co [26, 27].

In ES, grains placed in an electric field are separated as a result of differences in the ability to accumulate electric charges on grain surfaces [9]. The scheme of the electrostatic drum separator used in the study is shown in Fig. 1.

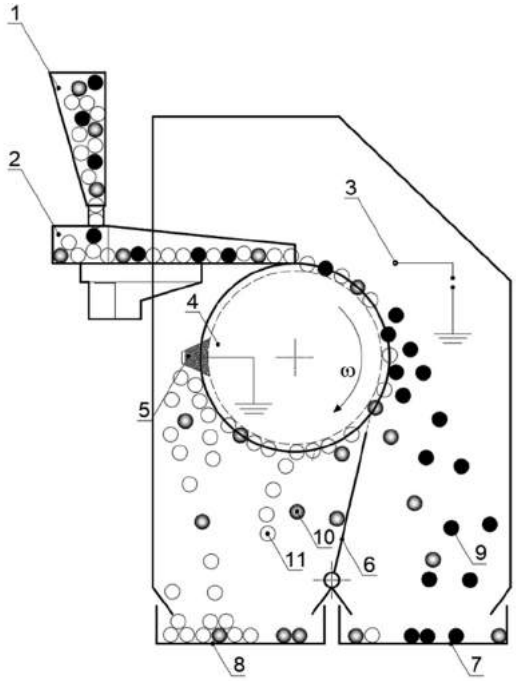

Fig. 1 Scheme of electrostatic drum separator:
1 – feed container, 2 – vibrating feeder, 3 – electrode, 4 – drum, 5 – brush, 6 – partition, 7 – conductors container (concentrate), 8 – non-conductors container (waste), 9 – grains with good electrical conductivity, 10 – complex grains folded with metals and non-metals, 11 – grains with weak electrical conductivity

Placing the grain that has accumulated electric charge in the electric field induces the electric field force. The value of the resultant force depends on the value of the electric field force in which the grain is located. The surface electric charge is generated on the surface of any material, and depends on time and the type of material. Materials with high electrical conductivity (metals) quickly get rid of the accumulated electrical charge [9]. However, the electrostatic force is not the only one acting on the grain during the separation process. There are also (in the electrostatic drum separator): gravity force, image forces and centrifugal force. The resultant force acting on well-conductive grains is directed outwards, contrary to grains with low conductivity (non-metals) [1].

Consequently, the performance of the electrostatic drum separator is mainly dependent on the electrical conductivity of the grain, as well as the grain size and its density [9]. Electrical conductivity of selected metals, the values of electrical resistance of plastic materials, and their densities are shown in Table 1

Based on the experimental research carried out by the authors of the paper and the literature review, it can be concluded that purity of the concentrate is most impacted by the size of grain. According to Niu et al, Dascalescu et al. and Hogzhou, changes in parameters such as voltage and rotational speed do not significantly affect the purity of the concentrate [4, 18, 19]. That is why the choice of the method and device for crushing PCB is very important. According to the authors, Kozłowski et al. and Franke and Suponik, grinding can be carried out in a knife mill [6, 11].

Table 1
Densities and electrical properties of selected metals and plastics

	Material		Density, g/cc	Electrical conductivity, $10^6\ \Omega^{-1}\ m^{-1}$
Metals	Gold	Au	19.30	44.35
	Lead	Pb	11.30	4.74
	Silver	Ag	10.50	61.84
	Copper	Cu	8.96	58.41
	Iron	Fe	7.87	10.13
	Silicone	Si	2.33	0.04
	Material		**Density, g/cc**	**Electrical resistivity, $10^6\ \Omega\ m$**
Plastics	Fiberglass reinforced plastics	FRP	1.80-2.00	10^6
	Polyesters	PET vs. PBT	1.31-1.39	$1\text{-}1.4 \times 10^7$
	Polypropylene	PP	0.90	10^9

Source: [3, 21, 28].

METHODS

Preparation for electrostatic separation

PCB from personal computers, hard disks, graphic cards and RAMs were used in this study. The way of preparing and grinding electronic waste is presented in the paper written by Franke and Suponik [6]. The knife mill manufactured by TESTCHEM was used to grind the PCB. The rotation speed of mill was 2815 rpm. The blades used were made of hardened steel and perforated sieve with a mesh size of 2 mm. Four grain classes were obtained from the grinded material: 2.00-0.56 mm, 0.56-0.32 mm, 0.32-0.10 mm and < 0.10 mm. The grain class of 0.32-0.10 mm was 40% of the total. This was a feed for the electrostatic separator. Results for the grain class of 0.56-0.32 were presented in the paper by Franke and Suponik [6]. So far, remaining grain classes have not been tested for the following reasons: in the grain class of 2.00-0.56 mm there were significant connections of metals with non-metals parts that reduce the purity of the concentrate, while for grains lower than 0.1 mm, the damage of electrode triggered by high risk of spark discharge [16] can occurred. In addition, the aggregation effect may appear for this class, which may also affect the efficiency of separation [13, 14]. However, despite this, it is planned that the efficiency of electrostatic separation will be tested for grain size < 0.1 mm.

Electrostatic separation

The drum separator used in the study allows to change three operating parameters. As a result of the experimental research, the following parameters were used: shaft rotation speed 100 rpm, electrical voltage at the electrode 17 kV and distance of the electrode from the shaft 0.03 m.

Product analysis

The feed and products obtained from ES were digested and the concentrations of the elements were measured with the JY 2000 spectrometer (by Yobin-Yvon) using the ICP-AES method. The source of induction was a plasma torch coupled with a frequency generator of 40.68 MHz.

Furthermore in the feed, concentrate and waste phase composition have been determined on the basis of the X-ray diffraction measurements, performed with the Panalytical X'Pert Pro MPD diffractometer, utilizing filtered radiation of a copper-anode lamp ($\lambda_{K\alpha}$ 0.154 nm). The diffraction lines were recorded in the Bragg-Brentano geometry, using the step-scanning method by means of a PIXcell 3D detector on the diffracted beam axis, in the angle range from 20-95° [20] (1 step 0.05°, count time per step 120 s). The diffractograms obtained were analyzed with the use of Panalytical High Score Plus software with the PAN-ICSD database.

The morphology of the feed and products from ES, as well as the chemical composition in microareas, were analyzed by means of the Zeiss Supra 35 high resolution electron microscope, equipped with EDAX EDS chemical analysis system.

RESULTS AND DISCUSSION

As a result of ES, the grinded PCB with grain size of 0.32-0.10 mm were separated into concentrate and waste. The concentrate was about 1/3 of the mass of the tested sample (Table 2), what confirms the average metal content in PCB ranging from 20% to 40%, assessed by authors such as Kumar et al., Bizzo et al., Burat et al. and Wu et al. [8, 17, 26, 27]. The waste was 2/3 of the mass. A high concentrate density of about 11 g/cc indicates high separation efficiency, while waste density of 3 g/cc may indicate the penetration of metal parts into the waste. The analysis of the ferromagnetic content shows that the waste did not contain ferromagnetic parts, in contrast to the concentrate, which had the ferromagnetic content of 0.3% (see Table 2).

Table 2
The results of ES

Product	Density of product, g/cc	Yield of product, %	Content of ferromagnetics in product, %
Feed	5.4	-	0
Waste	3.0	67.7	0
Concentrate	11.1	32.3	0.3

The results of measurements carried out in the ICP-AES of the feed, concentrate and waste products are presented in Table 3.

Out of the 91.44% elements identified in the concentrate, over 90% were metals. Si and Br content was over 8%. They form a lead-barium borosilicate glass on PCB. This relatively high content of impurities indicates that PCB needs to be ground into grain classes smaller than 0.32-0.10 mm. In this way, metals would be free of impurities. These elements were probably mechanically bonded to metals.

Table 3
Elemental concentrations in the feed and in ES products: A – this study, B – study by Guo et al. for a similar grain class [10], "-" no data

Element	Content of the element [%] in					
	Feed		Concentrate		Waste	
	A	B	A	B	A	B
Al	3.33	1.51	1.89	2.63	0	0.93
Si	15.6	-	5.15	-	0.0989	-
K	0.0589	-	0.00980	-	0	-
Ca	8.99	-	1.11	-	0.0095	-
Mg	0.0045	-	0.00890	1.23	0.00055	0.28
Mn	0.0355	-	0.10	-	0	-
Fe	0.3821	1.38	0.93	3.74	0	0.19
Ni	0.185	0.28	0.85	0.75	0	0.039
Cu	19.5	27.08	59.70	72.81	1.22	3.99
Zn	0.25	0.79	1.09	2.12	0	0.11
Br	13.8	-	2.98	-	0.00055	-
Ag	0.1415	0.0019	0.4996	-	0	-
Au	0.0019	0.0069	0.0101	-	0	-
Sn	2.38	3.23	7.83	9.63	0.0045	0.01
Ba	2.2	-	1.27	-	0.0075	-
Pb	1.95	2.44	8.00	9.63	0	0.12
Totality based on this study (A)	68.81		91.44		1.34	
Totality based on study by Guo et al. (B)		36.72		99.99		5.65

An example of connection of metal parts with plastics is shown in Fig. 4, while Table 4 presents the results of the chemical analysis. On the other hand, the non-metallic elements could have penetrated into the concentrate as a result of imperfections in the separation process. This issue should be checked in further studies. A similar problem concerned waste. Over 1% of copper was found in this group of products. Probably, the reason for contamination by copper was the layered construction of the PCB. According to Tatariants et al. and LaDou, some very thin elements consists of several layers, and the segments responsible for connecting them together are often made of copper [12, 20]. It can be assumed that, if the PCB were grinded to smaller fractions, this element would not penetrate into non-metals.

Guo et al. [10] (see Table 3) received a cleaner concentrate from the ES of a similar grain class. But in their analyzes, they did not take into account such elements as Si, Ca, Br, Ba neither in feed nor in the product of ES.

The creation of a semiproduct chamber in the electrostatic separator can improve the efficiency of metal recovery. Metals mechanically bonded to plastics or glass can be found in this product. They could be ground again to separate metals from plastics. Then this product could be separated again.

The concentrate contained the following valuable metals: Cu, Pb, Sn, Al, Zn, Ni, Ag, Au. The amount of the metals identified depends on the date of production, the manufacturer or the quality of the PCB and the type of the components used [22]. As provided by Bizzo et al., over the years PCB have had various metal contents i.e. Cu 12-28%,

Al 1.7-7%, Pb 1-3%, Zn 0.08-2.7%, Ag 79-3300 ppm, Au 29-11200 ppm [27].

To determine the morphology of the feed and products obtained from the ES, SEM observations and chemical analysis in micro-regions, by means of energy-dispersive X-ray spectroscopy (EDS) were performed. Imaging of the tested samples using the backscatter electron detection technique (QBSD) (Fig. 2 and 3), allowed to investigate the morphology.

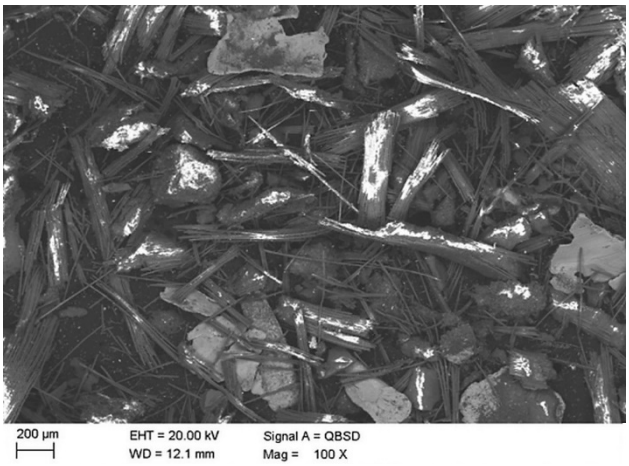

Fig. 2 Image of the feed (QBSD SEM)

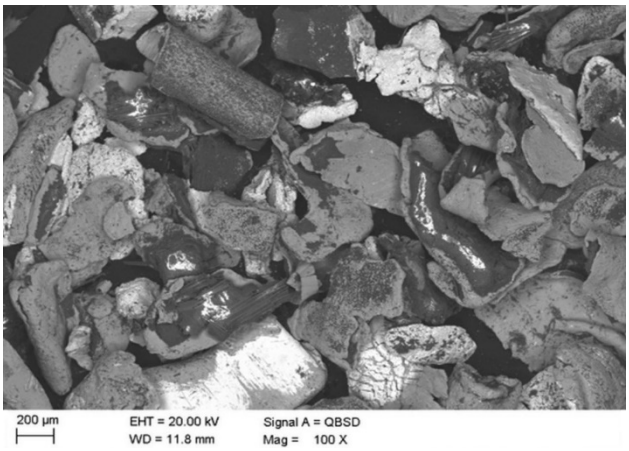

Fig. 3 Image of the concentrate from ES (QBSD SEM)

The contrast obtained in these pictures is a result of differences in the chemical composition. The areas containing elements with a high atomic number are clearly brighter compared to the areas consisting of lower Z-number elements. In the tested feed sample (Fig. 2), both metallic particles of various shapes and dimensions mostly in the range of 100 to 400 µm, as well as many fragments of non-metallic fibers and particles, were observed. In many cases, these non-metallic particles are bonded with metal, which may be due to the PCB production process, in which thin films of good electrical conductivity metals (mainly Cu and Sn, Au, Ag, Pt) are applied on a glass fiber and epoxy laminate [7, 29, 31]. This may create difficulties in the ES process, leading to "contamination" of the metallic product with non-metallic particles.

The SEM analysis of the concentrate (Fig. 3 and 4) showed the presence of mainly metal particles with a small amount of non-metallic materials, such as glass fiber, polymers, and ceramics, which were not separated from the metallic particles in the milling process. These metal particles with various geometry and dimensions approx. 300-400 µm (a few particles of the order of 800 µm were also observed) were characterized by different chemical composition, even within one particle, which was demonstrated by means of the chemical composition analysis in micro-areas (Fig. 4 and Tab. 4).

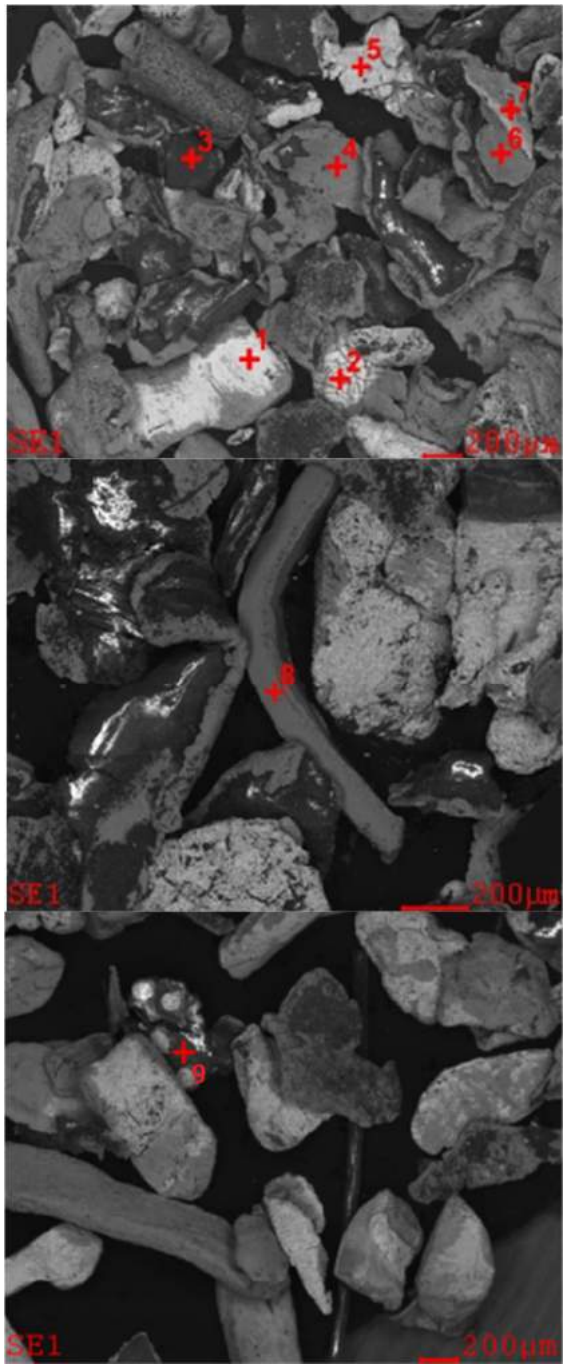

Fig. 4 Images of the concentrate obtained from ES with marked points of chemical microanalysis

Table 4
Results of chemical composition microanalysis for points shown in Figure 4

Element	Point of analysis/Concentration [% at.]								
	1	2	3	4	5	6	7	8	9
Cu	9.71	49.43	38.47	83.39	88.37	38.62	-	-	3.84
Sn	16.76	0.73	3.04	-	-	-	100	-	1.07
Ni	5.19	30.20	-	-	-	2.71	-	37.59	-
Au	68.35	2.65	-	-	-	-	-	-	-
O	-	5.25	30.41	11.66	-	25.23	-	-	38.19
Al	-	7.05	23.81	3.56	-	29.28	-	-	22.33
Si	-	2.69	4.27	1.39	-	0.7	-	2.24	26.55
Pb	-	2.01	-	-	11.63	-	-	-	-
Ti	-	-	-	-	-	1.56	-	-	0.38
P	-	-	-	-	-	0.81	-	-	-
K	-	-	-	-	-	0.5	-	-	-
Mo	-	-	-	-	-	-	-	0.72	1.28
Ag	-	-	-	-	-	-	-	1.45	-
Mn	-	-	-	-	-	-	-	0.67	-
Fe	-	-	-	-	-	-	-	57.35	-
Br	-	-	-	-	-	-	-	-	5.28

The results of the XRD (qualitative phase analysis) of the feed and concentrate and waste products are presented in Fig. 5. For the feed sample, diffraction lines from metallic phases (Cu, Sn, Pb, CuSn) and oxides phases SiO_2 and BaO were recorded. The same phases were indicated in the waste sample, while the intensity of lines obtained from metallic phases significantly decreased, which indicates a much lower volume share of these phases. It can be assumed, that these are mainly the residues of small metal fragments which, combined with larger non-metallic particles of PCB, got into the waste during the separation process. On the diffractogram obtained from the concentrate sample, only the diffraction lines from Cu, Sn, Pb, CuSn metallic phases were identified. However, the presence of other metallic phases in a lower volume share being under detection limit cannot be excluded, as well as with this method it is difficult to identify the small amounts of amorphous phases (polymers, glass).

CONCLUSION

As a result of the research analysis, it can be concluded that the products obtained from the ES were contaminated. Based on the ICP analysis, approximately 91% of metals were identified in the concentrate. These were Cu, in the largest amount (ca. 60%), and then Pb , Sn, Si, Br, Al, Ba, Ca, Zn and small amounts of Fe, Ni, Ag, Mn, Au, K and Mg. It can be assumed that the maximum of 9% of the mass was contaminated. The EDS analysis, as well as the ICP-AES, confirmed appearance of these elements: Cu, Sn, Ni, Au, Al, Si, Pb, K, Ag, Mn, Fe and Br. Quantitative analysis was difficult to perform for both methods. The authors used a larger amount of material in ICP than in EDS, in which only microscopic survey was carried out. The XRD analysis revealed that the concentrate contained mainly Cu, Sn, Pb, CuSn metallic phases, as well as small amounts of oxides phases such as SiO_2 and BaO.

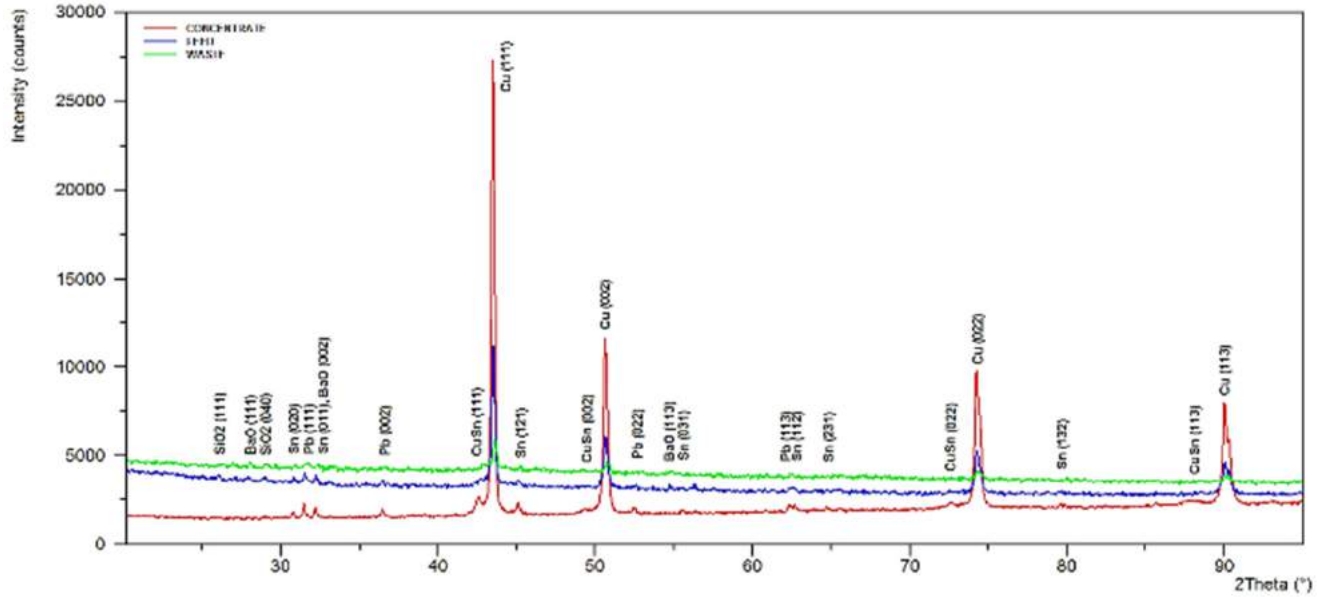

Fig. 5 X-ray diffraction patterns of feed (blue line), concentrate (red line) and waste (green line)

The SEM analysis of the concentrate showed the presence of mainly metal particles with a small amount of non-metallic materials, such as glass fiber, polymers, and ceramics, which were not separated from the metallic particles in the milling process. These metal particles, with various geometry and dimensions, were characterized by different chemical compositions, even within a single particle.

The analyzes of the waste indicated that the small amounts of metallic phases were in the waste sample. They were mainly Cu (ca. 1%) but also Ca, Mg, Sn, Ba in smaller quantities. Presumably, they were mainly the residues of small metal fragments which, combined with larger non-metallic particles of PCB, got into the waste during the separation process.

In conclusion, the results of the research confirmed that the efficiency of metal recovery for the grain class of 0.32-0.10 mm was still insufficient. It is reasonable to optimize the separation process for significantly smaller grains in subsequent works. Consideration should also be given to extending the separator with an additional receiver for semi products, i.e. for grains containing both metals and non-metals.

REFERENCES

[1] A. Cieśla, W. Kraszewski, M. Skowron, A. Surowiak, P. Syrek. "Wykorzystanie bębnowego separatora elektrodynamicznego do separacji odpadów elektronicznych." *Mineral resources management*, vol. 32(1), pp. 155-174, 2016.

[2] A. Kumar, M. E. Holuszko, T. Janke. "Characterization of the non-metal fraction of the processed waste printed circuit boards." *Waste Management*, vol. 75, pp. 94-102, 2018.

[3] A. Tuncuk, V. Stazi, A. Akcil, E.Y. Yazici, H. Deveci. "Aqueous metal recovery techniques from e-scrap: Hydrometallurgy in recycling." *Minerals Engineering*, vol. 25**,** pp. 28-37, 2012.

[4] B. Niu, Z. Chen, Z. Xu. "Recovery of Valuable Materials from Waste Tantalum Capacitors by Vacuum Pyrolysis Combined with Mechanical-Physical Separation." *ACS Sustainable Chemistry & Engineering*, vo. 5(3), pp. 2639-2647, 2017.

[5] C.P. Baldé, V. Forti, V. Gray, R. Kuehr, P. Stegmann, 2017. "The Global E-waste Monitor–2017" *United Nations University (UNU), International Telecommunication Union (ITU) & International Solid Waste Association (ISWA)*, Bonn/Geneva/Vienna.

[6] D. Franke, T. Suponik. "Metals recovery from e-scrap using gravity, electrostatic and magnetic separations." IOP Conf. Series: Materials Science and Engineering 545(012016), 2019.

[7] D. Shangguan (Ed.). "Lead-Free Solder Interconnect Reliability." ASM International, Ohio, 2005.

[8] F. Burat, M. Özer. "Physical separation route for printed circuit boards." *Physicochemical Problems of Mineral Processing*, vol. 54(2), pp. 554-566, 2018.

[9] J. Drzymała. "Mineral processing." Ofic. Wyd. PWr, Wrocław, 2007.

[10] J. Guo, J. Guo, Z. Xu. "Recycling of non-metallic fractions from waste printed circuit boards: A review." *Journal of Hazardous materials*, vol. 168(2-3), pp. 567-590, 2009.

[11] J. Kozłowski, W. Mikłasz, D. Lewandowski and H. Czyżyk, "Research on hazardous waste - management part I", *Archives of Waste Management and Environmental Protection*, vol. 15, no. 2, pp. 69-76, 2013.

[12] J. LaDou. "Printed circuit board industry" *International Journal of Hygiene and Environmental Health*, vol.209 (3), pp. 211-219, 2006.

[13] J. Li, Q. Zhou, Z. Xu, "Real-time monitoring system for improving corona electrostatic separation in the process of recovering waste printed circuit boards", *Waste Manag Res*, vol. 32, no. 12, pp. 1227-1234, 2014.

[14] J. Li, Z. Xu, and Y. Zhou, "Application of corona discharge and electrostatic force to separate metals and nonmetals from crushed particles of waste printed circuit boards", *Journal of Electrostatics*, vol. 65, no. 4, pp. 233-238, 2007.

[15] J. Sohaili, S.K. Muniyandi, S.S. Mohamad. "A review on printed circuit board recycling technology." *Journal of Emerging Trends in Engineering and Applied Sciences*, vol. 3(1), pp. 12-18, 2012.

[16] J. Wu, J. Li, and Z. Xu, "Electrostatic Separation for Recovering Metals and Nonmetals from Waste Printed Circuit Board: Problems and Improvements", *Environ. Sci. Technol.*, vol. 42, no. 14, pp. 5272-5276, 2008.

[17] J. Wu, J. Li, Z. Xu. "Electrostatic separation for multi-size granule of crushed printed circuit board waste using two-roll separator." *Journal of hazardous materials*, vol. 159(2-3), pp. 230-23, 2008.

[18] L. Dascalescu, A. Tilmatine, F. Aman, M. Mihailescu. "Optimization of electrostatic separation Processes using response surface modeling." *IEEE Transactions on Industry Applications*, vol. 40 (1), pp. 53-59, 2004.

[19] L. Hongzhou, L. Jia, G. Jie, X. Zhemning. "Movement behavior in electrostatic separation: Recycling of metal materials from waste printed circuit board." *Journal of Materials Processing Technology*, vol. 197 (1-3), pp. 101-108, 2008.

[20] M. Tatariants, S. Yousef, R. Sidaraviciute, G. Denafas, R. Bendikiene. "Characterization of waste printed circuit boards recycled using a dissolution approach and ultrasonic treatment at low temperatures." RSC Adv. 7 , pp. 37729-37738, 2017.

[21] N. P. Cheremisinoff, P. N. Cheremisinoff. "Fiberglass Reinforced Plastics." Noyes Publications, USA, 1995.

[22] R. G. Charles, P. Douglas, I. L. Hallin, I. Matthews, G. Liversage. "An investigation of trends in precious metal and copper content of RAM modules in WEEE: Implications for long term recycling potential." *Waste Management* vol. 60, pp. 505-520, 2017.

[23] A. Elbakian, B. Sentyakov, P. Bozek, I. Kuric, K. Sentyakov. Automated separation of basalt fiber and other earth resources by the means of acoustic vibrations. *Acta Montanistica Slovaca*. Vol. 23, no. 3, pp. 271-281, 2018.

[24] S. Zhang, Y. Ding, B. Liu, D.A. Pan, C.C. Chang, A.A. Volinsky. "Challenges in legislation, recycling system and technical system of waste electrical and electronic equipment in China." *Waste management*, vol. 45, pp. 361-373, 2015.

[25] V. Goodship, A. Stevels, J. Huisman, J. "Waste electrical and electronic equipment (WEEE) handbook", *Woodhead Publishing*, 2019.

[26] V. Kumar, J. C. Lee, J. Jeong, M. K. Jha, B.S. Kim, R. Singh. "Recycling of printed circuit boards (PCB) to generate enriched rare metal concentrate." *Journal of Industrial and Engineering Chemistry*, vol. 21, pp. 805-813, 2015.
[27] W. Bizzo, R. Figueiredo, V. de Andrade. "Characterization of printed circuit boards for metal and energy recovery after milling and mechanical separation." *Materials*, vol. 7(6), pp. 4555-4566, 2014.
[28] W. M. Haynes (Ed.). "CRC Handbook of Chemistry and Phisics", CRC Press, 2017.
[29] P. Bozek, Y. Nikitin, P. Bezak, G. Fedorko, M. Fabian. Increasing the production system productivity using inertial navigation. *Manufacturing technology*. Vol. 15, no. 3, online, pp. 274-278. 2015.
[30] R. Qiu et al., "Recovering full metallic resources from waste printed circuit boards: A refined review", *Journal of Cleaner Production*, vol. 244, p. 118690, 2020.
[31] Y. Chen, G. Zhu, Y. Zhou, M. Wang, X. Jia, X. Zhu. "Reflow soldering method with gradient energy band generated by optical system." *Optics express*, vol. 26(22), pp. 29103-29215, 2018.

Dawid Franke
ORCID ID: 0000-0002-5522-6889
Silesian University of Technology
Faculty of Mining, Safety Engineering
and Industrial Automation
Akademicka Str., 44-100 Gliwice, Poland
e-mail: dawid.franke@polsl.pl

Tomasz Suponik
ORCID ID: 0000-0002-4251-4275
Silesian University of Technology
Faculty of Mining, Safety Engineering
and Industrial Automation
Akademicka Str., 44-100 Gliwice, Poland
e-mail: tomasz.suponik@polsl.pl

Paweł M. Nuckowski
ORCID ID: 0000-0002-2606-0525
Silesian University of Technology
Faculty of Mechanical Engineering
Department of Engineering Materials and Biomaterials
18A Konarskiego Str., 44-100 Gliwice, Poland
e-mail: pawel.nuckowski@polsl.pl

Klaudiusz Gołombek
ORCID ID: 0000-0001-5188-1950
Silesian University of Technology
Faculty of Mechanical Engineering
Department of Engineering Materials and Biomaterials
18A Konarskiego Str., 44-100 Gliwice, Poland
e-mail: klaudiusz.golombek@polsl.pl

Kamila Hyra
ORCID ID: 0000-0002-9533-0066
Silesian University of Technology
Faculty of Mechanical Engineering
Department of Engineering Materials and Biomaterials
18A Konarskiego Str., 44-100 Gliwice, Poland
e-mail: kamilahyra.65@gmail.com

Physicochem. Probl. Miner. Process., 57(4), 2021, 63-77

http://www.journalssystem.com/ppmp

Physicochemical Problems of Mineral Processing

ISSN 1643-1049

Received April 16, 2021; reviewed; accepted June 03, 2021

Evaluation of the efficiency of metal recovery from printed circuit boards using gravity processes

Dawid M. Franke [1], Tomasz Suponik [1], Paweł M. Nuckowski [2], Justyna Dubaj [3]

[1] Institute of Mining, Faculty of Mining, Safety Engineering and Industrial Automation, Silesian University of Technology, 2 Akademicka Street, 44-100 Gliwice, Poland; dawid.franke@polsl.pl; tomasz.suponik@polsl.pl;

[2] Materials Research Laboratory, Faculty of Mechanical Engineering, Silesian University of Technology, 18A Konarskiego Street, 44-100 Gliwice, Poland; pawel.nuckowski@polsl.pl

[3] Health and Safety Inspectorate, Silesian University of Technology, 2 Akademicka Street, 44-100 Gliwice, Poland; justyna.dubaj@polsl.pl

Corresponding author: dawid.franke@polsl.pl (Dawid Franke)

Abstract: This paper evaluates the efficiency of metal recovery from printed circuit boards (PCBs) using two gravity separation devices: a shaking table and a cyclofluid separator. The test results were compared with the results obtained from previous research, where an electrostatic separation process was used for an identically prepared feed. The feed for the separators consisted of PCBs shredded in a knife mill at cryogenic temperatures. The separation efficiency and purity of the products were evaluated based on microscopic analysis, ICP-AES, SEM-EDS, XRD, and specific density. The yield of concentrates (valuable metals) obtained from the shaking table and the cyclofluid separator amounted to 25.7% and 18.9%, respectively. However, the concentrate obtained from the cyclofluid separator was characterised by much higher purity, amounting to ~88% of valuable metals, compared to ~72% for the shaking table. In both cases, middlings formed a significant share, their yield amounting to ~25%, with the share of valuable metals of ~15%. The yield of waste obtained from the shaking table and the cyclofluid separator were 42.6% and 52.5%, respectively. In both cases, as a result of the applied process, the waste was divided into two homogeneous groups differing in grain size and shape. The recovery of metals through gravity separation is possible, in particular, by using a shaking table. These processes can also be applied to separate waste (plastics) into two groups to be selectively processed to produce new materials in line with a circular economy.

Keywords: metals recovery, printed circuit board, gravity separation, ICP-AES, SEM-EDS

1. Introduction

Electronic waste is an increasing challenge to the modern world driven by the doctrines of circular economy and sustainable development (Geissdoerfer et al., 2017; Kumar et al., 2015). As a result of technological progress, more and more waste of electrical and electronic equipment (WEEE) is produced, containing various hazardous additives and substances, such as mercury, brominated flame retardants, and chlorofluorocarbons or hydrochlorofluorocarbons (Forti et al., 2020). In addition, almost all WEEE contains printed circuit boards (PCBs) (Kumar et al., 2015), rich in valuable metals, the share of which is significantly higher than in natural metal ores (Dascalescu et al., 1992; Johnson et al., 2007). Therefore, despite the already known WEEE recycling technologies (Huang et al., 2009; Li et al., 2007; Schluep et al., 2006), it is necessary to carry on research to develop environmentally friendly and cost-effective technologies that can be applied in specific business and industrial conditions of a given country, using the existing technological installations and other technical resources.

PCBs are estimated to contain 30% of metals (hereinafter referred to as metals) in a free state and 70% of components such as glass fibre reinforced epoxy resin and polyesters (hereinafter referred to as

DOI: 10.37190/ppmp/138471

plastics) (Huang et al., 2009; Kumar et al., 2018a). PCBs are divided into different types depending on the purpose, but the most popular and most frequently used ones are FR-4 (Weil and Levchik, 2004). The plastic part of FR-4 mainly consists of SiO_2 (approx. 40%), CaO (approx. 20%), and, to a lesser extent, Al_2O_3, MgO, and BaO (Muniyandi, 2014). In addition, to improve the thermal resistance properties of PCBs, flame retardants (bromine and antimony compounds) are added (Duan et al., 2016). It is estimated that the metallic part of PCBs is composed of approx. 16% Cu, 3% Fe, 3% Sn, 2% Pb, 1% Zn, as well as Al, Ni, Cr, Na, Cd, Mo, Ti, and Co in smaller amounts (Bizzo et al., 2014; Kumar et al., 2018b). What is worth noting is the share of noble metals such as Au, Ag, and Pd, mainly used as contact metals (Cayumil et al., 2016), which is estimated to amount to 0.05%, 0.03%, and 0.01%, respectively (Charles et al., 2017).

Among the methods of recovering metals from PCBs, chemical and physical processes can be distinguished. The use of chemical methods often involves interference with the natural environment by discharging pollutants into the water and air (Leung et al., 2007; Qiu et al., 2020; Xiang et al., 2007) and generating waste. Currently, the most commonly used methods include pyrometallurgical, hydrometallurgical, biohydrometallurgical (Kaya, 2017), and plasma (Changming et al., 2018) separation. The last two can be classified as environmentally friendly. Still, in the case of biohydrometallurgy, the disadvantage is the long-term impact of micro-organisms on the components of PCBs during the catalysis of the metal recovery process. In the case of an installation for the production of metals via metallurgy functioning in a given region, it seems reasonable to separate metals from PCBs using cost-effective physical methods and process them in this installation. The non-metallic part (plastics) can then, following the principles of circular economy, be used to produce prefabricated elements, such as, for example, composite boards. The physical recovery methods include: electrostatic (Dascalescu et al., 1992; Franke et al., 2020; Jiang et al., 2009; Wu et al., 2008), magnetic (Suponik et al., 2019; Veit et al., 2005), and gravity separation in the air (Eswaraiah et al., 2008; Yoo et al., 2009) and water medium (Duan et al., 2009; Zhu et al., 2020). Metal recovery from PCBs can also be carried out by flotation using flotation reagents (Gallegos-Acevedo et al., 2014; Otunniyi et al., 2013) or without them (Ogunniyi and Vermaak, 2009). One of the popular gravity methods of metal recovery is separation on a shaking table, enabling the effective separation of metals from plastics (Burat and Özer, 2018; Zhu et al., 2020). In all these methods, it is necessary to adjust the degree of grinding and release the valuable substance, i.e., metals in the free state.

This research aimed to evaluate the efficiency of metal recovery from PCBs via two methods based on grain density difference: a shaking table and a cyclofluid separator, for the option, verified in the paper (Suponik et al., 2021), of grinding the feed (PCBs) in a knife mill with the use of liquid nitrogen as a medium for lowering the process temperature.

2. Materials and methods

2.1. Material

Popular motherboards from well-known manufacturers such as Intel, MSI, Asus, Nvidia, and Gigabyte were used in the study. The boards were disassembled from damaged or obsolete desktops assembled in 2007-09. The dismantled PCBs belonged to the most numerous group of FR-4, the laminate of which consists of glass fibre and epoxy resin (Sanapala, 2008). To minimise the diversity of material properties and thus facilitate the grinding process, the following elements have been removed from the boards: resistors, transistors, capacitors, EMI filters, connectors, batteries, chips, screws, and switches (Lee et al., 2012). Simple workshop tools were used for the disassembly process.

2.2. Grinding and preparation of feed for gravity separators

The feed for the LMN-100 knife mill by TestChem consisted of PCB parts cut into 3 cm x 3 cm pieces. The grinding was performed at cryogenic temperatures (<-150^{o}C). The cooling of the feed was carried out by placing the material in a container with liquid nitrogen. The cooling time was defined as the time from placing the material in the container until the liquid nitrogen ceased to boil and was equal to approximately 1 minute per 20 grams of material. The grinding parameters were as follows: sieve perforation in the mill 1 mm, mill load 20 g/min, rotator speed 2815 rpm, the gap between the knives

0.5 mm. The method of grinding with the use of various process parameters was the subject of the research presented in the paper (Suponik et al., 2021), where an electrostatic separator was used to separate metals from plastics after the grinding process. Due to the difficulties in dampening some parts of the ground material and the presence of grains with a density lower than that of water (Tuncuk et al., 2012), the feed for gravity separation was carried out in an aqueous medium was adequately prepared. For this purpose, before separation, the material was placed in a mechanical mixer for approx. 30 minutes, and then floating grains were collected from the water surface. These grains were not included in the gravity processes.

2.3. Gravity separation in an aqueous medium

Two devices for gravity separation of fine grains were used in the study: a shaking table (ST) and a cyclofluid separator (CS). The ST was equipped with a slatted aluminium plate, two independent nozzles for feeding water, and a feeder. As a result of separation, it is possible to obtain ten feed separation products. The separation of products into concentrate, middlings and waste resulted from the difference in the specific density of the grains. Based on previous observations (Franke et al., 2020; Suponik et al., 2021), the concentrate included products with a specific density >7.5 g/cm^3, the middlings included grains with a density of 7.4-3.5 g/cm^3, and waste I and II included grains with densities of 3.4-2.5 g/cm^3 and <2.4 g/cm^3, respectively. The separation parameters were as follows: table load: 9 dm^3/min (water with the material); the mass of material used for testing: 400 g, water flow rate of the first nozzle 5.7 dm^3/min, a water flow rate of the second nozzle 5.4 dm^3/min; table stroke 1.5 mm; table movement frequency 260 strokes/min; longitudinal slope angle: 1˚; transverse slope angle: 6˚; duration of separation: 3 min 45 sec.

The second method of separation was carried out in the CS (Fig. 1). For this purpose, a laboratory cyclofluid separator was built. Its operating principle corresponding to the operation of a semi-industrial U-shaped cyclofluid separator with continuous motion (patent application no. P.424161, Poland). The main elements of the laboratory CS structure were a cylindrical tank filled with water and a separation chamber immersed in it. The chamber was equipped with a sieve with a mesh size of 0.5 mm in the lower part. In the upper part, a drive was fixed that caused a vertical movement of its medium. The principle of operation is based on separation by cyclic fluidisation of the grains from the suspension according to their different densities. The pulsating and vertical movement of the liquid in the working chamber immersed in the tank exerts a thrust force on the grains. The stream lifts and loosens the material, and after it is throttled, the grains fall and are stratified by density. After the separation process is completed, the layers of products with specific densities are formed in the separation chamber – with grains characterised by the highest densities at the bottom of the cylinder. In the case of ground PCBs, no layers with visible characteristic boundaries were formed. Therefore, the contents of the chamber were separated into 0.5 cm-high layers. Layers of similar densities were combined: concentrate I consisted of products with a density above 8.5 g/cm^3; concentrate II consisted of material with a density from 8.4 to 8.0 g/cm^3; middlings I from 7.9 to 6.5 g/cm^3; middlings II from 6.4 to 5.0 g/cm^3; intermediate III from 4.9 to 3.5 g/cm^3; and waste I and II from 3.4 to 2.5 g/cm^3 and <2.4 g/cm^3, respectively. To increase the thrust force (liquid stream) acting on the grains, a band with one-way valves was attached to the body of the working chamber. The upward movement of the working chamber caused the valves to open, and when the direction of movement was changed, they were closed. The parameters of the separation process in the CS were as follows: volume of used water 13 dm^3, material density - 200 g of material per 0.5 dm3 of water; separation chamber stroke 4 cm; separation chamber movement frequency 53 movements/minute; duration of separation: 1 min. 30 sec.

2.4. Product analysis

The purity of the concentrates, middlings, and waste was evaluated using Inductively Coupled Plasma Atomic Emission Spectroscopy (ICP-AES), specific density analysis using a pycnometer and ethyl alcohol (PN-EN 1097-7: 2001), Scanning Electron Microscope (SEM) with Energy Dispersive X-ray Spectroscopy (EDS), and microscopic analysis using Stereo Microscope and X-ray Powder Diffraction (XRD). The following analyses were carried out for the separation products obtained from the shaking table and cyclofluid separator:

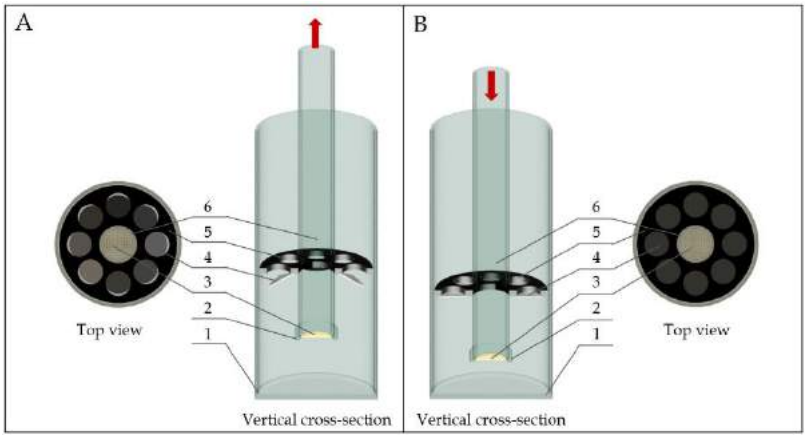

Fig. 1. Diagram of a laboratory cyclofluid separator: A – upper position, B – lower position, 1 – cylindrical tank ($Ø_{in}$ 19.5 cm), 2 – sieve clamp, 3 – sieve (mesh size 0.5 x 0.5 mm), 4 – valves, 5 – band, 6 – separation (working) chamber: $Ø_{in}$ 5 cm

- ICP-AES – using the Jy2000 spectrometer (by Yobin-Yvon) to assess the share of elements in products. The source of the induction was a plasma torch coupled with a 40.68 MHz frequency generator. The products were diluted beforehand;
- Specific density – with the use of Gay-Lussac pycnometers based on PN-EN 1097-7:2001 with the use of ethyl alcohol with a density of 0.7893 g/cm^3;
- Microscopic – using the Modular Stereo Microscope, Zeiss SteREO Discovery (Carl Zeiss AG, Germany).

The following additional analyses were carried out for the concentrates and middlings obtained as a result of separation:

- High resolution scanning electron microscope Zeiss SUPRA 35 (Carl Zeiss AG, Germany), equipped with EDAX Energy Dispersive X-ray Spectroscopy (EDS) chemical analysis system (EDAX, US);
- Qualitative phase analysis was performed with the use of a Panalytical X'Pert Pro MPD diffractometer (Panalytical, the Netherlands), utilising filtered radiation of a cobalt-anode lamp ($\lambda K\alpha$ = 0.179 nm). The diffraction lines were recorded in Bragg-Brentano geometry, using the step-scanning method by means of a PIXcell 3D detector on the diffracted beam axis, in the angle range from 20–100° [2θ] (step 0.05°, count time per step 200s). The obtained diffractograms were analysed with the use of Panalytical High Score Plus (v. 3.0e) software with the PAN-ICSD database.

3. Results and discussion

The feed for both separators was the material shredded in a knife mill with the cooling of the PCBs to cryogenic temperatures. Detailed results of the feed grinding study are presented in the publication (Suponik et al., 2021). The particle size distribution of the feed is shown in Table 1. Due to the nature of the material, the analysis was carried out using sieves and particle size analyser. More detailed information on this material is provided in the article (Suponik et al., 2021).

As a result of separation on the ST, in line with the assumed separation, four products T1 - T4 were obtained, while on CS seven products C1 - C7 were obtained. Product yields and their densities are presented in Table 2 and 3, respectively. In both cases, the floating material, which constituted approx. 3% of the feed was removed before separation. This material was named T0 and C0 according to the process used. Considering that the density of metals is much higher than that of plastics and fibreglass, it can be concluded that this material did not contain any metallic parts.

The highest yield of concentrate was obtained for the ST. It was quantitatively comparable to the yield obtained in the research with the use of electrostatic separation (Suponik et al., 2021). Due to the construction of the CS, two groups of concentrate were obtained from this device: C1 – grains that passed through the sieve and C2 – grains that remained directly at the up of the sieve. The yield of these

Table 1. Particle size distribution of the feed (Suponik et al., 2021)

Grain Class, mm	Yield of the feed, %	
	Analysis carried out with Fritsch screens	Analysis carried out with the particle size analyser
>2.0	0.0	0.0
2.0–1.4	0.0	0.0
1.4–1.0	0.4	0.0
1.0–0.71	3.6	1.6
0.71–0.50	13.0	10.4
0.50–0.36	19.5	22.1
0.36–0.25	17.0	14.2
0.25–0.18	10.6	6.5
0.18–0.13	10.8	5.3
0.13–0.09	8.5	4.3
<0.09	16.6	35.6

groups amounted to less than 19%. For both analysed devices, a significant share was exhibited by separation middlings (T2 and C3 - C5), whose total yields were comparable for both processes and amounted to more than 25%, while the share of the intermediate obtained from electrostatic separation in the paper (Suponik et al., 2021) was much lower and amounted to less than 3%. Based on the density analysis, products T3, C6 and T4, C7 were classified as waste with comparable yields and densities. In both cases of separation, the most numerous wastes were T4 (33.7%) and C7 (44%), made up of the smallest grains.

An essential parameter for the assessment of the purity of separation products was their density. As the density increased, the metal share increased as well, while the lower the density, the higher the share of plastics and fibreglass. The highest density was obtained for t he product C1 (8.9 g/cm^3), followed by C2 (8.1 g/cm^3), and T1 (8.0 g/cm^3). The relatively low density of the concentrate obtained from the ST may indicate its high contamination with plastics and fibreglass. Referring to the research results presented in the publication (Suponik et al., 2021, p. 21), the product density of C1 was comparable to that of the concentrate resulting from electrostatic separation. The density of the product T2 was 4.5 g/cm^3, while the densities of the products C3 – C5 ranged from 7.0 g/cm^3 to 4.1 g/cm^3. The high density of the C3 product indicates the penetration of a high metal share into it – there is no clear boundary between the densities corresponding to the concentrates and middlings. The reason for the significant differences in the density of the middlings obtained from CS and the high density of the C3 product is the separation of the resulting material column into layers. The thickness of the C3 layer was 0.5 cm, which is the assumed minimum division into layers. If a cyclofluid separator was used on a semi-technical scale and the process was automated, the problem of the high density of the middlings could be eliminated and part of the material from C3 would go to the concentrate with the assumed density >7.5 g/cm^3. Waste densities for both devices were <3.1 g/cm^3.

For economic and environmental reasons, the amount of water used should also be noted. Water was continuously supplied to the ST separation processes. The water circuit can be closed, but in this case, the station should be equipped with a filtering installation to remove fine particles from the water. In the case of the CS, on the other hand, water is consumed as a result of filling the tanks and during the collection of products remaining on the sieve. During the tests with the use of the ST, about 77 dm^3 of water was used, while in the case of the CS it was only 13 dm^3, which makes it more economical and environmentally friendly in terms of water consumption. In both cases, however, the products obtained have to be dried, which also requires the use of energy. This problem does not exist in the case of electrostatic separation, which is carried out dry (Suponik et al., 2021).

Photographs of the products (made with a Zeiss microscope) obtained from the ST and CS are presented in Figures 2 and 3, respectively. In both cases, a characteristic separation of metallic grains from composed of plastics or fibreglass grains can be noticed. In the concentrates (Fig. 2a, 3a, and b), mainly homogeneous metallic grains were present, along with a small number of grains with a mixed

Table 2. Yield and density of products obtained from the shaking table

Products	T0	T1	T2	T3	T4
Yield of product, %	2.8	25.7	28.9	8.9	33.7
Amount of water in the product, dm^3	0.5	0.5	12.0	12.5	51.5
Specific density, g/cm^3	1.9	8.0	4.5	2.9	2.4

T0 – floating grains removed before the separation process

Table 3. Yield and density of products obtained from the laboratory cyclofluid separator

Products	C0	C1	C2	C3	C4	C5	C6	C7
Yield of product, %	3.1	6.4	12.5	12.1	7.1	6.3	8.5	44.0
Distance of layer from the sieve, cm	-	-	0÷0.5	0.5÷1	1÷1.5	1.5÷2	2÷3.5	3.5÷9.5
Specific density, g/cm^3	2.0	8.9	8.1	7.0	5.3	4.1	3.1	2.3

C0 – floating grains removed before the separation process

C1 – grains that have passed through the sieve

chemical composition (conglomerates) of metals, plastics, and fibreglass. However, there were no homogeneous grains composed of plastics and fibreglass. Taking into account all the products obtained, the concentrates showed the greatest variation in terms of grain size and shape. There were mainly irregular, polyhedral, globular, and patch grains. Compared to other concentrates, product T1 (Fig. 2a) exhibited the largest differences in size, while the largest share was exhibited by conglomerates composed of metals, plastics, and fibreglass. The T1 product was dominated by globular grains (ranging from 200 μm to 600 μm) and patch grains (patch thickness >30 μm; width of the most numerous ones □ 600 μm). The least numerous polyhedral grains exhibited transverse dimensions of approx. 400 μm. The shape of the irregular grains demonstrates that they were mostly formed as a result of crushing patch grains. In product C1 (Fig. 3a), the grains were smaller. This is connected to the use of a sieve with a mesh size of 0.5 mm in the CS separation process. Compared to other concentrates, no mixed grains composed of metals, plastics, and fibreglass were established in visible light. Globular grains (ranging from 200 μm to 450 μm) and patch grains (patch thickness> 30 μm; the width of the most numerous ones ranged from 200 μm to 350 μm) were predominant. The dimensions of the polyhedral grains were approx. 400 μm. The C2 product (Fig. 3b) was composed mainly of grains with a globular shape ranging from 500 μm to 850 μm, irregular and polyhedral (transverse dimensions ranging from 400 μm to 600 μm). The share of patch grains was the smallest (patch thickness >30 μm; width in the range of 500 μm to 850 μm).

The middlings were composed of a patch, fibrous, and globular grains. Compared to all other products, the largest grains were observed here. In the case of the T2 product (Fig. 2B), patch grains (with a width ranging from 200 μm to 1100 μm) with a layered structure characteristic of PCBs predominated. The thickness and width of these grains were greater compared to the patch grains found in the concentrates. The T2 product contained grains with a mixed chemical composition (conglomerates) of metals, plastics, and fibreglass, as well as homogeneous grains composed of plastics and fibreglass, mainly fibrous (fibre length up to 1800 μm) and globular (ranging from 600 μm to 1000 μm). In the C3 – C5 products, a gradually decreasing proportion of patch-shaped homogeneous metallic grains can be noticed. The C3 product (Fig. 3c) was composed of homogeneous, metallic patch grains (similar in size to T1), a few metallic polyhedral grains and mixed patch grains. However, there were no homogeneous grains composed of plastics and fibreglass. Such grains appeared in the C4 product (Fig. 3d) and, to a greater extent, in C5 (Fig. 3e). Large patch grains, approx. 2000 μm wide, appeared in the C4 and C5 products. These grains were probably "pushed through" the sieve in the knife mill as a result of the big forces in the grinding chamber.

The products T3 (Fig. 2c) and C6 (Fig. 3f) consisted mainly of fibrous, patch, and globular grains. In the case of the T3 product, fibrous grains (up to 2000 μm long) and patch grains (up to 800 μm wide) were the most numerous. The coloured grains (green, blue, and red) were of a globular shape. No metal-containing grains were found here, unlike the C6 product, where such grains were scarce but present.

Fibrous grains also predominated in the C6 product, but with more varied transverse dimensions. These fibrous grains ranged from the thickness of a single fibre to even 200 μm. Similarly to the T3 product, there were coloured globular grains. The products, T4 (Fig. 2d) and C7 (Fig. 3g), were composed of fibrous grains and a small amount of small globular grains (<100 μm) - mainly plastics, and a small amount of metallic powder, smaller than 20 μm. The C7 product contained fibrous grains characterised by a more variable size than in the case of the T4 waste.

As it can be seen, the largest share of large grains (over 700 μm) was established in middlings, and these grains were mostly composed of metal, plastic, and ceramic conglomerates. This may indicate that the middlings contain large amounts of grains with insufficient level of metal release from the remaining PCB parts and imperfections of gravity processes compared to electrostatic methods. Figs. 2c and 2d show that no metal grains were identified in the waste obtained from the ST. However, they may be covered with plastic and ceramic grains, which is confirmed by the results presented in Table 4. Additionally, this waste has been divided into two groups due to grain size, which may be advantageous in the case of its use – e.g., for the production of prefabricated products. The waste obtained from the CS was characterised by a higher share of metallic impurities and lower grain size uniformity. Fewer metallic grains were present in the intermediate and the waste obtained from the ST than in the case of the CS. The reason for the penetration of these grains towards the waste in the CS could lie in too wide a division into layers which, due to the limited size of the separation chamber, could not be reduced.

(a) **(b)** **(c)** **(d)**

Fig. 2. Products obtained from the shaking table (stereo microscope): (a) – concentrate (T1), (b) – middling (T2), (c) – waste (T3), (d) – waste (T4)

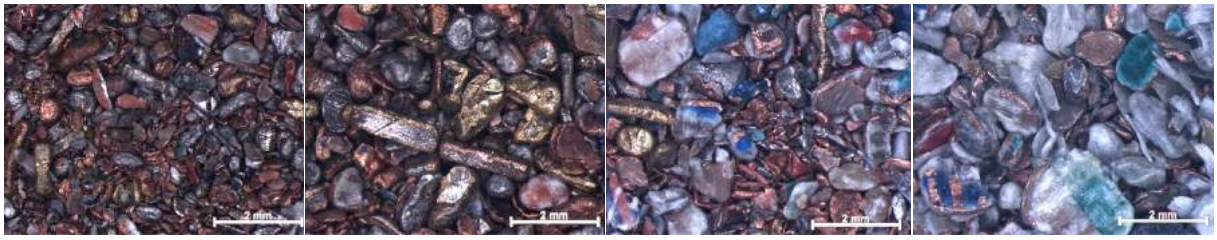

(a) **(b)** **(c)** **(d)**

(e) **(f)** **(g)**

Fig. 3. Products obtained from the laboratory cyclofluid separator (stereo microscope): (a) – concentrate (C1), (b) – concentrate (C2), (c) – middling (C3), (d) – middling (C4), (e) – middling (C5), (f) – waste (C6), (g) – waste (C7)

The chemical composition of the feed and separation products was an important element in the evaluation of the efficiency of the separation processes used. The results of these studies are presented in Table 4. Based on the economic value, a separation into valuable and non-valuable elements was

introduced. Valuable elements include metals the recovery of which can lead to economic benefits and which are present in PCBs in free form. The second group of elements includes the components of epoxy resins, such as Sb, Ca, Br, Ba, Mg, Mn (Muniyandi, 2014), and Si as the main component of glass fibre (Kumar et al., 2018a). Unidentified components are probably components of epoxy resins (mainly polyphenols, less often polyglycols, and epichlorohydrin or oligomers) (Pham and Marks, 2005; Sood et al., 2010; Sood and Pecht, 2018). 17.70% Cu, 2.92% Sn, 0.0301 Ag, 0.0029 Au, 12.02% Sn, 6.56% Ca, 1.64% Br and other elements in low concentrations were identified in the feed (Table 4).

Attention should be paid to the tendencies of changes in the share of individual elements in the separation products. The proportion of valuable elements in the concentrates should be the highest, and non-valuable elements to be the lowest. Among the group of valuable elements, the share of almost all elements decreased towards waste. The exception was Al, the share of which was increasing. The largest share of this metal was identified in the T3 product, followed by T4, C5, and C6. Taking into account the density of this metal equal to 2.7 g/cm^3, in the case of using gravity separation, one could expect its values to vary in different separation products. The difference in the density of this metal is small to plastics and fibreglass, and the small Al grains may not have been fully separated and transferred to the group of grains with higher densities, i.e., to other metals. In the group of non-valuable elements, the shares of Ca, Br, and Si increased towards waste. The highest Sb share was identified in middlings, then in the concentrate, and the lowest in the waste.

In the products T1, C1, and C2, the following concentrations of all valuable metals were identified: 72.00%, 88.79%, and 88.78%, respectively. Among all concentrates, the T1 product contained the least valuable metals, i.e., 71.97%, including 59.20% Cu, 6.3% Sn, and 0.0098% Au. Similar shares were identified in C1 and C2: 88.79% in C1, including 72.10% Cu, 8.10% Sn% and 0.0096% Au, and 87.78% in C2, including 68.10% Cu, 11.40% Sn, and 0.0078% Au. The lowest share of the identified non-valuable elements in the concentrates, which translates into the highest purity of these products, characterised the C1 product, with this value equal to 7.13%, followed by the T1 product with 7.51%. The most contaminated concentrate was C2 with 12.55%. Similar shares of valuable and non-valuable elements were identified in the middlings, which amounted to ~16% and from ~16% to ~18%, respectively. The exception was the C5 product, which contained 6.81% of the identified valuable elements and 21.46% of non-valuable elements. The T3, T4, and C6 products, characterised as waste, contained a comparable amount of valuable and non-valuable elements, i.e. ~6% and ~22%, respectively. The C7 product was the least contaminated with metals, where the share of valuable elements was equal to 4.89%, with the share of non-valuable elements equal to 17.25%.

To examine the morphology of the concentrate and intermediate grains obtained from both gravity separation devices and to determine the chemical composition in the grain micro-areas, as well as to demonstrate the amount and type of metal, plastic, and ceramic or metal and metal conglomerates, photographs were taken (Fig. 4 and 5) via scanning electron microscope using the quadrant backscatter electron detection method (QBSD). Moreover, a local quantitative microanalysis of chemical composition (EDS) (Table 5 and 6) was carried out. These methods primarily allowed to identify the number and type of connections present in mixed grains. The differences in the contrast visible in the photographs (Figs. 4 and 5) may indicate a heterogeneous chemical composition of the grains. Elements with a higher atomic mass are characterised by light colour, in contrast with the elements with a lower atomic mass, which appear as dark areas in the figures. Very bright areas, which are formed as a result of the accumulation of surface charges by plastics, may be an exception.

In the T1 product (Fig. 4a), about half of the surface displayed in the picture is occupied by homogeneous grains (points 1^{T1}, 2^{T1}, 3^{T1}), composed mainly of Cu, Sn, Zn, and a small amount of Al (Table 5). These are mainly globular grains (with a diameter from ~100 μm to ~900 μm) and polyhedral grains (with a transverse dimension of ~350 μm). This product also contains fewer homogeneous patch grains with a diameter of less than 250 μm. Grains with a mixed chemical composition (metal, plastic, and ceramic conglomerates), manifested by high-contrast areas, are mainly patch and irregular grains of various sizes. As can be noticed, the patch grains are covered with a very thin layer of plastic and fibreglass. The T2 product (Fig. 4b) contains grains of mixed chemical composition and grains composed of plastics and fibreglass. Conglomerates constitute the vast majority of the intermediate and mainly take a patch (the diameter of the most numerous ones ranges from 400 μm to 700 μm) and irregular

shape. Compared to the T1 product (Fig. 4a), the proportion of grains <200 μm in diameter is much lower. The results of the chemical composition analysis for micro-areas 2^{T2} and 3^{T2} (Table 5) confirm the presence of Cu in mixed grains, which is still mechanically bonded to the PCB substrate composed of plastics and fibreglass. Due to their chemical composition, it can be assumed that these grains come from internal PCB layers. Grain with a diameter of ~2000 μm, marked with point 2^{T2} (Fig. 4b), was probably pushed through the knife mill sieve during grinding as a result of big forces occurring in the grinding chamber.

In the C1 product (Fig. 5a), homogeneous grains of globular (with the most numerous ones with a diameter of 200 μm to 450 μm), irregular and polyhedral shape (with a maximum transverse dimension up to 200 μm) constituted the largest share. The patch grains present there were small (the most numerous ones less than 100 μm in diameter). Differences in contrast in a small number of patch grains indicate a small number of conglomerates. The chemical composition of grains in the 1^{C1}-4^{C1} micro-areas (Table 6) indicates a high Cu share, which confirms the high purity of the concentrate. In the case of the C2 product (Fig. 5b), polyhedral grains (the most numerous ones with a transverse dimension of ~600 μm) had the largest share. Almost every analysed grain was composed of approximately 50% Cu, 11% Al, 11% Ni, 11% Zn, 9% Sn, 5% Si, 1.5% Ca, and 1% Fe (Table 6). The shape and chemical composition of the grains may indicate that they come from various contacts (sockets) present in the PCBs. Occasionally, irregular grains occurred (point 3^{C2}, Fig. 5b), the shape of which indicated deformed patch grains. Based on the differences in contrast visible in the photographs (Fig. 5b), it can be concluded that the grains are covered with a small layer of plastics and fibreglass. The C3 product is composed mainly of heterogeneous irregular and patch grains (the most numerous ones with a width ranging from 450 μm to 750 μm). Homogeneous metallic patch grains (up to 300 μm wide) were present to a small extent. The results of the chemical composition analysis showed that most of the grains present in the C3 intermediate were composed of Cu, Al, Sn, and Si. Small amounts of Ag were established in the micro-area 2^{C3}. No homogeneous grains composed of plastics and fibreglass have been identified here. The C4 product (Fig. 5d) also includes mainly heterogeneous, irregular grains and patch grains (the most numerous ones with a diameter ranging from 500 μm to 850 μm) and homogeneous fibrous grains (with a transverse dimension up to 300 μm). The results of the analysis of the chemical composition of fibrous grains (point 4^{C4}, Table 6) indicated that these grains were mainly composed of Si, which is the main component of the glass fibre.

For concentrates obtained from the shaking table and cyclofluid separator, an X-ray qualitative phase composition analysis was performed (Fig. 6). Low amounts of metallic or non-metallic phases may have

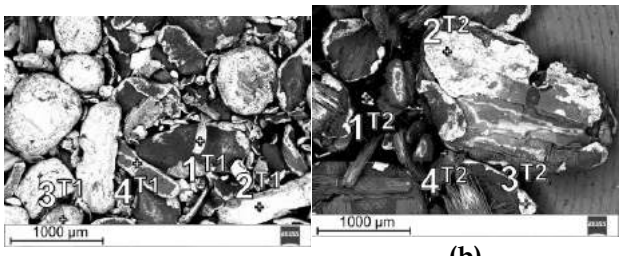

Fig. 4. The T1 and T2 products obtained from the shaking table (SEM, QBSD mode (Table 4) with marked EDS analysis points): (a) – product T1, (b) – product T2

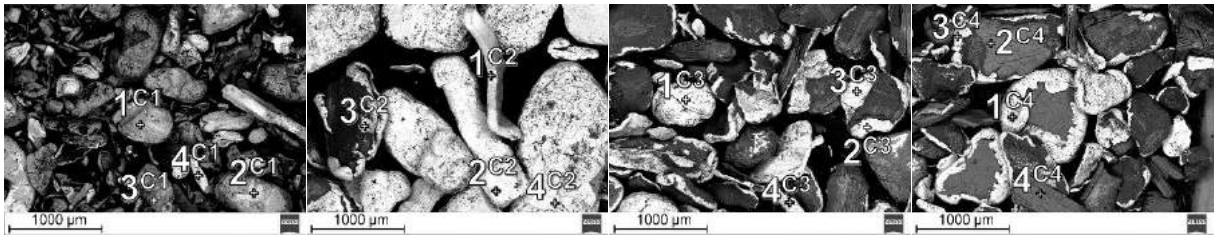

Fig. 5. Products obtained from the laboratory cyclofluid separator (s SEM, QBSD mode (Table 5) with marked EDS analysis points): (a) – product C1, (b) – product C2, (c) – product C3, (d) – product C4

Table 4. Elemental share in the feed and separation products [in %]

	Element	Feed	T1	T2	T3	T4	C1	C2	C3	C4	C5	C6	C7
Valuable elements	Cu	17.70	59.20	9.50	2.44	1.55	72.10	68.10	11.30	10.20	2.88	2.55	1.88
	Al	1.95	0.89	1.61	3.30	3.02	1.09	0.85	1.57	2.17	2.88	2.86	2.49
	Pb	0.39	1.10	0.64	0.02	0.02	1.50	1.40	0.88	0.91	0.05	0.02	0.01
	Zn	0.69	1.90	0.60	0.11	0.06	2.30	2.40	0.65	0.54	0.18	0.11	0.05
	Ni	0.19	0.59	0.19	0.08	0.06	1.09	1.07	0.32	0.36	0.08	0.06	0.01
	Fe	0.38	0.94	0.25	0.38	0.28	1.35	1.44	0.36	0.27	0.41	0.38	0.18
	Sn	2.92	6.30	2.67	0.27	0.36	8.10	11.40	1.10	0.90	0.10	0.11	0.07
	Cr	0.06	0.14	0.07	0.08	0.06	0.21	0.14	0.07	0.08	0.09	0.13	0.08
	Ti	0.26	0.91	0.15	0.13	0.09	0.99	0.89	0.24	0.21	0.15	0.21	0.13
	Ag	0.0301	0.0216	BDL	BDL	BDL	0.0582	0.0078	0.0012	BDL	BDL	BDL	BDL
	Au	0.0029	0.0072	BDL	BDL	BDL	0.0096	0.0078	BDL	BDL	BDL	BDL	BDL
	Sum	24.57	72.00	15.68	6.81	5.50	88.80	87.71	16.49	15.64	6.82	6.43	4.90
Non-valuable elements	Sb	0.22	0.10	0.34	0.18	0.11	0.50	0.30	0.09	0.08	0.15	0.17	0.12
	Ca	6.56	0.90	5.10	6.99	8.10	0.98	1.20	6.10	5.40	7.10	7.40	6.90
	Br	1.64	0.53	0.78	0.92	1.89	0.32	0.45	0.52	0.96	1.50	2.11	2.30
	Ba	0.31	0.71	0.15	0.19	0.12	0.92	0.84	0.09	0.07	0.21	0.25	0.22
	Si	12	3.10	9.30	15.10	13.10	0.92	5.50	6.30	9.20	13.80	15.20	9.80
	Mn	0.01	0.0065	0.0022	BDL	BDL	0.0078	0.0067	0.0054	0.0056	0.0077	0.0062	0.0012
	Sum	20.74	5.35	15.67	23.38	23.32	3.65	8.30	13.11	15.72	22.77	25.14	19.34

*BDL - below detection limit

DOI: 10.37190/ppmp/138471

Table 5. Element concentration [% at.] (EDS) in the micro-areas marked in Figure 4

Product	Point of analysis	Element concentration, % at.														
		Mg	Al	Al	Si	S	Ca	Ti	Cr	Fe	Ni	Cu	Zn	Ag	Sn	Ba
T1	1	-	-	-	-	-	-	-	-	2.7	-	92.2	-	-	5.1	-
	2	-	1	-	-	-	-	-	-	-	9	59.3	28.7	-	2	-
	3	-	1.2	-	1.4	-	-	-	-	-	51.4	34.8	11.2	-	-	-
	4	-	2.5	-	1.9	-	-	-	-	-	-	92.1	-	-	-	3.5
T2	1	-	2	-	3.6	-	-	44.8	-	-	-	-	7.2	-	-	42.4
	2	-	2.5	-	-	-	-	-	-	-	-	85.1	-	-	12.4	-
	3	-	11.3	-	14.5	-	-	-	-	-	-	74.2	-	-	-	-
	4	-	61.9	-	28.6	-	8.3	-	-	-	-	-	-	-	-	1.2

Table 6. Element concentration, [% at.] (EDS) in the micro-areas marked in Figure 5

Product	Point of analysis	Element concentration, % at.														
		Mg	Al	Al	Si	S	Ca	Ti	Cr	Fe	Ni	Cu	Zn	Ag	Sn	Ba
C1	1	-	-	-	-	-	-	-	-	0.6	-	99.4	-	-	-	-
	2	-	-	-	-	-	-	-	-	0.1	-	99.9	-	-	-	-
	3	-	-	8.4	-	-	-	-	-	-	-	91.6	-	-	-	-
	4	-	-	1.4	-	-	-	-	-	-	-	98.6	-	-	-	-
C2	1	-	10.8	-	4.7	-	1.6	-	-	1.9	11	50	11.3	-	8.7	-
	2	-	10.5	-	4.8	-	1.8	-	-	1.8	11.5	49.1	12.2	-	8.3	-
	3	-	10.7	-	4.7	-	1.7	-	-	1.7	12.9	48.3	11.8	-	9.2	-
	4	-	10.1	-	4.9	-	1.7	-	-	1.7	11.1	49.1	12.3	-	9.1	-
C3	1	1.3	18.9	-	18.3	-	-	-	-	-	-	9.3	-	-	52.2	-
	2	0.5	1.0	-	13.5	-	-	-	1.3	6.6	-	33.3	-	1.3	42.5	-
	3	-	4.1	-	-	-	-	-	-	-	2.5	56.2	-	-	37.2	-
	4	-	17.9	-	-	-	-	-	-	-	-	82.1	-	-	-	-
C4	1	-	10.2	-	4	-	1.5	-	1.5	5	-	74.3	3.5	-	-	-
	2	7.4	6.2	-	14.8	39.5	-	-	-	-	-	-	-	-	-	32.1
	3	-	-	-	-	-	-	-	-	4.7	-	95.3	-	-	-	-
	4	-	-	96.3	3.7	-	-	-	-	-	-	-	-	-	-	-

not been identified due to the limited sensitivity of the method. In each of the concentrates, diffraction lines were identified corresponding to Cu, tin bronze CuSn (3.68/0.32), Ni, and Sn phases. Conversely, no diffraction lines were established for the group of non-valuable elements, which may indicate a relatively high purity of the concentrates for a specific concentration range resulting from the detection of the measuring device.

Based on the conducted research, it can be concluded that the correlations between the density, yields, and the share of valuable and non-valuable elements may constitute a parameter determining the quality of separation products (Fig. 7). In the most optimal separation process, the concentrate should contain as many valuable elements as possible and thus should be characterised by the highest possible density. It should be the opposite in the case of waste, which should contain the least valuable elements and exhibit the lowest possible density. Comparing the quality of the products obtained from the shaking table, cyclofluid separator, and electrostatic separator (Fig. 7), it can be concluded that the best efficiency for the analysed material is provided by the electrostatic separator. It should be added that for this device, the amount of the middling is minimised and does not exceed 3%. In comparison with the other tested devices, i.e., the ST and CS, it is a value lower by more than 26% and 22%, respectively. However, it should be noted that the critical factor determining the efficiency of electrostatic separation is the size of the feed grains (Lu et al., 2008; Wu et al., 2009), unlike gravity separators, where the tolerance to grain size changes is greater. The recovery rates of valuable elements for the ST, CS and electrostatic separator were roughly 75%, 70%, 95%, respectively, while metal losses

DOI: 10.37190/ppmp/138471

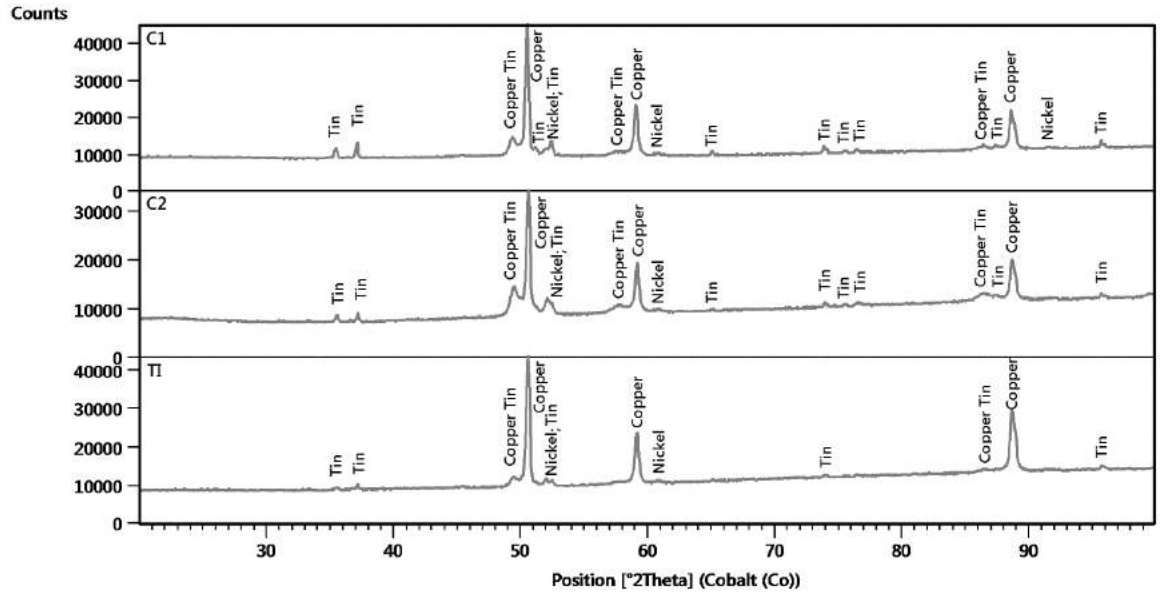

Fig. 6. X-ray diffraction patterns of C1, C2, and T1 products

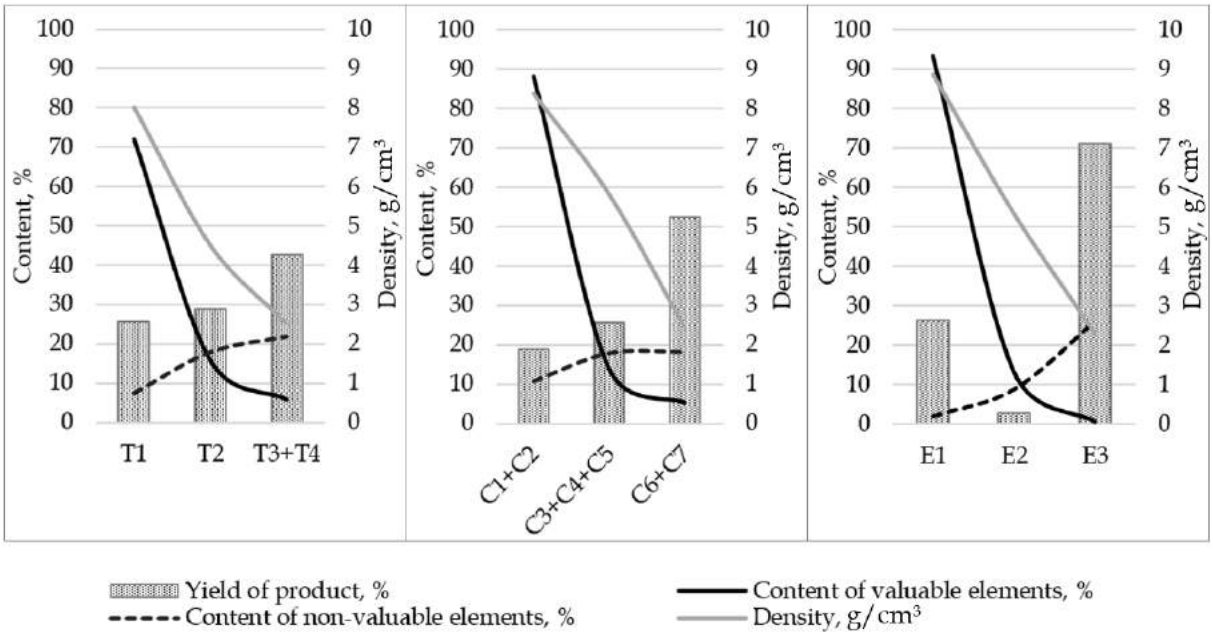

Fig. 7. Yield of separation products as a function of their density and quality parameters (valuable and non-valuable elements); E1 – concentrate, E2 – middlings, and E3 – waste from electrostatic separation (Suponik et al., 2021)

were 10%, 15% and 1%. In the case of the ST and CS, the content of valuable elements in the middlings was very high and amounted roughly 15%, in contrast to the electrostatic separator, in which it was 4%. As already mentioned, the middlings can be further processed, e.g. biohydrometallurgy or next grinding and processing.

4. Conclusions

The efficiency of metal recovery from ground PCBs using a shaking table and a cyclofluid separator is high. The yield of concentrate, intermediate, and waste obtained from the shaking table were 25.7%, 28.9, and 45.4%, respectively. For the cyclofluid separator these values were 18.9%, 31.7%, and 61.9%, respectively. In both cases, the obtained concentrates were characterised by relatively high purity, i.e., the content of valuable elements and the lack of contaminants, i.e., plastics and fibreglass. The

disadvantage of these processes was the high yield of middlings and the related losses of valuable elements.

Therefore, considering the environmental aspects (water consumption and energy consumption when drying the separation products) and the purity of all obtained products, the electrostatic separation presented in the paper (Suponik et al., 2021) seems to be a more favourable process for separating metals from plastics. Furthermore, gravity processes could be used as auxiliary operations, for example, to separate waste (i.e., the mixture of plastics obtained from electrostatic separation) into two groups according to grain size and shape to obtain substrates for the production of various composite materials. These processes could also prove to be highly effective in recovering metals from PCBs in the large variability of the grain composition of the feed.

Acknowledgments

Publication supported by Own Scholarship Fund of the Silesian University of Technology in the year 2019/2020, grant number: 26/FSW18/0003-03/2019.

References

BIZZO, W., FIGUEIREDO, R., DE ANDRADE, V., 2014. *Characterisation of Printed Circuit Boards for Metal and Energy Recovery after Milling and Mechanical Separation*. Materials 7, 4555–4566.

BURAT, F., ÖZER, M., 2018. *Physical separation route for printed circuit boards*. Physicochem. Probl. Miner. Process., 54(2), 554-566.

CAYUMIL, R., KHANNA, R., RAJARAO, R., MUKHERJEE, P.S., SAHAJWALLA, V., 2016. *Concentration of precious metals during their recovery from electronic waste*. Waste Manage. 57, 121–130.

CHANGMING, D., CHAO, S., GONG, X., TING, W., XIANGE, W., 2018. *Plasma methods for metals recovery from metal–containing waste*. Waste Manage. 77, 373–387.

CHARLES, R.G., DOUGLAS, P., HALLIN, I.L., MATTHEWS, I., LIVERSAGE, G., 2017. *An investigation of trends in precious metal and copper content of RAM modules in WEEE: Implications for long term recycling potential.* Waste Manage. 60, 505–520.

DASCALESCU, L., IUGA, A., MORAR, R., 1992. *Corona–Electrostatic Separation: An Efficient Technique for the Recovery of Metals and Plastics From Industrial Wastes*. Magn. Electr. Separ. 4, 241-255.

DUAN, C., WEN, X., SHI, C., ZHAO, Y., WEN, B., HE, Y., 2009. *Recovery of metals from waste printed circuit boards by a mechanical method using a water medium*. J. Hazard. Mater. 166, 478–482.

DUAN, H., HU, J., YUAN, W., WANG, Y., YU, D., SONG, Q., LI, J., 2016. *Characterising the environmental implications of the recycling of non-metallic fractions from waste printed circuit boards*. J. Clean. Prod.137, 546–554.

ESWARAIAH, C., KAVITHA, T., VIDYASAGAR, S., NARAYANAN, S.S., 2008. *Classification of metals and plastics from printed circuit boards (PCB) using air classifier*. Chem. Eng. Process. 47, 565–576.

FORTI, V., BALDÉ, C.P., KUEHR, R., BEL, G., 2020. *The Global E-waste Monitor 2020: Quantities, flows and the circular economy potential*. United Nations University (UNU)/United Nations Institute for Training and Research (UNITAR) – co-hosted SCYCLE Programme, International Telecommunication Union (ITU) & International Solid Waste Association (ISWA), 1-120.

FRANKE, D., SUPONIK, T., NUCKOWSKI, P.M., GOŁOMBEK, K., HYRA, K., 2020. *Recovery of Metals from Printed Circuit Boards By Means of Electrostatic Separation*. Management Systems in Production Engineering 28, 213–219.

GALLEGOS-ACEVEDO, P.M., ESPINOZA-CUADRA, J., OLIVERA-PONCE, J.M., 2014. *Conventional flotation techniques to separate metallic and non-metallic fractions from waste printed circuit boards with particles nonconventional size*. J. Min. Sci. 50, 974–981.

GEISSDOERFER, M., SAVAGET, P., BOCKEN, N.M.P., HULTINK, E.J., 2017. *The Circular Economy – A new sustainability paradigm?* J. Clean. Prod.143, 757–768.

HUANG, K., GUO, J., XU, Z., 2009. *Recycling of waste printed circuit boards: A review of current technologies and treatment status in China*. J. Hazard. Mater. 164, 399–408.

JIANG, W., JIA, L., ZHEN-MING, X., 2009. A new two-roll electrostatic separator for recycling of metals and nonmetals from waste printed circuit board. J. Hazard. Mater. 161, 257–262.

JOHNSON, J., HARPER, E.M., LIFSET, R., GRAEDEL, T.E., 2007. Dining at the Periodic Table: Metals Concentrations as They Relate to Recycling. Environ. Sci. Technol. 41, 1759–1765.

KAYA, M., 2017. *Recovery of Metals and Nonmetals from Waste Printed Circuit Boards (PCBs) by Physical Recycling Techniques*, in: ZHANG, L. et al. (Eds.), Energy Technology 2017. The Minerals, Metals & Materials Series. Springer, Cham., https://doi.org/10.1007/978-3-319-52192-3_43.

KUMAR, A., HOLUSZKO, M.E., JANKE, T., 2018A. *Characterisation of the non-metal fraction of the processed waste printed circuit boards*. Waste Manage. 75, 94–102.

KUMAR, A., KUPPUSAMY, V., HOLUSZKO, M., JANKE, T., 2018b. *Improving the Energy Concentration in Waste Printed Circuit Boards Using Gravity Separation*. Recycling 3, 21.

KUMAR, V., LEE, J., JEONG, J., JHA, M.K., KIM, B., SINGH, R., 2015. *Recycling of printed circuit boards (PCBs) to generate enriched rare metal concentrate*. J. Ind. Eng. Chem. 21, 805–813.

LEE, JAERYEONG, KIM, Y., LEE, JAE-CHUN, 2012. *Disassembly and physical separation of electric/electronic components layered in printed circuit boards (PCB)*. J. Hazard. Mater. 241–242, 387–394.

LEUNG, A.O.W., LUKSEMBURG, W.J., WONG, A.S., WONG, M.H., 2007. *Spatial distribution of polybrominated diphenyl ethers and polychlorinated dibenzo-p-dioxins and dibenzofurans in soil and combusted residue at Guiyu, an electronic waste recycling site in southeast China*. Environ. Sci. Technol. 15;41(8):2730-7

LI, J., LU, H., GUO, J., XU, Z., ZHOU, Y., 2007. *Recycle Technology for Recovering Resources and Products from Waste Printed Circuit Boards*. Environ. Sci. Technol. 41, 1995–2000.

LU, H., LI, J., GUO, J., XU, Z., 2008. *Movement behavior in electrostatic separation: Recycling of metal materials from waste printed circuit board*. J. Mater. Process. Technol. 197, 101–108.

MUNIYANDI, S.K., SOHAILI, J., HASSAN, A., 2014. Encapsulation of non-metallic fractions recovered from printed circuit boards waste with thermoplastic. J. Air. Waste. Manag .Assoc. 64:9, 1085-1092.

OGUNNIYI, I.O., VERMAAK, M.K.G., 2009. *Investigation of froth flotation for beneficiation of printed circuit board comminution fines*. Minerals Engineering 22, 378–385.

OTUNNIYI, I.O., VERMAAK, M.K.G., GROOT, D.R., 2013. *Particle size distribution and water recovery under the natural hydrophobic response flotation of printed circuit board comminution fines*. Mining, Metallurgy & Exploration 30, 85–90.

PHAM, H.Q., MARKS, M.J., 2005. *Epoxy Resins*. In Ullmann's Encyclopedia of Industrial Chemistry, (Ed.), Germany.

QIU, RUIJUN, LIN, M., RUAN, J., FU, Y., HU, J., DENG, M., TANG, Y., QIU, RONGLIANG, 2020. *Recovering full metallic resources from waste printed circuit boards: A refined review*. J. Clean. Prod.244, 118690.

SANAPALA, R., 2008. *Characterisation of FR-4 Printed Circuit Board Laminates Before and After Exposure to Lead-free Soldering Conditions*. M.S. thesis, Dept. Mech. Eng., Univ. Maryland, College Park, MD, USA.

SCHLUEP, M., HAGELUEKEN, C., KUEHR, R., MAGALINI, F., MAURER, C., 2009. *Recycling – from e-waste to resources*. Sustainable Innovation and Technology Transfer Industrial Sector Studies, Berlin, Germany.

SOOD, B., PECHT, M., 2018. *The effect of epoxy/glass interfaces on CAF failures in printed circuit boards*. Microelectronics Reliability 82, 235–243.

SOOD, B., SANAPALA, R., DAS, D., PECHT, M., HUANG, C.Y., TSAI, M.Y., 2010. *Comparison of Printed Circuit Board Property Variations in Response to Simulated Lead-Free Soldering*. IEEE Trans. Electron. Packag. Manufact. 33, 98–111.

SUPONIK, T., FRANKE, D., NUCKOWSKI, P., 2019. *Electrostatic and magnetic separations for the recovery of metals from electronic waste*. IOP Conf. Ser.: Mater. Sci. Eng. 641, 012017.

SUPONIK, T., FRANKE, D.M., NUCKOWSKI, P.M., MATUSIAK, P., KOWOL, D., TORA, B., 2021. *Impact of Grinding of Printed Circuit Boards on the Efficiency of Metal Recovery by Means of Electrostatic Separation*. Minerals 11, 281.

TUNCUK, A., STAZI, V., AKCIL, A., YAZICI, E.Y., DEVECI, H., 2012. *Aqueous metal recovery techniques from e-scrap: Hydrometallurgy in recycling*. Minerals Engineering 25, 28–37.

VEIT, H.M., DIEHL, T.R., SALAMI, A.P., RODRIGUES, J.S., BERNARDES, A.M., TENÓRIO, J.A.S., 2005. *Utilisation of magnetic and electrostatic separation in the recycling of printed circuit boards scrap*. Waste Manage. 25, 67–74.

WEIL, E.D., LEVCHIK, S., 2004. *A Review of Current Flame Retardant Systems for Epoxy Resins*. J. Fire Sci. 22, 25–40.

WU, J., LI, J., XU, Z., 2008. *Electrostatic separation for multi-size granule of crushed printed circuit board waste using two-roll separato*r. J. Hazard. Mater. 159, 230–234.

WU, J., QIN, Y., ZHOU, Q., XU, Z., 2009. *Impact of nonconductive powder on electrostatic separation for recycling crushed waste printed circuit board*. J. Hazard. Mater. 164, 1352–1358.

XIANG, D., MOU, P., WANG, J., DUAN, G., ZHANG, H.C., 2007. *Printed circuit board recycling process and its environmental impact assessment*. Int. J. Adv. Manuf. Technol. 34, 1030–1036.

YOO, J.-M., JEONG, J., YOO, K., LEE, J., KIM, W., 2009. *Enrichment of the metallic components from waste printed circuit boards by a mechanical separation process using a stamp mill*. Waste Manage. 29, 1132–1137.

ZHU, X., NIE, C., WANG, S., XIE, Y., ZHANG, H., LYU, X., QIU, J., LI, L., 2020. *Cleaner approach to the recycling of metals in waste printed circuit boards by magnetic and gravity separation*. J. Clean. Prod.248, 119235.

GOSPODARKA SUROWCAMI MINERALNYMI – MINERAL RESOURCES MANAGEMENT

2022 Volume 38 Issue 1 Pages 171–188

DOI: 10.24425/gsm.2022.140605

DAWID M. FRANKE[1], UMUT KAR[2], TOMASZ SUPONIK[3], TOMASZ SIUDYGA[4]

Evaluation of the use of flotation for the separation of ground printed circuit boards

Introduction

Due to the rapid advancement of technology, the global production of electrical and electronic equipment is increasing rapidly (Tuncuk et al. 2012). Along with technological innovations, economic growth and market expansion, a significant increase is observed in waste electrical and electronic equipment (WEEE) and this increase generates environmental problems (He et al. 2006; Khetriwal et al. 2009). If this waste is incinerated in a smelter, it pollutes the air; if it is disposed of in landfill or leached out to recover metals, harmful substances can be released into the soil and contaminate groundwater (Nnorom and Osibanjo 2009).

✉ Corresponding Author: Dawid Marek Franke; e-mail: dawid.franke@polsl.pl
[1] Silesian University of Technology, Gliwice, Poland; ORCID iD: 0000-0002-5522-6889; e-mail: dawid.franke@polsl.pl
[2] Eskisehir Osmangazi University, Turkey; ORCID iD: 0000-0002-4722-5878; e-mail: umutkar@icloud.com
[3] Silesian University of Technology, Gliwice, Poland; ORCID iD: 0000-0002-4251-4275; e-mail: tomasz.suponik@polsl.pl
[4] University of Silesia, Katowice, Poland; ORCID iD: 0000-0003-4646-6810; e-mail: tomasz.siudyga@gmail.com

The rapidly growing amount of WEEE is becoming a challenge for companies recovering various substances from it. In 2019, the global production of WEEE was 53.6 Mt and is expected to increase to 74.7 Mt in 2030. The estimated value of raw materials contained in e-waste produced in 2019 was 57 billion USD, but considering the current level of WEEE collection and recycling, the potential value for the recovery of raw materials was 10 billion USD (Forti et al. 2020). Increasing the levels of recycling by implementing innovative approaches and technologies allows the reduction of the negative impact on the environment and may bring material benefits to recycling companies.

Printed circuit boards (PCBs), which are an indispensable component of almost all electronic products, can be described as the basis of electronics. PCBs contain large amounts of metals such as Cu, Fe, Al, Sn and rare metals Ta, Ga and other rare metals of the platinum group (PGM) as well as precious metals Au, Ag and Pd (Kaya 2016). They also contain hazardous metals such as Cr, Pb, Be, Hg, Cd, Zn and Ni (Zhang and Forssberg 1997; Kaya 2016). The concentrations of these metals are dozens or even hundreds of times higher than in the mined ores (Yu et al. 2010). The metal concentrations in PCBs and in the corresponding metal ores are presented in Table 1.

Table 1. Metal content in PCBs and in metal ores

Tabela 1. Zawartość metali w PCBs i w rudach metali

Metals	PCBs	Metal ores
	Content (%)	Content (%)
Cu	6–27	0.5–2.0
Fe	1.2–8.0	<65
Al	2.0–7.2	30–60
Sn	1.0–5.6	5–25
Pb	1.0–4.2	–
Ni	0.3–5.4	1–1.5
Zn	0.2–2.2	5–15
Sb	0.1–0.4	5–60
Au (ppm)	250–2,050	0.0001–0.0006
Ag (ppm)	110–4,500	–
Pd (ppm)	50–4,000	–
Pt (ppm)	5–30	–
Co (ppm)	1–4,000	–

Source: Zhang and Forssberg 1997; Kaya 2016; Schwarz 2004; Muwanguzi et al. 2012; Zhou et al. 2004; Haldar 2018; Wang 2016; Anderson 2012.

There are many methods for the recovery of metals from PCBs, including pyrometallurgical, plasma, and (bio)hydrometallurgical separation. However, the use of some of these has some disadvantages. The combustion of non-metal parts by pyrometallurgical methods causes the formation of brominated organic and other toxic compounds (Bidini et al. 2015). Additionally, it produces about 20–25% of ashes containing a large number of heavy metals that require further processing (Long et al. 2010). In hydrometallurgical methods, there is a significant level of high-risk wastewater that can contaminate groundwater and soil (Ma et al. 2018). These methods are also time-consuming.

Physical (or mechanical) and physicochemical processing technologies are considered to be the most environmentally friendly alternative to recovering resources from end-of-life (EoL) products such as PCBs (Goosey and Kellner 2002). Some mechanical processing technologies have advantages with regard to PCB recycling (Zhao et al. 2004; Duan et al. 2009; Zhao et al. 2012) but involve problems in the processing of fine particles (Sarvar et al. 2015). It is scientifically known that froth flotation is an effective technique for fine fraction enrichment (Ogunniyi and Vermaak 2009). This process is based on the selective separation of hydrophobic from hydrophilic materials. It has been used in wastewater treatment, mineral processing, and the paper/waste recycling industries for a long time (Kaya 2019). It has also been employed in the processing of PCBs (Ogunniyi and Vermaak 2009). Flotation technology is widely applied and efficient, especially in the processing of metal ores. However, it requires the use of aqueous solutions. Separation in flotation is achieved by the difference in physicochemical properties of different particles (Farrokhpay 2011; He and Duan 2017). While hydrophilic particles settle down to the bottom of the aqueous medium, hydrophobic particles float due to selective bubble adsorption (Shean and Cilliers 2011). The contact angle, as a parameter that determines the hydrophobic properties of materials, is the angle between the gas and solid phases, through the water phase. This angle is 0° for hydrophilic materials and a maximum of 110° for hydrophobic materials (Drzymala 2007). The ease of separation is directly proportional to the magnitude of the differences in the chemical properties of different particle surfaces (Wills and Finch 2016). For this reason, various reagents called collectors are used to change the hydrophobic properties of the particles. The hydrophobizing power of the collectors is due to their chemical and physical interactions with the surface. The role of frothers is to accelerate flotation, create a stable foam, and disperse the gas. These tasks are accomplished when frothers are preferentially adsorbed at the water-gas interface. A decrease in surface tension accompanies sorption. The reduction in the size of the air bubbles is achieved by adding the frother to the solution. The reduction in the surface tension of the solution is associated with a reduction in bubble size (Drzymala 2007).

The aim of the research was to assess the possibility of recovering metals from ground PCBs by means of flotation. For this purpose, the contact angle of various materials was measured and a series of flotation tests was carried out to select the reagent and its dose, the airflow rate through the flotation tank, and the concentration of the feed. The test results were then compared with the results of electrostatic separation (Suponik et al. 2021) and gravity separation (Franke et al. 2021) used for the same feed.

1. Materials and methods

1.1. Material preparation

The surface of printed circuit boards includes many components that do not contain metals or that can cause considerable problems when grinding. These components can be easily dismantled by simple methods – manual and/or mechanical. These components were first manually separated from the PCBs using basic tools such as screwdrivers and pliers. These manually separated components include resistors (which contain: Ni, Cr, Cd, Al, Pb, and Ta), transistors (Pb and Cu), batteries, chips (Pb, Ni, Sn, Ga, Al, and Ag), capacitors (Sn, Cu, and Zn), electromagnetic interference filters (Fe, Cu, and Zn), connectors (Pb, Ni, and Sn), screws and wrenches (Lee et al. 2012). After manual separation, the pre-cleaned PCBs were cut into 4 × 4 cm pieces due to the limitations of the blade mill.

An LMN-100 blade mill by Testchem (Radlin, Poland) with blades mounted on the chamber body and rotator was used for grinding the material. The mill was also equipped with a sieve to determine the size of the ground material. A perforated sieve with a mesh of 1 mm was used to obtain the finest particle sizes suitable for flotation applications. The rotation speed of the mill was 2815 rpm. Liquid nitrogen was used to reduce the temperature of the previously cut PCB parts to a level of cryogenic temperatures (below –150°C) to avoid the formation of conglomerates (solid metal-plastic-ceramic compounds) that could be formed in the chamber during grinding at high temperatures. An overload of the mill was also prevented for this reason and a load of 20 g/min was applied. The cooling process consisted in placing the feed in a container filled with liquid nitrogen. The feed was cooled until the liquid nitrogen ceased to boil. In this way, the temperature increase in the working chamber of the mill was controlled.

The particle size composition of the feed, which was ensured using Frisch sieves, is presented in Table 2. Most of the feed grains were smaller than 0.5 mm (83 wt%). The rest of the feed consisted of grains up to 0.71 mm (13%) and grains 1.4–0.71 mm (4%). Based on microscopic analysis, it was observed that plastic grains mainly consisted of needle-shaped and fibrous grains, with sizes from less than 50 µm (fiber thickness) to 2000 µm. The less numerous plastic grains were patch-shaped with dimensions up to 1000 µm. This kind of grain

Table 2. Particle size distribution of the feed

Tabela 2. Skład ziarnowy nadawy

Grain classes (mm)	1.4–1.0	1.0–0.71	0.71–0.50	0.50–0.36	0.36–0.25	0.25–0.18	0.18–0.13	0.13–0.09	<0.09
Yield (%)	0.4	3.6	13.0	19.5	17.0	10.6	10.8	8.5	16.6

Source: Suponik et al. 2021.

was characteristic for woven fiberglass. The greatest variation in shape was seen in metal grains. The most numerous shapes were globular (mostly 250 to 500 μm), then patch shape (about 30 μm thick and 500 μm wide) and polyhedral and irregular grains (200–350 μm). In the feed, the conglomerate grains (plastic-metal) were also found. The shape of these grains was mainly patch and globular (approx. 150–1000 μm), which had a layer structure characteristic of PCBs.

1.2. Contact angle measurement

The purpose of measuring the contact angle was to assess the effect of the pH value and the type of reagent on the hydrophobic properties of various materials: metals (copper, molybdenum, niobium, steel, titanium alloy) and poly(tetrafluoroethylene) (PTFE), representing plastics. The greater the difference in the contact angle of metals and PTFE, the better the flotation conditions. PCBs contain roughly 65% of fiberglass and over 30% of hydrophobic materials such as PE, PP, PS, epoxy, PVC, PTFE, and nylon (Kumar et al. 2018; Zhang and Forssberg 1997; Kaya 2016). The assessment of the contact angle on the PCB surface prepared with sandpaper (P5000) was impossible due to the instability of the droplet and its absorption by the PCB structure. This may be due to the deterioration of the fiber structure by polishing. Therefore, PTFE was chosen as the material representing plastics.

The contact angle was measured with a Kernco optical goniometer. Before measurement, each surface was first cleaned with ethanol (30 vol.%), then rinsed with distilled water and quickly dried. For more accurate results for each plate, three drops of the respective solution were spotted onto the surfaces and the contact angles of both the right and left sides of each drop were read. The result was obtained by calculating the arithmetic mean of the six obtained values.

Eleven different aqueous solutions and six different materials were used to measure the contact angle. Plates of copper, PTFE, steel, molybdenum, niobium, and titanium alloys were used for the tests. Solutions of specific concentrations were obtained by dissolving the following reagents in tap water: tannic acid (60 mg/dm^3), 2-octanol (450 mg/dm^3), tannic acid (60 mg/dm^3) + 2-octanol (450 mg/dm^3), dimethoxy dipropyleneglycol (450 mg/dm^3), tannic acid (60 mg/dm^3) + dimethoxy dipropyleneglycol (450 mg/dm^3), calcium oleate (60 mg/dm^3), sodium xanthate (60 mg/dm^3). The given reagents were selected based on the articles by Han et al. Ximei et al. and Langa et al. (Han et al. 2018; Ximei et al. 2017; Langa et al. 2014). The pH values of the presented solutions were 7.57, 7.85, 7.60, 7.83, 7.59, 7.81 and 7.85, respectively. The parameters of tap water were as follows: pH 7.75, redox potential 124 mV, conductivity 0.552 mS, total dissolved solids 323 mg/dm^3, and temperature 16.9°C.

Additionally, the impact of the pH value of tap water on the contact angle was measured in the research. The measurements of the contact angle were made for tap water with different pH values: 2, 4, 7.75 (tap water) and 9. Appropriate pH values were obtained by changing the pH of the tap water with sulfuric acid (0.1 M) or sodium hydroxide (0.1 M).

1.3. Flotation experiments

Flotation experiments were carried out using the laboratory Mechanobr flotation machine produced by "IMN Gliwice; Apparatus Construction Plant of the Institute of Non-Ferrous Metals" using a 1-liter flotation tank. In all tests, the PCB samples were first mixed in tap water for five minutes using a magnetic stirrer. They were then transferred to a flotation tank. The sample doses are given in Table 3. After remixing for two minutes in the flotation tank, if the reagent was not added, the airflow was opened and the test was started (see test number 1 in Table 3). In the case of using one reagent (see tests 2, 3, 6–13 in Table 3), after adding the reagent and mixing for two minutes, the airflow was opened and the test was commenced. In cases where two reagents were used (see tests 4, 5 in Table 3), after the addition of the second reagent, the suspension was stirred for two minutes, then the airflow was opened and the experiment was started. In all tests, the speed of the magnetic stirrer, the rotator speed in the flotation tank and the flotation time remained constant at 100 rpm, ca. 400 rpm and five minutes, respectively.

Table 3. Flotation parameters for different test stages

Tabela 3. Parametry flotacji dla poszczególnych etapów badań

Test No.	Reagent	Solids content	Airflow
First stage: reagent selection			
1	without any reagent	25 g/dm^3	200 dm^3/h
2	tannic acid (60 mg/dm^3)	25 g/dm^3	200 dm^3/h
3	dimethoxy dipropyleneglycol (450 mg/dm^3)	25 g/dm^3	200 dm^3/h
4	tannic acid (60 mg/dm^3), dimethoxy dipropyleneglycol (450 mg/dm^3)	25 g/dm^3	200 dm^3/h
5	tannic acid (60 mg/dm^3) + 2 octanol (450 mg/dm^3)	25 g/dm^3	200 dm^3/h
6	2 octanol (450 mg/dm^3)	25 g/dm^3	200 dm^3/h
Second stage: dose selection			
7	dimethoxy dipropyleneglycol (225 mg/dm^3)	25 g/dm^3	200 dm^3/h
8	dimethoxy dipropyleneglycol (157 mg/dm^3)	25 g/dm^3	200 dm^3/h
9	dimethoxy dipropyleneglycol (60 mg/dm^3)	25 g/dm^3	200 dm^3/h
Third stage: airflow selection			
10	dimethoxy dipropyleneglycol (157 mg/dm^3)	25 g/dm^3	400 dm^3/h
11	dimethoxy dipropyleneglycol (157 mg/dm^3)	25 g/dm^3	600 dm^3/h
Fourth stage: selection of solids content			
12	dimethoxy dipropyleneglycol (157 mg/dm^3)	50 g/dm^3	200 dm^3/h
13	dimethoxy dipropyleneglycol (157 mg/dm^3)	100 g/dm^3	200 dm^3/h

Flotation experiments were divided into four stages (Table 3). The first stage was performed in order to find the best reagent using as a reference the collector and frother doses used in the article by Han et al. (Han et al. 2018) and keeping other parameters constant, with the exception of the reagent types. Additionally, one test was performed with the same parameters without the use of any reagents (test No. 1). The aim of the second stage was to find the optimal dose for the reagent selected in stage 1. The third stage was performed to determine the most effective airflow using the type of reagent and the dose selected in stages 1 and 2. In the fourth stage, the amount of feed was increased by maintaining the most efficient airflow at the optimal dose.

1.4. Methods of analysis

The flotation efficiency (purity of the products obtained) was assessed for all four test stages by means of density measurement. This quick analysis was chosen because PCBs contain plastics with a density below 2.0 g/cm^3, one light metal with a density of 2.7 g/cm^3 (Al, usually at low concentrations in PCBs), and heavy metals with a density above 7 g/cm^3, mainly Cu and ferromagnets (Zhang and Forssberg 1997, 1999). Specific density analysis of flotation products was performed with Gay-Lussac pycnometers based on the PN-EN 1097-7:2001 standard with the use of ethyl alcohol with a density of 0.7893 g/cm^3. There were always three density measurements taken and the result was presented as the arithmetic mean.

The products obtained under optimal flotation conditions (i.e. reagent type – dimethoxy dipropyleneglycol at a concentration of 157 mg/dm^3, airflow and feed concentration of 200 dm^3/h and <50 g/dm^3, respectively) were analyzed using the following analytical techniques:

- Energy dispersive X-ray fluorescence (ED/XRF) by means of a ED-XRF Epsilon 4 Spectofotometer (Malvern Panalytical, Malvern, United Kingdom), equipped with a 10 W X-ray tube with an Ag anode, Silicon Drift Detector type and helium flush system;
- microscopic analysis using Zeiss SteREO Discovery Modular Stereo Microscope (Carl Zeiss AG, Jena, Germany).

2. Results and discussion

2.1. Analysis of flotation tests

The results of the contact angle tests for various pH values of tap water and for various aqueous solutions of the reagents used are presented in Tables 4 and 5, respectively. These values provide rough information on the possibility of separating metals from plastics by flotation.

Table 4. Results of the contact angle tests for different pH values of tap water

Tabela 4. Kąt zwilżania dla wody wodociągowej o różnych wartościach pH

pH	The value of the contact angle (in degrees) for					
	Copper	PTFE	Steel	Molybdenum	Niobium	Titanium Alloy
2	78	107	46	54	50	62
4	78	102	42	59	57	61
7.75 (Tap Water)	62	102	51	57	48	58
9	72	100	52	56	49	58

Table 5. Contact angle test results for various aqueous solutions of the reagents used for different materials

Tabela 5. Kąt zwilżania dla roztworów wodnych reagentów otrzymany dla różnych materiałów

Reagent (concentration)	The value of the contact angle (in degrees) for					
	Copper	PTFE	Steel	Molybdenum	Niobium	Titanium Alloy
tannic acid (60 mg/dm^3)	63	101	54	52	64	58
2 octanol (450 mg/dm^3)	42	95	56	59	54	64
tannic acid (60 mg/dm^3) + + 2 octanol (450 mg/dm^3)	43	93	58	58	66	63
dimethoxy dipropyleneglycol (450 mg/dm^3)	48	109	38	55	48	58
tannic acid (60 mg/dm^3) + dimethoxy dipropyleneglycol (450 mg/dm^3)	55	108	42	50	63	57
calcium oleate (60 mg/dm^3)	69	105	64	58	52	51
sodium xanthate (60 mg/dm^3)	71	104	75	56	43	60

Based on the results of the tests presented in Table 4, displaying the effect of the pH value on the wettability of the samples, it can be concluded that for almost all samples, the contact angle decreased with increasing pH. The best conditions for the separation of plastic grains from metals by the flotation method, i.e. with the greatest difference in the contact angle for PTFE and the analyzed metals, occurred at the pH value of 7.75. These studies concerned the flotation process from aqueous solutions without the use of reagents, i.e. for tap water.

The reagent that generated the greatest difference between the contact angles for PTFE and for the tested metals was dimethoxy dipropyleneglycol at a concentration of 450 mg/dm^3 (this also applies to the lack of reagents, i.e. tap water) (see Table 5). However, the selection of the best reagent was based on laboratory flotation tests with the use of a flotation machine.

The results of these tests are presented in Table 6. They confirm that dimethoxy dipropyleneglycol at a concentration of 450 mg/dm^3 was the best of the tested reagents, generating two products: metals and plastics with densities of 5.6 g/cm^3 and 2.9 g/cm^3, respectively (see first stage – test No. 3 in Table 6). The yield of these products was 42.3% and 57.7%, respectively. Regarding the selection of the best dose for dimethoxy dipropyleneglycol and the best airflow, these parameters were 157 mg/dm^3 and 200 dm^3/h, respectively (both for test No. 8 in Table 6). The metal and plastic densities for these process conditions and their

Table 6. Flotation test results

Tabela 6. Wyniki badań flotacji

Test No.	Yield (%)		Density (g/cm^3)	
	Hydrophobic product (plastics)	Hydrophilic product (metals)	Hydrophobic product (plastics)	Hydrophilic product (metals)
First stage: reagent selection				
1	32.80	67.20	2.9	5.4
2	0.83	99.17	*	4.7
3	57.71	42.29	2.9	5.6
4	19.25	80.75	2.7	4.8
5	16.39	83.61	2.8	4.3
6	53.20	46.80	2.9	5.0
Second stage: dose selection				
3	57.71	42.29	2.9	5.6
7	52.85	47.15	2.8	6.8
8	56.56	43.44	2.7	7.4
9	54.98	45.02	3.0	6.4
Third stage: airflow selection				
8	56.56	43.44	2.7	7.4
10	56.68	43.32	2.9	6.4
11	53.25	46.75	3.1	6.6
Fourth stage: selection of feed concentration				
8	56.56	43.44	2.7	7.4
12	55.08	44.92	2.7	7.2
13	53.92	46.08	2.5	5.4

* No results due to lack of product.

yields were 7.4 g/cm^3, 2.7 g/cm^3, and 43.4 and 56.6%, respectively (second and third stages in Table 6 test No. 8). Based on the research carried out in stage 4, it can be concluded that the flotation efficiency decreases with increasing feed concentration, and is acceptable at the level of 50 g/dm^3. Under these conditions, the metal density decreases from 7.4 g/cm^3 (for feed concentration = 25g/dm^3) to 7.2 g/cm^3. The product yield is very similar, ranging from 43.4% to 44.9%.

2.2. Analysis of products for optimal flotation conditions

The microscopic analysis showed that the hydrophobic product (float fraction) obtained in test No. 8 (see Figure 1a) mainly comprised grains consisting of plastic-ceramic materials of a fibrous and needle shape (< 1100 µm; fiber thickness approx. 150 µm), and less often patch-shaped grains (diameter < 600 µm) with a characteristic PCB composite structure. Individual patch-shaped metal grains with a diameter of up to 230 µm were also observed. Penetration of these grains into the float fraction may be due to their entrapment inside a plastic powder. Moreover, no larger metal grains were found in the float fraction, which may indicate the high purity of this product. The hydrophilic product obtained in test 8 (see Figure 1b) consisted mainly of metal grains of various shapes and sizes, with a fairly large number of plastic-ceramic grains with a specific layered structure. Most of the metals were patch-shaped grains with a diameter of 300 to 700 µm and irregular grains of similar dimensions. Globular grains (diameters from 600 to 800 µm) and polyhedral grains (< 1500 µm; transverse dimensions < 150 µm) were found in smaller numbers. The grains consisting of plastic-ceramic materials visible in the sink fraction were mostly in the patch shape (diameter from 800 to 1000 µm) and, very rarely, the shape of a fiber with a length of 1500 µm and

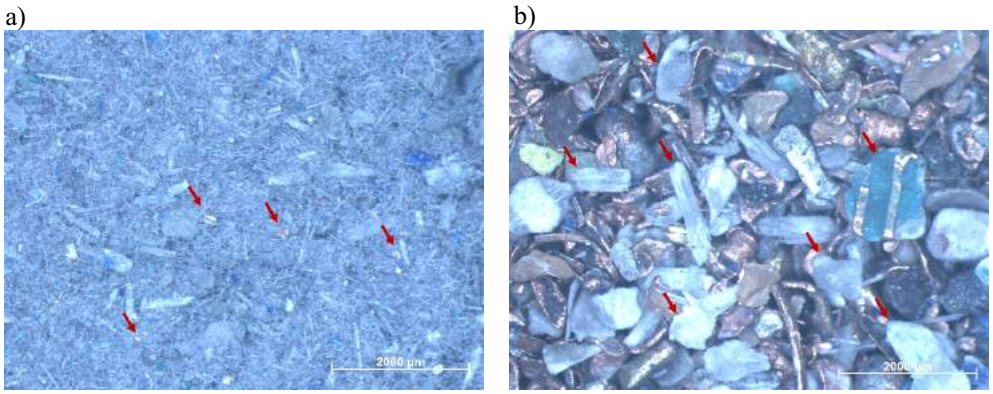

Fig. 1. Microscopic images of a) hydrophobic products (plastics) and b) hydrophilic products (metals) taken for test No. 8 (examples of impurities marked with a red arrow)

Rys. 1. Zdjęcia mikroskopowe: a) produkt górny (produkt hydrofobowy) i b) produkt dolny (hydrofilowy) dla testu nr 8 (zanieczyszczenia oznaczone czerwonym kolorem)

a transverse dimension of up to 300 µm. Moreover, grains of metal-plastic conglomerates (800 µm to 1200 µm in diameter) with a layered structure characteristic of PCBs were observed. The penetration of grains consisting of plastic-ceramic materials and metal-plastic conglomerates into the hydrophilic product was undesirable due to the deterioration of the purity of the concentrate. This was probably due to the large size of these grains. This demonstrates the need to improve the grinding in the knife mill. In the case of electrostatic separation, these products went to the middlings.

To evaluate the efficiency of flotation performed for the best option (test No. 8), a chemical composition analysis was carried out using the ED/XRF method (Table 7). The float fraction contained mainly non-valuable elements (29.82%), which are mostly concentrated

Table 7. Chemical composition of the products obtained using Dimethoxy dipropyleneglycol 157 mg/dm^3 (test No. 8)

Tabela 7. Skład chemiczny produktu otrzymanego przy zastosowaniu eteru dimetylowego glikolu dipropylenowego 157 mg/dm^3 (test nr 8)

	Element	Hydrophobic product	Hydrophilic product	Recovery ratio (%)
Valuable elements	Cu	2.33	39.94	93%
	Al	1.71	1.10	33%
	Zn	0.69	0.92	51%
	Ni	0.34	0.64	59%
	Fe	0.49	0.97	60%
	Sn	1.12	7.80	84%
	Cr	0.31	0.05	11%
	Ti	0.52	0.49	42%
	Ag	0.0918	0.5797	83%
	Au	0.0048	0.0140	69%
	Sum	8.01	53.13	84%
Non-valuable elements	Sb	10.40	0.09	–
	Ca	2.89	3.24	–
	Br	0.69	2.16	–
	Ba	0.0065	0.73	–
	Si	15.84	5.02	–
	Mn	0.0014	0.0083	–
	Sum	29.82	11.29	–

in epoxy resins, glass fabrics and flame retardants (Kumar et al. 2018; Muniyandi et al. 2014). The most numerous were Si (15.84%), Sb (10.40%) and Ca (2.89%). About 8% of valuable metals such as Cu (2.33%), Al (1.71%), and Sn (1.12%) were identified in this product. Considering that metals such as Cu and Sn impact the PCB value, their penetration into the float fraction was unfavorable.

53.13% of valuable metals were identified in the chemical composition of the hydrophilic product, mostly Cu (39.91%), Sn (7.80%), and Al (1.10%), and in smaller amounts, Zn, Ti, Cr, Fe and Ni. Significant amounts of precious metals such as Ag (0.5797%) and Au (0.0240%) were also identified in this product. In addition to valuable metals, over 11% of impurities (non-valuable elements) were found in it. The largest share was comprised of Si (5.02%), Ca (3.24%) and, in smaller amounts, Br, Ba, Sb, and Mn. As can be seen from microscopic and ED/XRF analysis, the sink fraction was significantly contaminated with materials from the non-metallic parts of the PCB composite.

The same feed as the one used for flotation has been used for electrostatic separation (Suponik et al. 2021) and gravity separation (Franke et al. 2021). Compared to the above methods of recovering metals from PCBs, flotation is not the most efficient process due to the impurities in both products and their yields. The penetration of the metal grains into the hydrophobic product may be caused by the patch shape of the grains, which tend to float. It mostly concerns Ag grains, but due to the presence of thin tracks in PCBs, it is also true of Cu grains (Allan and Woodcock 2001). This problem was also noticed in the work of Ogunniya and Vermaak (Ogunniya and Vermaak 2009), and is difficult to correct due to the kinetics of the flotation process. The purity of the hydrophobic product is important due to the minimization of metal losses and the production of composites (Mrówka et al. 2021) or concrete (Mohammed and Hama 2022) with specific properties from the obtained plastics.

The presence of significant amounts of fiberglass grains in the hydrophilic product may be due to their large dimensions (above 800 μm). These grains, given their weight, may not have floated to the surface of the tank and may have remained at the bottom of the tank, or been in suspension, despite the fact that fiberglass is hydrophobic (Gallegos-Acevedo et al. 2014). It is therefore necessary to optimize the grinding process to obtain even smaller grains and thus to reduce the amount of impurities in the hydrophilic product. However, much higher efficiency and product purities were obtained, for the same feed, in the case of electrostatic separation.

The recovery ratio (Figure 2) is relatively high for the most valuable metals occurring in PCBs. The highest ratio was obtained for Cu, Sn, Ag, and Au, which amounted to 93%, 84%, 83%, and 69%, respectively. In the work of Han et al. 2018, a similarly high level of copper recovery (90.5%) was achieved, using tannic acid and 2-octanol as flotation reagents. However, in the studies by Ogunniya and Vermaak (Ogunniya and Vermaak 2009), in which no flotation reagents were used, the recovery of Cu was 66%. In this case, such a large loss of this metal can make recovery unprofitable. Therefore, reagents are needed to separate the metals from PCBs by flotation.

The greatest losses of metals (Figure 2) were recorded for Cr, Al, and Ti: 89%, 77% and 58%, respectively. The low Cr recovery may have resulted from the formation of chromium compounds such as nitrides, carbides and oxides in the production process, and thus physicochemical changes, including density (Lynn Davis et al. 1992). On the other hand, in the case of Al and Ti, the grains could be lifted due to their relatively low specific density.

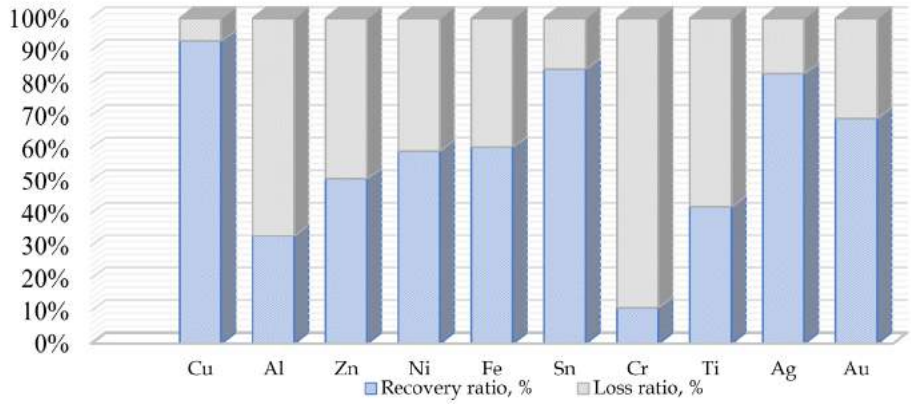

Fig. 2. Recovery and loss ratio for test No. 8

Rys. 2. Wskaźniki odzysku i strat dla testu nr 8

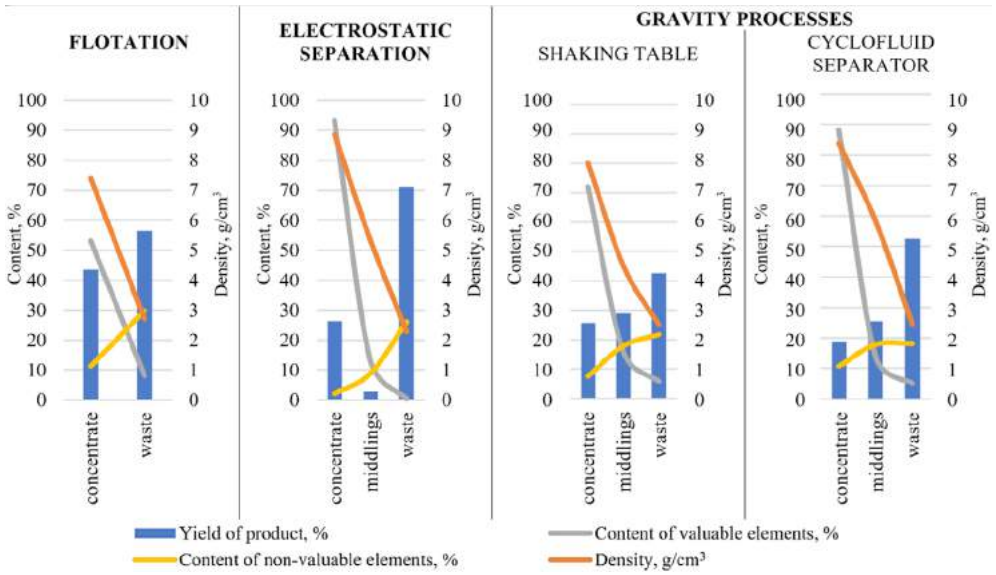

Fig. 3. Yield of separation products as a function of their density and quality parameters (Suponik et al. 2021; Franke et al. 2021)

Rys. 3. Udział produktów separacji w funkcji ich gęstości i parametrów jakościowych

Due to the low values of these metals, their loss should not significantly affect the profitability of the recovery process. New goods generated from the hydrophobic product, due to its content of chromium, should be analyzed in terms of their impact on the environment.

The use of flotation to recover metals from PCBs was an inefficient process compared to electrostatic separation. In this process, the best separation of the metallic product (concentrate) from plastics was obtained (Figure 3). The yield of this product was 26.2%wt., and had the highest amount of valuable elements (above 93.3%, mainly 68.5% Cu, 11.5% Sn, 1074 ppm Ag and 92 ppm Au), and furthermore, it had the lowest amount of impurities (less than 3%). In this method, the yield of plastics product was 71%wt. and had 0.54% valuable elements (mainly Cu). In the case of electrostatic separation, 2.8%wt. middlings were obtained, which mainly consisted of conglomerate grains (plastic-metal) (Suponik et al. 2021). The products obtained by the method of gravity separation were of lower quality. Through use of a shaking table, the following products was obtained: 25.7%wt. metals product (72% valuable elements, mainly 59.2% Cu, 6.3% Sn, 2160 ppm Ag and 72 ppm Au; 8.35% impurities), 28.9%wt. middlings (9.5% Cu), and 45.4%wt. plastics product (5.8% of valuable elements, mainly Cu). The products obtained using a cyclofluid separator were similar to those obtained from the shaking table (Franke et al. 2021).

Conclusions

As a result of the research, optimal conditions were obtained for the flotation process in which the process of metal-plastic separation from ground PCBs achieved the highest efficiency.

This was achieved with the combination of solids content <50 g/dm^3 with the airflow of 200 dm^3/h, and using dimethoxy dipropyleneglycol at a concentration of 157 mg/dm^3. The hydrophilic product thus obtained consisted mainly of copper (39.9%), tin (7.8%), and trace amounts of silver (0.5797%) and gold (0.024%). In addition to valuable elements, over 11% of contaminants were also identified, making the product significantly contaminated.

The flotation efficiency might possibly be improved by using different flotation parameters and the particle composition of the feed. The fact that the measured contact angle given in the material methodology is correlated with flotation efficiency may be helpful in finding better process conditions. The main concern for low efficiency could be the degree of milling and the strongly heterogeneous feed due to various particle size and shapes (from dozens μm to even 2 mm).

As compared to the other methods (specifically, electrostatic separation, gravity separation with the use of a concentration table, and a cyclofluid separator), the hydrophilic product obtained as a result of optimization of the flotation process was characterized by the lowest content of valuable metals and the highest level of contamination. In addition, this process was also associated with a number of other disadvantages, such as:

- relatively high negative impact on the environment caused by high water consumption and the use of chemical reagents,

- higher energy consumption of the process than dry methods resulting from the need to use additional devices for filtration and drying of the obtained products and compressed air installations,
- significant additional workload due to the number of devices used in the process.

In conclusion, the use of a flotation process to recover metals from ground PCBs is possible; however, it is not economically or environmentally viable. Much better results were obtained for the same feed using an electrostatic separator, which is characterized by a higher reliability, its predominantly low energy consumption and environmental impact, as well as its low costs.

Publication supported by the Silesian University of Technology, grant number: 06/050/BKM21/0122.

REFERENCES

Allan, G.C. and Woodcock, J.T. 2001. A review of the flotation of native gold and electrum. *Minerals Engineering* 14, pp. 931–962, DOI: 10.1016/S0892-6875(01)00103-0.

Anderson, C.G. 2012. The metallurgy of antimony. *Geochemistry* 72, pp. 3–8, DOI: 10.1016/j.chemer.2012.04.001.

Bidini et al. 2015 – Bidini, G., Fantozzi, F., Bartocci, P., D'Alessandro, B., D'Amico, M., Laranci, P., Scozza, E. and Zagaroli, M. 2015. Recovery of precious metals from scrap printed circuit boards through pyrolysis. *Journal of Analytical and Applied Pyrolysis* 111, pp.140–147.

Drzymala, J. 2007. *Mineral processing. Foundations of theory and practice of minerallurgy*. Wroclaw: Oficyna Wydawnicza Politechniki Wrocławskiej, pp. 510.

Duan et al. 2009 – Duan, C., Wen, X., Shi, C., Zhao, Y., Wen, B. and He, Y. 2009. Recovery of metals from waste printed circuit boards by a mechanical method using a water medium. *Journal of Hazardous Materials* 166, pp. 478–482, DOI: 10.1016/j.jhazmat.2008.11.060.

Farrokhpay, S. 2011. The significance of froth stability in mineral flotation — A review. *Advances in Colloid and Interface Science* 166, pp. 1–7, DOI: 10.1016/j.cis.2011.03.001.

Forti et al. 2020 – Forti, V., Baldé, C.P., Kuehr, R. and Bel, G. 2020. The Global E-waste Monitor 2020: Quantities, flows and the circular economy potential. *United Nations University/United Nations Institute for Training and Research – co-hosted SCYCLE Programme, International Telecommunication Union & International Solid Waste Association*, pp. 1–120.

Franke et al. 2021 – Franke, D., Suponik, T., Nuckowski, P. and Dubaj, J. 2021. Evaluation of the efficiency of metal recovery from printed circuit boards using gravity processes. *Physicochemical Problems of Mineral Processing* 57, pp. 63–77.

Gallegos-Acevedo et al. 2014 – Gallegos-Acevedo, P.M., Espinoza-Cuadra, J. and Olivera-Ponce, J.M. 2014. Conventional flotation techniques to separate metallic and nonmetallic fractions from waste printed circuit boards with particles nonconventional size. *Journal of Mining Science* 50, 974–981, DOI: 10.1134/S1062739114050172.

Goosey, M. and Kellner, R. 2002. A scoping study: End-of-life printed circuit boards. Department of Trade and Investment, *Shipley Europe Limited*.

Haldar, S.K. 2018. Mineral Processing, [In:] *Mineral Exploration*. Elsevier, pp. 259–290.

Han et al. 2018 – Han, J., Duan, C., Li, G., Huang, L., Chai, X. and Wang, D. 2018. The influence of waste printed circuit boards characteristics and nonmetal surface energy regulation on flotation. *Waste Management* 80, pp. 81–88, DOI: 10.1007/s10163-021-01310-8.

He, J. and Duan, C. 2017. Recovery of metallic concentrations from waste printed circuit boards via reverse floatation. *Waste Management* 60, pp. 618–628, DOI: 10.1016/j.wasman.2016.11.019.

He et al. 2006 – He, W., Li, G., Ma, X., Wang, H., Huang, J., Xu, M. and Huang, C. 2006. WEEE recovery strategies and the WEEE treatment status in China. *Journal of Hazardous Materials* 136, pp. 502–512, DOI: 10.1016/j.jhazmat.2006.04.060.

Kaya, M. 2016. Recovery of metals and nonmetals from electronic waste by physical and chemical recycling processes. *Waste Management* 57, pp. 64–90, DOI: 10.1016/j.wasman.2016.08.004.

Kaya, M. 2019. *Electronic waste and printed circuit board recycling technologies.* Cham, Switzerland: The Minerals, Metals & Materials Series. Springer International Publishing, pp. 351.

Khetriwal et al. 2009 – Khetriwal, D.S., Kraeuchi, P. and Widmer, R. 2009. Producer responsibility for e-waste management: Key issues for consideration – Learning from the Swiss experience. *Journal of Environmental Management* 90, pp. 153–165, DOI: 10.1016/j.jenvman.2007.08.019.

Kumar et al. 2018 – Kumar, A., Holuszko, M.E. and Janke, T. 2018. Characterization of the non-metal fraction of the processed waste printed circuit boards. *Waste Management* 75, pp. 94–102, DOI: 10.1016/j.wasman.2018.02.010.

Langa et al. 2014 – Langa, N.T.N., Adeleke, A.A., Mendonidis, P. and Thubakgale, C.K. 2014. Evaluation of sodium isobutyl xanthate as a collector in the froth flotation of a carbonatitic copper ore. *International Journal of Industrial Chemistry* 5, pp. 107–110, DOI: 10.1007/s40090-014-0025-5.

Lee et al. 2012 – Lee, J., Kim, Y., and Lee, Jae-Chun 2012. Disassembly and physical separation of electric/electronic components layered in printed circuit boards (PCB). *Journal of Hazardous Materials* 241–242, pp. 387–394, DOI: 10.1016/j.jhazmat.2012.09.053.

Long et al. 2010 – Long, L., Sun, S., Zhong, S., Dai, W., Liu, J. and Song, W. 2010. Using vacuum pyrolysis and mechanical processing for recycling waste printed circuit boards. *Journal of Hazardous Materials* 177, pp. 626–632, DOI: 10.1016/j.jhazmat.2009.12.078.

Lynn Davis et al. 1992 – Lynn Davis, J., Williams, M., Kevin Arledge, J. and Swirbel, T. 1992. Spectroscopic studies of the chemical properties of thin metal films on poly(ether imide). *Thin Solid Films* 220, pp. 217–221.

Ma et al. 2018 – Ma, H., Du, N., Lin, X., Li, C., Lai, J. and Li, Z. 2018. Experimental study on the heat transfer characteristics of waste printed circuit boards pyrolysis. *Science of the Total Environment* 633, pp. 264–270, DOI: 10.1016/j.scitotenv.2018.03.180.

Mohammed, T.K. and Hama, S.M. 2022. Mechanical properties, impact resistance and bond strength of green concrete incorporating waste glass powder and waste fine plastic aggregate. *Innovative Infrastructure Solutions* 7, pp. 49.

Mrówka et al. 2021 – Mrówka, M., Woźniak, A., Prężyna, S. and Sławski, S. 2021. The Influence of Zinc Waste Filler on the Tribological and Mechanical Properties of Silicone-Based Composites. *Polymers* 13, p. 585, DOI: 10.3390/polym13040585.

Muniyandi et al. 2010 – Muniyandi, S.K., Sohaili, J. and Hassan, A. 2014. Encapsulation of nonmetallic fractions recovered from printed circuit boards waste with thermoplastic. *Journal of the Air & Waste Management Association* 64, pp. 1085–1092, DOI: 10.1080/10962247.2014.911221.

Muwanguzi et al. 2012 – Muwanguzi, A.J.B., Karasev, A.V., Byaruhanga, J.K. and Jönsson, P.G. 2012. Characterization of Chemical Composition and Microstructure of Natural Iron Ore from Muko Deposits. *International Scholarly Research Notices*, art. ID 174803.

Nnorom, I.C. and Osibanjo, O. 2009. Toxicity characterization of waste mobile phone plastics. *Journal of Hazardous Materials* 161, pp. 183–188, DOI: 10.1016/j.jhazmat.2008.03.067.

Ogunniyi, I.O. and Vermaak, M.K.G. 2009. Froth flotation for beneficiation of printed circuit boards comminution fines: An overview. *Mineral Processing and Extractive Metallurgy Review* 30, pp. 101–121, DOI: 10.1080/08827500802333123.

Sarvar et al. 2010 – Sarvar, M., Salarirad, M.M. and Shabani, M.A. 2015. Characterization and mechanical separation of metals from computer printed circuit boards (PCBs) based on mineral processing methods. *Waste Management* 45, pp. 246–257, DOI: 10.1016/j.wasman.2015.06.020.

Schwarz, H.G. 2004. Aluminium Production and Energy. [In:] Cutler, J.C. ed. *Encyclopedia of Energy*. United States: Elsevier, pp. 81–95.

Shean, B.J. and Cilliers, J.J. 2011. A review of froth flotation control. *International Journal of Mineral Processing* 100, pp. 57–71, DOI: 10.1016/j.minpro.2011.05.002.

Suponik et al. 2021 – Suponik, T., Franke, D., Nuckowski, P., Matusiak, P., Kowol, D., and Tora, B. 2021. Impact of Grinding of Printed Circuit Boards on the Efficiency of Metal Recovery by Means of Electrostatic Separation. *Minerals* 11, p. 281, DOI: 10.3390/min11030281.

Tuncuk et al. 2010 – Tuncuk, A., Stazi, V., Akcil, A., Yazici, E.Y. and Deveci, H. 2012. Aqueous metal recovery techniques from e-scrap: Hydrometallurgy in recycling. *Minerals Engineering* 25, pp. 28–37, DOI: 10.1016/j.mineng.2011.09.019.

Wang, G.C. 2016. Nonferrous metal extraction and nonferrous slags. [In:] *The Utilization of Slag in Civil Infrastructure Construction*. United States: Woodhead Publishing, pp. 35–61.

Wills, B.A. and Finch, J.A. 2016. Introduction to the practical aspects of ore treatment and mineral recovery. Froth Flotation. [In:] *Wills' Mineral Processing Technology.* (Ed. 8). Butterworth-Heinemann, Oxford: *Elsevier*, pp. 265–380.

Ximei et al. 2017 – Ximei, L., Yunfan, W., Mingze, M., Shuixiang, S., Ying, Z., Jiushuai, D. and Jian, L. 2017. Role of dissolved mineral species in quartz flotation and siderite solubility simulation. *Physicochemical Problems of Mineral Processing* 53(1), pp. 1241–1254, DOI: 10.5277/ppmp18154.

Yu et al. 2010 – Yu, J., Williams, E. and Ju, M. 2010. Analysis of material and energy consumption of mobile phones in China. *Energy Policy* 38, pp. 4135–4141.

Zhang, S. and Forssberg, E. 1997. Mechanical separation-oriented characterization of electronic scrap. *Resources, Conservation & Recycling* 21, pp. 247–269.

Zhang, S. and Forssberg, E. 1999. Intelligent liberation and classification of electronic scrap. *Powder Technology* 105, pp. 295–301.

Zhao et al. 2004 – Zhao, Y., Wen, X., Li, B. and Tao, D. 2004. Recovery of copper from waste printed circuit boards. *Mining, Metallurgy & Exploration* 21, pp. 99–102.

Zhao et al. 2012 – Zhao, Y.M., Duan, C.L., Wu, L.L., Zhang, H.J., He, J.F. and He, Y.Q. 2012. The separation mechanism and application of a tapered diameter separation bed. *International Journal of Environmental Science and Technology* 9, pp. 719–728, DOI: 10.1007/s13762-012-0105-z.

Zhou et al. 2004 – Zhou, J., Jago, B. and Martin, C. 2004. Establishing the Process Mineralogy of Gold Ores. *SGS Minerals Technical Bulletin* 2004(03), pp. 16.

EVALUATION OF THE USE OF FLOTATION FOR THE SEPARATION OF GROUND PRINTED CIRCUIT BOARDS

Keywords

printed circuit boards, recycling, flotation, recovery, metals

Abstract

The paper presents an assessment of flotation efficiency in the separation of plastics from metals derived from printed circuit boards (PCBs). The PCBs were ground in a knife mill prior to flotation. The contact angles of various materials corresponding to the grains from ground PCBs were measured, and a series of flotation tests was carried out to obtain the best product. The impact of the following parameters were investigated: the reagent and its dose, the airflow rate through the flotation tank and the feed concentration. The highest efficiency of metal recovery from PCBs was achieved for Dimethoxy dipropyleneglycol at a concentration of 157 mg/dm^3 and with an airflow of 200 dm^3/h and a feed concentration of <50 g/dm^3. In the hydrophilic product (concentrate), it was mainly Cu (40%) and Sn (7.8%) that were identified by means of XRF, but there were also trace amounts of pre-

cious metals such as Au (0.024%), Ag (0.5797%) and Pd (149 ppm). Impurities in the form of Si (5%), Ca (3.2) and Br (2.1) were also identified in this product. Small amounts of metals in their metallic form were identified in the hydrophobic product (waste), mainly Cu (2.3), Al (1.7) and Sn (1.1). As a result of the research, high recovery ratios were obtained for Cu (93%), Sn (84), Ag (83) and Au (69). The purity of obtained metal concentrate with this method was lower in comparison with the other methods of the recovery of metals from ground PCBs for the same feed, i.e. electrostatic or gravity separation. Also considering other factors such as the environmental impact of the flotation process, the number of facilities and their energy consumption, this process should not be used in the developed metal recovery technology. Using electrostatic separation for the same feed obtained much better results.

OCENA ZASTOSOWANIA FLOTACJI W ODZYSKU METALI Z ROZDROBNIONYCH PŁYT OBWODÓW DRUKOWANYCH

Słowa kluczowe

płyty obwodów drukowanych, recykling, flotacja, odzysk, metale

Streszczenie

W artykule przedstawiono ocenę zastosowania flotacji do rozdziału metali od tworzyw sztucznych z rozdrobnionych w młynie nożowym płyt obwodów drukowanych (PCBs). Zmierzono kąty zwilżania różnych materiałów odpowiadających ziarnom zmielonych PCBs oraz określono wypływy odczynników i ich stężeń, wydatków powietrza oraz zagęszczenia materiału na sprawność procesu flotacji. Najwyższą sprawność odzysku metali z PCBs uzyskano przy zastosowaniu eteru dimetylowego glikolu dipropylenowego w stężeniu 157 mg/dm^3, wydatku powietrza 200 dm^3/h i zagęszczeniu materiału poniżej 50 g/dm^3. W produkcie hydrofilowym (metalach), wykorzystując metodę XRF, zidentyfikowano głównie Cu (40%) i Sn (7,8%) oraz śladowe ilości metali szlachetnych takich jak Au (0,024%), Ag (0,5797%) i Pd (0,015%). W produkcie tym rozpoznano również zanieczyszczenia takie jak Si (5%), Ca (3,2%) i Br (2,1%). W produkcie hydrofobowym (tworzywach sztucznych) występowały nieznaczne ilości metali, głównie były to Cu (2,3%), Al (1,7%) i Sn (1,1%). W wyniku przeprowadzonych badań uzyskano wysokie wskaźniki odzysku dla Cu (93%), Sn (84%), Ag (83%) i Au (69%). Niemniej jednak, w porównaniu do separacji elektrostatycznej, która była prowadzona dla tej samej nadawy, czystość produktów uzyskanych za pomocą flotacji była mniejsza. Biorąc pod uwagę również inne czynniki, między innymi takie jak oddziaływanie procesu flotacji na środowisko naturalne, ilość urządzeń oraz ich energochłonność, stwierdzono w konkluzji artykułu, że proces ten nie powinien być stosowany w tworzonej technologii odzysku metali z PCBs. Znacznie lepsze efekty rozdziału uzyskano bowiem dla tej samej nadawy, stosując proces separacji elektrostatyczny, który ma niewielki wpływ na środowisko przyrodnicze, a powstające produkty mogą być w pełni wykorzystywane.

Recycling of waste printed circuit boards – application potential and selection of eco-efficient methods

Authors (names and surnames): Dawid M. Franke[a], Tomasz Suponik[b]

[a]Department of Geoengineering and Raw Materials Extraction, Faculty of Mining, Safety Engineering and Industrial Automation, Silesian University of Technology, Akademicka 2, 44-100 Gliwice, Poland, dawid.franke@polsl.pl

[b]Department of Geoengineering and Raw Materials Extraction, Faculty of Mining, Safety Engineering and Industrial Automation, Silesian University of Technology, Akademicka 2, 44-100 Gliwice, Poland, tomasz.suponik@polsl.pl

Corresponding author: Dawid M. Franke, Silesian University of Technology, Akademicka 2, 44-100 Gliwice, Poland, dawid.franke@polsl.pl, +48 515 738 435

Abstract: This article evaluates selected physical metal recovery methods from waste printed circuit boards (WPCBs) in terms of cost, efficiency, and human and environmental impact. Frequently-used chemical PCB recycling methods such as (bio)hydrometallurgical and high-energy (pyrometallurgical and plasma) methods are characterized by a high recovery efficiency and high environmental impact, while physical methods have a negligible environmental impact because they operate in accordance with the principles of a circular economy and sustainable development. They allow the production of a mixture of metals free of plastics and fiberglass, which constitutes a separate product for the production of, among others, composite materials. The mixture of metals is to be transferred to metal

production companies to produce individual metals in their installations without incurring additional costs or causing any additional impact on the natural environment. Due to the high potential of physical methods and the high environmental impact of chemical methods, and their high costs, it was decided to evaluate the applicability of electrostatic and gravity separation and flotation in WPCB recycling processes. An important issue in the case of physical recycling methods was the grinding of WPCBs using liquid nitrogen, which increased the efficiency of the process and allowed for the appropriate release of metals from the WPCB composite. The best separation method in terms of energy consumption, efficiency, and environmental impact was electrostatic separation, which resulted in a product in the form of a mixture of very high-purity metals. The plastic and glass fiber residues, after separation, will be used as additives during the production of composite materials such as construction screeds.

Keywords: recycling, printed circuit boards, separation, eco-efficient, technology

Funding: This work was supported by the Silesian University of Technology [grant numbers 06/050/BKM_22/0140]

1. Introduction

As humankind develops, the consumption of primary raw materials continually increases, and fast-growing economies demand critical raw materials whose deposits may be depleted shortly. The cause of this situation is the economic model that operated in earlier decades, which involved the extraction of materials, the production of goods, and their disposal without processing to obtain secondary raw materials. This resulted in raw materials, even valuable ones, becoming waste (Xavier et al., 2021). The main reasons for this were economic factors and the lack of developed waste management technologies and systems (Araujo Galvão et al., 2018), as well as the lack of legal regulations forcing holders of these goods to deal with them properly. In the era of rising energy prices, depleting deposits, and increasingly worsening environmental pollution, the transformation of the old, linear economic model into a circular one has begun, whose aim is to extend the life cycle of raw materials while retaining their value (Xavier et al., 2021). This model has been called the circular economy, and its implementation is necessary to maintain raw material security and ensure sustainability (Dantas et al., 2021).

Electro-waste is one of the fastest-growing waste streams. According to the United Nations Institute for Training and Research, humanity generated 53.6 million tonnes of waste electronic and electrical equipment (WEEE) in 2019, valued at 57 billion USD. This waste stream is estimated to grow to 74.7 Mt in 2030 and as much as 110 Mt in 2050 (Forti et al., 2020).

Printed circuit boards (PCBs) are the basis of almost every electronic device (Silva et al., 2021), most of which are FR-4 type PCBs, which are constructed from a composite made of glass fiber and epoxy resin in which metal tracks are embedded (Tatariants et al., 2017). The

63 composition of PCBs depends mainly on the manufacturer, the type of technology used to
64 produce them, and their intended use. It is estimated that the average PCB contains about
65 35% of metals such as copper, aluminum, gold, silver, and traces of palladium and platinum
66 (Fig. 1). As can be seen, gold, palladium, silver, and copper are the most valuable metals
67 used in PCBs, and their recovery can bring significant economic benefits to companies
68 recycling PCBs. In addition, the protection of the earth's natural resources and the security
69 of raw materials must be kept in mind. Therefore, the Royal Society of Chemistry has
70 developed an index of relative supply risk to assess the problems of future raw material
71 availability. As can be seen from Figure 1, most metals in PCBs have an index above six on a
72 10-point scale, where 1 means very low supply risk and 10 means very high supply risk (Royal
73 Society of Chemistry, 2022). Therefore, to protect metal deposits, manufactured PCBs
74 should be treated in accordance with the principles of a circular economy and sustainable
75 development.

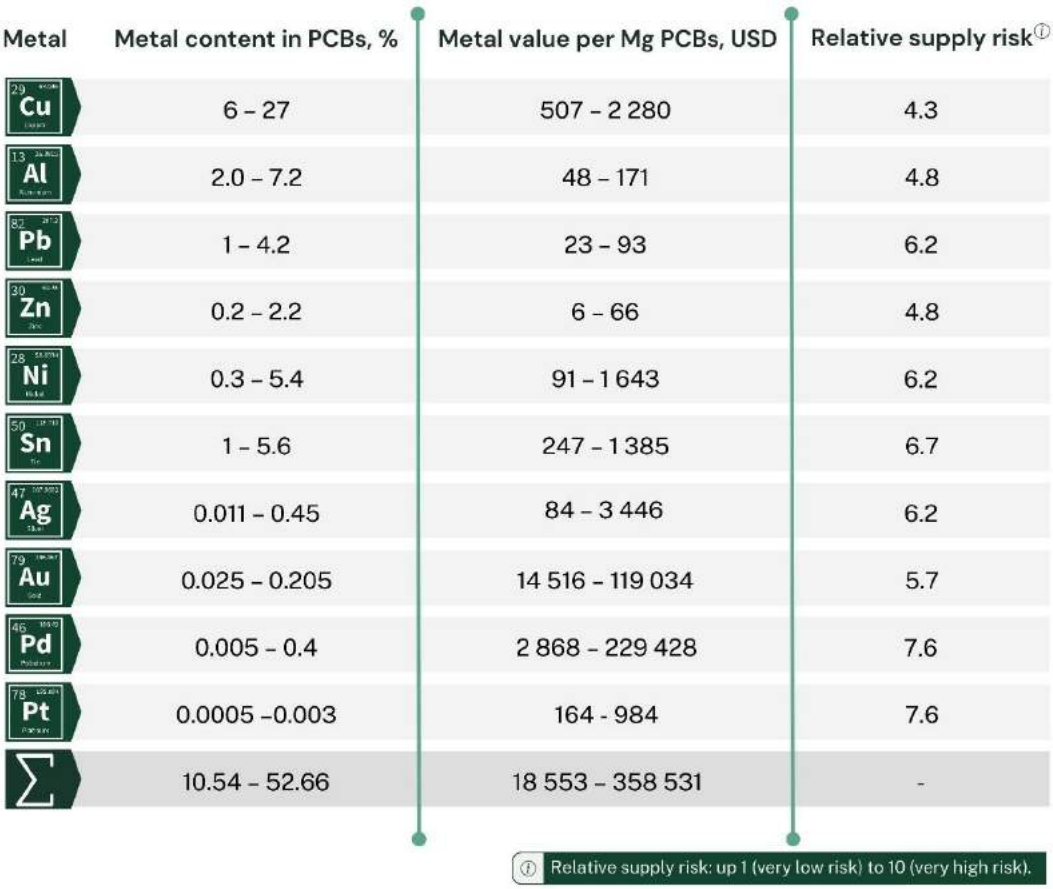

Metal	Metal content in PCBs, %	Metal value per Mg PCBs, USD	Relative supply risk ⓘ
Cu	6 – 27	507 – 2 280	4.3
Al	2.0 – 7.2	48 – 171	4.8
Pb	1 – 4.2	23 – 93	6.2
Zn	0.2 – 2.2	6 – 66	4.8
Ni	0.3 – 5.4	91 – 1 643	6.2
Sn	1 – 5.6	247 – 1 385	6.7
Ag	0.011 – 0.45	84 – 3 446	6.2
Au	0.025 – 0.205	14 516 – 119 034	5.7
Pd	0.005 – 0.4	2 868 – 229 428	7.6
Pt	0.0005 –0.003	164 - 984	7.6
∑	10.54 – 52.66	18 553 – 358 531	-

ⓘ Relative supply risk: up 1 (very low risk) to 10 (very high risk).

Figure 1. Estimates of metal content in printed circuit boards, their economic values, and relative supply risk (Kaya, 2017; Royal Society of Chemistry, 2022; "The London Metal Exchange," 2022).

The lack of locally-available WPCB recycling facilities is at the root of the growing problem of WEEE management. It is estimated that almost 83% of the world's electronic waste has no clearly-documented treatment history. The situation is slightly better for WPCBs, as the management of around 66% is unknown, partly due to the high value of the metals they contain (Baldé et al., 2022; Forti et al., 2020). This waste is mainly processed in domestic facilities, poses a high risk to people and the environment, and is exported to countries where recycling or management costs are lower and often more environmentally damaging.

The recovery of metals from WPCBs can be carried out using chemical methods, i.e., (bio)hydrometallurgy, pyrometallurgy, and plasma, or physical methods, which include grinding and separation, e.g., electrostatic or air separation (without using water). Each of these methods has different environmental impacts (Fig. 2) and specific characteristics (Fig. 3). Among the most common chemical methods is hydrometallurgy, which has a high environmental impact due to the use of toxic chemical reagents (Yaashikaa et al., 2022). However, it is one of the few methods by which full separation of metals is possible. A variant of this method is biohydrometallurgy, which uses microorganisms as catalysts. Due to its speed, pyrometallurgy is another frequently used chemical method, but it also has a significant environmental impact, mainly due to the emission of fumes and gases into the atmosphere and the generation of industrial waste (Ma, 2019). To reduce emissions, expensive filters are required, which significantly reduces the cost-effectiveness of installations. Chemical methods result in the loss of some non-metallic PCBs, which in turn produces additional waste streams. In the two WPCB recycling methods presented above, neither plastics nor glass fiber are treated or recovered – they are either a waste or a source of various emissions to the natural environment.

In contrast to the above, physical methods have the lowest environmental impact, and recovery is carried out according to the principles of a closed-loop economy and sustainable development. They are also low-cost methods (Franke et al., 2022; Suponik et al., 2021), and the separation processes allow valuable substances to be recovered and the remaining substances to be used to manufacture new products without creating waste. Part of the shredded WPCB composites from which the metals have been removed remains chemically unchanged, which creates a wide range of possible applications, e.g., to produce other composite materials. Thus, recycling in this way can be considered waste-free. It should be

borne in mind that the use of physical methods in WPCB recycling does not allow obtaining separated metals, and they produce a mixture of metals free of non-metallic parts.

Therefore, taking into account the cumulative impact of WPCB recycling methods on the environment, the need to incur costs, and the regulatory conditions regarding the technology, physical recycling methods provide the best solution.

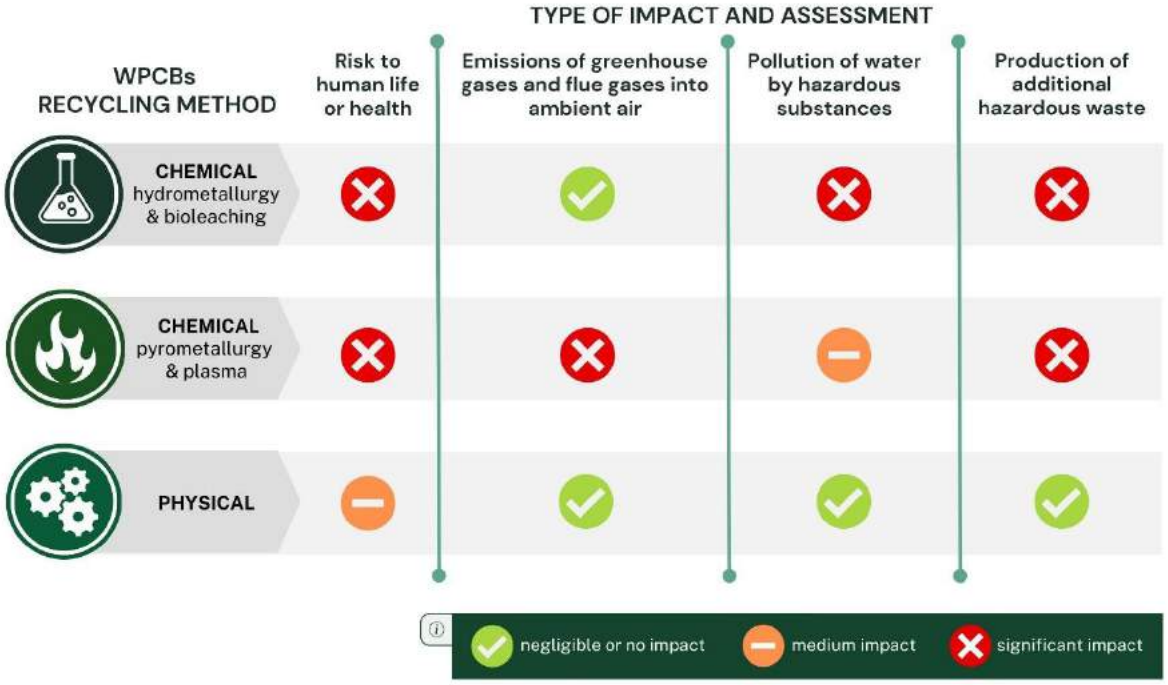

Figure 2. Assessment of the environmental impact of selected WPCB recycling methods

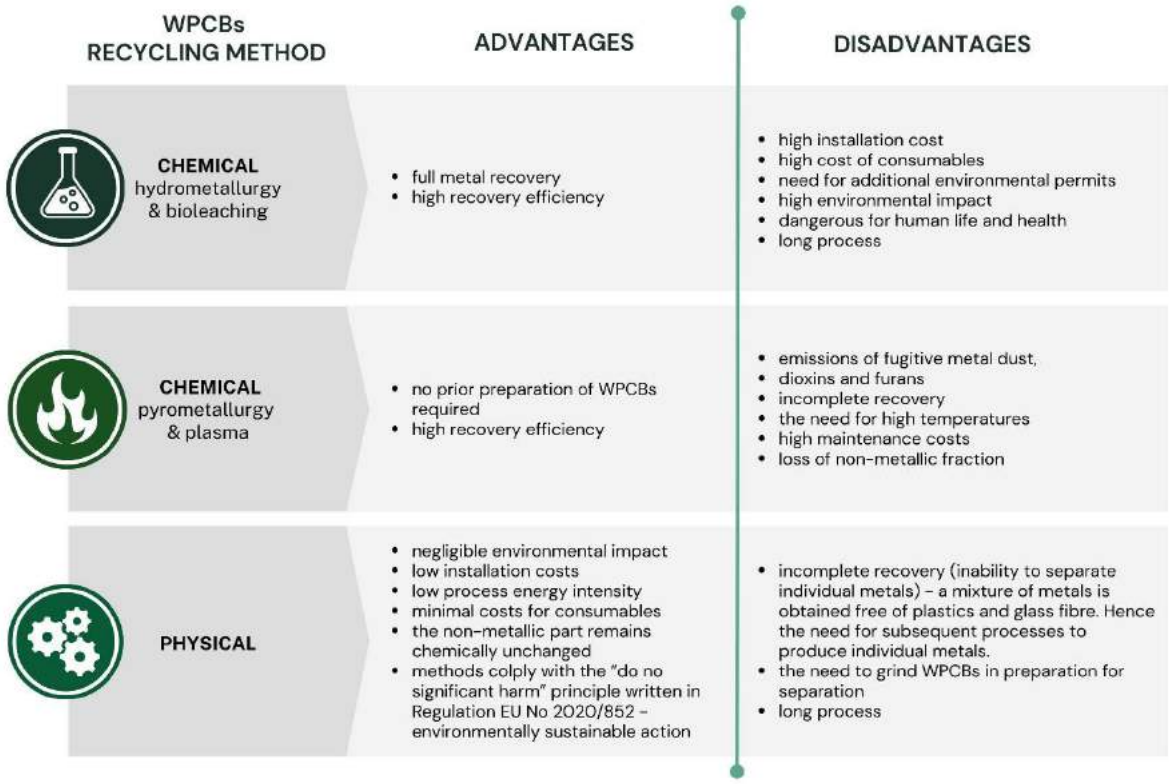

118

119 **Figure 3.** The main advantages and disadvantages of selected WPCB recycling methods (Ma,
120 2019; Maurice et al., 2021; Yaashikaa et al., 2022)

121 This paper presents the physical WPCB recycling methods to separate metals from plastics
122 and glass fibers and their economic applications, in accordance with the principles of a
123 circular economy and sustainable production. The article also presents the results of
124 environmental assessments, efficiency analyses, and financial aspects of the applied physical
125 separation methods. This serves as a foundation for the selection of components in the
126 designed eco-efficient WPCB recycling technology.

2. Material and methods

2.1. Unit processes of WPCB recycling technology

Considering the relatively high environmental impact of WPCB recycling by chemical methods and the high potential for the application of physical methods, the authors of the publication decided to assess the applicability of selected mineral engineering methods. As part of the research, it was decided to apply and evaluate methods characterized by different physical interaction modes, i.e., electrostatic separation (Franke et al., 2020; Suponik et al., 2021), gravity separation (Franke et al., 2021), and flotation (Franke et al., 2022) to select the most eco-efficient method. Before separating metals from the WPCB composite, the WPCBs were properly prepared and ground. For this purpose, the different processes (stages) leading to efficient separation of metals from WPCBs by the above-mentioned methods have been developed and verified on a laboratory scale:

Stage I - disassembly

The first stage of the research was to remove components from the surface of the PCBs that may interfere with subsequent processes, i.e., sockets, resistors, transistors, processors, RAM, and others. Disassembly was carried out using handheld workshop tools. An initial selection was made of components with a high potential for reuse, such as processors and their cooling systems, various types of connectors, and RAM. The removal of these components is also possible using physical stripping methods.

Stage II – shredding

Disassembled WPCBs were crushed in a disintegrator to obtain pieces no larger than 1 x 1 cm. The size reduction of the WPCBs was necessary due to the size limitations of the mill feed.

Stage III – grinding

The appropriate release level of metal grains from the rest of the WPCB composite is one of the most critical measures for successfully recycling by all physical methods and for achieving high separation efficiencies. Previous work by the authors noted a significant positive effect of the use of liquid nitrogen on WPCB grinding. However, the process of cooling the WPCB pieces cannot take place directly in the working chamber of the mill, so this step was divided into two parts. First, the ground WPCB pieces were cooled to below 150 ^{o}C using liquid nitrogen (stage IIIA) and a special liquid nitrogen tank equipped with a sieve. The cooled WPCB pieces were then ground in a Testchem LMN-100 laboratory knife mill (Radlin, Poland) equipped with a sieve with a mesh size of 1 mm (stage IIIB). The result was a WPCB powder with a maximum particle size of 1.5 mm.

Stage IV – separation

The separation of metals from the WPCB composite was carried out using four pieces of laboratory equipment with different modes of interaction, i.e., an electrostatic drum separator, a shaking table, a cyclofluid separator, and a flotation machine. The machines were fed with the same material from which four representative samples were separated. Gravity separation and flotation used water for separation, so the resulting products had to be dried.

The first separation process studied was electrostatic separation, which is based on differences in surface charge storage capacity and conductivity of the particles. In electrostatic drum separators, non-conductive particles adhere to a rapidly rotating drum, which is electrified by friction against a brush that also acts to mechanically scrape these particles (plastics). The conductive particles (metals) rapidly release their surface charge,

allowing them to be easily ‘stripped’ from the drum surface. To increase the efficiency of this process, the electrostatic separator is equipped with a high-voltage electrode that bombards the particles with electrons. A Boxmag-rapid (Aston, Birmingham, UK) laboratory electrostatic drum separator was used, which was designed to receive three products, i.e., metal grains, conglomerates, and plastic grains. Separation was carried out with the following parameters: a shaft speed of 100 rpm, a voltage of 17 kV, and a distance between the electrode and drum of 0.03 m (Franke et al., 2020).

The second method of separation investigated was gravity separation, and it was used to separate grains with different densities. Due to the wide range of devices and different designs within this type of separation, it was decided to use two types of equipment that interacted with the grains in different ways. In both cases, the separation took place in an aqueous medium. The first piece of equipment used in gravity separation was a shaking table. In this case, the separation of the grains took place on a longitudinal working plate that was inclined up to 10^{o} transversely to the axis. The plate made reciprocating movements so that the particles in suspension, which were fed onto the plate surface, were separated along the plate according to their density. The lightest particles (plastics) were stripped from the plate surface the fastest, while the heaviest particles (metals) overcame the hydrostatic pressure of the liquid and were carried along the plate as a result of its movement. Spray nozzles were placed at the top of the plate to increase the efficiency of the separation process.

Separation was carried out using a laboratory shaking table equipped with a grooved plate. The separation parameters were as follows: table load of 9 dm^3/min (slurry of water with material), water flow rate of the first nozzle of 5.7 dm^3/min, water flow rate of the second

196 nozzle of 5.4 dm^3/min; table stroke of 1.5 mm, table movement frequency of 260
197 strokes/min, longitudinal inclination angle of 1°, and transverse inclination angle of 6°
198 (Franke et al., 2021).

199 The second device was a laboratory cyclofluid separator, in which separation was achieved
200 by vertical fluidization of the particles, where the vertical movement of the liquid caused the
201 particles to separate according to their density. The heaviest particles (metals) fell to the
202 bottom of the separator, while the lightest particles were lifted to the surface. The principle
203 of operation of the laboratory cyclofluid separator involved the use of a semi-industrial U-
204 shaped cyclofluid separator with continuous movement (patent application No. P.424161,
205 Poland). This separator was equipped with a water-filled tank in which a cylinder was placed.
206 The cylinder that contained the WPCB powder suspension was closed at the bottom by a
207 sieve with a mesh size of 0.5 mm and performed a vertical reciprocating motion. This
208 created a cyclical fluid thrust in the cylinder and allowed for density separation of the
209 particles. In the cyclofluid separator, separation was achieved by fluidizing the particles in a
210 vertical direction.

211 A laboratory cyclofluid separator was used for the separation. The following parameters
212 were used: volume of water of 13 dm^3, cylinder stroke of 4 cm, and frequency of cylinder
213 movement of 53 movements/minute (Franke et al., 2021).

214 The final separation process studied in the research was flotation, which involved the
215 separation of grains based on differences in their ability to either repel or attract water
216 molecules. The flotation process took place in aerated water so that hydrophilic grains
217 (metals) could ‘stick’ to air particles and float to the surface of the vessel. During flotation, it
218 is possible to use various flotation reagents that change the surface properties of the grains

or form a froth in which the floated grains will remain. However, due to the relatively low density of the plastics, with estimated densities ranging from 0.9 g/cm^3 to 3.5 g/cm^3, a reverse flotation process was used in the studies.

Flotation was carried out using a laboratory flotation machine Mechanobr, from IMN Gliwice (Instrumentation Building Plant of the Institute of Non-Ferrous Metals, Gliwice, Poland), with a 1 litre flotation tank. During the flotation process, a flotation reagent (dipropylene glycol dimethyl ether) was used at a concentration of 157 mg/dm^3. The rotation speed of the magnetic stirrer and the rotation speed of the rotator in the flotation tank were 100 rpm, approximately 400 rpm, and 5 minutes, respectively (Franke et al., 2022).

Stage V – Distribution and usage

A final step that also needs to be considered when designing eco-efficient technology is securing products for transfer to others and their distribution and sale. This is because the packaging of products can have hazardous effects on people and the environment, and, because of the aggregate form of the products, they should be secured in a way that prevents them from being scattered or wasted.

The obtained products represent significant economic value and possess considerable income-generating potential for enterprises involved in WPCB recycling. Based on data sourced from the Polish WEEE recycling company - Enviropol (Poland, Gliwice), it has been estimated that the annual accumulation of WPCBs in Poland amounts to 27 metric tons per 1 million residents. Consequently, the potential annual value of recovered metals approaches approximately 1.8 million USD per 1 million residents (computed according to the mean metal contents in WPCBs, without accounting for operational, investment, and maintenance expenses). The plastics remaining after the separation process can be utilized as additives to

epoxy or polyester resins, up to a maximum of 10% by weight, to manufacture composite materials. These products can be applied as surface materials for flooring or other items, such as composite boards. The method for producing composite materials based on epoxy or polyester resins with the inclusion of plastics has been described in a patent application (patent application No. P.438999, Poland).

2.2. Evaluation of unit processes

All unit processes of the proposed technology concept (Stages I–V) were subjected to a comprehensive assessment to determine the most eco-efficient recycling method. The analyses were carried out only for processes and equipment integrated at the laboratory scale.

As part of the work, a comprehensive assessment of occupational hazards was conducted. When extrapolated to a larger technical scale, this process enables the identification of potential hazards and the formulation of suitable countermeasures to ensure the safety of workers. It should be noted that the introduction of appropriate procedures and protective measures in workplaces is legally required by most European countries and directly contributes to minimizing accidents and hazards. Workplace hazard identification was conducted by a meticulous analysis of hazardous factors present in each unit process. Harmful factors such as dust and noise, as well as hazardous factors, were identified. The dust level was determined by measuring the mass of fallout accumulated over a one-hour period on the surface of a glass plate placed 1 meter from the dust source. These values were subsequently adjusted for an eight-hour workday (the estimated exposure time to this factor). Noise intensity was measured using a Bentech GM1356 Sonometer. Hazardous factors encompass elements of equipment that may cause accidents. It is important to note

that these studies were not conducted by accredited entities; therefore, the results presented are solely indicative.

An analysis was also carried out in the context of potential factors that may negatively impact the environment. Recycling processes may produce harmful emissions, generate toxic waste, or consume excessive natural resources, which is contrary to the requirements of an eco-efficient technology. Furthermore, accurate identification of potential environmental impacts will allow appropriate preventive measures to be taken to minimize negative environmental impacts.

An important part of the assessment of the unit recycling technology processes was the assessment of the technical and economic parameters for both operations and investments. A thorough evaluation of these parameters made it possible to determine the effectiveness of the recycling technology in terms of both operating and investment costs. Technical and economic parameters were presented per kilogram of WPCBs to allow informed decisions to be made regarding the implementation of WPCB recycling processes. Investment costs were limited to the necessary equipment required during recycling processes, excluding the costs of administration and premises, space rental, provision of welfare facilities, lighting, and maintaining the internal climate. The prices for consumable equipment were established through market research. Energy costs were computed by considering the energy intensity of the equipment and the current market price of electricity in Poland (Polskie Sieci Elektroenergetyczne, 2023). The cost of labor was determined by factoring in the labor burden associated with the projected process productivity and the average monthly employer cost in 2023 in Poland, which was approximately 1,000 USD per month. The mentioned amounts do not include taxes.

One final facet of the analysis, yet one of paramount significance from a business perspective, involved studying and assessing both qualitative and quantitative parameters of the products obtained using different separation methods. The chemical composition of the separation products was assessed using different analytical techniques, i.e., ICP-AES, XRF, SEM-EDS, and XRD. The yields of the different recycling processes were also determined. The quantitative and qualitative data of the products obtained were essential for assessing the effectiveness of the separation technology and will be used in the future to make decisions on further developments and industrial implementation feasibility.

3. Results

The first analysis was the identification and assessment of hazards in the workplace, as presented in Table 1. The harmful factors identified were dust present in the workplace and the noise generated by the equipment. The highest level of dust per eight-hour working day occurred during electrostatic separation and was 0.064 g/m^2×8 h, followed by 0.048 and 0.016 g/m^2×8 h during the grinding and packing processes, respectively. The highest noise intensities were measured during gravity separation on the concentration table, followed by grinding, comminution, and flotation, whose values did not exceed 133 dB, 132 dB, 117 dB, and 116 dB, respectively. An important element of worker safety is the risk of personal injury. In the recycling process, based on the opinion and knowledge of the senior health and safety inspector, the main hazards identified were moving and sharp machine parts. However, during electrostatic separation, there is also a risk of high-voltage shock (> 15 kV), and during grinding, there is a risk of direct contact with very low temperatures due to the use of liquid nitrogen.

Each of the proposed process steps had an indirect or direct impact on the natural environment, e.g., through the depletion of natural resources or the consumption of non-renewable energy sources due to the need to manufacture machinery or equipment. However, as part of the work undertaken, it was decided to assess the impacts resulting directly from the operation of the equipment and the emission of pollutants into the environment, i.e., dust and process water emissions. The highest dust emissions capable of contaminating the atmosphere were found for electrostatic precipitation and grinding at 0.008 g/m^2×h and 0.006 g/m^2×h, respectively. Gravity and flotation separations gave rise to process water emissions. The highest water flow required for management occurred during separation on a concentration table and amounted to more than 1000 l/h, while water emissions were about three times lower when a cyclofluid separator was used (about 375 l/h). It should be noted that flotation uses a chemical reagent that does not contain components that are considered toxic and bioaccumulative, but it does require appropriate management. In the case of the electrostatic separator, there are no process water emissions due to the dry nature of the separation.

One of the main technical parameters examined was the estimated throughput of each process (Table 2). The highest efficiency was achieved during shredding with a disintegrator, with an estimated value of 20 kg_{WPCBs}/h. The next step after shredding was grinding, whose capacity was estimated to be about 2.5 kg_{WPCBs}/h. For the separation processes, the highest efficiency was obtained for the cyclofluid separator (7.5 kg_{WPCBs}/h) and the concentration table (6 kg_{WPCBs}/h). However, the efficiency of the stage associated with these devices was limited by the need to dry the resulting products, with a yield of 2.5 kg kg_{WPCBs}/h, which was comparable to that of electrostatic separation (2 kg_{WPCBs}/h). The lowest efficiency was obtained using a flotation machine at 0.15 kg_{WPCBs}/h. All processes were carried out by the

author, and only one operator was assumed for each step. Another important technical parameter is the energy consumption of the equipment used during the recycling process. The highest energy demand (7.5 kW/h) was found during the shredding of WPCBs due to the operation of the disintegrator. Another energy-intensive process was the drying of the separation products, which required 3 kW/h of dryers. Similar energy requirements (3 kW/h) were determined for the flotation process, which consisted of two pieces of equipment: a flotation machine and a compressor.

An important aspect to consider when planning a recycling technology is the investment costs, which can be a critical parameter in determining the establishment of a WPCB recycling facility. As mentioned above, the investment costs refer only to the necessary tools and equipment used during the recycling processes. In the case of the first stage, these costs were set at approximately 715 USD and consisted of a disassembly table equipped with workshop tools, a soldering iron, and containers for segregating the elements disassembled from the WPCB surface. The next process, shredding, required the highest investment of the identified stages of 15,715 USD. This was due to the special design of the shredder, which allows shredding of other WEEE, such as hard disks containing neodymium magnets, which would not be shredded if traditional ferromagnetic materials were used in the design of the shredder. For grinding, the costs of vessels and tanks for procedures involving liquid nitrogen and a knife mill were considered. The cost of the equipment required for electrostatic separation consisted of an electrostatic separator and a high-voltage generator. The capital cost for flotation was the price of the flotation machine and compressor. In contrast, the capital cost for gravity separation was only the price of the cyclofluid separator and shaking table. The last and smallest capital expenditure was the purchase of a precision and certified scale, which was required during the packing stage.

Another aspect included in the economic parameters was the cost of operating equipment, i.e., the cost of energy, water, workforce, and other consumables required for the proper functioning of equipment. Taking into account the operating costs of all stages except separation, almost 80% of the costs were incurred during grinding and feed cooling. The average total operating cost of preparing WPCB for separation was 10.7 USD/kg_{WPCBs}, of which almost half was the cost of purchasing mill knives. The highest eclectic energy cost per kg of WPCBs was calculated for the flotation process, which was more than 2.4 USD/kg_{WPCBs} and also required filtration (3.6 USD/kg_{WPCBs}), product drying (0.15 USD/kg_{WPCBs}), and the use of a flotation reagent (7.7 USD/kg_{WPCBs}). Flotation also had the highest calculated cost per employee (27.8 USD/kg_{WPCBs}). In view of the above, the total operating costs resulting from the flotation process alone were more than 41 USD/kg_{WPCBs}. On the other hand, the lowest total operating costs were incurred for the cycloid separation process, which amounted to about 0.9 USD/kg_{WPCBs}.

The aspect that determines the monetary value of the printed circuit board recycling process is the efficiency of the separation process, determined based on the qualitative and quantitative parameters of the resulting products (Fig. 4). The effectiveness of the separation process was determined by comparing the content of valuable (Cu, Al, Pb, Zn, Ni, Sn, Cr, Ti, Ag, Au) and other (mainly Ca, Si and Br) elements in the obtained products called metals, middlings, and plastics.

The best products, evaluated in terms of the above parameters, were obtained by electrostatic separation. The metallic product was about 26% by weight and consisted of more than 93% valuable metals and about 2% impurities. In contrast, almost 0.5% of valuable metals were identified in the plastic product, demonstrating the very high level of

recyclability and efficiency of the device. Electrostatic separation also resulted in an intermediate product of about 3%, which consisted of conglomerate grains containing about 13% valuable metals. In view of the above, the efficiency of recycling precious metals using an electrostatic separator was estimated to be over 95%. In the case of other separation processes, the obtained products were characterized by a lower purity and content of valuable metals. For example, the metal product obtained using a shaking table was characterized by a metal content of 71% and a contamination level of approximately 7.5%, while the product containing plastics contained more than 5% of valuable metals. The worst product quality parameters were obtained by flotation. The metal product contained about 53% valuable elements and more than 11% impurities.

391 **Table 1**. Evaluation of unit technology processes for their impact on workers and the natural environment.

Stages			Impact categories				
			Identification of harmful and hazardous factors in the workplace			Impact on the natural environment	
			Hazardous factors		Harmful factors	Dust emission to air (dust fallout), g/m^2×h	Process water emissions, l/h
			Dusting, g/m^2×8h	Noise, db	Type of harmful factor		
I Disassembly			no	no	sharp tool parts	no	no
II Shredding			no	<89, peak <117	moving parts of the disintegrator	no	no
III Grinding		IIIA Cooling	no	no	temperatures of -198^{o}C (liquid nitrogen)	no	no
		IIIB Grinding	0.048	<94, peak <132	sharp moving parts	0.006	no
IV Separation	ELECTROSTATIC SEPARATOR		0,064	<71	separator moving parts, high voltage approx. 15kV	0.008	no
	SHAKING TABLE	IVA SEPARATION	no	<133	separator moving parts	no	1020
		IVB DRYING	no	<50	no	no	no
	CYCLOFLUID SEPARATOR	IVA SEPARATION	no	<102	separator moving parts	no	375
		IVB DRYING	no	<50	no	no	no
	FLOTATION MACHNIE	IVA SEPARATION	no	<116	separator moving parts	no	3
		IVB DRYING	no	<50	no	no	no

V Distribution and usage[1]	0.016	no	no	0.002	no		

[1] Only the impact of packaging was assessed. The manufacturing processes of the composite materials were not evaluated due to the experimental level of the research work, and the ways of further processing the metal mixture were not assessed due to the different processes of the enterprises.

Table 2. Evaluation of unit processes of technologies in terms of technical, operational, and economic parameters

Stages		Impact categories							
		Technical specifications		Economic parameters					
				Investment costs				Operation and maintenance aspects	
		Estimated process efficiency, kg_{WPCBs}/h	Energy consumption, kWh	Purchase of equipment, USD	Energy costs, USD/kg_{WPCBs}	Process water costs, USD/kg_{WPCBs}	Employee costs, USD/kg_{WPCBs}	Consumables	Costs of consumables, USD/kg_{WPCBs}
I Disassembly		12	no	715	0	0	0.59	no	
II Shredding		20	7.5	15,715	0.05	0	0.36	cutting shaft components (36 pcs./2 Mg_{WPCBs})	1.1
III Grinding	IIIA Cooling	2,5	no	1,071	0	0	2.85	liquid nitrogen (1 l/kg_{WPCBs})	1
	IIIB Grinding		2.2	5,952	0.12	0		mill knives (pcs./50 kg_{WPCBs})	4.66
IV Separation	ELECTROSTATIC SEPARATOR	2	1.5	7,380	0.1	0	2.09	electrode (1pcs. /4 Mg_{WPCBs})	<0.01

	SHAKING TABLE	IVA SEPARATION	6	2.0	6,190	0.04	0.52	0.70	no	0
		IVB DRYING	2.5	3.0	1,071	0.15	0		Bag for liquid filtration 5um, 1pcs./250l	0.77
	CYCLOFLUID SEPARATOR	IVA SEPARATION	7.5	0.7	4,761	0.01	0.15	0.56	no	0
		IVB DRYING	2.5	3.0	1,071	0.15	0		Bag for liquid filtration 5um, 1pcs./250l	0.18
	FLOTATION MACHNIE	IVA SEPARATION	0.15	3.0	4,285	2.52	0.06	27.90	flotation reagent	7.7
		IVB DRYING	2.5	3.0	1,071	0.15			Bag for filtration 5um, 1pcs./250l	3.64
V Distribution and usage[2]			n/a.[3]		571	0	0	0	no	0

396

397 [2] Not applicable. Due to the very short packing time, which depends on the user's efficiency.

398 [3] Only the impact of packaging was assessed.

399

Figure 4. Summary of the obtained qualitative and quantitative parameters of the separation products (Franke et al., 2021, 2022; Suponik et al., 2021)

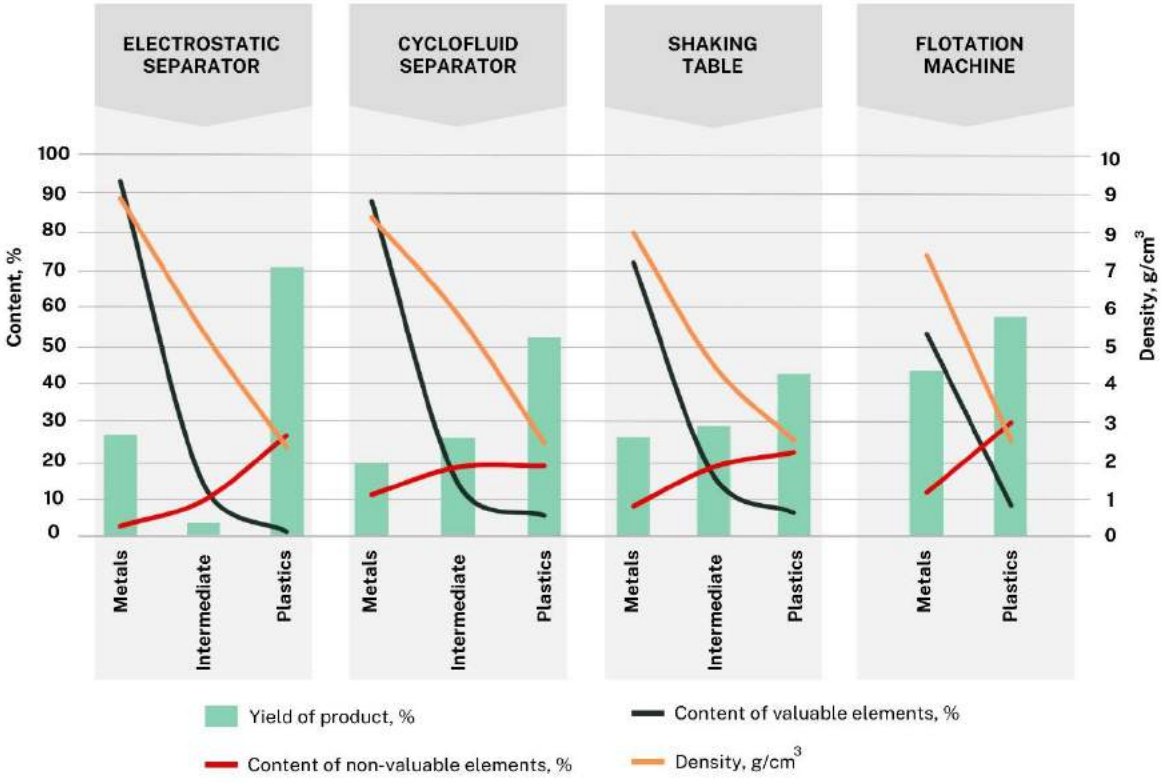

4. Discussion

WPCBs are one of the most problematic types of electronic waste due to their complexity and content of valuable raw materials and environmentally hazardous substances (Liu et al., 2021). In a publication by Hischier et al. (Hischier et al., 2005), an LCA analysis of WPCB recycling processes showed that the recycling of secondary raw materials has a significantly lower impact on the natural environment than conventional raw material extraction. However, it is important to remember that every recycling process has some impact on the natural environment. Furthermore, as the analysis by Pokhrel et al. (Pokhrel et al., 2020) showed, despite the economic benefits and conservation of natural resources resulting from WPCB recycling, the environmental costs may be higher than when raw materials are extracted from deposits. Therefore, the development of eco-efficient WPCB recycling technologies represents a huge potential for the recovery and reuse of these raw materials and may help reduce dependence on imported raw materials and reduce negative environmental impacts.

The results presented in this paper show that efficient recycling of WPCBs can be achieved using physical methods, particularly electrostatic separation. Thus, the negative environmental impacts of recycling can be reduced. A similar conclusion can be found in the publication by Hao et al., which further emphasized the need for further processing of the metal mixtures obtained by physical separation to separate them into elemental forms (Hao et al., 2020). In addition, a number of authors have pointed out that the chemically unchanged non-metallic part of the WPCB composites can be a valuable product. Powder containing plastics, resins, and glass fibers can be used to strengthen new resin-based composites (Ma et al., 2021) and asphalt materials (Li et al., 2022), and it is also possible to

recover the resin (Wei et al., 2021) and use it in other processes. In view of the above, physical methods appear to be the most appropriate option for WPCB recycling.

One of the most important processes for separating metals from plastics is grinding. Our previous results indicate that near-complete release of metals occurs for grains below 0.3 mm, with small impurities found for grains below 0.8 mm, but effective separation was still possible (Suponik et al., 2021). According to Li et al. (Li et al., 2007), complete metal release occurs for grains < 0.6 mm, while Kaya (Kaya, 2016) showed that it only occurs for grains < 0.15 mm. Both studies involved multi-stage grinding in hammer mills without the use of liquid nitrogen, which may have had a significant influence on the results obtained. In addition, the use of liquid nitrogen during grinding was found to significantly increase the efficiency of the process and reduce dust levels. As grinding is one of the most energy-intensive processes, it is detrimental to grind too deeply, and this process, in particular, should be optimized when moving to a technical scale. Grains that are too small can also adversely affect the separation efficiency. It has been observed that very small metal grains (< 0.1 mm) can become stuck in glass fiber grains and enter plastic products, causing losses.

Another important aspect of the work was an evaluation of physical processes. It was important to use the same feed when comparing the products obtained from different separation processes. PCBs are characterized by highly variable chemical compositions (Yazıcı et al., 2010), which can significantly affect the efficiency of separation processes (Hou et al., 2010) and make it difficult to reliably select the most effective method. Evaluation of the products showed that the most efficient separation was electrostatic separation, while the least efficient was flotation. The efficiency of electrostatic separation was about 95%, and the metallic product (26% by weight) consisted of more than 93% valuable metals and

about 2% impurities. The efficiency of electrostatic separation was also confirmed by Mir and Dhawan (Mir and Dhawan, 2022), De Oliveira et al. (De Oliveira et al., 2022), Hamerski et al. (Hamerski et al., 2019), and Dascalescu et al. (Dascalescu et al., 1992). The outputs of the electrostatic separation products were also similar to this work, i.e., about 25% metals, 5% intermediates, and 70% non-metallic parts. In the case of an intermediate containing conglomerate grains, it is possible to return it for regrinding to minimize metal losses. One of the key parameters of electrostatic separation is the voltage across the electrode. Wu et al. (Wu et al., 2008) indicated that the maximum efficient voltage was 20 kV, while higher voltages can lead to a high risk of spark discharge, which may damage the equipment or reduce the separation efficiency. As mentioned above, electrostatic separation was carried out with a voltage across the electrode of 17 kV and high-purity products were obtained. This reduced the risk of spark discharge.

The next subject of evaluation was the products of gravity separation methods. The highest efficiency of these methods was obtained using a shaking table. The metallic product, with an output of about 25%, contained more than 70% metals, but more than 28% of the intermediate product was obtained, which must be reseparated or transferred to other processes. De Oliveira et al. (De Oliveira et al., 2022) also used a concentration table and obtained higher efficiencies, but the separation process was carried out only for selected grain classes. For feeds with particle sizes of 0.3–0.6 mm and 0.6–1.18 mm, metal contents of 89% and 76%, respectively, were found in the metal product. In the study by Burat and Ozer (Burat and Özer, 2018), it was necessary to integrate a concentration table with an electrostatic and magnetic separator, as the use of gravity alone was insufficient. Separation was also carried out for three selected grain sizes. The processes resulted in a metal recovery efficiency of 95.4%, similar to the electrostatic separation in this study. It should be

noted that grain size had a significant effect on the separation efficiency using physical methods. Narrower grades allowed the process to be optimized more precisely, but this increased the complexity of the technology. Flotation produced the worst products in terms of purity. The metallic product of 43% by weight contained approximately 53% metals, while approximately 8% metals were identified in the non-metallic product (57% by weight), indicating high losses of valuable materials. Attempts to separate WPCBs by flotation can be found in the literature, but this method is used for very fine grains and requires precise chemical dosing, mixing speeds, and air flow rate (Mir and Dhawan, 2022). Yao et al. (Yao et al., 2020) also used a reverse flotation process and achieved a metal recovery of 92.7%, but the feed consisted of grains between 0.25 mm and 0.5 mm in size and used anhydrous alcohol as the reagent. In the work of Jeon et al., the Au recovery increased from 32 to 51% using MIBC as a foaming agent (40.5 g/Mg) and paraffin as a collector (405 g/Mg) (Jeon et al., 2018). Han et al. achieved a copper recovery of almost 91% using tannic acid at a concentration of 60 mg/cm^3 (Han et al., 2018). It is important to stress the need to use chemical reagents during flotation, the use of which is questionable when designing eco-efficient technologies. Not all reagents have toxic or carcinogenic effects, but this creates problems with the management or treatment of process water and, in some cases, the concentration of substances can be detrimental to human health.

Operating costs are also an important consideration when designing a technology. The most demanding process in this respect was cooling and grinding, which accounted for almost 80% of all costs associated with preparing WPCBs for separation processes. Taking all stages together, the costs of dismantling, grinding, milling, and electrostatic separation were 4%, 10%, 60%, and 25% respectively. This means that the preparation of the feed to the separator accounted for ¾ of the operating costs. Therefore, these processes, especially

497 grinding, can determine the economic viability of WPCB recycling. When moving to the
498 technical scale, the proportion of costs may be different, but grinding will definitely be the
499 costliest process. Another factor affecting the economic viability of recycling is energy
500 consumption (Pokhrel et al., 2020), which, depending on the energy mix (for Poland, more
501 than 70% of energy comes from fossil sources), may contribute to higher environmental
502 burdens than the traditional mining of certain metals. When water was used for separation
503 processes, a longer drying time was required for the resulting products, which increased the
504 energy consumption of these methods. In an era of volatile energy prices and the drive to
505 decarbonize industries, a low energy consumption should become the standard for modern
506 recycling technologies. Furthermore, according to Kaya (Kaya, 2016), electrostatic separation
507 is relatively easy to scale up and achieves high efficiencies of 95–99%.

508 Another aspect to consider when designing a technology is its potential impact on workers'
509 health. Ahirwar et al. pointed out that WPCBs may contain substances toxic to humans and
510 the environment (Ahirwar and Tripathi, 2021). It is, therefore, important to identify
511 potentially harmful factors in the workplace, such as dust and noise. It has been found that
512 the amount of dust emitted from equipment does not depend on the material load of the
513 equipment but on the duration of its operation. The highest dust concentrations were
514 observed during electrostatic separation, which may be caused by a leaking separator
515 housing. In the case of crushing, the use of liquid nitrogen significantly reduced the dust, and
516 no dust was detected during gravity separation and flotation. It should be remembered that
517 uncontrolled emissions of WPCB dust can be harmful to humans and the environment (Kaya,
518 2018), making it necessary to use protective masks during work, as well as a ventilation
519 system to capture airborne particles. Another identified harmful factor was noise, the
520 highest intensity of which was studied during the use of a shaking table that was driven by a

motor. In the case of crushing and grinding, the source of the noise was the crushing of WPCB parts, while in the case of flotation, the source of the noise was the compressor generating the compressed air needed to produce aerated water. According to Polish legislation, earmuffs are required for the noise levels found during the tests. The use of water during the gravity separation and flotation processes was an important factor and had a significant environmental impact. Therefore, when moving to a technical or semi-technical scale, it is necessary to close the water circuit. However, it should be borne in mind that WPCBs contain aluminium and magnesium in metallic form, which, when fragmented and in high concentrations, can cause chemical reactions when in prolonged contact with water (Corcoran et al., 2013).

5. Conclusions

The recycling technologies for WPCBs were analyzed using various methods, each characterized by different environmental and human impacts, cost-effectiveness, and efficiency. Therefore, it is essential to choose the most efficient method in terms of these aspects. Based on the analyses conducted in this study, it can be concluded that the proposed recycling technology employing electrostatic separation is eco-efficient.

The presented technology consisted of five primary stages (Fig. 5) and was characterized by a relatively low environmental impact, minimal effects on human health, modest financial investments, and high efficiency. The selected components of this technology did not involve complex or challenging procedures. Hazardous chemicals that pose risks to the environment and human health were not used. Furthermore, no process water was utilized, which, if not properly treated, may release hazardous metals into the environment.

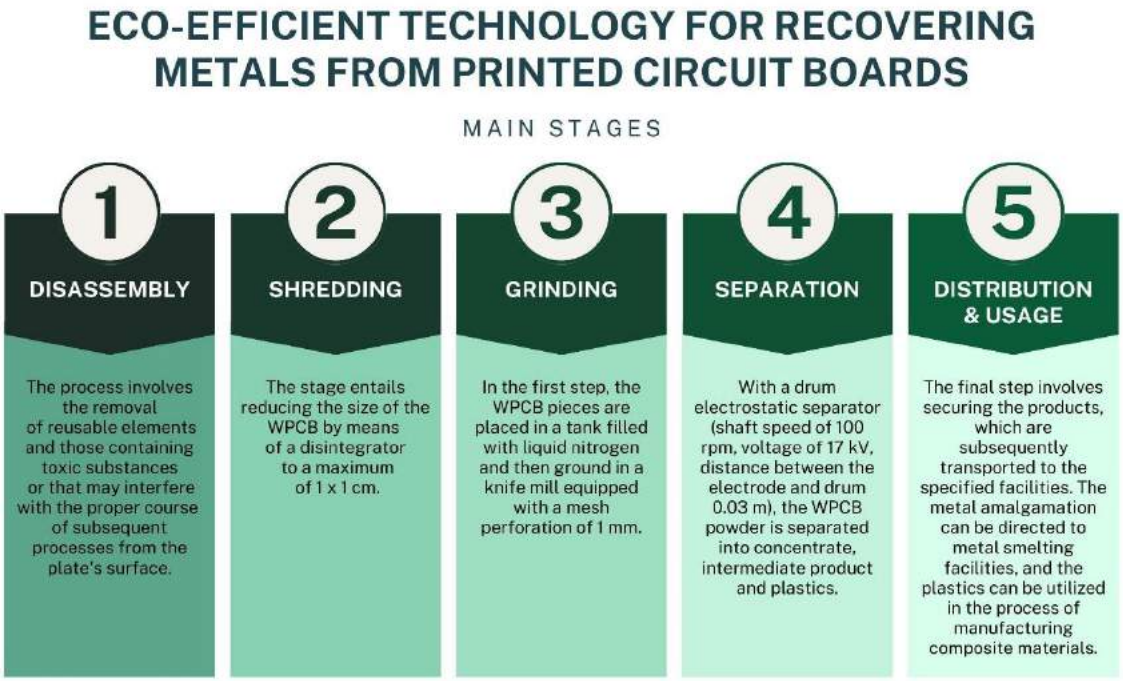

Figure 5. The main stages of an eco-efficient WPCB recycling technology.

The obtained metal mixture can be sold to metal smelting facilities, while the plastics can be used for composite production. As a result, over 95% of pure WPCBs become products that find applications, rendering this technology nearly waste-free. Therefore, the proposed technology aligns with the principles of sustainable production and the closed-loop economy and thus holds significant implementation potential, particularly in economies lacking reserves of the metals found in WPCBs.

References

Ahirwar, R., Tripathi, A.K., 2021. E-waste management: A review of recycling process, environmental and occupational health hazards, and potential solutions. Environmental Nanotechnology, Monitoring & Management 15, 100409. https://doi.org/10.1016/j.enmm.2020.100409

Araujo Galvão, G.D., de Nadae, J., Clemente, D.H., Chinen, G., de Carvalho, M.M., 2018. Circular Economy: Overview of Barriers. Procedia CIRP 73, 79–85. https://doi.org/10.1016/j.procir.2018.04.011

559 Baldé, C.P., D'Angelo, E., Luda, V., Deubzer, O., Kuehr, R., 2022. Global Transboundary E-
560 waste Flows Monitor 2022.
561 Burat, F., Özer, M., 2018. Physical separation route for printed circuit boards.
562 Physicochemical Problems of Mineral Processing; ISSN 2084-4735.
563 https://doi.org/10.5277/PPMP1858
564 Corcoran, A., Mercati, S., Nie, H., Milani, M., Montorsi, L., Dreizin, E.L., 2013. Combustion of
565 fine aluminum and magnesium powders in water. Combustion and Flame 160, 2242–
566 2250. https://doi.org/10.1016/j.combustflame.2013.04.019
567 Dantas, T.E.T., de-Souza, E.D., Destro, I.R., Hammes, G., Rodriguez, C.M.T., Soares, S.R., 2021.
568 How the combination of Circular Economy and Industry 4.0 can contribute towards
569 achieving the Sustainable Development Goals. Sustainable Production and
570 Consumption 26, 213–227. https://doi.org/10.1016/j.spc.2020.10.005
571 Dascalescu, L., Iuga, A., Morar, R., 1992. Corona–Electrostatic Separation: An Efficient
572 Technique for the Recovery of Metals and Plastics From Industrial Wastes. Magnetic
573 and Electrical Separation 4, 241–255. https://doi.org/10.1155/1993/59037
574 De Oliveira, C.M., Bellopede, R., Tori, A., Zanetti, G., Marini, P., 2022. Gravity and
575 Electrostatic Separation for Recovering Metals from Obsolete Printed Circuit Board.
576 Materials 15, 1874. https://doi.org/10.3390/ma15051874
577 Forti, V., Baldé, C.P., Kuehr, R., Bel, G., 2020. The Global E-waste Monitor 2020: Quantities,
578 flows and the circular economy potential. United Nations University (UNU)/United
579 Nations Institute for Training and Research (UNITAR) – co-hosted SCYCLE
580 Programme, International Telecommunication Union (ITU) & International Solid
581 Waste Association (ISWA), 1-120.
582 Franke, D., Suponik, T., Nuckowski, P., Dubaj, J., 2021. Evaluation of the efficiency of metal
583 recovery from printed circuit boards using gravity processes. Physicochem. Probl.
584 Miner. Process. 57, 63–77. https://doi.org/10.37190/ppmp/138471
585 Franke, D., Suponik, T., Nuckowski, P.M., Gołombek, K., Hyra, K., 2020. Recovery of Metals
586 from Printed Circuit Boards By Means of Electrostatic Separation. Management
587 Systems in Production Engineering 28, 213–219. https://doi.org/10.2478/mspe-2020-
588 0031

589 Franke, D.M., Kar, U., Suponik, T., Siudyga, T., 2022. Evaluation of the use of flotation for the
590 separation of ground printed circuit boards.
591 https://doi.org/10.24425/GSM.2022.140605
592 Hamerski, F., Krummenauer, A., Bernardes, A.M., Veit, H.M., 2019. Improved settings of a
593 corona-electrostatic separator for copper concentration from waste printed circuit
594 boards. Journal of Environmental Chemical Engineering 7, 102896.
595 https://doi.org/10.1016/j.jece.2019.102896
596 Han, J., Duan, C., Li, G., Huang, L., Chai, X., Wang, D., 2018. The influence of waste printed
597 circuit boards characteristics and nonmetal surface energy regulation on flotation.
598 Waste Management 80, 81–88. https://doi.org/10.1016/j.wasman.2018.09.002
599 Hao, J., Wang, Y., Wu, Y., Guo, F., 2020. Metal recovery from waste printed circuit boards: A
600 review for current status and perspectives. Resources, Conservation and Recycling
601 157, 104787. https://doi.org/10.1016/j.resconrec.2020.104787
602 Hischier, R., Wäger, P., Gauglhofer, J., 2005. Does WEEE recycling make sense from an
603 environmental perspective? Environmental Impact Assessment Review 25, 525–539.
604 https://doi.org/10.1016/j.eiar.2005.04.003
605 Hou, S., Wu, J., Qin, Y., Xu, Z., 2010. Electrostatic Separation for Recycling Waste Printed
606 Circuit Board: A Study on External Factor and a Robust Design for Optimization.
607 Environ. Sci. Technol. 44, 5177–5181. https://doi.org/10.1021/es903936m
608 Jeon, S., Ito, M., Tabelin, C.B., Pongsumrankul, R., Kitajima, N., Park, I., Hiroyoshi, N., 2018.
609 Gold recovery from shredder light fraction of E-waste recycling plant by flotation-
610 ammonium thiosulfate leaching. Waste Management 77, 195–202.
611 https://doi.org/10.1016/j.wasman.2018.04.039
612 Kaya, M., 2018. Current WEEE recycling solutions, in: Waste Electrical and Electronic
613 Equipment Recycling. Elsevier, pp. 33–93. https://doi.org/10.1016/B978-0-08-
614 102057-9.00003-2
615 Kaya, M., 2017. Recovery of Metals and Nonmetals from Waste Printed Circuit Boards (PCBs)
616 by Physical Recycling Techniques, in: Zhang, L., Drelich, J.W., Neelameggham, N.R.,
617 Guillen, D.P., Haque, N., Zhu, J., Sun, Z., Wang, T., Howarter, J.A., Tesfaye, F.,
618 Ikhmayies, S., Olivetti, E., Kennedy, M.W. (Eds.), Energy Technology 2017. Springer
619 International Publishing, Cham, pp. 433–451. https://doi.org/10.1007/978-3-319-
620 52192-3_43

621 Kaya, M., 2016. Recovery of metals and nonmetals from electronic waste by physical and
622 chemical recycling processes. Waste Management 57, 64–90.
623 https://doi.org/10.1016/j.wasman.2016.08.004
624 Li, J., Lu, H., Guo, J., Xu, Z., Zhou, Y., 2007. Recycle Technology for Recovering Resources and
625 Products from Waste Printed Circuit Boards. Environ. Sci. Technol. 41, 1995–2000.
626 https://doi.org/10.1021/es0618245
627 Li, S., Sun, Y., Fang, S., Huang, Y., Yu, H., Ye, J., 2022. Recycling Non-Metallic Powder of
628 Waste Printed Circuit Boards to Improve the Performance of Asphalt Material.
629 Materials 15, 4172. https://doi.org/10.3390/ma15124172
630 Liu, T., Cao, J., Wu, Y., Weng, Z., Senthil, R.A., Yu, L., 2021. Exploring influencing factors of
631 WEEE social recycling behavior: A Chinese perspective. Journal of Cleaner Production
632 312, 127829. https://doi.org/10.1016/j.jclepro.2021.127829
633 Ma, C., Sánchez-Rodríguez, D., Kamo, T., 2021. A comprehensive study on the oxidative
634 pyrolysis of epoxy resin from fiber/epoxy composites: Product characteristics and
635 kinetics. Journal of Hazardous Materials 412, 125329.
636 https://doi.org/10.1016/j.jhazmat.2021.125329
637 Ma, E., 2019. Recovery of Waste Printed Circuit Boards Through Pyrometallurgy, in:
638 Electronic Waste Management and Treatment Technology. Elsevier, pp. 247–267.
639 https://doi.org/10.1016/B978-0-12-816190-6.00011-X
640 Maurice, A.A., Dinh, K.N., Charpentier, N.M., Brambilla, A., Gabriel, J.-C.P., 2021. Dismantling
641 of Printed Circuit Boards Enabling Electronic Components Sorting and Their
642 Subsequent Treatment Open Improved Elemental Sustainability Opportunities.
643 Sustainability 13, 10357. https://doi.org/10.3390/su131810357
644 Mir, S., Dhawan, N., 2022. A comprehensive review on the recycling of discarded printed
645 circuit boards for resource recovery. Resources, Conservation and Recycling 178,
646 106027. https://doi.org/10.1016/j.resconrec.2021.106027
647 Pokhrel, P., Lin, S.-L., Tsai, C.-T., 2020. Environmental and economic performance analysis of
648 recycling waste printed circuit boards using life cycle assessment. Journal of
649 Environmental Management 276, 111276.
650 https://doi.org/10.1016/j.jenvman.2020.111276
651 Polskie Sieci Elektroenergetyczne, 2023. Rynkowa cena energii elektrycznej z dnia
652 25.04.2023 [WWW Document]. URL https://www.pse.pl/dane-

systemowe/funkcjonowanie-rb/raporty-dobowe-z-funkcjonowania-rb/podstawowe-wskazniki-cenowe-i-kosztowe/rynkowa-cena-energii-elektrycznej-rce (accessed 4.25.23).

Royal Society of Chemistry, 2022. Periotic Table [WWW Document]. URL https://www.rsc.org/periodic-table/ (accessed 12.29.22).

Silva, L.H. de S., Júnior, A.A.F., Azevedo, G.O.A., Oliveira, S.C., Fernandes, B.J.T., 2021. Estimating Recycling Return of Integrated Circuits Using Computer Vision on Printed Circuit Boards. Applied Sciences 11, 2808. https://doi.org/10.3390/app11062808

Suponik, T., Franke, D., Nuckowski, P., Matusiak, P., Kowol, D., Tora, B., 2021. Impact of Grinding of Printed Circuit Boards on the Efficiency of Metal Recovery by Means of Electrostatic Separation. Minerals 11, 281. https://doi.org/10.3390/min11030281

Tatariants, M., Yousef, S., Sidaraviciute, R., Denafas, G., Bendikiene, R., 2017. Characterization of waste printed circuit boards recycled using a dissolution approach and ultrasonic treatment at low temperatures. RSC Adv. 7, 37729–37738. https://doi.org/10.1039/C7RA07034A

The London Metal Exchange [WWW Document], 2022. URL https://www.lme.com/en/ (accessed 12.29.22).

Wei, X., Nie, C., Yu, Y., Wang, J., Lyu, X., Wu, P., Zhu, X., 2021. Environment-friendly recycling of resin in waste printed circuit boards. Process Safety and Environmental Protection 146, 694–701. https://doi.org/10.1016/j.psep.2020.12.008

Wu, J., Li, J., Xu, Z., 2008. Electrostatic Separation for Recovering Metals and Nonmetals from Waste Printed Circuit Board: Problems and Improvements. Environ. Sci. Technol. 42, 5272–5276. https://doi.org/10.1021/es800868m

Xavier, L.H., Giese, E.C., Ribeiro-Duthie, A.C., Lins, F.A.F., 2021. Sustainability and the circular economy: A theoretical approach focused on e-waste urban mining. Resources Policy 74, 101467. https://doi.org/10.1016/j.resourpol.2019.101467

Yaashikaa, P.R., Priyanka, B., Senthil Kumar, P., Karishma, S., Jeevanantham, S., Indraganti, S., 2022. A review on recent advancements in recovery of valuable and toxic metals from e-waste using bioleaching approach. Chemosphere 287, 132230. https://doi.org/10.1016/j.chemosphere.2021.132230

683 Yao, Y., Bai, Q., He, J., Zhu, L., Zhou, K., Zhao, Y., 2020. Reverse flotation efficiency and
684 mechanism of various collectors for recycling waste printed circuit boards. Waste
685 Management 103, 218–227. https://doi.org/10.1016/j.wasman.2019.12.030
686 Yazıcı, E., Deveci, H., Alp, I., Akçil, A., Yazıcı, R., 2010. Characterisation of Computer Printed
687 Circuit Boards for Hazardous Properties and Beneficiation Studies 8.
688

materials

MDPI

Article

Morphology, Phase and Chemical Analysis of Leachate after Bioleaching Metals from Printed Circuit Boards

Kamila Hyra [1], Paweł M. Nuckowski [2,*], Joanna Willner [3], Tomasz Suponik [4,*], Dawid Franke [4], Mirosława Pawlyta [2], Krzysztof Matus [2] and Waldemar Kwaśny [5]

1 Department of Engineering Materials and Biomaterials, Faculty of Mechanical Engineering, Silesian University of Technology, 18A Konarskiego Street, 44-100 Gliwice, Poland; kamila.hyra@polsl.pl
2 Materials Research Laboratory, Faculty of Mechanical Engineering, Silesian University of Technology, 18A Konarskiego Street, 44-100 Gliwice, Poland; miroslawa.pawlyta@polsl.pl (M.P.); krzysztof.matus@polsl.pl (K.M.)
3 Department of Metallurgy and Recycling, Faculty of Materials Engineering, Silesian University of Technology, 8 Krasińskiego Street, 40-019 Katowice, Poland; joanna.willner@polsl.pl
4 Department of Geoengineering and Raw Materials Extraction, Faculty of Mining, Safety Engineering and Industrial Automation, Silesian University of Technology, 2 Akademicka Street, 44-100 Gliwice, Poland; dawid.franke@polsl.pl
5 Department of Welding, Faculty of Mechanical Engineering, Silesian University of Technology, 18A Konarskiego Street, 44-100 Gliwice, Poland; waldemar.kwasny@polsl.pl
* Correspondence: pawel.nuckowski@polsl.pl (P.M.N.); tomasz.suponik@polsl.pl (T.S.)

Abstract: The article presents the assessment of solutions and dried residues precipitated from solutions after the bioleaching process of Printed Circuit Boards (PCB) utilizing the *Acidithiobacillus ferrooxidans*. The obtained dried residues precipitated from bioleaching solution (leachate) and control solution were tested using morphology, phase, and chemical composition analysis, with particular emphasis on the assessment of crystalline and amorphous components. The analysis of the dried residues from leachate after bioleaching as well as those from the sterile control solution demonstrated a difference in the component oxidation—the leachate consisted of mainly amorphous spherical particles in diameter up to 200 nm, forming lacy aggregates. In the specimenform control solution larger particles (up to 500 nm) were observed with a hollow in the middle and crystalline outer part (probably Fe_2O_3, $CuFeS_2$, and Cu_2O). The X-ray diffraction phase analysis revealed that specimen obtained from leachate after bioleaching consisted mainly of an amorphous component and some content of Fe_2O_3 crystalline phase, while the dried residue from control solution showed more crystalline components. The share of the crystalline and amorphous components can be related to efficiency in dissolving metals during bioleaching. Obtained results of the investigation confirm the activity and participation of the *A. ferrooxidans* bacteria in the solubilization process of electro-waste components, with their visible degradation–acceleration of the reaction owing to a continuous regeneration of the leaching medium. The performed investigations allowed to characterize the specimen from leachate and showed that the application of complementary cross-check of the micro (SEM and S/TEM) and macro (ICP-OES and XRD) methods are of immense use for complete guidance assessment and obtained valuable data for the next stages of PCBs recycling.

Keywords: metals recovery; recycling; bioleaching; scanning electron microscopy (SEM); high resolution transmission electron microscopy (S/TEM); X-ray diffraction (XRD)

Citation: Hyra, K.; Nuckowski, P.M.; Willner, J.; Suponik, T.; Franke, D.; Pawlyta, M.; Matus, K.; Kwaśny, W. Morphology, Phase and Chemical Analysis of Leachate after Bioleaching Metals from Printed Circuit Boards. *Materials* **2022**, *15*, 4373. https://doi.org/10.3390/ma15134373

Academic Editor: Shanshan Yang

Received: 14 April 2022
Accepted: 8 June 2022
Published: 21 June 2022

1. Introduction

Year after year, a significant increase in the amount of produced waste of electrical and electronic equipment (WEEE) is recorded, and in 2014, its mass equaled 41.8 Mt (metric ton), in 2016—44.7 Mt, and 53.6 Mt was generated in 2019 [1–3]. In 2014, approximately 35% of electro-waste was recycled [4]. One of the electro-waste components is Printed

Circuit Board (PCB). It is a laminate and constitutes about 3% of the mass of the whole electronic equipment [5–7]. A printed circuit board is manufactured from materials belonging to metals (about 30–40% of the whole component) and non-metals (plastics, ceramics, composites, about 60–70% of the whole component) [3,8–10]. It is possible to identify the diversified element composition: Cu, Zn, Ni, Al, Fe, Si, Ca, Pb, Sn, Cr, Mn, Mo, Ti, Pd, Pt, Ag, Au, etc. In some cases, a PCB consists of even as much as 60 elements, also toxic and hazardous [3,9–13]. Actions related to the recycling of WEEE and PCB protect the natural environment by limiting the use of ores, as well as reducing the amount of generated waste and pollutants (storage of heavy metals and other toxic substances). Additionally, recovery processes are less energy-consuming than the extraction of metals from primary sources [4,14]. Metal recycling from printed circuit boards is a complex issue, mostly due to the complicated construction of these components. The difficulty in developing effective methods of processing and recovery of those materials is connected mostly with the toxicity of some of the elements used to manufacture PCB, which is mentioned, among others, by Priya et al. [3] and Sohaili et al. [5], as well as a small concentration of metallic elements [3,5].

This paper is a continuation of research [15] aimed at the application of physical methods of metal recovery from PCB, which are economical and environmentally friendly. For this purpose, the material was prepared with a knife mill and in the next stage the fine grains were subjected to electrostatic separation. This method allows to separate grains into three products: concentrate (a mixture of metals), waste (mainly consisting of plastics and ceramics) for which two applications have been found, and a small amount of a difficult-to-manage intermediate (mixture of metals, plastics, and ceramics combined by strong connections). Due to its complicated structure and chemical composition, its processing with simple and cheap methods was difficult. Therefore, for this small amount of intermediate, it was decided to use bioleaching, which is also environmentally friendly, but its disadvantage is the long-term impact of micro-organisms on the components of PCBs during the catalysis of the metal recovery process. As a result of bioleaching, a metal-free sludge is to be formed, which will be combined with the waste (plastics) to produce composites and a solution containing metal ions that will be recovered in the next stage of the research [15]. It is a cost-effective process, and there are no required high energy inputs or advanced technology apparatus. Bioleaching with *Acidithiobacillus ferrooxidans* is a bacteria-assisted course (they provide and accelerate Fe ions oxidation), yielding solubilization of metals from material to leachate. Biological processes are inherently environment-friendly, but the kinetics are long-lasting. *A. ferrooxidans*, "iron bacteria", are usually used both in laboratorial tests and industrial processes of bioleaching of copper, gold, nickel, or cobalt. They are chemolithoautotrophs, which live in the optimal temperature of 20–45 °C and pH = 1.3 ÷ 4.5. These bacteria take energy by oxidizing the reduced sulfur compounds (in the case of the oxidation of pyrite), but mostly from the oxidation of Fe^{2+} ions to Fe^{3+}, thus ensuring continuous regeneration of the leaching agent, which is not possible in the case of traditional leaching [14,16–24]. The Fe^{2+} ions oxidize chemically with oxygen to Fe^{3+} ions for a very long time in a strongly acidic environment, but it is they who are responsible for the occurrence of the leaching reaction when bioleaching sparingly soluble sulfide minerals, whereas the presence of iron bacteria significantly accelerates the oxidation processes and Fe^{3+} regeneration with the pH value below 4, and only iron bacteria are capable of accelerating the oxidation with the indicated pH value. The process characterizes in high elasticity, due to the high adaptation ability of the microorganisms to extreme living conditions. The adaptation process, consisting in a gradual increase of the agent's concentration in the bacterial environment makes it possible for the microorganisms to adapt to high metal concentrations. However, with a properly high concentration of heavy metals or some salts, the bacteria's metabolism becomes disturbed, which may lead to their death [16]. In their study, Zhu et al. [17] emphasize also that plastics can contribute to bacteria's faded activity during the bioleaching process, which, without the strain's adaptation to such conditions, can also result in their necrobiosis. The presence of iron-oxidizing bacteria also

increases the probability of the formation of secondary iron compounds (mainly jarosites), which are the undesirable products of bioleaching, as they form envelopes around the ore's particles, thus inhibiting the kinetics of mineral solubilization [25]. In turn, solutions from bioleaching processes usually have very low pH values and high concentrations of sulfates and iron (III). Especially solubilized iron can disturb the further processes of separation and recovery of the metals [26,27]. After bioleaching, leachate (solid crystals of metals dispersed in liquid) and residue (non-metals and non-digested metals) are obtained. In the presented study, the leachate was the basis for metal recovery, hence the sludge has not been analyzed in detail.

The article analyzes the dried residues precipitated from solution after bioleaching using modern measurement techniques to evaluate and select applicable methods of recovering metals from solutions, such as e.g., the reduction of metal ions in the reactor in accordance with patent application No. P.410550 [28]. In order to properly design the process of recovering metals from a bio-solution, the input material for this process, in particular its chemical composition and morphology, should be identified. The aim of the study was to present possible and necessary analytical methods for testing solutions and the sequence of these analyzes. The intermediate in an amount less than 3% of total electrostatic separator feed (Suponik et al. [15]), which was subjected to the bioleaching process in this study, had a different chemical composition (especially in the amount of plastics) and structure from typical PCBs waste undergoing biological oxidation.

Metal separation and recovery from solutions are commonly achieved by technologies such as solvent extraction (SX), electrolysis/electro-winning (EW), or ion exchange (IX). The effectiveness of these processes is diversified, and the range of results shows the influence of many factors on their course. Therefore, in order to apply and select the best method of recovering metals from solution obtained after bioleaching process of PCBs, these solutions must be fully characterized not only in terms of chemical composition but also crystalline and amorphous components should be assessed. This article was devoted to these issues. A secondary goal of this work was to demonstrate the possibility of using bacteria for effective leaching of PCBs waste materials.

2. Materials and Methods

This publication is a continuation of previous research presented in the paper Suponik et al. [15], in which the electrostatic separation of grinded PCBs was conducted. As a result, the following products were obtained: concentrate, intermediate, and waste, with yields of 26.2%, 2.8%, and 71.0%, respectively. The obtained concentrate and waste were pure and could be easily processed by known methods, unlike the intermediate, which consisted mostly of conglomerate grains (metal–non-metals–ceramics material). The release of metals from the conglomerate grains by mechanical means is time-consuming, costly, and difficult, mainly due to strong and undefined connections. Therefore, this material was biochemically processed with *A. ferrooxidans* bacteria in this study. A small amount of intermediate product (less than 3% after electrostatic separation) makes it possible to apply bioleaching as part of the recovery of metals from PCBs, which makes this long-lasting method effective and cheap compared with other methods.

The bioleaching was carried out in Erlenmeyer flasks (0.3 dm^3) containing 3 g of the intermediate fraction samples and 0.18 dm^3 of nutrient medium 9K (Silverman and Lundgren medium, composition in g/dm^3: $FeSO_4 \cdot 7\ H_2O$—44.30, $Ca(NO_3)_2$—0.01, $(NH4)_2SO_4$—3.00, K_2HPO_4—0.50, KCl—0.10, $MgSO_4 \cdot 7\ H_2O$—0.50) inoculated by 0.02 dm^3 of *A. ferrooixdans*. A pure strain of *A. ferrooxidans* (F3-02) was isolated from the source of mineral water coming from Głębokie (Nowy Sącz county, Poland) [29]. Metals concentration in the intermediate product of electrostatic separation (bioleached material) in %: Cu—6.68 ± 0.67, Al—1.34 ± 0.13, Pb—0.74 ± 0.07, Zn—0.74 ± 0.09, Ni—0.31 ± 0.03, Fe—1.5 ± 0.15, Sn—1.18 ± 0.12, Ti—0.39 ± 0.04 [25]. The bioleaching process was conducted for 64 days at ambient temperature, through systematic measurements of pH and Eh (every 3–5 days). To maintain the optimal solution pH, the samples were acidified (5M H_2SO_4) to pH = 2.0.

After the end of the bioleaching, the solutions were filtered, by way of separating the remaining liquid with the use of medium filter papers (Macherey—Nagel, Allentown, PA, USA, MN 640 d, 18.5 cm ∅) to separate the solutions and the residues from each other. Simultaneously, the sterile control samples were performed, under identical experiment conditions (chemical leaching).

For the pH and Eh measurements, a KnickPortamesstype 913 pH meter with an electrode by WTW pH—ElectrodeSenTix 41 with automatic temperature compensation (used to read off the liquid temperature) and an Elmetron CP—551 m with a Radelkis OP—7171—1A electrode were used, respectively. The specimens made from the solutions and the residue underwent further analyses—Inductively Coupled Plasma Optical Emission Spectrometry (ICP-OES), Ultra–high resolution Scanning-Transmission Electron Microscopy (S/TEM), Scanning Electron Microscopy (SEM), and X-Ray Diffraction (XRD).

The main analysis was carried out on the following specimens: made from filtered solution obtained after bioleaching process (described as leachate) and filtered solution obtained in chemical leaching (described as control solution). In order to perform SEM, S/TEM, and XRD analysis, dried residues precipitated from leachate samples and control solution samples were examined. To obtain representative results of electron microscopy analytical methods it was necessary to dilute the leachate and control solution with pure ethyl alcohol (1:1000) before the samples were dried. Without this procedure, it would be impossible to reveal the morphology of the particles placed in solutions, as well as obtain full information about the qualitative phase and chemical composition. Residue (sediment and solid phase filtered form leachate) from bioleaching process was tested only by using ICP-OES technique to show the chemical balance after the bioleaching process.

A high-resolution scanning electron microscope (SEM) Zeiss Supra 35 (Carl Zeiss AG, Aalen, Germany) was equipped with the EDAX Energy dispersive X-ray spectroscopy (EDS) system (EDAX, Mahwah, NJ, USA) and enabled to analyze the chemical composition in micro-areas. The voltage accelerating the electron beam reached 15 kV. The solutions were mixed in a magnetic mixer for 15 min, then applied on a carbon band and dried at the temperature of 60 °C. The tests have been carried out on the diluted (morphology and chemical composition of selected areas) and undiluted solutions (only chemical composition).

In order to illustrate the morphology and structure of the examined specimens, a high resolution transmission electron microscope S/TEM TITAN 80-300 (FEI, Hillsboro, OR, USA) was used, the microscope was equipped with an X-ray energy dispersion spectrometer (EDS). The electron beam energy was 300 kV. For the analysis of the obtained results, the DigitalMicrograph by Gatan (v. 2.32.888), TEM Imaging & Analysis (v. 4.17) and Crystal Maker (v. 4.0) software was applied. To prepare the specimens, a proper number of the solutions was collected, which was then mixed in a magnetic mixer and applied in a small amount onto a copper mesh. In the EDS analyses, light elements were excluded ($Z < 11$), as their qualitative evaluation is burdened with too much error.

The X-ray diffraction tests were made on an X'Pert Pro diffractometer (Panalytical, Almelo, The Netherlands), with the use of filtered X-ray lamp radiation (filter Fe) with a cobalt anode (KαCo λ = 1.7909 Å), powered by voltage 40 kV, with the filament current intensity = 30 mA. The examined specimens were applied on a non-reflective base made of silicon mono-crystal. The X-ray diffraction measurements were performed in the Bragg–Brentano geometry in the angular scope 10–70° [2θ] with the step 0.026° and the step count time 70 s. The obtained diffractograms were analyzed by means of the X'Pert High Score Plus software (v. 3.0e) with a dedicated Inorganic Crystal Structure Database—ICSD (FIZ, Karlsruhe, Germany).

In order to check and confirm the metals concentration in leachate and residue ICP-OES method was employed, using the Jy2000 spectrometer (by Horiba Yobin-Yvon, Hessen, Germany). The source of the induction was a plasma torch coupled with a 40.68 MHz frequency generator; the bioleaching products were previously dissolved.

3. Results

3.1. Bioleaching Process

Figure 1 shows the changes in the potential of Eh and pH during bacterial and chemical leaching. For the system inoculated with the bacteria, a constant increase of Eh was observed—from the initial value of 255 mV to about 700 mV, obtained on the 52nd day of the experiment. The *A. ferrooxidans* bacteria gradually oxidized Fe (II) to Fe (III), which, in connection with a low pH during the bioleaching, points to growth of the microorganisms and proves a biological course of the reaction. At the same time, the value of Eh in the control solution remained in the scope of 300–400 mV. Due to the alkaline nature of the PCB waste [26,27] and to provide favorable conditions for microorganisms, the pH of the samples was corrected using 5M H_2SO_4. The reaction of the leaching solution inoculated with the bacteria was corrected several times in the preliminary phase of the process. The self-acidification effect with the maintained value of pH = 2 was observed on the 9th day of the performed process. In the case of the control solution, the pH correction was made regularly, thus ensuring an acidic environment during the 64 days of chemical leaching.

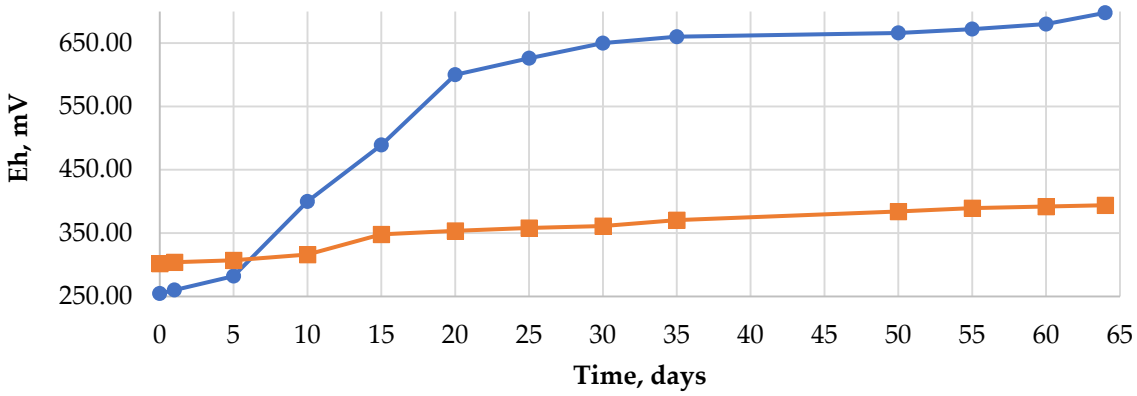

(**a**)

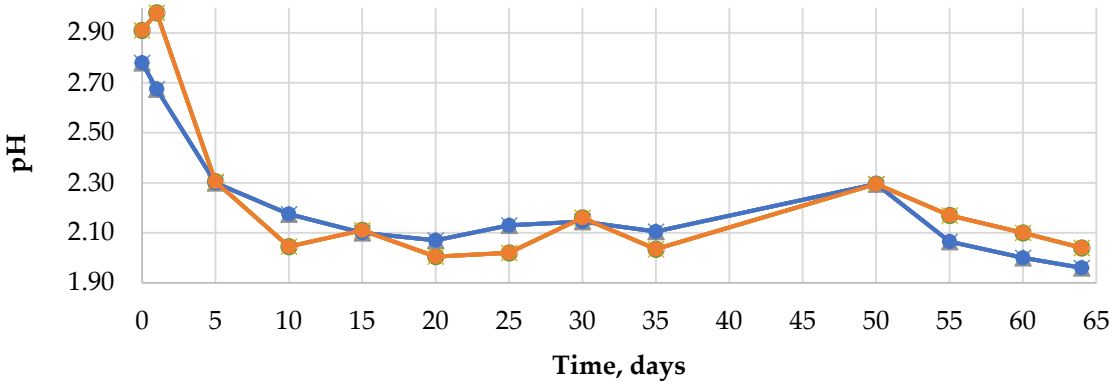

(**b**)

Figure 1. Graphs showing changes in: (**a**) redox potential (Eh), (**b**) pH, during bacterial (blue line) and chemical (orange line) leaching.

3.2. Scanning Electron Microscopy

The observations of the dried residues precipitated from solution after the bioleaching specimen made on a scanning electron microscope enabled an evaluation of the specimens' morphology and chemical composition. Figure 2a,b shows the morphology of the dried residues precipitated from diluted specimen of the leachate and the control solution. The specimen obtained from leachate (Figure 2a) revealed mainly agglomerates with a spongy structure, probably formed as a result of evaporation of the liquid from the colloidal suspension. Similar structures, yet in a smaller content, were identified in the dried

specimen from control solution. There was observed numerous agglomerates with a compact structure.

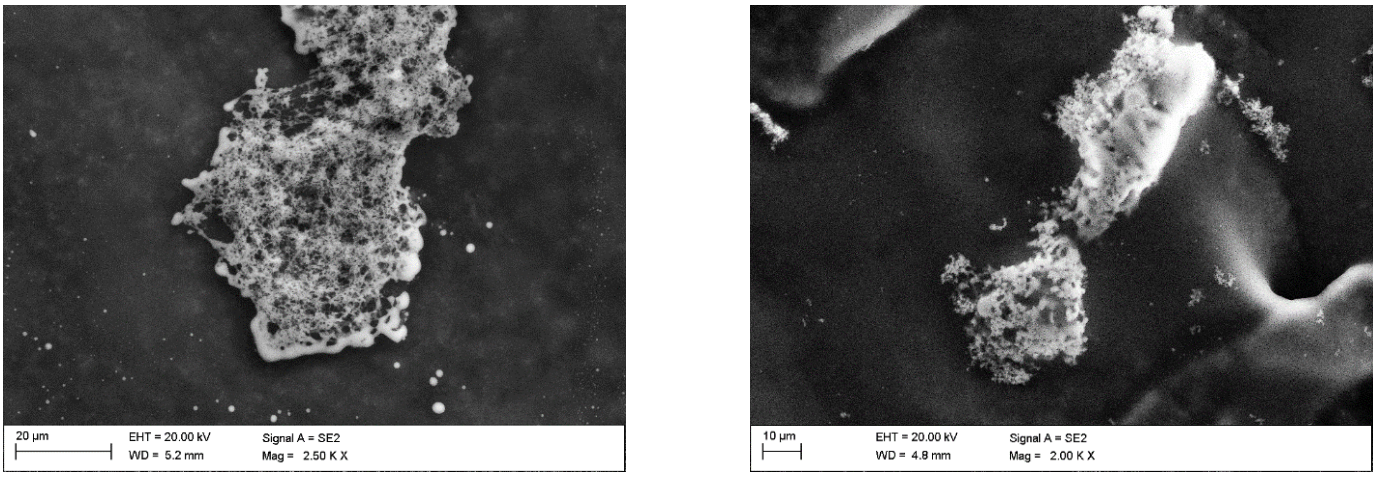

(**a**) (**b**)

Figure 2. Morphology of the: (**a**) leachate, (**b**) control solution, SEM (SE).

The chemical analysis in the micro-areas of the dried residues precipitated from leachate (Figure 3 and Table 1) and control solution (Figure 4 and Table 2) revealed a content of the following elements: Cu, Fe, Al, Mo, Si, Ca, S. In the dried residues form control solution, Ag and K were also identified. A difference in the chemical composition between the formulation from the dried specimens from diluted solution and the undiluted one within the same test was observed as well. In the dried specimen from the solutions after the bioleaching, after dilution, no copper, magnesium or sulfur were identified, whereas in the specimen prepared from control solution, also silicon and potassium were not found, which were present in the specimen from undiluted solutions. This could be associated with the phenomenon of sedimentation of larger particles after the solution's dilution.

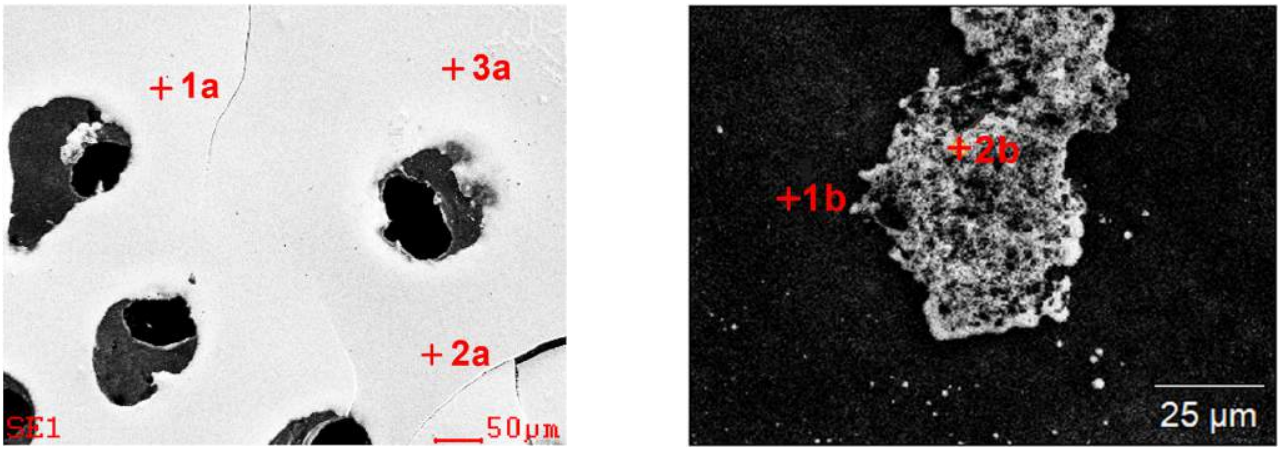

(**a**) (**b**)

Figure 3. *Cont.*

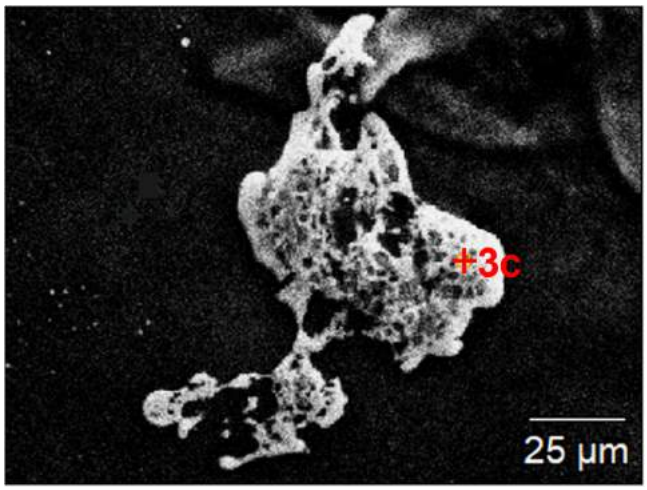

(**c**)

Figure 3. SEM images of the dried residues precipitated from leachate with marked chemical composition analysis points (results are presented in Table 1); (**a**) undiluted, (**b**,**c**) diluted.

Table 1. Results of chemical composition analysis of the dried residues precipitated from leachate (EDS, SEM) at points shown in Figure 3; specimen from undiluted solution (Figure 3a); specimen from diluted solution (Figure 3b,c).

Element	Dried Residues Precipitated from Undiluted Solution (Figure 3a)						Dried Residues Precipitated from Diluted Solution (Figure 3b,c)					
	Point of Analysis											
	1a		2a		3a		1b		2b		3c	
	% wt.	% at.	% wt.	% at.	% wt.	% at.	% wt.	% at.	% wt.	% at.	% wt.	% at.
Cu	4	3	4	3	2	-	-	-	-	-	-	-
Fe	40	29	39	26	40	26	-	-	32	40	25	29
Al	2	3	2	3	2	3	-	-	-	-	4	14
Mo	-	-	-	-	-	-	-	-	64	60	64	43
Si	-	-	-	-	-	-	-	-	-	-	4	-
Ca	2	3	2	3	2	3	-	-	5	-	4	14
S	53	63	54	65	55	68	-	-	-	-	-	-

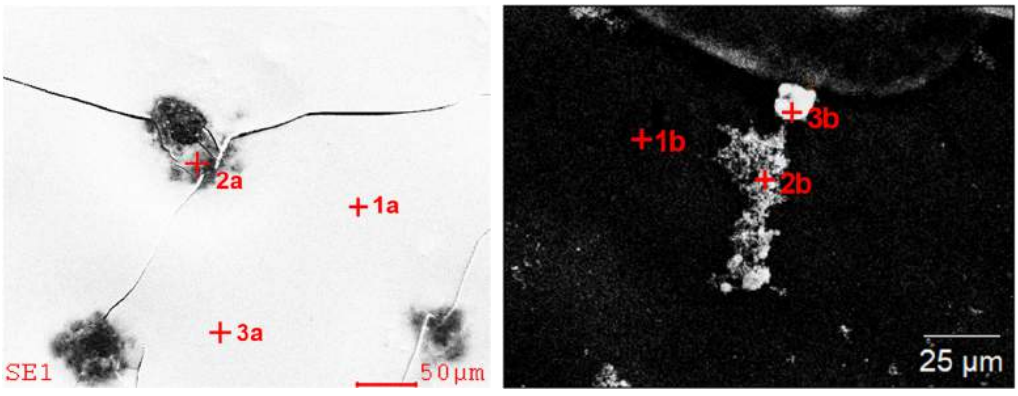

(**a**) (**b**)

Figure 4. SEM images with marked chemical composition analysis points (results are presented in Table 2), dried specimen made from the control solution; (**a**) undiluted, (**b**) diluted.

Table 2. Results of chemical composition analysis of the dried residues precipitated from control solution (EDS, SEM) at points shown in Figure 4; specimen from undiluted solution (Figure 4a), specimen from diluted solution (Figure 4b).

Element	Dried Residues Precipitated from Undiluted Solution (Figure 4a)						Dried Residues Precipitated from Diluted Solution (Figure 4b)					
	Point of Analysis											
	1a		2a		3a		1b		2b		3b	
	% wt.	% at.	% wt.	% at.	% wt.	% at.	% wt.	% at.	% wt.	% at.	% wt.	% at.
Cu	5	3	7	5	5	3	-	-	-	-	-	-
Fe	46	34	52	45	48	35	-	-	33	42	35	44
Al	2	3	2	-	2	3	-	-	3	8	2	6
Mo	-	-	-	-	-	-	-	-	62	50	59	44
Ag	-	-	-	-	-	-	-	-	3	-	2	-
Ca	-	-	-	-	-	-	-	-	-	-	2	6
K	2	3	2	-	2	3	-	-	-	-	-	-
S	46	58	36	50	44	58	-	-	-	-	-	-

3.3. High Resolution Transmission Electron Microscopy

Figure 5 shows the results of TEM observations of the dried residues precipitated from the solution obtained in the bioleaching process. The specimen from undiluted solution (Figure 5a) are characterized by a spongy structure. More precise analyses could be performed on dried specimen obtained from solution after dilution. Figure 5b shows particles of spherical shape, with a diameter of several tens to 200 nm, forming lacy aggregates. The diffraction made in this area (the example is marked by A in Figure 5b) confirms an amorphous structure (Figure 5c). Additionally, there are visible fragments with a different morphology (marked by B). Both the SAED (Selected Area Electron Diffraction) and the dark field image confirm the nanocrystalline structure of these fragments (Figure 5d). The analyses of the chemical composition (Figure 6a–e) obtained in STEM mode with the use of EDS confirmed that the aggregates made of spherical particles contain mainly Fe, S, and O (the presence of Cu in the recorded spectra may be omitted), while the irregular, nanocrystalline fragments contain additional Ca and Na.

Figure 7a–d shows the structure of dried residues precipitated from the control solution. A representative result of the specimen obtained from diluted solution is shown in Figure 7b. It shows spherical particles of various diameters (several dozen to 500 nm), which are not connected. Larger particles are hollow in the middle, while the outer part is crystalline (Figure 7c), which can prove incomplete oxidation. Spherical particles consist of Fe, S, and O. The presence of Ce is also visible in the spectra, which results from its presence in the PCB. Between the spherical particles, there are visible fragments with an irregular structure (marked as B in Figure 7d), which chemical composition that is similar to the spherical particles (Figure 7f).

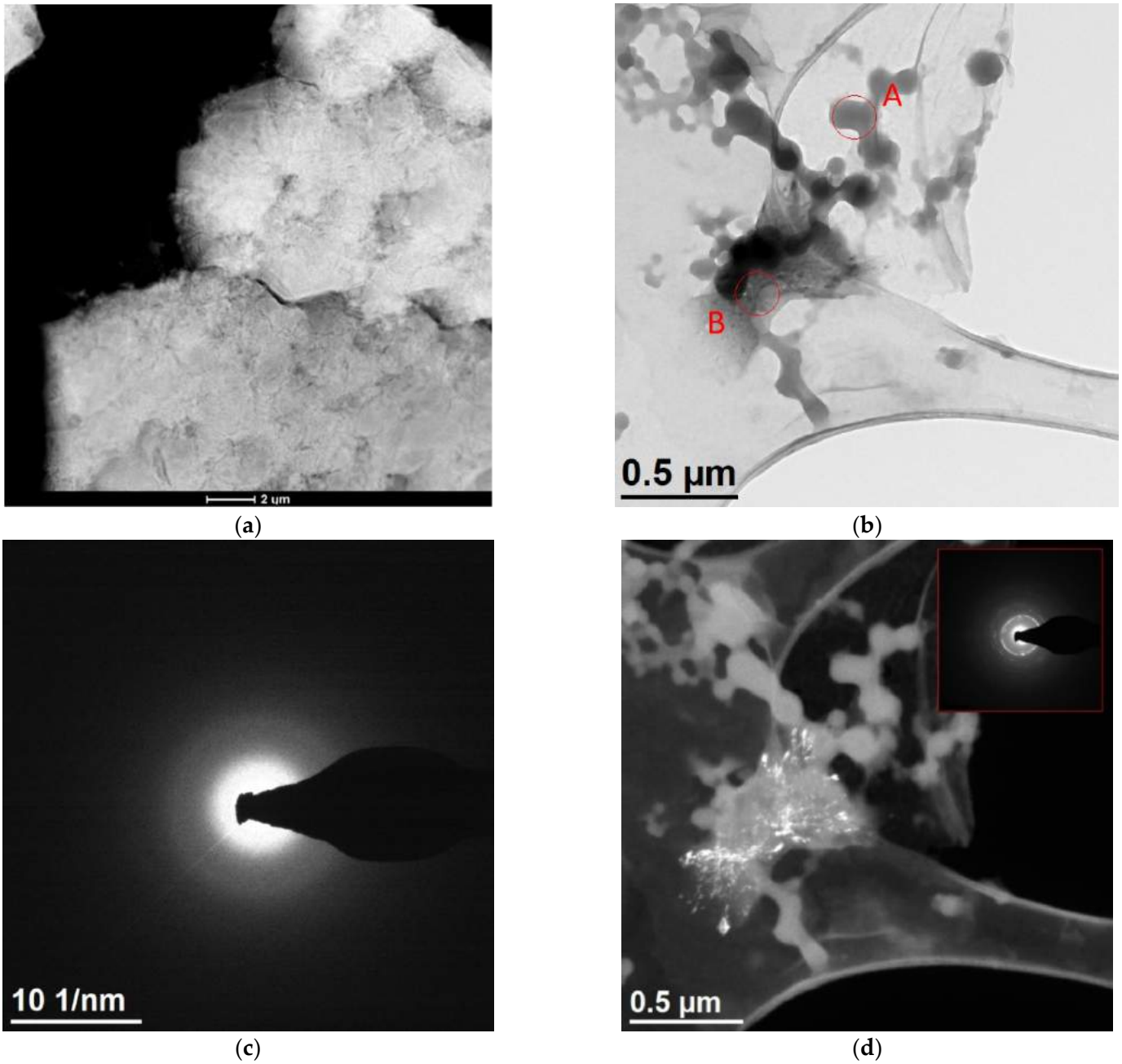

Figure 5. Microscope images of the dried residues precipitated from leachate; (**a**) undiluted (STEM HAADF—High-angle annular dark-field scanning transmission electron microscopy), (**b**) diluted (TEM), (**c**) selected area diffraction SAED obtained for area indicated by A image (**b**), (**d**) dark field image (TEM-DF), in right bottom part selected area electron diffraction from the area indicated by B in image (**b**).

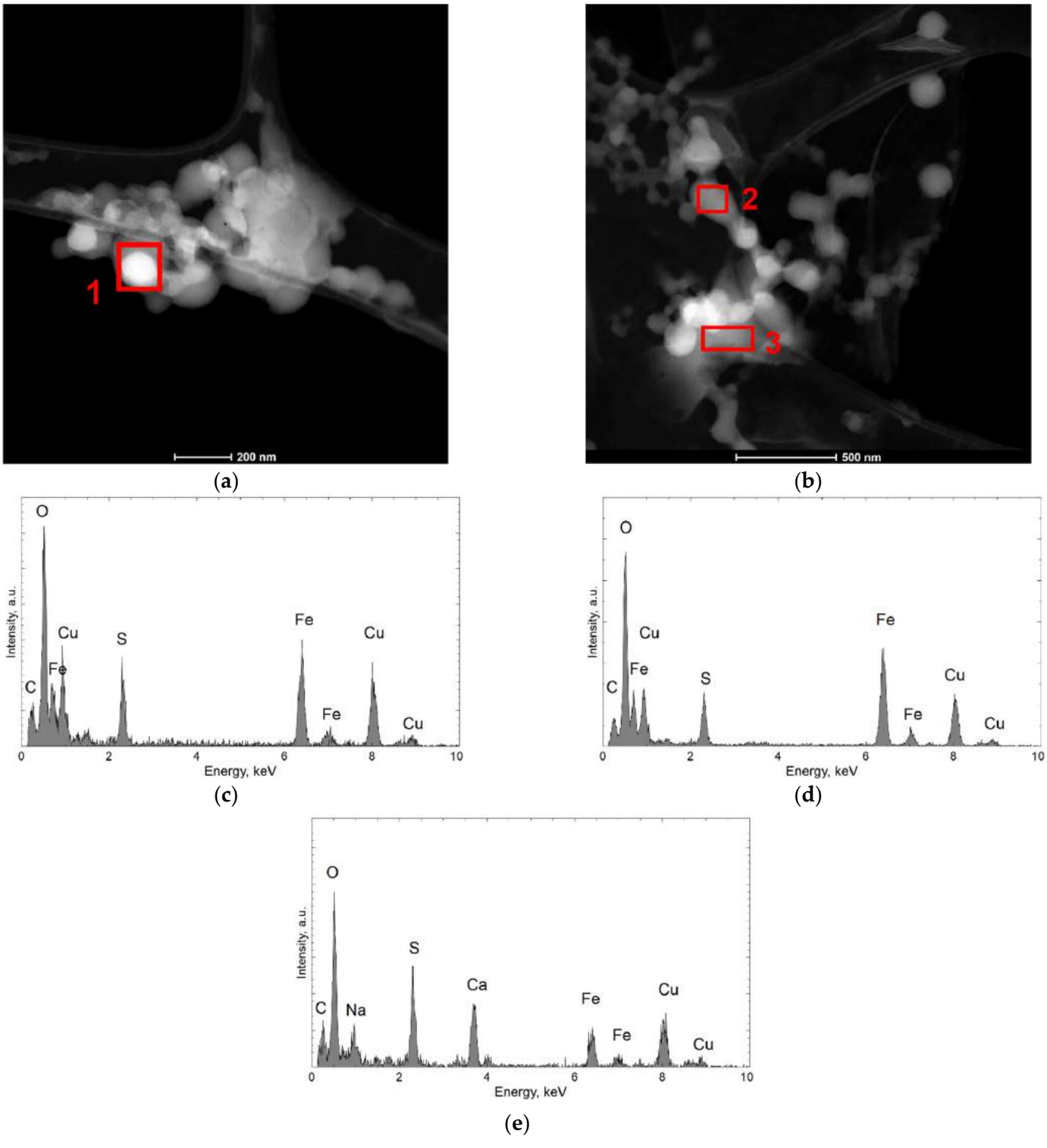

Figure 6. STEM-HAADF images of the dried residues precipitated from leachate, diluted; (**a**,**b**) spherical particle where EDS analysis were performed, (**c**) EDS result obtained in area indicated by 1 in (**a**), (**d**) EDS result obtained in area indicated by 2 in (**b**), (**e**) EDS result obtained in area indicated by 3 in (**b**).

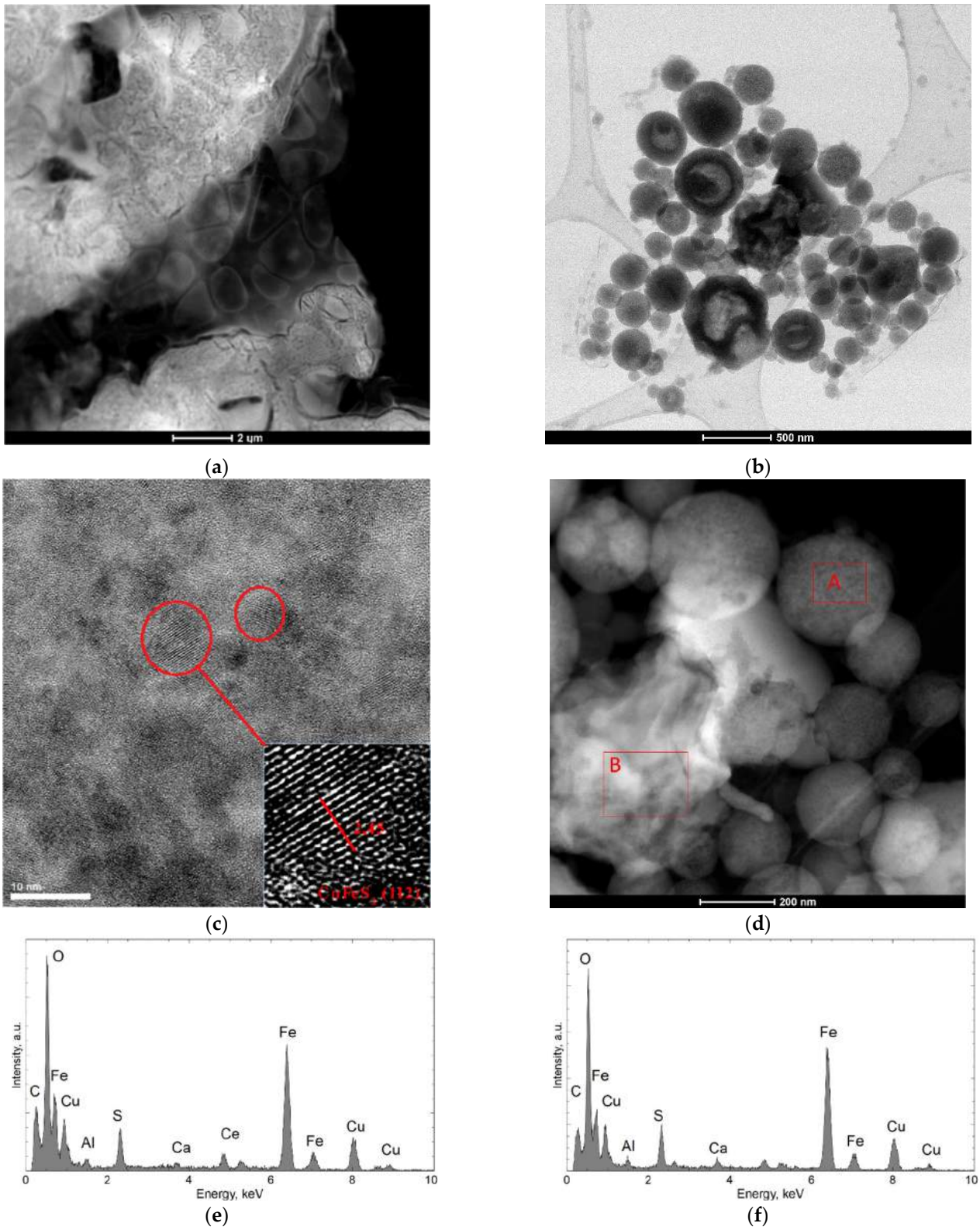

Figure 7. Microscope images of the dried residues precipitated from control solution; (**a**) undiluted (STEM HAADF), (**b**) diluted (STEM B), (**c**) TEM image of the outer part of bigger spherical particle from (**b**), (**d**) STEM-HAADF image consist of spherical and unregular fragments, where EDS analysis were performed, (**e**) EDS result obtained in area indicated by A in (**d**); (**f**) EDS result obtained in area indicated by B in (**d**).

3.4. X-ray Qualitative Phase Analysis

In the diffractogram of the specimen from the dried residues precipitated from solution after bioleaching (Figure 8) in the scope from 22 to 45° 2 Theta, we can see a very big, slightly asymmetric hump, characteristic of the amorphous component. A diffraction line in an angular orientation was also recorded, which corresponded to reflection from the crystalline planes (222) of iron oxide (III)—Fe_2O_3 (ICSD: 98-010-8905). The qualitative X-ray phase analysis of formulation made from dried residues from the control solution (Figure 9) revealed an amorphous component as well as diffraction lines which can be attributed to the strongest lines of the standard $CuFeS_2$ (ICSD: 98-003-0289), Fe_2O_3 (ICSD: 98-010-8905), Cu_2O (ICSD: 98-017-3983). In the case of the examined specimens, diffraction lines are characterized by low intensity, due to high content of an amorphous component.

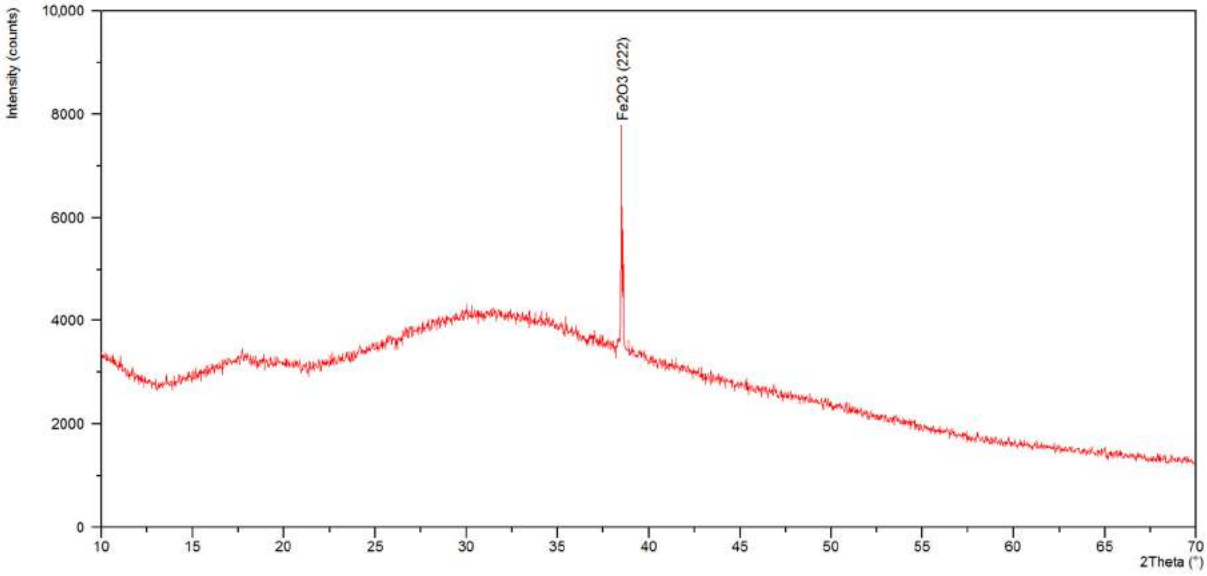

Figure 8. X-ray diffraction patterns of the leachate.

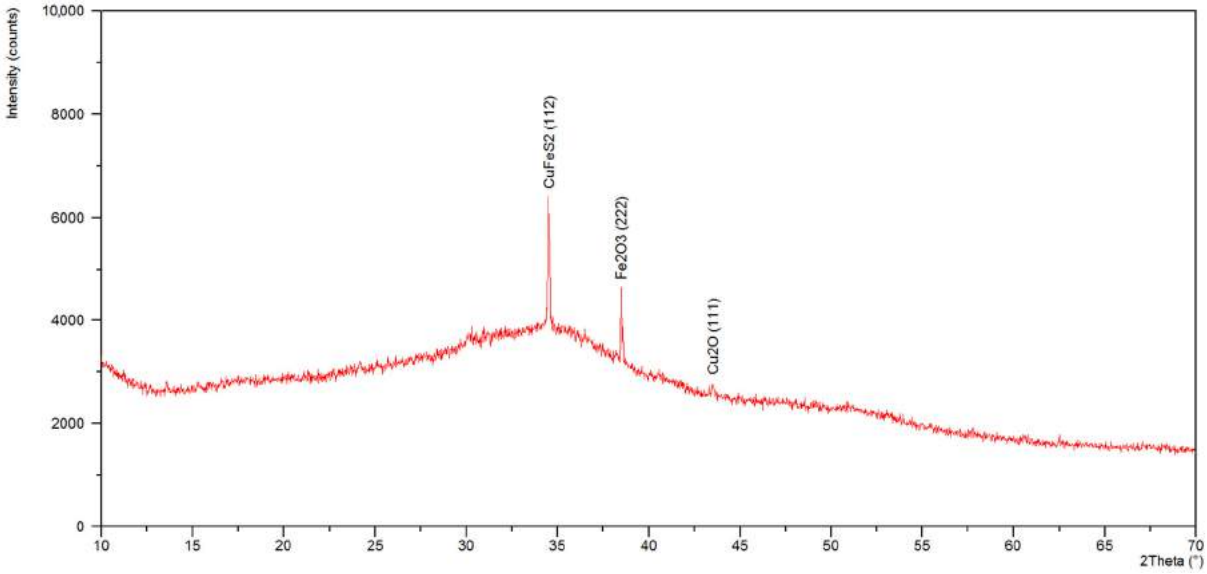

Figure 9. X-ray diffraction patterns of the control solution.

3.5. ICP-OES Analysis

The chemical composition of leachate and residue is presented in Table 3. The theoretical maximum content of elements can be calculated in accordance with metals composition

in the intermediate product of electrostatic separation which was later bioleached. The calculated theoretical maximum content of Cu, Al, Pb, Zn, Ni, and Sn was 1000, 200, 110, 140, 50, and 180 in ppm respectively. It could be observed that in the case of copper, aluminum, zinc, and nickel, the larger quantity of each substance appears in the leachate. Lixiviation did not occur in all other cases (lead and tin), where a bigger amount of elements was recognized in the residue. As regards copper, the bioleaching process was the most efficient, subsequently: zinc, nickel, and aluminum.

Table 3. The chemical composition of the leachate and the residue (ICP-OES analysis).

Element	Quantity of the Substance /Element in the Leachate (ICP)	Quantity of the Substance /Element in the Residue (ICP)
	ppm	ppm
Cu	700	250
Al	150	60
Pb	20	70
Zn	75	60
Ni	34	20
Sn	10	200

4. Discussion

The tendency for a change in the level of oxidation-reduction potential and pH in time (Figure 1) is in agreement with the studies published so far (Willner et al. [30]). During the bioleaching procedure, the microorganisms were provided with the optimal growth conditions; however, the experiment time was longer than it had been assumed. Probably, the waste composition—a ground PCB fraction rich in metals and an unseparated metallic fraction—had a slowing effect on the metabolism of the bacterial cells. The plastics present in the sample could have extended the time of the bacteria's adaptation to the environment, which is mentioned by Zhu et al. [17].

Referring to the composition of metallic elements of the initial material (chemical composition of ground PCB after the separation of the plastic fraction (Franke et al.) [12]) as well as the solutions after the bioleaching, it can be stated that the iron percentage in the specimen increased significantly, which is related to the course of the leaching process and continuous oxidation of Fe^{2+} to Fe^{3+} guaranteeing a transition of the metal from the solubilized material into the solution. Analyzing the obtained SEM and TEM results, we can assume that the demonstrated small differences in the chemical composition between the obtained dried specimen from the undiluted solution and that from the diluted one were mainly connected with the applied research technique (analysis in micro-areas) as well as the preparatory procedure. The concentration of some elements in the formulation was low, and, with heavier/bigger agglomerates in the specimen made from undiluted solution, sedimentation could have taken place. However, the obtained results of the chemical composition confirm the presence of elements used to manufacture PCB in the solution, which is mentioned by Seif El-Nasr et al. [9], Liang et al. [10], Szałatkiewicz [11] van Houwelingen [13], and de Andrade et al. [31].

Bioleaching with *A. ferrooxidans* bacteria provides acquiring elements such as copper, zinc, and aluminum from leached material (Willner et al. [16], Kremser et al. [32], Rouchalova et al. [33]). It was confirmed in the ICP-OES results in the solution samples. Moreover, it was proved by SEM EDS and TEM EDS analysis results—in the dried residues precipitated from solutions the following elements have been identified: Cu, Fe, Al, Mo, Si, Ag, K, S, Ca, and Na. In the examined specimen from solutions, appearance of Pb and Sn has not been supported as opposed to residue (ICP-OES analysis findings). Similar observations were presented in previous papers by Brandl et al. [34], Ilyas et al. [35], and

others—Bryan et al. [36], Willner et al. [30], Willner et al. [37], Hubau et al. [38]. It was reported that during PCB bioleaching, Sn was detected in residues in the form of precipitated SnO together with Pb in the form of $PbSO_4$. Additionally, performed analysis results validate that a strong combination of metal–nonmetal–ceramics conglomerate were broken and elements from conglomerate probably entered the solution. The metal content in the leachate (Table 3) is sufficient for the reduction and precipitation of metal ions from the solutions using e.g., iron reactor (patent application No. P.410550, [28]), which is planned to be carried out in the second stage of the research.

TEM observations show that the morphology of dried residues precipitated from leachate after dilution consisted of mainly amorphous spherical particles in diameter up to 200 nm, forming lacy aggregates. Chemical composition confirmed that these aggregates contain mainly Fe, S, and O. In the dried specimen from control solution larger particles (up to 500 nm) were observed with hollow in the middle and crystalline outer part. The obtained investigation allowed the conclusion that the differences in the morphology of these spherical particles observed in the dried specimen made from leachate and the control solution are the result of activity of the bacteria and their participation in the solubilization of the waste components, with their visible degradation–acceleration of the reaction owing to a continuous regeneration of the leaching agent (Cui et al. [39]). Also, Arshadi et al. [40] point to the fact that the factor of the change in the morphology of the spherical particles are the bacterial metabolites, which, through their chemical operation, intensify the process of their degradation.

Qualitative X-ray phase analysis of ground PCBs performed by Erust et al. [41] and Franke et al. [12] made it possible to identify mainly metallic phases (iron and copper). The investigation results presented in this article point to the presence of mostly oxides and sulfides of these metals in dried residues precipitated from solution, which is a consequence of bioleaching. The specimen made from leachate is characterized by a spongy structure, composed of spherical particles of iron oxide III, exhibiting features of an amorphous substance, which was confirmed by XRD. The specimen made from control solution, in turn, demonstrated the presence of Fe_2O_3 as well as a large content of fine-dispersive crystals, probably $CuFeS_2$ and Cu_2O, in the base of the amorphous phase. It can be assumed that these compounds were formed during the leaching process, with participation of elements present in nutrient medium, which also was confirmed by the study of Sethurajan et al. [8].

The application of such a variety of test methods has enabled comprehensive information on the leachates. Each of the analyses complemented each other and gave different data on the specimen. Neither could be omitted—without SEM it is impossible to perform XRD data, and without XRD it is difficult to identify the phase composition only by TEM analysis. The only difficulty in conducting the tests was the preparation of specimens which must be dried under the same conditions. It required a lot of attempts to achieve the intended goal—as indicated in the presentation of the results, it was necessary to dilute the solution to reveal the morphology of the particles in dried specimen (SEM and TEM), or multistage evaporation of water from leachate to prepare the specimen for XRD testing. The chemical composition analysis was difficult in terms of identifying some heavy elements that could fall to the bottom of the vial immediately after the mixing process was completed. Therefore, it took several attempts to collect test materials to obtain clear results. However, the obvious advantage of combining the above-mentioned research methods is the simultaneous obtaining of information about the material on a micro and macro scale. Previous publications on bioleaching have not used all the methods indicated in this study, most often it was confined only to the analysis of the chemical composition. This concerns in particular the intermediate obtained from electrostatic separation [28], which had different chemical composition and structure from typical PCBs. The use of electron microscopy made it possible to visualize the morphology of the specimen, which is interesting information and could potentially be used to define bioleaching mechanisms that are not yet explicitly defined. All the data obtained from the investigation using presented analytical techniques allow to assess the applicability of the best method of recovering

metals from bio-leachate and to select the best one. This study will be carried out in the next step of the research.

5. Conclusions

The chemical composition of the leachate is similar to the composition of the elements used to manufacture PCB boards (Cu, Al, Mo, Ca, Ag, Mg, Si). The dominating amount of iron is involved with the continuous oxidation of Fe^{2+} to Fe^{3+}, which ensures the transition of the metals from the solubilized material into the solution. According to copper the bioleaching process was the most effective.

The application of comprehensive scientific techniques allowed to evaluate the morphology of the obtained products and identify the components of the analyzed solutions, mainly the oxide and sulfide phases (Fe_2O_3, Cu_2O, $CuFeS_2$), which were presented as a consequence of the leaching processes. These complementary methods allow for a quick and complex analysis that gives full information about the analyzed solutions (ICP-OES analysis) and dried residues precipitated from leachate and control solution (SEM, S/TEM, and XRD), which is needed in the next step of PCBs recycling to conduct a qualitative and quantitative assessment of precipitates, obtained as a result of metal recovery from leachates by e.g., reduction of ion metals using an iron reactor.

The morphology of the dried residues precipitated from leachate after bioleaching consisted of mainly amorphous spherical particles in diameter up to 200 nm, forming lacy aggregates. In the dried residues precipitated from the control solution larger particles (up to 500 nm) were observed with hollow in the middle and crystalline outer part. The obtained investigation allows to conclude that the differences in morphology and phase composition of these spherical particles observed in specimen obtained from the leachate and the control solution are the result of activity of *A. ferrooxidans* bacteria and can be related to efficiency in dissolving metals during the bioleaching.

Obtained results of the investigation confirm the activity and participation of the *A. ferrooxidans* bacteria in the solubilization process of electro-waste components, with their visible degradation–acceleration of the reaction owing to a continuous regeneration of the leaching medium.

Electron microscopy was useful to assess the chemical composition and to obtain the images of solutions morphology, in order to examine the input and effectiveness of metal–nonmetal–ceramics conglomerates bioleaching. However, in a full assessment of the bioleaching process, complementary cross-checks of the micro (SEM and S/TEM) and macro (ICP-OES and XRD) methods are required.

Author Contributions: Research concept, K.H., P.M.N., J.W. and T.S.; conducting the process of bacterial and chemical leaching, K.H., J.W. and D.F.; SEM analysis, K.M.; TEM analysis, M.P.; XRD analysis, P.M.N., W.K.; investigation, K.H., P.M.N. and J.W.; writing—original draft preparation, K.H.; writing—review and editing, P.M.N., J.W., T.S., M.P., W.K. and D.F. All authors have read and agreed to the published version of the manuscript.

Funding: The APC was funded by grant number 10/010/BKM20/0377, and statutory financial grant of the Faculty of Mechanical Engineering, Silesian University of Technology and the Rector's pro-quality grant, Silesian University of Technology, 10/100/RGJ21/0003.

Institutional Review Board Statement: Not applicable.

Informed Consent Statement: Not applicable.

Data Availability Statement: Not applicable.

Conflicts of Interest: The authors declare no conflict of interest.

References

1. Forti, V.; Baldé, C.P.; Kuehr, R.; Bel, G. *The Global E-Waste Monitor 2020: Quantities, Flows and the Circular Economy Potential*; United Nations University (UNU)/United Nations Institute for Training and Research (UNITAR)—co-hosted SCYCLE Programme, International Telecommunication Union (ITU) & International Solid Waste Association (ISWA): Bonn, Germany, 2020; Available online: https://ewastemonitor.info/wp-content/uploads/2020/11/GEM_2020_def_july1_low.pdf (accessed on 20 January 2021).
2. Baldé, C.P.; Forti, V.; Gray, V.; Kuehr, R.; Stegmann, P. *The Global E-Waste Monitor–2017*; United Nations University (UNU), International Telecommunication Union (ITU) & International Solid Waste Association (ISWA): Bonn, Germany, 2017; Available online: https://ewastemonitor.info/wp-content/uploads/2020/11/Global-E-waste-Monitor-2017-electronic-spreads.pdf (accessed on 10 December 2020).
3. Priya, A.; Hait, S. Comparative assessment of metallurgical recovery of metals from electronic waste with special emphasis on bioleaching. *Environ. Sci. Pollut. Res.* **2017**, *24*, 6989–7008. [CrossRef] [PubMed]
4. Cieszyńska, A. Waste electronic and electrical equipment (WEEE)—Scraps or valuable source of precious metals. *Polish J. Commod. Sci.* **2016**, *4*, 43–54. [CrossRef]
5. Sohaili, J.; Muniyandi, S.K.; Mohamad, S.S. A review on printed circuit boards waste recycling technologies and reuse of recovered nonmetallic materials. *Int. J. Sci. Eng. Res.* **2012**, *3*, 138–144.
6. Li, J.; Shrivastava, P.; Gao, Z.; Zhang, H.-C. Printed circuit board recycling: A state-of-the-art survey. *IEEE Trans. Electron. Packag. Manufact.* **2004**, *27*, 33–42. [CrossRef]
7. LaDou, J. Printed circuit board industry. *Int. J. Hyg. Environ. Health* **2006**, *209*, 211–219. [CrossRef]
8. Sethurajan, M.; van Hullebusch, E.D. Leaching and selective recovery of Cu from printed circuit boards. *Metals* **2019**, *9*, 1034. [CrossRef]
9. Seif El-Nasr, R.; Abdelbasir, S.M.; Kamel, A.H.; Hassan, S.S.M. Environmentally friendly synthesis of copper nanoparticles from waste printed circuit boards. *Sep. Purif. Technol.* **2020**, *230*, 115860. [CrossRef]
10. Liang, G.; Li, P.; Liu, W.; Wang, B. Enhanced bioleaching efficiency of copper from waste printed circuit boards (PCBs) by dissolved oxygen-shifted strategy in *Acidithiobacillus ferrooxidans*. *J. Mater. Cycles Waste Manag.* **2016**, *18*, 742–751. [CrossRef]
11. Szałatkiewicz, J. Metals content in printed circuit board waste. *Pol. J. Environ. Stud.* **2014**, *23*, 2365–2369.
12. Franke, D.; Suponik, T.; Nuckowski, P.M.; Gołombek, K.; Hyra, K. Recovery of metals from printed circuit boards by means of electrostatic separation. *Manag. Syst. Prod. Eng.* **2020**, *28*, 213–219. [CrossRef]
13. Van Houwelingen, J.A. Identification and recovery of rare metals in electric and electronic scrap. In *Thirtteenth International Waste Management and Landfill Symposium*; S. Margherita di Pula (Cagliari): Sardinia, Italy, 2011.
14. Akcil, A.; Erust, C.; Sekhar Gahan, C.; Ozgun, M.; Sahin, M.; Tuncuk, A. Precious metal recovery from waste printed circuit boards using cyanide and non-cyanide lixiviants—A review. *Waste Manag.* **2015**, *45*, 258–271. [CrossRef] [PubMed]
15. Suponik, T.; Franke, D.M.; Nuckowski, P.M.; Matusiak, P.; Kowol, D.; Tora, B. Impact of grinding of printed circuit boards on the efficiency of metal recovery by means of electrostatic separation. *Minerals* **2021**, *11*, 281. [CrossRef]
16. Willner, J.; Pacholewska, M.; Fornalczyk, A.; Saternus, M. *Introduction to Hydrometallurgy and Biometallurgy of Non-Ferrous Metals*, 1st ed.; Wydawnictwo Politechniki Śląskiej: Gliwice, Poland, 2015; pp. 87–129. (In polish)
17. Zhu, N.; Xiang, Y.; Zhang, T.; Wu, P.; Zhi, D.; Li, P.; Wu, J. Bioleaching of metal concentrates of waste printed circuit boards by mixed culture of acidophilic bacteria. *J. Hazard. Mater.* **2011**, *192*, 614–619. [CrossRef] [PubMed]
18. Valdés, J.; Pedroso, I.; Quatrini, R.; Dodson, R.; Tettelin, H.; Blake, R.; Eisej, J.; Holmes, D. *Acidithiobacillus ferrooxidans* metabolism: From genome sequence to industrial applications. *BMC Genom.* **2008**, *9*, 597. [CrossRef]
19. Rohwerder, T.; Gehrke, T.; Kinzler, K.; Sand, W. Bioleaching review part A. *Appl. Microbiol. Biotechnol.* **2003**, *63*, 239–248. [CrossRef] [PubMed]
20. Quatrini, R.; Appia-Ayme, C.; Denis, Y.; Jedlicki, E.; Holmes, D.S.; Bonnefoy, V. Extending the models for iron and sulfur oxidation in the extreme acidophile *Acidithiobacillus ferrooxidans*. *BMC Genom.* **2009**, *10*, 394. [CrossRef]
21. Zhang, Y.; Zhang, S.; Zhao, D.; Ni, Y.; Wang, W.; Yan, L. Complete genome sequence of *Acidithiobacillus ferrooxidans* YNTRS-40, a strain of the ferrous iron- and sulfur-oxidizing acidophile. *Microorganisms* **2020**, *8*, 2. [CrossRef]
22. Lundgren, D.G.; Vestal, J.R.; Tabita, F.R. Chapter 18—The iron-oxidizing bacteria. In *Microbial Iron Metabolism: A Comprehensive Treatise*, 1st ed.; Neilands, J.B., Ed.; Academic Press: London, UK, 1974; pp. 457–471.
23. Carlos, J.G. Bioleaching and Biomining for the Industrial Recovery of Metals. In *Comprehensive Biotechnology*, 2nd ed.; Moo-Young, M., Ed.; Pergamon—Elsevier: Oxford, UK, 2011; pp. 717–729.
24. Fenchel, T.; King, G.M.; Blackburn, T.H. Chapter 1—Bacterial metabolism. In *Bacterial Biogeochemistry*, 3rd ed.; Fenchel, T., King, G.M., Blackburn, T.H., Eds.; Academic Press—Elsevier: Amsterdam, The Netherlands, 2012; pp. 1–34.
25. Grishin, S.I.; Bigham, J.M.; Tuovinen, O.H. Characterization of jarosite formed upon bacterial oxidation of ferrous sulfate in a packed-bed reactor. *Appl. Environ. Microbiol.* **1988**, *54*, 3101–3106. [CrossRef]
26. Nurmi, P.; Özkaya, B.; Sasaki, K.; Kaksonen, A.H.; Riekkola-Vanhanen, M.; Tuovinen, O.H.; Puhakka, J.A. Biooxidation and precipitation for iron and sulfate removal from heap bioleaching effluent streams. *Hydrometallurgy* **2010**, *101*, 7–14. [CrossRef]
27. Willner, J.; Fornalczyk, A.; Saternus, M. Selective recovery of copper from solutions after bioleaching electronic waste. *Nova Biotechnol. Chim.* **2015**, *14*, 32–37. [CrossRef]
28. Suponik, T.; Kurzyca, M. Recovery of copper from water by using a reactor of iron. *J. Pol. Miner. Eng. Soc.* **2015**, *2*, 293–299.

29. Pacholewski, A.; Pacholewska, M. Natural ability to oxidize iron (II) compounds by ferric bacteria from the Łomniczanka mineral water source. In *Modern Problems of Hydrogeology*; Bocheńska, T., Staśko, S., Eds.; Printing House "Sudety": Wrocław, Poland, 2001; pp. 389–396. (In Polish)
30. Willner, J.; Fornalczyk, A. Extraction of metals from electronic waste by bacterial leaching. *Environ. Prot. Eng.* **2013**, *39*, 197–208. [CrossRef]
31. De Andrade, L.M.; Rosario, C.G.A.; de Carvalho, M.A.; Espinosa, D.C.R.; Tenório, J.A.S. Copper recovery from printed circuit boards from smartphones through bioleaching. In *TMS 2019 148th Annual Meeting & Exhibition Supplemental Proceedings*; The Minerals, Metals & Materials Society; Springer: Cham, Switzerland; Pittsburgh, PA, USA, 2019; pp. 837–844. [CrossRef]
32. Kremser, K.; Gerl, P.; Pellis, A.; Guebitz, G.M. A new bioleaching strategy for the selective recovery of aluminum from multi-layer beverage cans. *Waste Manag.* **2021**, *120*, 16–24. [CrossRef] [PubMed]
33. Rouchalova, D.; Rouchalova, K.; Janakova, I.; Cablik, V.; Janstova, S. Bioleaching of iron, copper, lead, and zinc from the sludge mining sediment at different particle sizes, pH, and pulp density using *Acidithiobacillus ferrooxidans*. *Minerals* **2020**, *10*, 1013. [CrossRef]
34. Brandl, H.; Bosshard, R.; Wegmann, M. Computer-munching microbes: Metal leaching from electronic scrap by bacteria and fungi. *Hydrometallurgy* **2001**, *59*, 569–576. [CrossRef]
35. Ilyas, S.; Anwar, M.A.; Niazi, S.B.; Ghauri, M.A. Bioleaching of metals from electronic scrap by moderately thermophilic acidophilic bacteria. *Hydrometallurgy* **2007**, *88*, 180–188. [CrossRef]
36. Bryan, C.G.; Watkin, E.L.; McCredden, T.J.; Wong, Z.R.; Harrison, S.T.L.; Kaksonen, A.H. The use of pyrite as a source of lixiviant in the bioleaching of electronic waste. *Hydrometallurgy* **2015**, *152*, 33–43. [CrossRef]
37. Willner, J.; Fornalczyk, A.; Gajda, B.; Saternus, M. Bioleaching of indium and tin from used LCD panels. *Physicochem. Probl. Miner. Process.* **2018**, *54*, 639–645. [CrossRef]
38. Hubau, A.; Minier, M.; Chagnes, A.; Joulian, C.; Silvente, C.; Guezennec, A.G. Recovery of metals in a double-stage continuous bioreactor for acidic bioleaching of printed circuit boards (PCBs). *Sep. Purif. Technol.* **2020**, *238*, 116481. [CrossRef]
39. Cui, H.; Anderson, C.G. Literature review of hydrometallurgical recycling of printed circuit boards (PCBs). *J. Adv. Chem. Eng.* **2016**, *6*, 142–153. [CrossRef]
40. Arshadi, M.; Yaghmaei, S.; Mousavi, S.M. Study of plastics elimination in bioleaching of electronic waste using *Acidithiobacillus ferrooxidans*. *Int. J. Environ. Sci. Technol.* **2019**, *16*, 7113–7126. [CrossRef]
41. Erust, C.; Akcil, A.; Tuncuk, A.; Panda, S. Intensified acidophilic bioleaching of multi-metals from waste printed circuit boards (WPCBs) of spent mobile phones. *J. Chem. Technol. Biotechnol.* **2020**, *95*, 2272–2285. [CrossRef]

Zgłoszenia patentowe

URZĄD PATENTOWY
RZECZYPOSPOLITEJ POLSKIEJ

al. Niepodległości 188/192
00-950 Warszawa, skr. poczt. 203
tel.: (+48) 22 579 05 55 | fax: (+48) 22 579 00 01
e-mail: kontakt@uprp.gov.pl | www.uprp.gov.pl

Departament Zgłoszeń

Warszawa, 22.09.2021 r.

Nasz znak: DZ-NZ.P.438999.2.dbiel
Wasz znak: 4658/71/RPCITT

CENTRUM INKUBACJI I TRANSFERU TECHNOLOGII POLITECHNIKA ŚLĄSKA
rzecznik patentowy Justyna Duda
ul. Banacha 7
44-100 Gliwice

POTWIERDZENIE

Urząd Patentowy RP stwierdza, że dnia 2021-09-21 przyjęto w formie papierowej wniosek o udzielenie patentu na wynalazek pt.:

Sposób rozdziału metali od tworzyw sztucznych z płyt obwodów drukowanych

Zgłoszenie oznaczono numerem: **P.438999**
[WIPO ST 10/C PL438999]

Zgłaszający: **POLITECHNIKA ŚLĄSKA, Gliwice, POLSKA**

Dominik Bielski
Specjalista
/podpisano kwalifikowanym podpisem elektronicznym/

Pismo wydane w formie dokumentu elektronicznego

Pouczenie:

1. Strony oraz ich przedstawiciele i pełnomocnicy mają obowiązek zawiadomić Urząd o każdej zmianie swojego adresu. W razie zaniedbania tego obowiązku doręczenie pisma pod dotychczasowym adresem ma skutek prawny (art. 41 kpa).
2. O zgłoszeniu wynalazku Urząd Patentowy dokonuje ogłoszenia niezwłocznie po upływie 18 miesięcy od daty pierwszeństwa do uzyskania patentu. Zgłaszający może w okresie 12 miesięcy od daty pierwszeństwa złożyć wniosek o dokonanie ogłoszenia w terminie wcześniejszym (art. 43 ustawy z dnia 30 czerwca 2000r. Prawo własności przemysłowej (Dz. U. z 2021 r. poz. 324)).
3. W korespondencji należy powoływać się na nr P.438999.

Klauzula informacyjna

Sposób rozdziału metali od tworzyw sztucznych z płyt obwodów drukowanych

Przedmiotem wynalazku jest sposób rozdziału metali i tworzyw sztucznych z płyt obwodów drukowanych (PCB - *ang. printed circuit board*).

Szybki postęp technologii komputerowych przyczynił się do zmiany wzorców konsumpcyjnych, których skutkiem jest masowa wymiana urządzeń na nowe, o znacznie wyższych wydajnościach. Wynikiem tego jest wytwarzanie coraz większych ilości zużytego sprzętu elektrycznego i elektronicznego (WEEE – *ang. Waste from Electrical and Electronic Equipment*). W roku 2019 wygenerowano 53,6 milionów ton takich odpadów i było to o 9,2 milionów ton więcej w porównaniu do roku 2014 (Forti i in. 2020). Jednym z podstawowych elementów budowy WEEE są płyty obwodów drukowanych (PCB), w których zawartość metali jest znacząco wyższa od ich zawartości w naturalnych rudach (Sohaili i in. 2012, Tsydenova i Bengtsson 2011, Johnson i in. 2007). PCB zbudowane są w około 70% z części niemetalicznych takich jak włókno szklane, żywica epoksydowa, poliester i w 30% z metali w stanie wolnym (Huang i in. 2009, Kumar i in. 2018). Część niemetaliczna nazwana została w niniejszym wniosku tworzywem sztucznym.

PCB w zależności od producenta, daty produkcji i przeznaczenia zawierają różne ilości metali. Szacunkowa zawartość metali szlachetnych (Au, Ag, Pd) i półszlachetnych (Cu) w PCB wynosi odpowiednio 0,05%, 0,03%, 0,01%, oraz 16%. W PCB występują również inne metale w niewielkich stężeniach: 3% Fe, 3% Sn, 2% Pb, 1% Zn oraz w śladowych ilościach Al, Ni, Cr, Na, Cd, Mo, Ti, Co (Kumar i in. 2018, Charles i in. 2017, Bizzo i in. 2014). Szacuje się, że w roku 2019 wartość surowych materiałów zawartych w WEEE wynosiła 57 miliardów USD (Forti i in. 2020), przy czym dotyczyło to około 17 procent udokumentowanych w tym roku WEEE. Pozostała nieudokumentowana część pozostająca poza ewidencją była magazynowana ze względu na brak skutecznych, proekologicznych uniwersalnych i niskokosztowych technologii lub przetwarzana w sposób niezgodny ze standardami środowiskowymi (Forti i in. 2020, Song i in,

2015). Poprawny recykling WEEE jest więc konieczny nie tylko z powodu ochrony środowiska przyrodniczego i naturalnych zasobów, ale również z powodów ekonomicznych, tworzenia nowych miejsc pracy i ograniczenia wpływu składowisk i magazynów odpadów na krajobraz.

Wśród metod odzysku metali z PCB wyróżnia się metody chemiczne i fizyczne. Stosowanie metod chemicznych często wiąże się z ingerencją w środowisko naturalne poprzez zużycie energii, odprowadzanie zanieczyszczeń do wód i powietrza (Leung i in. 2007; Qiu i in. 2020; Xiang i in. 2007) oraz powstawanie odpadów. Głównie stosuje się metody pirometalurgiczne, hydrometalurgiczne, biohydrometalurgiczne (Kaya, 2017) oraz z wykorzystaniem plazmy (Changming et al., 2018). Dwie ostatnie można zaliczyć do przyjaznych dla środowiska, jednak w przypadku biohydrometalurgii wadą jest długotrwały czas oddziaływania mikroorganizmów na składniki PCB podczas katalizowania procesu odzysku metali. W przypadku istniejącej w danym regionie instalacji do wytwarzania metali na drodze metalurgicznej zasadne jest wydzielenie z PCB metali, tanimi fizycznymi metodami, i ich przetwarzanie w tej instalacji. worzywa sztuczne mogą być wtedy, zgodnie z zasadami gospodarki obiegu zamkniętego, wykorzystane do wytworzenia różnego rodzaju prefabrykatów.

Wśród metod fizycznych wyróżnić można m.in. separację elektrostatyczną (Dascalescu i in. 1992; Suponik i in. 2021; Jiang i in. 2009; Wu i in. 2008), magnetyczną (Suponik i in. 2019; Veit i in. 2005) oraz grawitacyjną w ośrodku powietrznym (Eswaraiah i in. 2008; Yoo i in. 2009) i w ośrodku wodnym (Duan i in. 2009; Zhu i in. 2020). Odzysk metali z PCBs może być prowadzony również za pomocą flotacji z wykorzystaniem odczynników flotacyjnych (Gallegos-Acevedo et al., 2014; Otunniyi et al., 2013) lub bez (Ogunniyi and Vermaak, 2009). W przypadku zastosowania wszystkich tych metod konieczne jest dostosowanie stopnia rozdrobnienia i uwolnienia substancji użytecznej, czyli metali w stanie wolnym. Metody fizyczne charakteryzują się niewielkim wpływem na środowisko przyrodnicze.

Istotą wynalazku jest sposób rozdziału metali od tworzyw sztucznych z płyt obwodów drukowanych w ośrodku powietrznym, różniących się zdolnością

do gromadzenia ładunków elektrostatycznych na powierzchni ziaren oraz własnościami przewodnictwa elektrostatycznego, w którym płyty odwodów drukowanych są uwolnione od pozostałości niewbudowanych, charakteryzujący się tym, że uwolnione od pozostałości płyty obwodów drukowanych tnie się na kawałki o wielkości do 5 cm, które następnie poddaje się chłodzeniu do temperatury kriogenicznej < - 150°C w komorze, następnie mieleniu w młynie nożowym do wielkości cząstek <0,5 mm przy chłodzeniu komory roboczej młyna, po czym płyty poddaje się rozdziałowi na metale, tworzywa sztuczne oraz półprodukt za pomocą elektrostatycznego separatora elektrostatycznego, przy napięciu rozdziału >17 kV, w temperaturze otoczenia i materiału w zakresie 10-30°C oraz wilgotności materiału <1% i wilgotności względnej w komorze rozdziału <5%, po czym półprodukt ponownie chłodzi się do temperatury kriogenicznej < - 150°C w komorze następnie mieli w młynie nożowym do wielkości cząstek <0,5mm, przy chłodzeniu komory roboczej młyna, po czym rozdziela się w separatorze elektrostatycznym, przy napięciu > 17 kV, w temperaturze otoczenia i materiału w zakresie 10-30°C oraz wilgotności materiału <1% i wilgotności względnej w komorze rozdziału <5%.

Chłodzenie do temperatury kriogenicznej < - 150°C, każdorazowo, prowadzi się w ciekłym azocie.

Przedstawiony sposób separacji metali i tworzyw sztucznych z PCB wykorzystuje metody fizyczne, które charakteryzują się niewielkim wpływem na środowisko przyrodnicze i powodują powstawanie, poza półproduktem, dwóch głównych produktów (metali tworzyw sztucznych) z łatwością zagospodarowywanych, co wpisuje się w promowaną w UE politykę zgodną z zasadami gospodarki o obiegu zamkniętym. W przypadku półproduktu można go recyrkulować w układzie mielenia bądź stosować inne proekologiczne, niskokosztowe metody pozyskiwania metalii jak na przykład biohydrometalurgię.

Sposób umożliwia· skuteczny rozdział metali. od' tworzyw sztucznych, pochodzących z płyt obwodów drukowanych.

Przedmiot wynalazku został przedstawiony w przykładzie pokazanym na rysunku, który przedstawia schemat sposobu separacji metali i tworzyw sztucznych z PCB.

Sposób opisano w przykładzie realizacji został na 5 etapów.

W pierwszym etapie 1 z płyt obwodów drukowanych należy usunąć wszelkie elementy elektroniczne i inne, korzystnie stosując dezintegrator łańcuchowy. Następnie w drugim etapie 2 tak przygotowane płyty obwodów drukowanych (PCB) poddaje się cięciu w dezintegratorze nożowym na części o wielkości mniejszej od 5 cm, aby w trzecim etapie 3 schładzając je do temperatury kriogenicznej < - 165^{o}C, za pomocą ciekłego azotu, następnie w czwartym etapie 4 zmielić je do wielkości cząstek 0 do 0,5mm, za pomocą młyna nożowego, stosując perforację w sicie młyna 1mm oraz szczelinę między nożami 0,5 mm. Tak powstały materiał stanowi nadawę do piątego etapu 5 na separator elektrostatyczny, w którym tworzy się optymalne warunki rozdziału metali od tworzyw sztucznych tj: Temperatura otoczenia i materiału wynosiła 23^{o}C, wilgotność materiału oraz wilgotność względna w komorze rozdziału wynosiła odpowiednio 0,1% i 3%, a napięcie rozdziału w komorze roboczej wynosiło 17 kV.

Zastrzeżenia patentowe

1. Sposób separacji metali od tworzyw sztucznych z płyt obwodów drukowanych w ośrodku powietrznym, różniących się zdolnością do gromadzenia ładunków elektrostatycznych na powierzchni ziaren oraz własnościami przewodnictwa elektrycznego, w którym płyty odwodów drukowanych są uwolnione od pozostałości niewbudowanych, **znamienny tym**, że uwolnione od pozostałości płyty obwodów drukowanych tnie się (2) na kawałki o wielkości do 5 cm, które następnie poddaje się chłodzeniu do temperatury kriogenicznej < - 150°C w komorze (3) następnie mieleniu w młynie nożowym (4) do wielkości cząstek <0,5 mm przy chłodzeniu komory roboczej młyna, po czym płyty poddaje się rozdziałowi na metale, tworzywa sztuczne oraz półprodukt za pomocą separatora elektrostatycznego (5), przy napięciu rozdziału > 17 kV, temperaturze otoczenia i materiału w zakresie 10-30°C oraz wilgotności materiału <1 % i wilgotności względnej w komorze rozdziału <5%, po czym półprodukt ponownie chłodzi się do temperatury kriogenicznej < - 150°C w komorze (3), następnie mieli w młynie nożowym (4) do wielkości cząstek <0,5 mm, przy chłodzeniu komory roboczej młyna, po czym rozdziela się w separatorze elektrostatycznym (5), przy napi1rciu rozdziału > 17 kV, temperaturze otoczenia i materiału w zakresie 10-30°C oraz wilgotności materiału <1 % i wilgotności względnej w komorze rozdziału <5%.

2. Sposób separacji metali według zastrz. 1 **znamienny tym**, że chłodzenie do temperatury kriogeniczne} < - 1 50°C, każdorazowo, prowadzi się w ciekłym azocie.

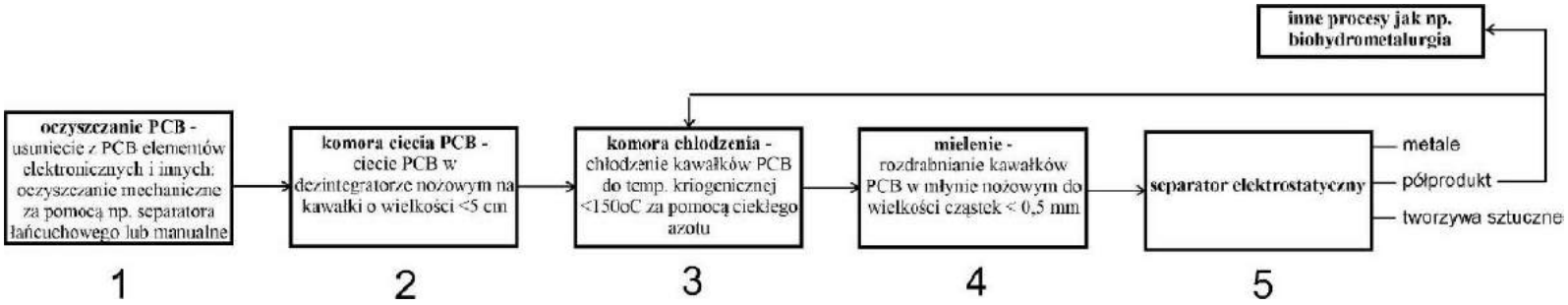
inne procesy jak np. biohydrometalurgia
oczyszczanie PCB - usunięcie z PCB elementów elektronicznych i innych: oczyszczanie mechaniczne za pomocą np. separatora łańcuchowego lub manualne
komora ciecia PCB - ciecie PCB w dezintegratorze nożowym na kawałki o wielkości <5 cm
komora chlodzenia - chłodzenie kawałków PCB do temp. kriogenicznej <150oC za pomocą ciekłego azotu
mielenie - rozdrabnianie kawałków PCB w młynie nożowym do wielkości cząstek < 0,5 mm
separator elektrostatyczny
metale
półprodukt
tworzywa sztuczne
1
2
3
4
5

Fig. 1

Skrót opisu

Sposób rozdziału metali od tworzyw sztucznych z płyt obwodów drukowanych w ośrodku powietrznym, różniących się zdolnością do gromadzenia ładunków elektrostatycznych na powierzchni ziaren oraz własnościami przewodnictwa elektrycznego, w którym płyty obwodów
drukowanych są uwolnione od pozostałości niewbudowanych, charakteryzuje się tym, że uwolnione od pozostałości płyty obwodów
drukowanych tnie się (2) na kawałki o wielkości do 5 cm, które następnie poddaje się chłodzeniu do temperatury kriogenicznej < - 150°C
w komorze (3), następnie mieleniu w młynie nożowym (4) do wielkości cząstek < 0,5 mm przy chłodzeniu komory roboczej młyna, po
czym płyty poddaje się rozdziałowi na metale, tworzywa sztuczne oraz półprodukt za pomocą separatora elektrostatycznego (5), przy napięciu
rozdziału > 17 kV, temperaturze otoczenia i materiału w zakresie 10–30°C oraz wilgotności materiału < 1% i wilgotności względnej w komorze rozdziału < 5%, po czym półprodukt ponownie chłodzi się do temperatury
kriogenicznej, - 150°C w komorze (3), następnie mieli w młynie nożowym (4) do wielkości cząstek < 0,5 mm, przy chłodzeniu komory roboczej
młyna, po czym rozdziela się w separatorze elektrostatycznym (5), przy napięciu rozdziału > 17 kV, temperaturze otoczenia i materiału w zakresie 10 - 30°C oraz wilgotności materiału < 1% i wilgotności względnej w komorze rozdziału < 5%.

Literatura

Bizzo, W.; Figueiredo, R.; de Andrade, V. Characterization of Printed Circuit Boards for Metal and Energy Recovery after Milling and Mechanical Separation. Materials 2014, 7, 4555–4566,

Charles, R.G.; Douglas, P.; Hallin, I.L.; Matthews, I.; Liversage, G. An investigation of trends in precious metal and copper content of RAM modules in WEEE: Implications for long term recycling potential. Waste Management 2017, 60, 505–520

Changming, D., Chao, S., Gong, X., Ting, W., Xiange, W., 2018. Plasma methods for metals recovery from metal–containing waste. Waste Management 77, 373–387

Duan, C., Wen, X., Shi, C., Zhao, Y., Wen, B., He, Y., 2009. Recovery of metals from waste printed circuit boards by a mechanical method using a water medium. Journal of Hazardous Materials 166, 478–482.

Dascalescu, L., Iuga, A., Morar, R., 1992. Corona–Electrostatic Separation: An Efficient Technique for the Recovery of Metals and Plastics From Industrial Wastes. Magnetic and Electrical Separation 4, 059037

Eswaraiah, C., Kavitha, T., Vidyasagar, S., Narayanan, S.S., 2008. Classification of metals and plastics from printed circuit boards (PCB) using air classifier. Chemical Engineering and Processing: Process Intensification 47, 565–576

Forti, V.; Baldé, C.P.; Kuehr, R.; Bel, G. The Global E-waste Monitor 2020. 120.

Huang, K.; Guo, J.; Xu, Z. Recycling of waste printed circuit boards: A review of current technologies and treatment status in China. Journal of Hazardous Materials 2009, 164, 399–408, doi:10.1016/j.jhazmat.2008.08.051.

Johnson, J.; Harper, E.M.; Lifset, R.; Graedel, T.E. Supporting information for "Dining at the Periodic Table: Metals"Concentrations as They Relate to Recycling. Environ. Sci. Technol. 2007, 41, 1759–1765

Jiang, W., Jia, L., Zhen-ming, X., 2009. A new two-roll electrostatic separator for recycling of metals and nonmetals from waste printed circuit board. Journal of Hazardous Materials 161, 257–262.

Kaya, M., 2017. Recovery of Metals and Nonmetals from Waste Printed Circuit Boards (PCBs) by Physical Recycling Techniques, in: Zhang, L., Drelich, J.W.,

Neelameggham, N.R., Guillen, D.P., Haque, N., Zhu, J., Sun, Z., Wang, T., Howarter, J.A., Tesfaye, F., Ikhmayies, S., Olivetti, E., Kennedy, M.W. (Eds.), Energy Technology 2017. Springer International Publishing, Cham, pp. 433–451

Kumar, A.; Holuszko, M.E.; Janke, T. Characterization of the non-metal fraction of the processed waste printed circuit boards. Waste Management 2018, 75, 94–102,

Leung, A.O.W., Luksemburg, W.J., Wong, A.S., Wong, M.H., 2007. Spatial distribution of polybrominated diphenyl ethers and polychlorinated dibenzo-p-dioxins and dibenzofurans in soil and combusted residue at Guiyu, an electronic waste recycling site in southeast China 12

Suponik, T., Franke, D.M., Nuckowski, P.M., Matusiak, P., Kowol, D., Tora, B., 2021. Impact of Grinding of Printed Circuit Boards on the Efficiency of Metal Recovery by Means of Electrostatic Separation. Minerals 11, 281

Suponik, T., Franke, D., Nuckowski, P., 2019. Electrostatic and magnetic separations for the recovery of metals from electronic waste. IOP Conf. Ser.: Mater. Sci. Eng. 641, 012017.

Tsydenova, O.; Bengtsson, M. Chemical hazards associated with treatment of waste electrical and electronic equipment. Waste Management 2011, 31, 45–58

Sohaili, J., Muniyandi, S. K., Mohamad, S. S. A review on printed circuit board recycling technology. Journal of Emerging Trends in Engineering and Applied Sciences, 3(1), 2012, 12-18

Song, Q.; Zeng, X.; Li, J.; Duan, H.; Yuan, W. Environmental risk assessment of CRT and PCB workshops in a mobile e-waste recycling plant. Environ Sci Pollut Res 2015, 22, 12366–12373

Veit, H.M., Diehl, T.R., Salami, A.P., Rodrigues, J.S., Bernardes, A.M., Tenório, J.A.S., 2005. Utilization of magnetic and electrostatic separation in the recycling of printed circuit boards scrap. Waste Management 25, 67–74

Wu, J., Qin, Y., Zhou, Q., Xu, Z., 2009. Impact of nonconductive powder on electrostatic separation for recycling crushed waste printed circuit board. Journal of Hazardous Materials 164, 1352–1358

Qiu, Ruijun, Lin, M., Ruan, J., Fu, Y., Hu, J., Deng, M., Tang, Y., Qiu, Rongliang, 2020. Recovering full metallic resources from waste printed circuit boards: A refined review. Journal of Cleaner Production 244, 118690

Xiang, D., Mou, P., Wang, J., Duan, G., Zhang, H.C., 2007. Printed circuit board recycling process and its environmental impact assessment. Int J Adv Manuf Technol 34, 1030–1036.

Yoo, J.-M., Jeong, J., Yoo, K., Lee, J., Kim, W., 2009. Enrichment of the metallic components from waste printed circuit boards by a mechanical separation process using a stamp mill. Waste Management 29, 1132–1137

Zhu, X., Nie, C., Wang, S., Xie, Y., Zhang, H., Lyu, X., Qiu, J., Li, L., 2020. Cleaner approach to the recycling of metals in waste printed circuit boards by magnetic and gravity separation. Journal of Cleaner Production 248, 119235